

**Interoceptive Awareness in Health and Depression –
Investigations of Underlying Neural and
Neurochemical Mechanisms
by Combining fMRI, PET and MRS**

**Inaugural-Dissertation
to obtain the academic degree
Doctor rerum naturalium (Dr. rer. nat.)**

**Submitted to the Department of Biology, Chemistry and Pharmacy
of Freie Universität Berlin**

by

Christine Wiebking

(born in Stadthagen, Germany)

December 2012

Time period, supervisor and institute of doctorate studies

2009

Department of Psychiatry,
Otto-von-Guericke University, Magdeburg, Germany

2009-2012

Institute of Mental Health Research,
University of Ottawa, Ottawa, Canada

Supervisor

Prof. Malek Bajbouj

Prof. Georg Northoff

1st Reviewer: Prof. Malek Bajbouj

2nd Reviewer: Prof. Constance Scharff

Date of defence: 08 May 2013

Acknowledgements

Firstly, I would like to thank Georg Northoff, my former colleagues from Germany as well as my colleagues here in Canada at the Mind, Brain Imaging and Neuroethics group for their important input, support, and motivation.

Thank you to Malek Bajbouj for his support and to Constance Scharff for her work as a reviewer.

Many thanks to the technical staff at the various scanning centres for their support.

I would also like to thank all participants taking part in these studies, especially to the patient group for their voluntarily participation.

Zum Schluß möchte ich mich bei meinen Freunden und vor allem bei meiner Familie bedanken, deren Unterstützung aus der Ferne eine große Hilfe war.

Contents

1	General introduction	1
1.1	Background	1
1.2	Questions	7
1.3	Methods	10
1.3.1	Magnetic resonance imaging (MRI)	10
1.3.2	Image contrast	13
1.3.3	Introduction to fMRI	14
1.3.4	Characteristics of the BOLD response	15
1.3.5	Positron emission tomography (PET)	17
1.3.6	Magnetic resonance spectroscopy (MRS)	20
2	Are emotions associated with activity during rest or interoception? An exploratory fMRI study in healthy subjects	21
2.1	Abstract	21
2.2	Introduction	22
2.3	Materials and methods	23
2.3.1	Participants	23
2.3.2	Paradigm	24
2.3.3	Behavioural Tests	24
2.3.4	fMRI data acquisition and analysis	25
2.4	Results	27
2.4.1	Behavioural data	27

2.4.2	Signal changes during rest	27
2.4.3	Relationship between signal changes during rest and emotions	31
2.5	Discussion	33
2.6	Acknowledgements	36
3	Abnormal body perception and neural activity in the insula in depression	
	– An fMRI study of the depressed “material me”	37
3.1	Abstract	37
3.2	Introduction	38
3.3	Materials and methods	40
3.3.1	Depressed participants and healthy controls	40
3.3.2	Paradigm	42
3.3.3	Behavioural tests	44
3.3.4	fMRI data acquisition and analysis	44
3.4	Results	47
3.4.1	Behavioural data	47
3.4.2	Signal changes during intero- and exteroceptive processing and rest in the insula	48
3.4.3	Relationship between signal changes in the insula and body perception	54
3.5	Discussion	58
3.6	Acknowledgements	61
4	Neural response to interoceptive awareness in the insula as state marker for depression - an fMRI study investigating healthy, depressed and remitted participants	63
4.1	Abstract	63
4.2	Introduction	65

4.3	Materials and methods	67
4.3.1	Participants	67
4.3.2	Paradigm	68
4.3.3	fMRI data acquisition and analysis	70
4.3.4	Definition of insula regions and statistical analysis	72
4.4	Results	73
4.4.1	Results in insula regions (Figure 4.1)	73
4.4.2	Results in the dAI (Figure 4.2)	76
4.4.3	Results in the PI (Figure 4.3)	79
4.5	Discussion	80
4.6	Acknowledgements	85
5	External awareness and GABA – A multimodal imaging study combining fMRI and [¹⁸F]flumazenil-PET	87
5.1	Abstract	87
5.2	Introduction	88
5.3	Materials and methods	91
5.3.1	Participants	91
5.3.2	Paradigm	91
5.3.3	fMRI data acquisition and analysis	92
5.3.4	PET-Image Acquisition and Reconstruction	96
5.4	Results	98
5.4.1	Behavioural data	98
5.4.2	fMRI	98
5.4.3	PET	100
5.5	Discussion	107
5.6	Acknowledgements	110

6	GABA in the insula – a predictor of the neural response to interoceptive awareness	111
6.1	Abstract	111
6.2	Introduction	112
6.3	Materials and Methods	114
6.3.1	Participants	114
6.3.2	fMRI paradigm	115
6.3.3	fMRI data acquisition and analysis	116
6.3.4	MRS acquisition and analysis	118
6.4	Results	120
6.4.1	GABA and interoceptive awareness	120
6.4.2	GABA and depressed affect	125
6.5	Discussion	127
6.6	Acknowledgements	131
7	Discussion	133
8	Perspectives	141
8.1	Neural mechanisms underlying abnormal arousal and body perception in adolescent anxiety patients	143
8.1.1	Introduction	143
8.1.2	Imaging studies in adolescent anxiety disorders	145
8.1.3	fMRI paradigm (in developmental phase)	146
8.1.4	Aims and hypotheses	148
8.1.5	Pilot data	149
9	Abstracts	153
	Bibliography	159

10 Papers in peer-refereed journals	209
10.1 Year 2012	209
10.2 Year 2011	210
10.3 Year 2010	211
10.4 Year 2009	211
10.5 Year 2008	211
10.6 Year 2007	212
10.7 Year 2006	212
10.8 Book chapters	213
11 List of contributions	215
11.1 Chapter 2: Are emotions associated with activity during rest or interoception? An exploratory fMRI study in healthy subjects [Wiebking et al., 2011]	215
11.2 Chapter 3: Abnormal body perception and neural activity in the insula in depression – An fMRI study of the depressed “material me” [Wiebking et al., 2010]	216
11.3 Chapter 4: Neural response to interoceptive awareness in the insula as state marker for depression - an fMRI study investigating healthy, depressed and remitted participants	216
11.4 Chapter 5: External awareness and GABA – A multimodal imaging study combining fMRI and [¹⁸ F]flumazenil-PET [Wiebking et al., 2012a]	217
11.5 Chapter 6: GABA in the insula — a predictor of the neural response to interoceptive awareness	218
A Supplementary material for Chapter 2	221
B Supplementary material for Chapter 4	223

C	Supplementary material for Chapter 5	229
D	Supplementary material for Chapter 6	235
E	List of abbreviations	241
F	Copies of original publications	245

List of Figures

- 1.1 The human insula cortex in lateral view 2
- 1.2 The insula cortex with three distinct subregions 5
- 1.3 Schematic time course of T_1 and T_2 relaxation 12
- 1.4 Schematic representation of BOLD hemodynamic response 16
- 1.5 Binding potential map of cortical GABA 19

- 2.1 Cortical midline regions implicated in the default-mode network and correlations between activity changes during rest and the Florida Affect Battery 29

- 3.1 fMRI paradigm used in groups of healthy and MDD participants 43
- 3.2 Comparing the total score of the Body Perception Questionnaire between healthy and depressed participants 47
- 3.3 Comparing the subscales of the Body Perception Questionnaire between healthy and depressed participants 48
- 3.4 Interoceptive awareness in healthy and MDD, left anterior insula 49
- 3.5 Interoceptive awareness in healthy and MDD, right anterior insula 50
- 3.6 Interoceptive awareness in healthy and MDD, left middle insula 51
- 3.7 Interoceptive awareness in healthy and MDD, right middle insula 52
- 3.8 Correlation in healthy and MDD participants between signal changes in the right insula during rest and Body Perception Questionnaire 56

3.9	Correlation in healthy and MDD participants between signal changes in the left insula during rest, Body Perception Questionnaire, and Beck Depression Inventory	57
4.1	Neural activity for interoceptive awareness in the dorsal anterior insula, ventral anterior insula, and the posterior insula in independent groups of healthy, depressed, and remitted participants	75
4.2	Neural activity for different conditions in healthy, depressed, and remitted participants in the left and right dorsal anterior insula	77
4.3	Neural activity for exteroceptive awareness in the right posterior insula in independent groups of healthy, depressed, and remitted participants and its relation to BHS	79
5.1	Signal changes (main and an independent data sample) for the three main conditions in cortical midline regions	99
5.2	GABA binding potentials in the left mPFC and their correlation with signal changes	101
5.3	GABA binding potential in the bilateral precuneus and its correlation with signal changes	103
5.4	Binding potentials of anatomically defined regions in whole brain regression analysis	104
6.1	Intero-/ exteroceptive awareness in the insula MRS voxel and its relation to GABA	121
6.2	Intero-/ exteroceptive awareness in the mPFC MRS voxel and its relation to GABA and BHS	122
6.3	Relation between GABA, BHS, and interoceptive awareness in the insula MRS voxel	125

6.4	Inter-relationship in the left insula between GABA, interoception, and depression	126
7.1	Overview of all study results	137
8.1	FMRI paradigm for a new study in adolescent anxiety patients	147
8.2	Single subject pilot fMRI data for a new study design showing the contrast [IA > Fix]	150
8.3	Single subject pilot fMRI data for a new study design showing the contrast [Self > Other]	151
A.1	Whole brain regression using scores of the Florida Affect Battery	221
B.1	Distribution of neural activity in the left and right dAI across healthy, depressed, and remitted participants for different conditions	226
C.1	GABA binding potential in the right mPFC and its correlation with signal changes	230
C.2	FMRI paradigm used in healthy participants in combination with PET and MRS	234
D.1	LCModel quantification of the representative ¹ H NMR spectrum obtained using MEGA-PRESS	235

List of Tables

2.1	Signal changes in the VMPFC, DMPFC, and PCC during the three main conditions	30
2.2	Neural activity in (independent) regions of the default-mode network and their correlation with psychological measures of emotion	32
3.1	Percent signal changes in the anterior and middle insula for healthy and MDD participants	54
3.2	Correlation between signal changes during rest and Body Perception Questionnaire	55
5.1	Binding potential values, percent signal changes, and their correlation for functionally defined cortical midline regions	102
5.2	Binding potential values, percent signal changes and their correlation for anatomically defined midline regions	106
6.1	Correlations between residuals for MRS metabolites and signal changes for single conditions as well as the Beck Hopelessness Scale	124
A.1	Correlation between signal changes of main interoceptive regions and tests for emotional processing, depression, and body perception	222
B.1	Demographics and clinical variables for healthy, depressed, and remitted participants	223
B.2	Group effects as revealed by MANOVA	224

B.3	Signal changes for healthy, depressed, and remitted participants in regions showing significant group effects	225
B.4	Correlation between signal changes in the dorsal anterior/ posterior insula and depression scores	227
C.1	Binding potential values, percent signal changes and their correlation for functionally defined regions that were not located along the cortical midline	231
C.2	Detailed overview of conducted whole brain regressions	233
D.1	Metabolite concentrations, CRLB values, correlation coefficients between Glu/ Gln (A) and signal changes (B) in the insula and mPFC	236
D.2	Results for SPM regression analysis in the insula, using insula MRS values and BHS scores as regressor	237
D.3	Results for SPM regression analysis in the mPFC, using mPFC MRS values and BHS scores as regressor	238
D.4	Whole brain regressions using GABA values from the insula as regressor	239

Chapter 1

General introduction

1.1 Background

The insula (Figure 1.1), located within the Sylvian fissure of each hemisphere, is an important structure involved in the processing of the physiological condition of the human body, which is termed interoception [Craig, 2002, 2003, 2008]. The meaning of this construct, originally restricted to sensations solely from the viscera [Sherrington, 1948], has been broadened to comprise a generalized sensory capacity, mainly due to findings of a phylogenetically novel ascending interoceptive pathway in primates. According to Craig [Craig, 2002, 2008], this so-called lamina I spinothalamocortical pathway from the body to the cortex (including the insula) is the neuroanatomical substrate that enables an interoceptive cortical representation of the body (which he terms “the material me”) [Craig, 2002].

In more detail, two parallel pathways, one containing sympathetic and the other parasympathetic information from small-diameter afferents, project via brainstem nuclei to distinct thalamo-cortical relay nuclei, which in turn project to posterior parts of the insula cortex [Craig, 2002, 2003, 2008]. As postulated by Craig, iterative processes integrating and then re-representing multimodal information gradually take place starting from the posterior, continuing to the mid and ending in the anterior part of the insula. Hence, specifically the anterior insula is seen to play an important role in human awareness

and particularly in interoceptive awareness, the awareness of stimuli originating inside the body.

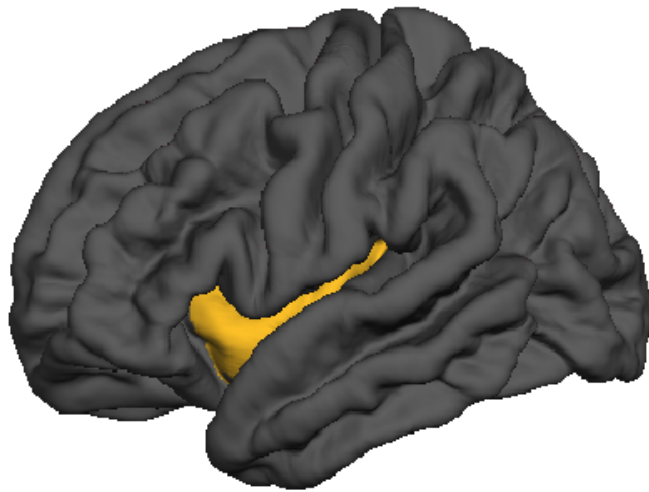


Figure 1.1: The human insula cortex (yellow) in lateral view. The bilateral structure was first described 1796 by Johann Christian Reil and is folded deep within the lateral sulcus.

In addition to connections with the insula, ascending projections of lamina I neurons also form a thalamocortical pathway in primates that innervates the anterior cingulate cortex [Craig, 2008], a brain structure located along the cortical midline of the human brain and involved in a variety of functions such as emotional processing [e.g. Etkin et al., 2011] alongside its activation by autonomic functions. Additionally, both structures, the anterior insula and the anterior cingulate cortex, are often seen to be functionally co-activated in imaging studies dealing with emotions, suggesting an involvement of both structures in human emotional processing.

Alongside neuroanatomical findings, the emergence of new imaging techniques like functional magnetic resonance imaging (fMRI), electroencephalography (EEG) and positron emission tomography (PET) have allowed active *in vivo* studies of interoceptive awareness to be carried out. These methods have contributed significantly to enlightening the neural and biochemical processes underlying awareness of ones own body and the environment, as well as its interplay with emotional processing.

An important early contribution to the imaging-based literature was an fMRI study by Critchley and colleagues [Critchley et al., 2004]. Similar to early work on the behavioural level by Schandry [Schandry, 1981], a heartbeat detection task in fMRI was used to induce interoceptive awareness on the neural level in healthy participants. During interoceptive conditions, participants had to judge if their own heartbeat was in sync with an external tone. In the control exteroceptive condition, participants had to judge if one of the applied external tones was played with a different pitch compared to the rest of the tones. In addition, anxiety was measured by a psychometric test, a procedure comparable to Schandry's. It was shown that neural activity during interoceptive awareness is increased in several brain regions such as the anterior cingulate cortex and, most importantly, the insula cortex (see Figure 1.1). Moreover, anxiety scores were positively correlated with interoceptive accuracy as well as with neural activity in the insula. As discussed by Critchley, psychiatric conditions like anxiety disorders are accompanied by somatic symptoms and increased attention to bodily processes. This supports the hypothetical relationship between interoceptive awareness and emotional processing, supporting key assumptions of the James-Lange theory of emotion, a classical construct of the late 19th century stating that the perception of bodily changes is essential for generating emotions [James, 1884, 1894]. The findings underline a putative abnormal interaction of interoceptive awareness, emotional processing, and insula activity in psychiatric disorders. The results of this study thus reinforce the fact that the insula is a crucial brain region for mediating awareness of bodily stimuli, as well as being implicated in emotional processing.

Further investigations into the neural activity in the insula during interoceptive awareness have supported and extended the findings of Critchley and colleagues. Importantly, a recent fMRI study by Zaki et al. (2012) showed for the first time that neural activity during emotional processing and interoceptive awareness overlaps in the region of

the insula cortex. Here they speak of a “convergence zone for the representations of the body and emotion” [Zaki et al., 2012, p. 498]. However, as noted above, other regions, such as the anterior cingulate cortex, are found to co-activate with the insula. Such patterns of co-activation occur not only during tasks dealing with interoceptive awareness, but have also been described in imaging studies investigating stimuli originating outside the body (i.e., exteroceptive awareness) such as tasks requiring cognitive control [Duncan and Owen, 2000] or attention to visual stimuli [Sterzer and Kleinschmidt, 2010]. Studies using diffusion weighted imaging to investigate the structural connectivity of the human insula have revealed connections with the cingulate cortex [Beckmann et al., 2009, van den Heuvel et al., 2009], although these results are not as consistent [Cloutman et al., 2012, Cerliani et al., 2012] as results gained using functional connectivity, where patterns of intrinsic activity are correlated over time. Here, an important network role for the insula is further underlined by studies showing functional connectivity between the insula and, amongst others, prefrontal regions [Deen et al., 2011, Farb et al., 2012a, Simmons et al., 2012, Cauda et al., 2011, Medford and Critchley, 2010] such as the anterior cingulate cortex.

Looking at the insula more closely, several imaging studies have revealed a threefold regional organization within it, as illustrated in Figure 1.2 [Chang et al., 2012, Deen et al., 2011]. In particular, the results of Deen and colleagues [Deen et al., 2011] suggest linked but dissociable networks across regions of the anterior insula and the cingulate cortex, specifically a dorsal network associated with cognitive control and a ventral network associated with emotional experience. A third functional connectivity network includes the posterior insula along with primary and secondary motor and somatosensory cortices. These results highlight the multimodal character of the insula and in particular its connection to anterior cortical midline structures, implying a potential role in decisional as well as emotional processes. Although involvement of cortical midline

structures, such as the cingulate cortex, has been noted in a broad range of different tasks, they also form a major part of the so-called “default-mode network”, a group of regions that show elevated activity levels in the absence of an active task [Raichle, 2009, Northoff et al., 2010a]. Interestingly, several studies have suggested that the default-mode network is connected to emotional functions [Harrison et al., 2008, Pitroda et al., 2008], which in turn have been associated with interoceptive processing [Panksepp, 1998, Pollatos et al., 2007a, Critchley et al., 2005, Craig, 2009]. This dual association of emotions with activity during rest and interoception raises the question as to the exact relationship between the two states in cortical midline structures and the insula, a question that remains to be investigated.

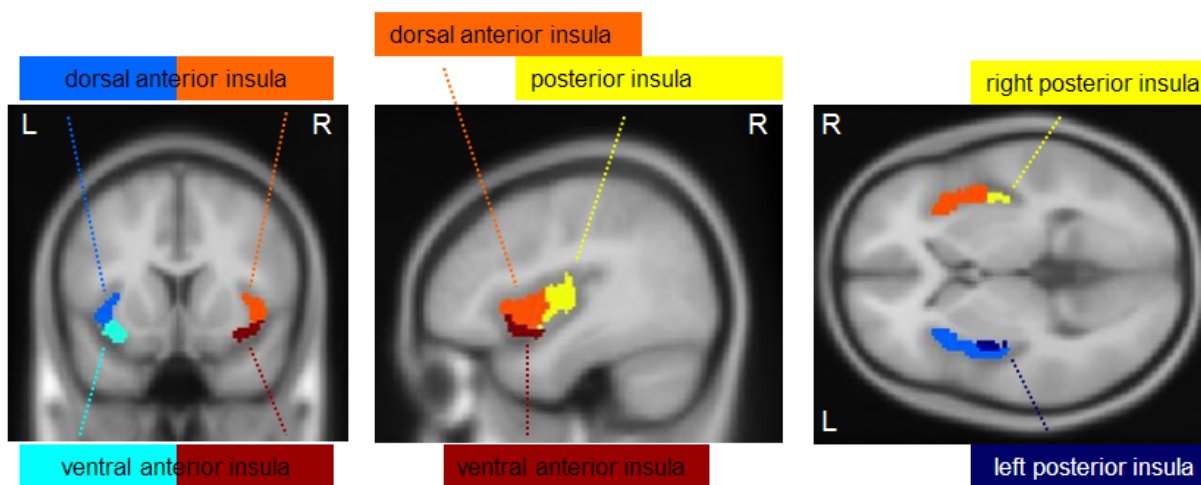


Figure 1.2: The insula cortex with three distinct subregions, as revealed by functional connectivity: dorsal anterior insula, ventral anterior insula, and posterior insula. Subdivisions shown here are taken from [Deen et al., 2011].

Studying psychiatric disorders opens the opportunity to further explore the role of interoceptive awareness by linking altered behaviour to neural activity. Thereby, conclusions can be drawn about particular brain structures involved in processes like interoceptive awareness and how neural dysfunction of a particular brain region like the insula can be related to behavioural symptoms seen in psychiatric populations. Findings in such

studies can provide novel insights into the neural underpinnings of mental disorders and may lead to potential reclassifications of psychiatric disorders on a neurobiological basis. Brain regions abnormally involved in processes like interoceptive awareness might serve due to their association with emotional processing (which is disrupted in major depression) as target regions for treating affective disorders. This can be seen as a way of stabilizing emotional processing by instead directly targeting an interacting behavioural feature [[Simmons et al., 2006](#), [Craig, 2008](#)].

Patients suffering from affective disorders like major depression are of particular interest for investigating an interaction between interoceptive awareness, emotional processing and the default-mode network, since these patients show abnormalities in each of these domains on the behavioural as well as neural levels. Major depressive disorder (MDD), one of the leading causes of disability worldwide [[Bromet et al., 2011](#), [WHO, 2002](#)], is apparently characterised by abnormalities in the processing of emotional stimuli. This includes feelings of hopelessness and guilt, loss of awareness of one's own feelings and over-attribution of negative stimuli to the own person, including the body [[Grimm et al., 2011a](#), [Rimes and Watkins, 2005](#), [Northoff, 2007](#), [Nyboe Jacobsen et al., 2006](#), [Henningesen et al., 2003](#)]. In addition, MDD patients often suffer from diffuse and persisting physical comorbidities such as headache, sensibility deficits in chest and abdomen, or increased muscle tension, which go along with altered awareness of bodily symptoms as well as altered awareness of external stimuli [[Beck, 1961](#), [Garcia-Cebrian et al., 2006](#), [Nyboe Jacobsen et al., 2006](#)]. These altered states of awareness have been described as decreased environment-focus and increased self-focus of MDD [[Grimm et al., 2011a](#), [Paulus and Stein, 2010](#), [Stewart et al., 2001](#), [Wiersma et al., 2011](#)]. At the same time the evaluation and accuracy of interoceptive heartbeat perception seems to be impaired in MDD [[Terhaar et al., 2012](#)], which can be seen as a result of impaired cognitive and decision-making functions. These deficits in MDD – on the one hand emo-

tional and on the other hand interoceptive deficits – present an interesting combination to target for further experimental studies. In addition, MDD is also characterised by deficits on two other levels – in the neural activity constituting the default-mode network [Gentili et al., 2009, Grimm et al., 2009a, 2011a] and deficits at the biochemical level of receptors and neurotransmitters [Alcaro et al., 2010, Kalueff and Nutt, 2007, Luscher et al., 2011, Brooks et al., 2009, Möhler, 2012] – providing multiple avenues for the study of underlying abnormalities in individuals suffering from MDD. These biochemical underpinnings of interoceptive awareness, however, also remain to be investigated in healthy participants. Here, psychiatric disorders can also serve as a valuable hypothesis generator, as the systems seen to be dysfunctional in MDD are likely to be those involved in healthy participants also.

Finally, as described above, the insula is seen as a region highly involved in mediating interoceptive awareness in combination with emotional processes. An involvement of this region in depression is supported by findings of altered functional [Liotti et al., 2002, Paulus and Stein, 2010], structural [Sprengelmeyer et al., 2011] and biochemical states [Zhao et al., 2012], suggesting a link between altered awareness of bodily stimuli and neural activity in the insula in depression.

1.2 Questions

Based on the above introduction into the processes of interoceptive awareness, emotional processing and neural activity in relevant brain areas, several questions can be formulated:

Firstly, based on the described link between the insula and anterior cingulate, the question arises as to whether emotions can be related to neural activity during rest or interoception in regions located along the cortical midline of the healthy human brain.

Secondly, since patients suffering from MDD typically show disturbances in the processing and perception of bodily stimuli, it remains to be investigated as to whether abnormalities can also be seen on the neural level in the insula in such individuals.

Thirdly, the described functionally different sub-regions of the insula - dorsal and ventral parts of the anterior insula as well as the posterior insula - need to be considered. Do the subdivisions of the insula reveal differences in neural activity when comparing healthy, depressed and remitted participants?

Finally, since ultimately neurotransmitters and receptors are the effectors of neural activity, an interesting question to ask concerns the underlying biochemical landscape of the regions discussed above, i.e. the cortical midline structures and the insula. Can the biochemical environment of these regions be connected to specific neural processes such as intero- or exteroceptive awareness?

In order to approach these points, the work presented here contains a set of multi-modal imaging studies in humans. In more detail, imaging data have been acquired from MDD patients, participants recovered from MDD, and two independent groups of healthy participants. Functional magnetic resonance imaging (fMRI) was combined with behavioural tests in the first three groups of healthy, depressed and remitted participants. In addition, fMRI was combined with positron emission tomography (PET) and magnetic resonance spectroscopy (MRS) in the fourth group of healthy participants. fMRI allows for excellent spatial localization of functional changes, whilst PET is used to measure neural receptor density in order to investigate biochemical underpinnings of the brain's neural activity. MRS is also used to acquire neurotransmitter concentration values from one of the main regions of interest in regard to interoceptive awareness, the insula cortex.

Importantly, all participants underwent the same fMRI paradigm (focusing on interoceptive awareness, exteroceptive awareness, and fixation periods), making the experiments an ideal instrument to have a closer look at underlying neural processes of interoceptive awareness in healthy and psychiatric populations in combination with the investigation of underlying biochemical entities.

The work is presented here as a series of stand-alone papers that have been published (Chapters 2, 3, and 5, see also Appendix F), or have been submitted for publication in peer-reviewed journals (Chapters 4 and 6). Although they can be read independently of each other, their underlying main theme combines them into an integrated overall picture. Supplementary (Suppl.) information is included in a series of appendices at the end of the work and is referenced within each paper's text. The chapters included can be summarized as follows:

- Chapter 2 consists of an analysis linking activity during rest in cortical midline structures to emotional processing in a group of healthy subjects.
- Chapter 3 investigates body perception and neural activity in the insula during rest in healthy and MDD participants and shows the decoupling of these processes in MDD.
- Chapter 4 also focuses on the insula, specifically on *a priori* defined functionally different sub-regions of the insula and their neural activity in comparison between healthy, depressed and remitted participants.
- Chapter 5 advances the findings of Chapter 2 by investigating the link between biochemistry and neural activity in cortical midline structures by combining fMRI and PET in a group of healthy subjects.
- Chapter 6 extends the insula findings of Chapters 3 and 4. Using MRS in the insula, this Chapter shows a specific association between neural activity during interoceptive awareness and GABA.

- Finally, Chapters 7 (Discussion) and 8 (Perspectives) provide general conclusions and a description of ongoing/ future research projects.

1.3 Methods

The following section describes the basics of magnetic resonance imaging (MRI), followed by an introduction to the method of functional magnetic resonance imaging (fMRI), positron emission tomography (PET), and magnetic resonance spectroscopy (MRS).

1.3.1 Magnetic resonance imaging (MRI)

For the relatively new imaging technique of magnetic resonance imaging, the properties of hydrogen atoms (^1H) are used. Firstly, hydrogen atoms are ubiquitous in biological systems like the human body and secondly, their nuclei consist of only one positively charged proton. Moreover, they have a rotation (spin), a fundamental property of elementary particles, so that the proton has a magnetic dipole moment and therefore behaves like a small magnet. The nucleus is said to possess the nuclear magnetic resonance (NMR) property. If no external magnetic field is present, the individual spin axes are aligned randomly. Hence, they cancel each other out and the sum of all magnetic moments of all spins is infinitesimally small. The introduction of an external magnetic field causes the alignment of each proton's axis of spin. The axes of spin align either along (parallel) or against (antiparallel) the external magnetic field. Without thermal influence, a system would tend to acquire the lowest energy state, which is parallel alignment of spins. When considering a physiological system, however, thermal energy must be taken into account. This is sufficient to enable some spins to get into a higher energy state, which is the antiparallel orientation. Consequently, a small imbalance between parallel and antiparallel aligned spins occurs. For example, at 1.5 Tesla and

physiological temperatures, only 10 of 1.000.000 spins add to give a net magnetization of the system, leading to a measurable longitudinal magnetization, i.e. parallel to the main magnetic field in z direction [Jezzard et al., 2002, Pooley, 2005]. For a typical imaging unit, the z direction is horizontal and corresponds to the long axis of a body. To illustrate the unit Tesla, the magnetic field of the earth can be used, which has a strength of 30 to 60 μT , roughly 1/ 50.000 Tesla.

Protons within an external magnetic field react with a compensating movement, which is known as precession. Here, the axis of the spin itself rotates around a central axis. This happens at a characteristic frequency, the so-called Larmor frequency, which is proportional to the strength of the magnetic field. For protons, the Larmor frequency within the earth's magnetic field is only about 1 kHz, but already 63.8 MHz at 1.5 T [Koechli and Marincek, 1998].

Precessing protons within an external magnetic field can precess around an axis that is either parallel (low-energy state) or antiparallel (high-energy state) to the magnetic field. The amount of electromagnetic energy that is necessary to create equal numbers of nuclei in the low- as well as high-energy state is called 90° excitation pulse. This high-frequency pulse tips the net magnetization into the transverse plane, i.e., perpendicular to the main magnetic field of the scanner (x-y axis). The x direction is usually the left-right direction of the individual and the y direction corresponds to the anterior-posterior direction. As spins return to a low-energy state after applying the high-frequency pulse, they emit energy that can be detected by a receiving coil. This takes place in the course of two independent processes, so that finally the stable initial low-energy state can be reached. These two processes are called spin-lattice (transverse) and spin-spin relaxation (longitudinal). The time constant of the longitudinal relaxation, i.e., the recovery of the longitudinal magnetization, is called T_1 and shows an exponential curve (see Figure 1.3). T_1 is defined as the time that it takes the longitudinal magnetization to grow back to 63% of its final value (assuming a 90° pulse). White matter has a very short T_1

time and relaxes rapidly, appearing bright on T_1 -weighted images. Cerebrospinal fluid (CSF) has a long T_1 and relaxes slowly, appearing dark on T_1 -weighted images. Gray matter has an intermediate T_1 and relaxes at an intermediate rate, appearing grey on T_1 -weighted images. The full recovery of the T_1 relaxation depends on the tissue type and takes about 0.5 - 5 s [Koechli and Marincek, 1998, Pooley, 2005].

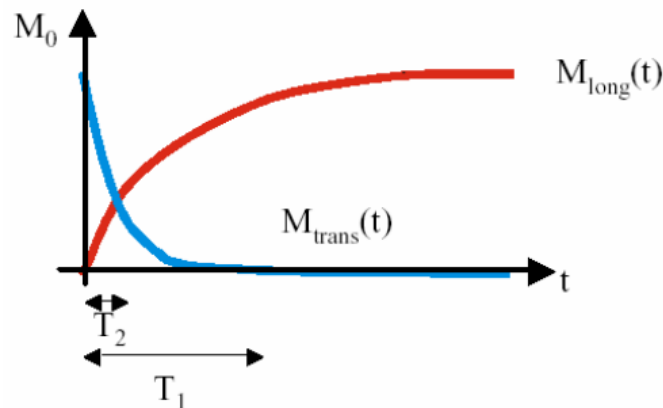


Figure 1.3: Schematic time course of the longitudinal (long) relaxation (red line, T_1 recovery) and transverse (trans) relaxation (blue line, T_2 decay).

The transverse relaxation is the loss of net magnetization within the transverse plane due to the loss of phase coherence of the spins. No energy is released to the environment, but the spins exchange energy among each other. This is the pure spin-spin relaxation with the time constant T_2 , due to which the MR signal decays within the first 100-300 ms (Figure 1.3). T_2 is defined as the time that it takes for the transverse magnetization to decay to 37% of its original value. White matter has a short T_2 and dephases rapidly, appearing dark grey on T_2 weighted images. CSF has a long T_2 and dephases slowly, appearing bright on T_2 weighted images. Grey matter has an intermediate T_2 and dephases intermediately, appearing grey on T_2 weighted images [Koechli and Marincek, 1998, Pooley, 2005].

Moreover, local magnetic field inhomogeneities cause spins to additional lose of coherence, which leads to a quicker decay: T_2^* . Field inhomogeneities occur for example near blood vessels. Here, the deoxygenated hemoglobin of the blood influences the T_2^* relaxation of the surrounding tissue. This effect constitutes the basis of the BOLD contrast (see below), the blood-oxygenation-level dependent contrast, which is crucial for functional MRI (fMRI) [Ogawa et al., 1992].

1.3.2 Image contrast

In order to determine the position of the protons in the part of the body that is of interest, the magnetic field is varied across the image volume by using gradient coils. These gradients cause changes in the MR signal and the position of the protons can be mathematically recovered from the measured MR signal.

Two factors govern the timing of MR image collection, i.e. the repetition time (T_R) and the echo time (T_E). The time between two consecutive excitations of the same slice is called repetition time, whilst the time interval between excitation through a 90° pulse and data acquisition is called echo time. The choice of T_R determines the T_1 weighting. Using a short T_R (less than 600 ms), T_1 significantly affects the image contrast since tissues with a short T_1 time constant relax fast and have a strong signal after reapplied excitation – the tissue appears bright in the resulting picture. The T_E determines the T_2 weighting. Using a long T_E (over about 60 ms), T_2 significantly affects the image contrast. Whilst tissues with a short T_2 time constant give little signal, tissues with a long T_2 value appear bright in the images, since they still have a lot of signal [Huettel et al., 2008, Koechli and Marincek, 1998]. CSF has the longest T_2 value due to its high water content and will appear brighter than grey or white matter. The signals are then be put together in two- or three-dimensional pictures (tomogram).

1.3.3 Introduction to fMRI

The underlying physiological principle of functional imaging of the brain is based on the close link between neural activity and energy metabolism, which was first described in 1890 by Roy and Sherrington. Due to neural activation, induced for example by a cognitive task, brain areas involved in the task show an increased metabolic activity. This causes an increased consumption of oxygen and glucose in brain areas involved in the task, that is supplied through hemoglobin within red blood cells. The increasing energy demands of oxygen and glucose in brain areas involved in the task leads to local increase in blood flow (HR, hemodynamic response).

Functional magnetic resonance imaging works on the basis of differing magnetic properties (susceptibility) of oxygen-rich (oxygenated) or oxygen-poor (not oxygenated, deoxygenated) hemoglobin. Oxygenated hemoglobin is diamagnetic and has no effect on the external magnetic field. The deoxygenated form is paramagnetic and leads to inhomogeneities in the magnetic field, leading to a faster dephasing and thus a signal increase in T_2^* -weighted measurements. Hence, changes in the concentration of deoxygenated blood, peaking at about 2 s and then declining [[Huettel et al., 2008](#)], provide a measure of brain function based on blood-oxygenation-level dependent (BOLD) contrast. Using fMRI, images of perfusion-related changes in the oxygen concentration are created that are correlated with neuronal activity – an indirect measure of neuronal activity [[Ogawa et al., 1992](#)].

Echo planar imaging (EPI), invented by Sir Peter Mansfield [[Mansfield, 1977](#)], is a specific MRI pulse sequence that enables fast data acquisition of the whole brain. EPI is the technique most frequently used to acquire the BOLD contrast [[Feinberg and Yacoub, 2012](#)]. This particularly fast measuring sequence enables whole brain recordings

of 30 layers in 1-3 seconds, and is thus ideal to fit with the temporal behaviour of the blood flow response. Although the temporal resolution of fMRI (in seconds) is lower compared to electroencephalography (EEG, in milliseconds), the link between neuronal activity and BOLD contrast has been shown [[Logothetis et al., 2001](#)].

On the basis of the strength of the BOLD signal conclusions can be drawn regards neuronal activity during a certain task. Another significant advantage of the fMRI technique is its non-invasive character – participants need no contrast agents. Moreover, exposure to radiation is not necessary. Overall, no long term effects have been observed so far. Functional magnetic imaging offers in addition a very high spatial resolution of up to 1.5 mm, so that even the appearance of cortical columns is possible [[Lutti et al., 2012](#)].

1.3.4 Characteristics of the BOLD response

The course of the hemodynamic response (HR) has to be taken into account for the design and analysis of an fMRI study. The schematic course of a BOLD response is shown in [Figure 1.4](#). After an initial signal drop (initial dip) immediately after the stimulus presentation, that has been associated with the increase in the amount of deoxygenated hemoglobin in a certain voxel, the signal rises over about 2 seconds, giving a maximum value around 4 s after stimulus presentation. After this, the intensity decreases continuously. About 10 s after stimulus onset, the signal has decayed.

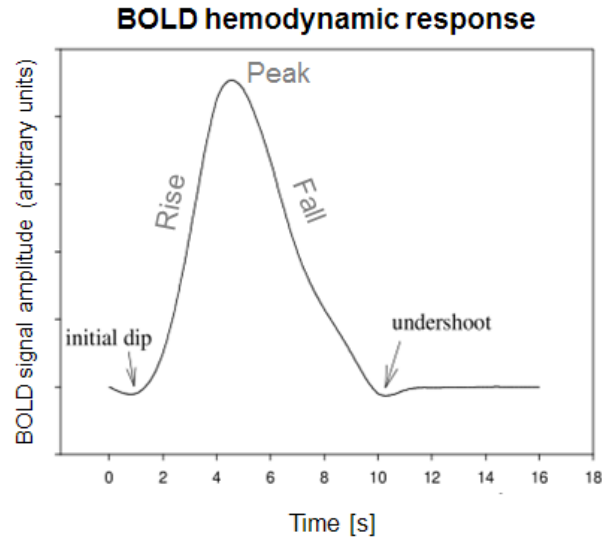


Figure 1.4: Schematic representation of the BOLD hemodynamic response, that peaks after about 4-5 s after stimulus onset before returning to baseline at about 10 s. Adapted from [Chein and Schneider, 2003, Huettel et al., 2008].

Thereafter, often a decrease in the negative range (below the baseline) is seen [Jezzard et al., 2002]. According to the balloon model [Buxton et al., 1998], this is associated with an increased amount of deoxygenated haemoglobin due to normalized blood flow but still expanded blood volume. To ensure a maximum of differentiation between different types of stimuli, the ratio of signal to noise has to be optimally adjusted. The noise, which is for example caused by the scanner or the participant, increases the variance of acquired data and leads to a lower signal-to-noise ratio. By integrating a control condition in the experiment, e.g. a baseline, stimulus-related changes of the BOLD signal can be considered in relation to the baseline.

1.3.5 Positron emission tomography (PET)

Positron emission tomography (PET) uses gamma rays to produce an image of body tissues and processes. Using a cyclotron, i.e. a particle accelerator, a radioactive isotope is created. This tracer is attached to a molecule, that - injected in the blood stream - is metabolized or can bind to a specific receptor site. The biological function of the molecule is not influenced by the attached tracer. Hence, by choosing an appropriate molecule with a known biological pathway or function, the PET technique can determine where it is taken up by cells and accumulates by imaging the tracer.

For example, fluorine-18 (^{18}F) is a commonly used tracer and can be attached to many substances, e.g. to fluorodeoxyglucose (FDG), an analogue of glucose. A bolus injection of FDG is given intravenously. Serving as an energy supply, FDG will be taken up by structures that require a high amount of energy, such as the brain. As positrons (anti-electrons) are emitted by the tracer, they eventually collide with an electron. Mutually annihilated, a pair of gamma waves are released in opposing directions. These waves are then detected by the PET camera, which generally takes the form of a ring around the body of the person and consists of scintillation crystals. The point in space from which the waves originated can be calculated from the positioning and relative timing of the two detections [Bailey et al., 2003]. In the example of FDG, different accumulation level can be used to infer the amount of energy being used within a particular region. This information can then be used to investigate neural activity [Phelps, 1981].

Taken together, PET scans can provide images specifically sensitive to a single substance and therefore many questions about underlying brain physiology and functioning can be investigated. However, disadvantages in human research are the radiation exposure and the poor temporal resolution. An image with a good signal-to-noise ratio requires the detection of many emissions, leading to very long acquisition times (see below).

Flumazenil

As mentioned above, tracers can be attached to different kinds of molecules, including molecules that bind to certain receptor types in the brain. PET imaging is an ideal method to provide information about the distribution and function of a specific receptor [Heiss and Herholz, 2006]. Since the GABA_A receptor is the major inhibitory receptor in the brain and distributed throughout the cortex [Olsen, 1981, Jacob et al., 2008], it has been the target of the work presented here. The ligand of this receptor, which consists of five subunits, is gamma-aminobutyric acid (GABA). For PET imaging in humans, the usage of competitive benzodiazepine antagonists is common, since this class binds reversibly to the benzodiazepine site without psychological side effects [Hunkeler et al., 1981]. Flumazenil (FMZ) is a common used benzodiazepine receptor antagonist. It can be radiolabelled with the isotopes ¹¹C or ¹⁸F, whilst the latter has the advantage of a longer half-life [la Fougere et al., 2011, Gründer et al., 2001]. Using this PET radioligand, the distribution of GABA_A receptors in the human brain can be visualized (see Figure 1.5).

After a bolus injection of FMZ, it is distributed in the body approximately according to a basic three-compartment model which consists of the free ligand in the blood plasma (C_a), non-specifically bound ligand (C_f), and ligand that is specifically bound to the tissue of interest (C_b). The change in concentrations across these compartments can be calculated by using the transfer rate of the ligand across the blood brain barrier as well as the association and dissociation rate from the receptor. To calculate the value of interest (C_b), it is necessary to acquire data about the arterial blood flow. Since this procedure is a challenge in human research studies, a simplified two-compartment model has been proposed [Innis et al., 2007]. It assumes a linear rate of association between receptor and ligand as well as constancy of non-specific binding in the tissue of interest to obtain an approximation of C_b , which is known as binding potential (BP).

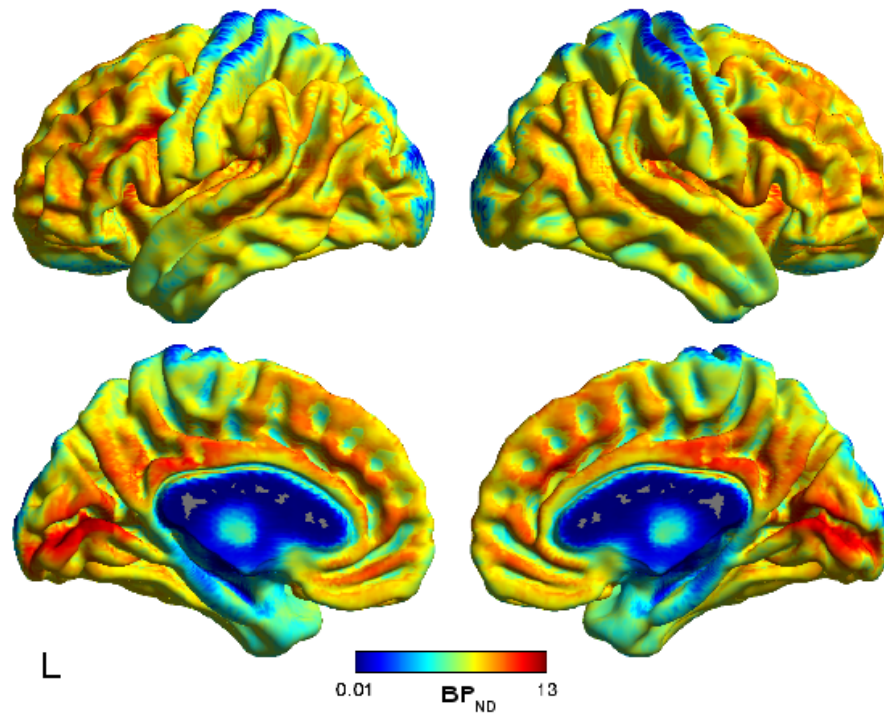


Figure 1.5: The image shows data from high-resolution [^{18}F]-labelled flumazenil (FMZ) PET imaging, that has been used to calculate cortical GABA_A binding potential maps (please refer to Chapter 5 for study details). Greater BP_{ND} corresponds to greater receptor density.

In the current study the BP_{ND} is used, i.e. the binding potential as compared to non-displaceable uptake. If the system has reached a steady state (equilibrium), the BP_{ND} can be calculated by comparing the concentration of radioligand in the receptor-rich region of interest with a reference region that has no receptors [Logan et al., 1996]. The pons has been commonly used as reference region [e.g., Klumpers et al., 2008], but recent studies have shown that it also shows specific binding of FMZ [e.g., Frankle et al., 2009]. Hence, in the study described in Chapter 5, the pons as well as the cortical white matter have been used to calculate BP_{ND} . In the case of FMZ, equilibrium is reached after about 30 minutes, which means that scans must be longer than this. In the current study, data have been acquired for 60 minutes (see Chapter 5.3.4). Of note is that BP_{ND} is not directly representative of the total amount of receptors, but is rather a combination of receptor density and ligand affinity of the receptor [Innis et al., 2007].

1.3.6 Magnetic resonance spectroscopy (MRS)

Magnetic resonance spectroscopy (MRS) is a technique basing on the principle characteristics of nuclear magnetic resonance. As described above, different tissues and ultimately different molecules can be distinguished from each other depending on their different relaxation times after a high radio frequency pulse. These different relaxation values of molecules are also dependent on their chemical and physical environment [Proctor and Yu, 1950]. For example, hydrogen molecules as part of water molecules have a different relaxation time compared to those bound into much more complex structures, as for example GABA.

Evaluating the concentration of particular molecules within a region of interest, with a typical a volume of 3 cm^3 , requires repeated measures of the different relaxation signals. Hence, when combining MRS with other techniques like fMRI in the same participant and same scanning session, the time investment of 10 to 15 minutes for measuring one region of interest is a restraining factor. Moreover, the set of molecules that can be discriminated from each other is limited, but does include the neurotransmitter GABA, as described in Chapter 6. This, in combination with its non-invasive and non-ionizing character in contrast to PET, makes it to an interesting technique for studying the role of neurotransmitters in the living human brain [Northoff et al., 2007, Horn et al., 2010].

Chapter 2

Are emotions associated with activity during rest or interoception? An exploratory fMRI study in healthy subjects

Neuroscience Letters 2011 Mar, 491(1), 87-92

<http://dx.doi.org/10.1016/j.neulet.2011.01.012>

2.1 Abstract

Imaging studies investigating the default-mode network (DMN) of the brain revealed the phenomenon of elevated neural responses during periods of rest. This effect has been shown to be abnormally elevated in regions of the DMN concerning mood disorders like major depressive disorder (MDD). Since these disorders are accompanied by impaired emotional functioning, this leads to the suggestion of an association between activity during rest conditions and emotions, which remains to be demonstrated in a healthy and clinical population. Controlling for interoceptive processing, a process often closely connected to emotional functioning, we here demonstrate in an fMRI study of 30 healthy subjects the connection between activity during rest conditions in regions of the DMN and emotions in a psychologically, regionally, and stimulus specific way.

2.2 Introduction

The significance of the high level of activity displayed by certain regions of the brain during rest is a topic of increasing interest [Raichle, 2009, Northoff et al., 2010a]. Central amongst these regions are those termed the default-mode network (DMN). This network consists mainly of cortical midline structures [Gusnard and Raichle, 2001, Raichle and Gusnard, 2005] and includes, for example, the perigenual anterior cingulate cortex (PACC), posterior cingulate cortex (PCC) as well as the ventro- and dorsomedial prefrontal cortex (VMPFC, DMPFC) [Fitzgerald et al., 2008, Greicius et al., 2007, Grimm et al., 2009b]. The DMN displays a deactivation from its level of activity at rest in response to attention-requiring tasks (task-induced deactivations, TID).

Several studies have suggested that the DMN, or components of the DMN, are connected to emotional functioning [Harrison et al., 2008, Pitroda et al., 2008]. This hypothesis is supported by the observation that a number of psychiatric disorders characterised by a deficit in emotional processing – such as major depressive disorder (MDD) and social phobia – are associated with an alteration in DMN functioning [Gentili et al., 2009, Wiebking et al., 2010].

Emotional processing has, however, also been associated with interoceptive processing [Panksepp, 1998, Pollatos et al., 2007a, Critchley et al., 2005, Craig, 2009]). The attention-requiring nature of interoceptive tasks means that such processing can be assumed to induce a deactivation in the DMN (i.e., TID). This, in conjunction with the dual association of emotions with activity during rest and interoception, thus raises the question as to whether the link between emotion and activity in the DMN described above is due to a relationship between emotion and activity during rest itself, or whether the observed relationship is instead a result of emotion-induced interoceptive activity within the DMN.

In order to investigate this issue in an exploratory study with healthy subjects, we utilised

a combination of fMRI and measures of emotions and bodily awareness. A well established fMRI paradigm for interoceptive processing [Pollatos et al., 2007c, Critchley et al., 2004] was slightly modified to include an operationalisation of resting-state (via fixation cross) within an event-related design [Wiebking et al., 2010]. This design allowed the BOLD signal observed during rest, and intero-/ exteroception (TID) to be related to the measures of emotions and bodily awareness.

Based on the DMN-related findings described above, it was hypothesised that emotional processing would be related to the level of rest activity within the DMN. In addition, it was further hypothesised that there would be no relationship between emotions and intero- or exteroceptive induced activity in these regions, as based on the assumption that it is the induced activity during rest itself in these regions that is tied to emotion, rather than any task-induced signal changes.

2.3 Materials and methods

2.3.1 Participants

We studied 30 subjects (15 female) with no psychiatric, neurological, or medical illness using fMRI. In order to evaluate the status of the subjects, they were questioned about psychiatric, neurological, or medical diseases as well as the use of psychoactive substances using a custom-made semi-structured clinical questionnaire. Participants were recruited from the University of Magdeburg and the local community. The study was approved by the local ethics committee and all participants gave written informed consent before participating in this study. Subjects were compensated for their participation.

2.3.2 Paradigm

The fMRI design was based on a paradigm introduced by Pollatos and Critchley [Pollatos et al., 2007b, Critchley et al., 2004]. Subjects were presented with three separate conditions: an interoceptive task, an exteroceptive task, and rest periods (fixation) - in a pseudo-randomised order. For a detailed description of the paradigm see Section 3.3.2 and Figure 3.1, where a separate dataset and independent analysis are presented.

2.3.3 Behavioural Tests

Intelligence was assessed through the nonverbal LPS-3 [Horn, 1983] and verbal MWT-B [Lehrl, 1995] tests.

For investigating the ability to recognize emotions, we used the Florida Affect Battery (FAB) [Bowers et al., 1991]. The FAB is a research tool that was designed to investigate disturbances in the perception of emotional signals (facial and prosodic affect) under a variety of task demands. In order to apply a comparable auditory emotional task in relation to the exteroceptive task in the scanner, we concentrated only on subtest 8a. It consists of a set of 15 semantically neutral sentences (e.g.: 'The chairs are made of wood') spoken in emotional tones of voice. The sentences show approximately the same length and were recorded by an experienced actress in five different emotional intonations: happy, angry, sad, fearful and neutral, so each affect was presented three times. Subjects were asked to verbally label the emotional prosody of each item. The Body Perception Questionnaire (BPQ) [Porges, 1993] was also used in order to test for the individuals' awareness and manner of processing bodily changes. It includes 4 subscales, e.g. for bodily awareness, with subjects scoring their answer on a 5-point scale (ranging from never to always). Since the resting-state network has been associated with depressive symptoms we also applied the 20-item Beck Hopelessness Scale (BHS) [Beck et al., 1974].

2.3.4 fMRI data acquisition and analysis

Scans were performed on a 3-Tesla whole body MRI system (Siemens Trio, Erlangen, Germany) using an eight-channel head coil. Slices were acquired parallel to the AC-PC plane in an odd-even interleaved acquisition order. Thirty-two T_2^* -weighted echo planar images per volume with BOLD contrast were obtained (matrix: 64 x 64; FoV: 224 x 224 mm²; spatial resolution: 3.5 x 3.5 x 4 mm³; $T_E = 30$ ms; $T_R = 2000$ ms; flip angle = 80°). Functional data were recorded in four scanning sessions containing 290 volumes per session for each subject. The first five volumes were discarded due to saturation effects.

The fMRI data were pre-processed and statistically analyzed by the general linear model approach [Friston et al., 1995] using the SPM2 software package (Statistical Parametric Mapping, <http://www.fil.ion.ucl.ac.uk>) and MATLAB 6.5 (The Mathworks Inc., Natick, MA, USA). For a detailed description of the pre-processing see Wiebking et al. [Wiebking et al., 2010].

All three conditions (rest, intero-/ exteroception) were included in the SPM model as separate events without their response phases. Regionally specific condition effects were tested by employing linear contrasts for each subject and different conditions. The resulting contrast images were submitted to a second level random-effects analysis. Here, one-sample t-tests were used on images obtained for each subjects' volume set and different conditions. To control for the multiple testing problem we performed a familywise error rate correction [Bennett et al., 2009, Nichols and Hayasaka, 2003]. The anatomical localization of significant neural responses in our main contrast [Rest > Intero-/ Exteroception] ($P \leq 0.01$, FWE-corrected, $k \geq 10$) was assessed with reference to the standard stereotactic atlas by superimposition of the SPM maps on a standard brain template provided by SPM2.

In a second step, the BOLD signals were analyzed. Applying sphere-shaped regions of interest (ROI, radius 5 mm), we extracted fMRI signal timecourses from regions of the DMN, as identified using the contrast [Rest > Intero-/ Exteroception] (VMPFC: -2, 52, -4, DMPFC: -2, 52, 40, PCC: 6, -48, 24) using the MarsBaR toolbox (<http://www.sourceforge.net/projects/marsbar>). Using a custom PERL script, fMRI signals were corrected for baseline shifts (applying a linear baseline correction algorithm) as well as normalized (dividing each value through the average fMRI signal of the time from -6s to 30s). The normalized average fMRI signal of the time-points -2s and 0s was then subtracted from each single fMRI value. This procedure ensured that all timecourses start from 0% signal change at 0 s. For each subject, mean fMRI signal changes for each of the three conditions were calculated by averaging the normalized fMRI signal values from 4s to 10s. For inter-subject statistical analysis, these values were Pearson-correlated with subjects' behavioural scores using SPSS (Statistical Package for the Social Sciences, Version 17.0).

Following the recommendations of Kriegeskorte et al. [[Kriegeskorte et al., 2009](#)], we also used independent coordinates (midline rather than right or left as criterion; except the DMPFC, see Table 1a). As described above, we calculated percent signal changes in similar regions found to be involved in mind-wandering and Pearson-correlated them with the behavioural test results. Independent coordinates were taken from Christoff et al. [[Christoff et al., 2009](#)] and transferred from Talairach in MNI coordinates using the WFU-pickatlas [[Maldjian et al., 2003](#), [Tzourio-Mazoyer et al., 2002](#)].

2.4 Results

2.4.1 Behavioural data

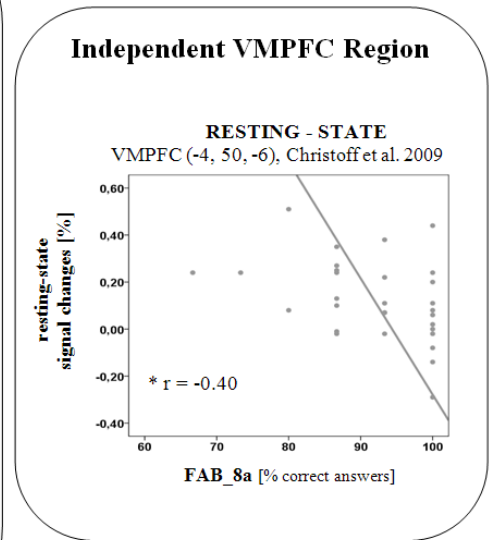
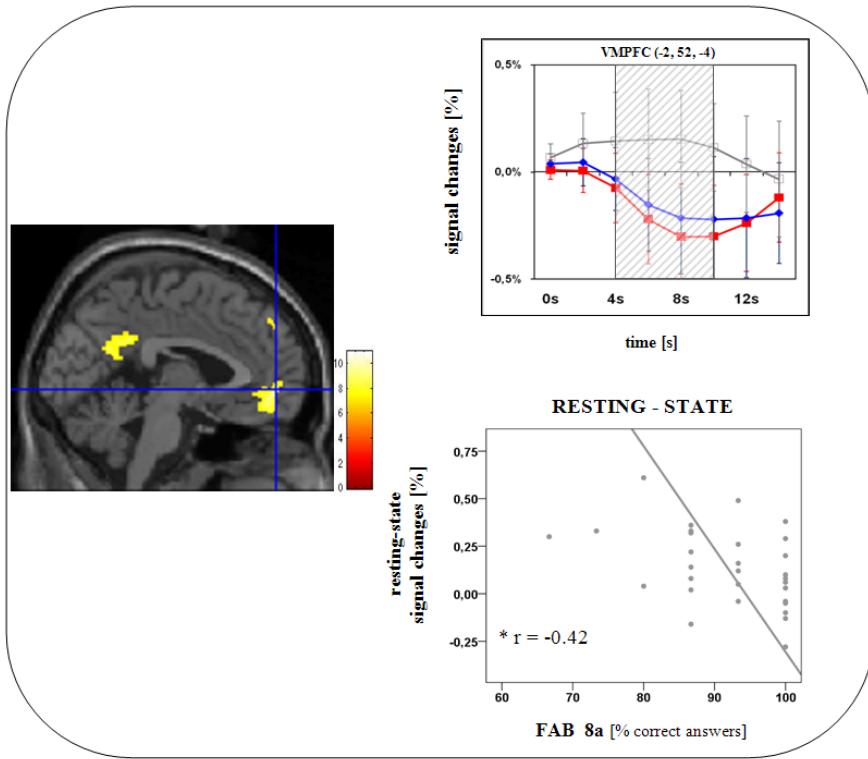
The group of 30 subjects had a mean age of 33.73 years (± 11.62 SD) and a mean time in education of 16.05 years (± 2.42 SD), with no sex differences. Their mean score for verbal intelligence was 114.23 (± 13.56 SD) and for nonverbal intelligence 118.40 (± 14.53 SD). Emotional tests included the BHS and the FAB_8a, with mean scores of 4.6 (± 3.9 SD) and 91.78 (percent correct answers ± 8.87 SD), respectively. The BPQ showed a total score of 199.03 (± 50.24) and for the subscale of bodily awareness a score of 107.80 (± 38.78).

2.4.2 Signal changes during rest

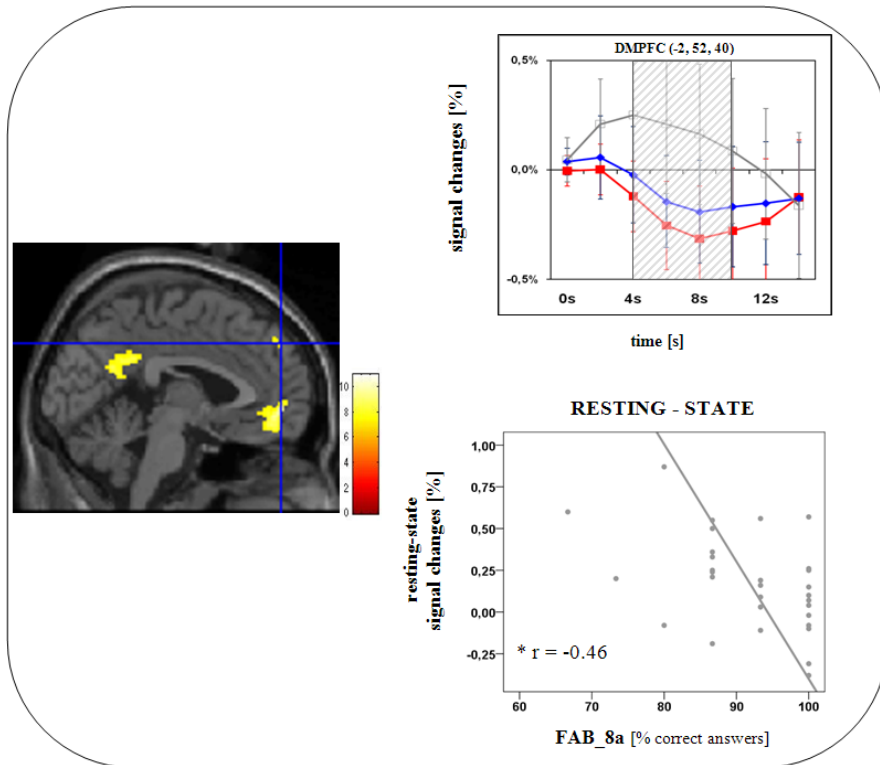
We firstly tested for the validity of our paradigm by analysing the contrast [Interoception > Exteroception] ($P \leq 0.05$, FWE corrected, $k \geq 10$), comparing relevant regions with those obtained from the same contrast by Critchley et al. [Critchley et al., 2004]. As detailed in Supplementary table A.1, this yielded almost identical regions, demonstrating that our modified paradigm can be considered to be valid.

Since we included the rest condition as a separate condition, we were able to calculate in a second step the main contrast [Rest > Intero-/ Exteroception] ($P \leq 0.01$, FWE corrected, $k \geq 10$), which showed significant signal changes in the VMPFC, DMPFC, and PCC (see Figure 2.1 and Table 2.1) mirroring regions implicated in the DMN (Table 2.2 A).

A



B



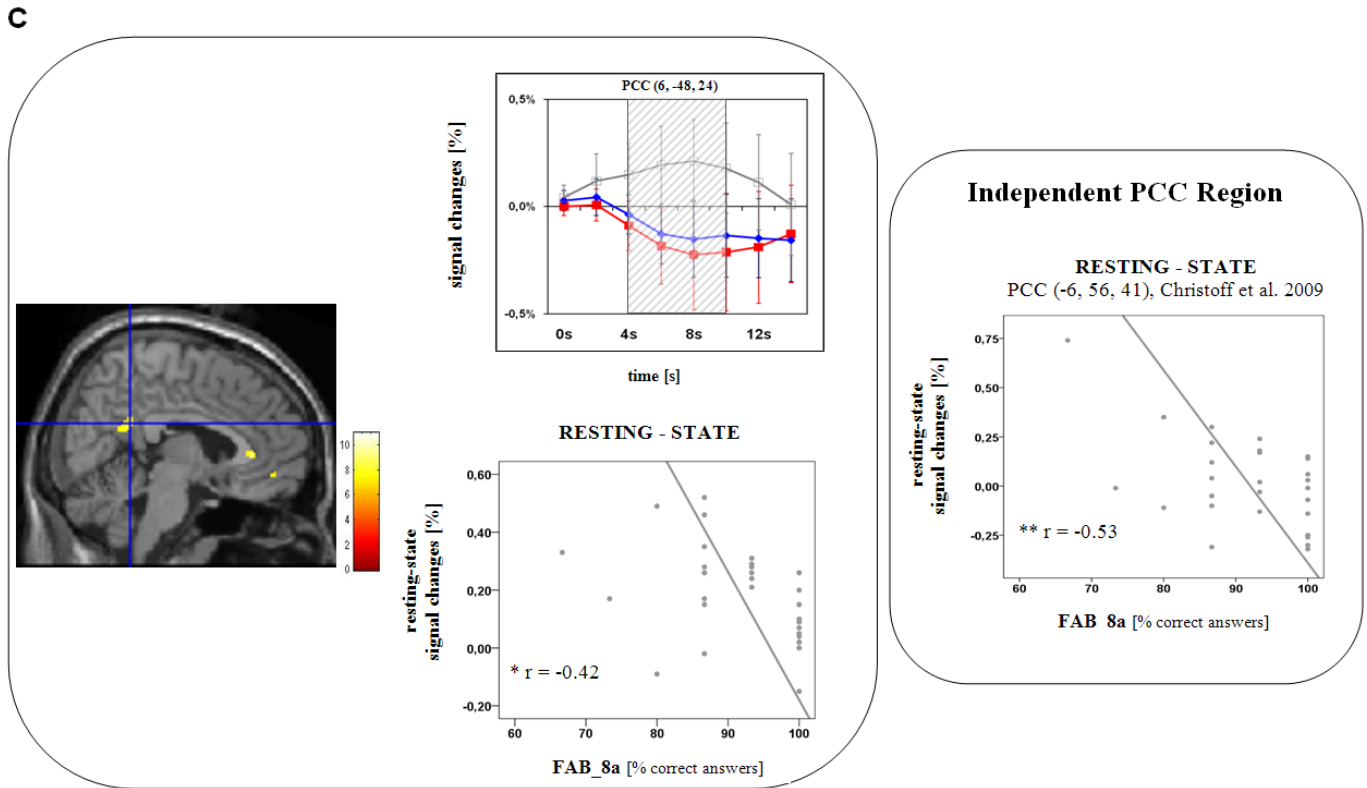


Figure 2.1: SPM images show activity changes for the contrast [Rest > Intero-/ Exteroception] ($P \leq 0.01$, FWE corrected, $k \geq 10$) in (A) the ventromedial prefrontal cortex (VMPFC) (x,y,z: -2, 52, -4), (B) the dorsomedial prefrontal cortex (DMPFC) (x,y,z: -2, 52, 40), and (C) the posterior cingulate cortex (PCC) (x,y,z: 6, -48, 24). Timecourse images show the mean percent signal changes (\pm SD) in these same regions during rest (grey line), interoceptive (red line) and exteroceptive (blue line) conditions. Correlation graphs for each region show the intraregional relationship between percent signal changes during rest conditions and FAB_8a scores. The separate boxes in figure A and C show the same correlation using signal changes from an independent region (see Methods 2.3.4), obtained in a similar imaging study (* $P \leq 0.05$). No independent region was available for the DMPFC (B).

With the rest periods used here being rather short in comparison to the periods used in the majority of resting-state studies, we compared the regions identified by the main contrast with those obtained in a study by Fox et al. [Fox et al., 2005], which measured activity during rest over a time interval of 5 min. In addition, we compared our regions with the ones obtained in a comparable study by Christoff et al. [Christoff et al., 2009]. Corresponding regions provide evidence that our rest periods show an acceptable representation of the resting-state (Table 2.2 A). Calculating percent signal changes in regions of the DMN obtained by the main contrast revealed task-induced deactivations (TID) during both intero- and exteroceptive processing (Table 2.1). Small positive BOLD responses (PBR) were observed in these regions during the rest condition (see also BOLD curves in Figure 2.1).

Region (x, y, z)	Signal Changes Resting-State mean \pm SD	Signal Changes Interoception mean \pm SD	Signal Changes Exteroception mean \pm SD
VMPFC (-2, 52, -4)	0.1390 \pm 0.20213	-0.2247 \pm 0.20382	-0.1560 \pm 0.21175
VMPFC (-4, 50, -6) Christoff et al. 2009	0.1277 \pm 0.17370	-0.1940 \pm 0.16592	-0.1097 \pm 0.18178
DMPFC (-2, 52, 40)	0.1770 \pm 0.28542	-0.2420 \pm 0.19459	-0.1313 \pm 0.21252
PCC (6, -48, 24)	0.1837 \pm 0.16449	-0.1777 \pm 0.18805	-0.1130 \pm 0.13598
PCC (-6, -56, 42) Christoff et al. 2009	0.0123 \pm 0.23018	-0.0963 \pm 0.13890	-0.0663 \pm 0.11716

Table 2.1: Signal changes (mean \pm SD) of the experimental conditions (rest, intero-/exteroception) in regions of interest in the VMPFC, DMPFC and PCC, which were defined by the main contrast [Rest > Intero-/ Exteroception] ($P \leq 0.01$, FWE corrected, $k \geq 10$). Additionally, values for independent regions of the VMPFC and PCC are shown.

2.4.3 Relationship between signal changes during rest and emotions

The observed signal changes in the regions identified in the main contrast were then correlated with the results of the emotion-related psychological tests. This revealed negative correlations between signal changes during rest (i.e., PBR) with scores of the FAB_8a (Figure 2.1, Suppl. figure A.1) and positive correlations with BHS scores (Table 2.2). A high FAB score indicates that the subject's ability to identify emotions correctly is good, while high scores in the BHS indicate depressive symptoms concerning emotional expectation and the future.

To look closer at the specificity of the association between emotions and induced activity during rest in regions of the DMN, we distinguished between stimulus, regional and psychological specificity. To test for the latter association, we correlated these signal changes with results of the BPQ, which tests for awareness of bodily changes. No significant correlation was observed (Table 2.2 B). In a further step we conducted a partial correlation using the individual's BHS scores as co-variables. No change in the correlation between activity during rest and FAB_8a was observed. To test for stimulus specificity, we correlated all three measures (FAB_8a, BHS and BPQ) with TID in regions of the DMN. There were two negative correlations between exteroceptive signal changes in the VMPFC and BHS, whereas no significant relationships concerning interoceptive signal changes could be observed (Table 2.2).

A)		Rest > Intero-/exteroception (x, y, z)	Default mode network (Fox et al. 2005) (x, y, z)	Mind wandering (Christoff et al. 2009) (x, y, z)	
VMPFC		-2, 52, -4	-3, 40, 0	-4, 50, -6	
DMPFC		-2, 52, 40	-	-	
PCC		6, -48, 24	-2, -39, 38	-6, -56, 42	
B)	Region	Test	Signal Changes Resting-State	Signal Changes Interoception	Signal Changes Exteroception
VMPFC (-2, 52, -4)	FAB 8a	r	-0.42 ¹ *	-0.27	0.03
		P	0.02	0.15	0.86
	BHS	r	0.32 (*)	-0.25	-0.39 *
	P	0.09	0.18	0.03	
BPQ_body	r	0.02	0.16	-0.04	
	P	0.92	0.40	0.83	
BPQ_total	r	-0.03	0.13	0.01	
	P	0.86	0.48	0.96	
VMPFC (-4, 50, -6) Christoff et al. 2009	FAB 8a	r	-0.4 *	-0.25	0.05
		P	0.03	0.19	0.78
	BHS	r	0.24	-0.27	-0.43 *
	P	0.203	0.14	0.02	
BPQ_body	r	0.003	0.19	-0.07	
	P	0.99	0.31	0.73	
BPQ_total	r	-0.02	0.19	-0.04	
	P	0.93	0.32	0.83	
DMPFC (-2, 52, 40)	FAB 8a	r	-0.46 *	.010	-.062
		P	0.01	0.96	0.75
	BHS	r	0.28	-0.28	-0.10
	P	0.14	0.13	0.59	
BPQ_body	r	-0.21	0.28	-0.16	
	P	0.26	0.28	0.40	
BPQ_total	r	-0.18	0.18	-0.04	
	P	0.35	0.33	0.82	
PCC (6, -48, 24)	FAB 8a	r	-0.42 ¹ *	-0.09	0.00
		P	0.02	0.65	1.00
	BHS	r	0.35 *	-0.31	-0.20
	P	0.05	0.10	0.29	
BPQ_body	r	-0.15	0.20	0.00	
	P	0.44	0.30	1.00	
BPQ_total	r	-0.15	0.15	-0.01	
	P	0.44	0.44	0.97	
PCC (-6, -56, 42) Christoff et al. 2009	FAB 8a	r	-0.53 **	-0.22	-0.18
		P	0.003	0.24	0.33
	BHS	r	0.22	-0.16	-0.28
	P	0.25	0.41	0.13	
BPQ_body	r	-0.19	0.03	0.01	
	P	0.31	0.86	0.10	
BPQ_total	r	-0.18	0.06	0.15	
	P	0.34	0.77	0.44	

Table 2.2: A) Cortical midline regions identified by the contrast [Rest > Intero-/ Exteroception] ($P \leq 0.01$, FWE corrected, $k \geq 10$) and comparison with regions of the DMN from two other studies [Christoff et al., 2009, Fox et al., 2005].

B) Neural responses (rest, intero-/ exteroception) in regions of the DMN (VMPFC, DMPFC, PCC) and their correlations with psychological measures of emotion (FAB: Florida Affect Battery, BHS: Beck Hopelessness Scale).

** $P \leq 0.01$, * $P \leq 0.05$, (*) $P \leq 0.1$

¹ A partial correlation between FAB_8a and signal changes in VMPFC and PCC remained significant when controlling for BHS. Significance level of $P \leq 0.05$ also remained on this level when excluding 2 subjects scoring < 75 % correct answers in the FAB_8a, except for the independent region of the PCC (changing to $P \leq 0.1$).

Finally, to test for regional specificity, we correlated measures for emotions with interoceptive signal changes in interoceptive regions, which did not yield significant results for the main interoceptive regions (just for somatomotor areas, see Suppl. table A.1). Since the extracted signal changes, which derived from regions of interest (ROI) found in the second level analysis, served for further correlations, the problem of a selection bias occurs and thus a potential increase of the non-independence error.

To test for statistical independence, in line with the recommendations made by Kriegeskorte et al. [Kriegeskorte et al., 2009], Poldrack et al. [Poldrack and Mumford, 2009] and Vul et al. [Vul et al., 2009], we used coordinates from a comparable study on mind-wandering by Christoff et al. [Christoff et al., 2009]. Application of these midline coordinates (except the DMPFC, which they did not obtain) yielded again a negative correlation with FAB_8a (correlation graphs on the bottom right in Figure 2.1 A and C), which provides an independent confirmation of the above described results.

2.5 Discussion

In an exploratory fMRI study with healthy subjects we demonstrate that measures of emotions correlate with induced activity during rest within regions of the DMN, including the VMPFC, DMPFC and PCC. In contrast, no relationship was seen between activity in these same regions during either intero- or exteroception (i.e., TID) and the measures of emotions.

These findings in healthy subjects may have future implications for subjects with mood disorders, like MDD or social phobia, who show both abnormal emotional functioning and abnormally high activity during rest in the same regions as those identified in this study [Grimm et al., 2009a, Gentili et al., 2009].

Our demonstration of a relationship between induced activity during rest within regions of the DMN and emotions, which was reduced here to identification of emotions, are in line with previous findings that show that emotions, as induced by the presentation of emotional stimuli, impact upon neural response changes in subsequent rest periods [Harrison et al., 2008, Pitroda et al., 2008]. While these prior studies indicated some indirect relationship between emotions and DMN regions, it remained unclear whether this effect was mediated by non-task-related rest activity itself or by interoceptive activity associated with emotions. By distinguishing induced activity during rest (PBR) in DMN regions from both intero- and exteroceptively-induced signal changes (TID) in the same regions, we were able to demonstrate psychological, regional, and stimulus specificity. Only emotional measures, and not bodily perception, were associated with PBR during rest indicating psychological specificity. Measures of emotions were only associated with activity during rest periods, but not with TID. This thus suggests a specificity of neural responses.

Finally, we observed an association of emotions only with signal changes in DMN regions, but not with those in intero- and exteroceptive regions, thus being indicative of regional specificity.

Our findings in emotions complement recent observations in healthy subjects that associated activity of the DMN with various internally-oriented functions like mind-wandering, episodic memory retrieval and self-relatedness [Mason et al., 2007, Buckner et al., 2008, Christoff et al., 2009]. This raises the question whether the observed relation between emotional functioning and induced activity during rest is mediated by psychological interaction with mind-wandering, episodic memory retrieval and self-relatedness rather than interoception. Such a psychological interaction between emotions and activity during rest remains to be directly demonstrated.

Moreover, the results of this exploratory study could serve for a better understanding of mood disorders. We could show that increases in rest activity in regions of the DMN are related to decreases in emotion perception (FAB_8a) and increases in hopelessness (BHS), although the latter point could not be replicated in independently selected regions. Since MDD patients are characterized by both deficits in emotional functioning as well as hopelessness, one could suggest a linkage between these deficits and their abnormally increased rest activity, as observed in various imaging studies [Fitzgerald et al., 2008, Grimm et al., 2009a, Mayberg, 2003]. One would consecutively expect that MDD subjects may be at the upper extreme end of a continuous relationship between DMN activity and emotion abilities, which remains to be tested in future studies.

Several limitations need to be mentioned. By using the FAB, we could test only for one part of the broad processes of emotional functioning. Other emotional functions, like emotion recognition, were not included. Analogously, emotion measures were controlled only by measures of body perception since one condition addressed interoception. In the future one might want to include more cognitive functions and cognitive-emotional regulation strategies to achieve further neuropsychological specification. Since recent research underlined the impact of depression as well as anxiety symptoms on interoceptive awareness [Paulus and Stein, 2010, Dunn et al., 2010a], future studies should also account for these interactive effects. Another major limitation is that correlations were not corrected for multiple comparisons.

Finally, the concept of resting-state needs to be discussed. We here defined resting-state in a purely operational sense, i.e., as the absence of an active task [see Shulman et al., 2009, for a similar definition], realized in our design by a fixation cross. One may however argue that even viewing a cross may induce some activity, thus precluding a 'pure' resting-state. Another issue is the timing of rest periods. Investigations target-

ing functional connectivity in rest conditions use time intervals of 5min in their designs [Damoiseaux et al., 2006, Fox et al., 2005]. In contrast, we were not interested in functional connectivity but rather in the induction of positive and negative BOLD responses in regions of the DMN during the three conditions of interest. This made it necessary to shorten the time interval and use 9-13 second periods of fixation cross as the rest condition. We are however aware that our results must be replicated for longer rest periods in order to be sure that they are not due to overlapping BOLD responses from preceding activation periods.

In conclusion, we demonstrate a relation between induced activity during rest in regions of the DMN and emotions, as distinguished from neural responses and psychological function associated with interoception. Demonstrating some degree of psychological, stimulus and regional specificity, our findings can serve for a better understanding of rest activity in both healthy and depressed subjects.

2.6 Acknowledgements

We thank the staff from the Department of Neurology (University of Magdeburg, Germany) and B. Enzi for their helpful comments on the manuscript. Financial contributions are acknowledged from the Hope of Depression Research Foundation, the EJLB-Michael Smith Foundation, the CRC, and the German Research Foundation (DFG-SFB 779 A6) to GN.

Chapter 3

Abnormal body perception and neural activity in the insula in depression – An fMRI study of the depressed “material me”

World Journal of Biological Psychiatry 2010 Apr, 11(3):538-49

<http://dx.doi.org/10.3109/15622970903563794>

3.1 Abstract

In addition to affective-cognitive symptoms, patients with major depressive disorder (MDD) suffer from somato-vegetative symptoms, suggesting abnormal interoceptive awareness of their “material me”. While recent imaging studies have extensively investigated affective-cognitive symptoms in MDD, the neural correlates of somato-vegetative symptoms and abnormal interoception remain unclear. Since the “material me” has been especially associated with the anterior insula in healthy subjects, we hypothesized abnormalities in this region during interoceptive awareness in MDD. We therefore investigated behavioural and neural correlates of interoception in healthy and depressed subjects using the Body Perception Questionnaire (BPQ) and a well established heart-beat perception task in fMRI. MDD patients showed significantly higher scores in the

BPQ and significantly reduced neural activity during rest periods, particularly in the bilateral anterior (and middle) insula. In contrast to healthy subjects, BPQ scores no longer correlated with activity during rest periods in the right (and left) anterior insula. Both BPQ scores and left anterior insula signal changes correlated with depression severity. Taken together, we here demonstrate for the first time abnormal body perception and altered activity in the insula during rest periods in MDD. Our results suggest that these behavioural and neural abnormalities are closely related to these patients' somato-vegetative abnormalities and their abnormal "material me".

3.2 Introduction

Patients with major depressive disorder (MDD) can be characterized by abnormalities in both mental and physical aspects of their self [Northoff, 2007]. Abnormalities in the mental self include abnormal emotions and cognition like ruminations, self-blame, and increased association of their self with negative emotions [Ingram, 1990, Treynor et al., 2003, Rimes and Watkins, 2005, Frodl et al., 2007, Northoff, 2007]; whilst alterations in the physical self are reflected in various persisting somato-vegetative symptoms, along with an apparent hyperawareness of bodily changes [Beck et al., 1961, Garcia-Cebrian et al., 2006, Nyboe Jacobsen et al., 2006]. Patients with MDD can thus be described as suffering from major abnormalities in their "material me".

Recent imaging studies of MDD have indicated an association of the mental aspects of the self - i.e., its emotional and cognitive abnormalities - with altered neural activity in the medial cortical regions, particularly the dorsomedial prefrontal cortex [Northoff, 2007, Grimm et al., 2009a]. In contrast, the neural correlates of the abnormal physical aspects of the self in MDD remain to be explored.

The physical aspect of our self [Panksepp, 1998, Damasio, 1999a, Gillihan and Farah, 2005, Northoff et al., 2006] has been conceptualized as our "bodily or proto-self" [Panksepp,

1998, Craig, 2002, 2003, 2004]. Craig [Craig, 2002, 2003, 2004] characterizes the “bodily or proto-self” as perception and awareness of one’s body, with him describing this interoceptive awareness as the “material me”. Consistent with the basics of the James-Lange theory of emotion and Damasio’s somatic marker hypothesis, he describes the representation of the interoceptive body in the anterior insula as essential for subjective feelings from the body and for emotional awareness. This “material me” is thought to be predominantly mediated by neural activity in the right anterior insula [Craig, 2002, 2003, 2004, 2009]. This has recently been further supported by imaging studies that have identified the anterior insula as a key region in interoceptive awareness [Critchley et al., 2004, 2005, Pollatos et al., 2007c].

The neural correlates of abnormal somato-vegetative symptoms and interoceptive awareness in MDD remain unclear however. Early PET, and more recent MRI studies, do show alterations to the insula in MDD, but these studies have been concerned only with the resting state or exteroceptive perception [Mayberg, 2002, 2003, Fitzgerald et al., 2008]. Emotional-cognitive stimulation has also been seen to induce abnormal neural activity in the insula in MDD [Mayberg, 2002, 2003, Philips et al., 2003, Keedwell et al., 2005, Paulus and Stein, 2006, Fitzgerald et al., 2008]. In contrast, studies targeting the insula specifically during interoceptive awareness, as distinguished from resting periods, exteroceptive awareness and affective components (as they are present in, for instance, pain perception; [Bär et al., 2007, Strigo et al., 2008a,b]) remain to be reported.

The aim of our study was to investigate the changes in neural activity in the insula during interoceptive awareness and their relation to abnormal body perception in MDD. Since previous findings demonstrated neural abnormalities in the insula during resting periods and exteroceptive, i.e., emotional-cognitive, stimulation (see above), we also investigated signal changes in the insula during both rest periods and exteroceptive stimulation. Our main focus was thus not on the activity of the rest period itself, but

on the modulation of interoception and exteroception by the rest period. Based on the above mentioned findings, we hypothesized abnormal neural activity in specifically the anterior insula in MDD, as well as abnormal body perception, as measured by the Body Perception Questionnaire [Porges, 1993]. To induce neural processing of interoception, we applied a modified and well established heartbeat perception task and compared it with activity during rest and tone perception mirroring exteroception [Critchley et al., 2004, Pollatos et al., 2007c].

3.3 Materials and methods

3.3.1 Depressed participants and healthy controls

We studied 22 psychiatric in-patients suffering from major depressive disorder (MDD), diagnosed according to the DSM-IV (Diagnostic and Statistical Manual of Mental Disorders (4th edition); American Psychiatric Association, 1994), using functional magnetic resonance imaging (fMRI). Patients with MDD were recruited in an acute state from either the Department of Psychiatry at the University of Magdeburg or from the state hospital of Uchtspringe. Eligibility screening procedures included the 21-item Beck Depression Inventory (BDI) [Beck et al., 1961] and the 20-item Beck Hopelessness Scale (BHS) [Beck et al., 1974]. Diagnoses of depression were made by the participants' treating psychiatrists. Inclusion criteria were a score of at least 16 on the BDI, while exclusion criteria were major medical illnesses, histories of seizures, metallic implants, a history of substance dependence, head trauma with loss of consciousness, pregnancy and criteria for any psychiatric disorder other than MDD.

The data for one depressed subject was excluded from the analysis due to structural abnormalities identified in their anatomical scan. A further four depressed subjects were excluded due to motion artefacts. Usable fMRI data was thus available for a total

of 17 depressed subjects. Behavioural test results were not available for two depressed subjects.

The group of depressed subjects (11 female and 6 male subjects, all right-handed) revealed a mean age of 41.88 (\pm 12.1 SD) and mean educational years of 15.44 (\pm 2.84 SD). Mean scores for verbal intelligence (MWT-B) [Lehrl, 1995] were 111.35 (\pm 9.86 SD) and for nonverbal intelligence (LPS-3) [Horn, 1983] 108.77 (\pm 13.56 SD). The mean BHS score was 32.13 (\pm 4.45 SD), the mean BDI score 29.93 (\pm 8.56 SD), and the mean score for the clinician rated Montgomery-Åsberg Depression Rating Scale (MADRS) [Montgomery and Asberg, 1979] was 26.07 (\pm 8.48 SD), indicating that patients were moderately depressed. Seventeen depressed subjects were taking one or more antidepressants from the following pharmacological classes: 6 subjects SSRIs, 5 subjects NaSSAs, 10 subjects NARIs/ MAOI/ others. None of the control subjects were taking any psychotropic medications at the time of the investigation.

Our healthy control group consisted of 17 subjects (11 female and 6 male subjects, all right-handed) with no psychiatric, neurologic, or medical illness. They had a mean age of 37.59 (\pm 12.84 SD) and mean educational years of 15.44 (\pm 2.71 SD). Their mean score for verbal intelligence was 117.47 (\pm 14.28 SD) and for nonverbal intelligence 117.56 (\pm 16.93 SD). The healthy group was thus well matched to the patient group for group size, sex, age, years of education, and verbal and general intelligence. Groups did not differ significantly in gender distribution, age, verbal/ nonverbal intelligence or years of education.

The study was approved by the local ethics committee and all participants gave written informed consent before participating in this study.

3.3.2 Paradigm

The paradigm was based on a design, which was introduced by Pollatos and Critchley [Pollatos et al., 2007b, Critchley et al., 2004]. Since the paradigm was applied to depressed patients, it was altered in order to make it more suitable for the use with a depressed population, i.e. the paradigm was made less complicated and the time that patients spent in the scanner was reduced. In this paradigm, subjects were presented with three separate conditions: an intero- and an exteroceptive task, as well as rest periods – in a pseudo-randomised order.

The task-type indicator for the interoceptive condition was a dark coloured heart on a light background. As long as it was displayed on the screen (9–13 s), subjects were asked to silently count their own heartbeat. Afterwards, subjects had to report the number of heartbeats counted via a simple visual analogue scale (4 s). The indicator on the scale was moved by the subject to the labelled position representing the number of beats that they counted. Similarly, exteroceptive conditions were indicated by a dark coloured musical note symbol on a light background (9–13 s). During these conditions, as long as the task-type indicator was visible, subjects had to count silently the number of tones heard during this period. Afterwards, subjects were asked to report the number of counted tones, again via a visual analogue scale (4 s). Two different tones with a duration of 200 ms were presented. They were alternating with each of the four scanning runs.

In order to make the difficulty of both tasks closely comparable, tones were presented at an individually determined volume (i.e. just audible, like the heartbeat). The general presentation frequency of the tones was adapted to correspond to each subject's pulse-rate. In order to control for habituation effects, the onset time of the tones was jittered by 200 ms from this general frequency. Resting state conditions were indicated by a dark fixation cross on light background (9–13 s). Subjects were instructed to relax and re-

duce any cognitive work during these periods. The total experiment consisted of 4 runs of 9.6 min (290 volumes), with each condition being presented 48 times in total. The paradigm was executed on a computer running the software package “Presentation” (Neurobehavioral Systems, <http://www.neurobs.com>). Visual stimuli were projected via an LCD projector onto a screen visible through a mirror mounted on the headcoil. Auditory stimuli were presented via the scanner loudspeaker.

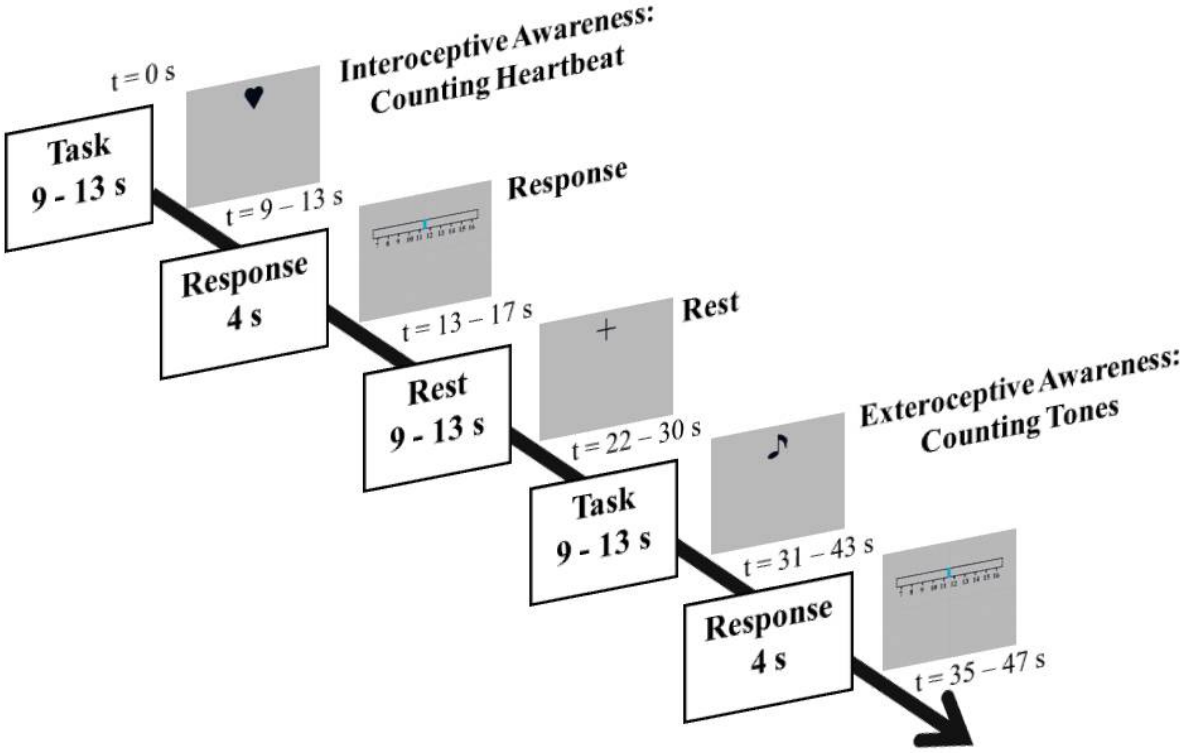


Figure 3.1: FMRI paradigm to study internal awareness, external awareness, and fixation periods.

3.3.3 Behavioural tests

To assess body perception, we applied after fMRI measurement the Body Perception Questionnaire (BPQ) [Porges, 1993], which includes several factors: The awareness subscale (A) of the BPQ includes 45 items. Subjects should imagine how aware they are of their body processes and rate their awareness. In the second subscale (S: stress response, 10 items), subjects are asked to imagine being in a very stressful situation and rate their awareness of perceived changes due to stress. The third subscale, autonomic nervous system reactivity (ANSR), requires that subjects answer 27 items about their own autonomous nervous system reactions. Finally, the stress style (SS) subscale contains 12 items and evaluates the manner in which the subject responds to stress. All ratings are made on a five-point Likert scale.

3.3.4 fMRI data acquisition and analysis

Functional measurements were performed on a 3-Tesla whole body MRI system (Siemens Trio, Erlangen, Germany) with echo planar imaging (EPI) using an eight channel head coil. The slices were acquired parallel to AC-PC plane in an odd-even interleaved acquisition order. Thirty-two T_2^* -weighted echo planar images per volume with blood oxygenation level-dependent (BOLD) contrast were obtained (matrix: 64 x 64; 32 slices per volume; FoV: 224 x 224 mm²; spatial resolution: 3.5 x 3.5 x 4 mm³; $T_E = 30$ ms; $T_R = 2000$ ms; flip angle = 80°). Functional data were recorded in four scanning runs, each containing 290 volumes. The first five volumes were discarded due to saturation effects.

The fMRI data were preprocessed and statistically analyzed according to the general linear model approach [Friston et al., 1995] using the SPM2 software package (SPM2, <http://www.fil.ion.ucl.ac.uk>) running on MATLAB 6.5 (The Mathworks Inc., Natick, MA, USA). All functional images were slice time corrected with reference to the first slice

acquired, corrected for motion artefacts by realignment to the volume taken nearest to the anatomical images, and spatially normalized to a standard T₁-weighted SPM template [Ashburner and Friston, 1999]. Four MDD patients were excluded due to head-movements of more than 2 mm. The normalization was generated by warping the subject's T₁-structural image to the T₁-template provided by the MNI (Montreal Neurological Institute) and applying these parameters to all functional images. The images were resampled to 2 x 2 x 2 mm³ and smoothed with an isotropic 6 mm full-width half-maximum Gaussian kernel. The time-series fMRI data were filtered using a high pass filter and cut-off of 128 s. A statistical model for each subject was computed by applying a canonical response function [Friston et al., 1998].

All 3 conditions (interoception, exteroception, and rest) were included in the SPM model as separate events. Regionally specific condition effects were tested by employing linear contrasts for each subject and each condition. The resulting contrast images were submitted to a second-level random-effects analysis by applying a one-sample t-test to the images created for all subjects in each condition. To control for the multiple testing problem we performed a false discovery rate correction [Nichols and Hayasaka, 2003]. The anatomical localization of significant activations was assessed with reference to the standard stereotactic atlas by superimposition of the SPM maps on the standard MNI brain template provided by SPM2.

Following the functional localizer approach [Saxe et al., 2006, Lamm and Decety, 2008, Vul et al., 2009], we next determined the regions involved in interoception through the comparison between interoceptive and exteroceptive awareness (count heartbeat > count tones). In accordance with Goldstein and colleagues [Goldstein et al., 2007] we calculated this contrast for a combined group of healthy and depressed subjects (n = 34). This was done to ensure that neither the group of healthy subjects nor the group

of depressive subjects should be favoured and therefore have a dominant influence on the determination of the regions of interest (ROI). This contrast yielded significant signal changes in the bilateral anterior and middle insula. Spherical ROIs (radius 5 mm) were then located at the peak voxel within the left (x,y,z: -32, 14, 6) and right (x,y,z: 36, 16, 6) anterior insula, and left (x,y,z: -42, 12, -2) and right (x,y,z: 43, 8, 0) middle insula. Signal changes in these ROIs during interoception, exteroception and rest were then extracted using the Marseille Region of Interest Toolbox software package (MarsBaR 1.86, <http://www.sourceforge.net/projects/marsbar>) [Brett et al., 2002].

Mean normalized fMRI signal values from 4-10 s of the BOLD response for each condition were first compared between healthy and depressed subjects (two-sample t-test, two tailed) using SPSS 16.0 (SPSS inc., Chicago). In a second analysis, intero- and exteroceptive trials that followed a rest period were identified. The signal changes during these trials were thus assumed to represent the change from the baseline state; as opposed to those events which followed another trial type, which would represent a change from a stimulus-induced state. This allowed the effect of differences in resting-state activity on subsequent stimulus-induced signal changes to be characterised. These so-called baseline corrected signal changes were then compared between healthy and depressed subjects (two-sample t-test, two tailed). Finally, the signal changes during the rest condition were correlated with the subscales of the Body Perception Questionnaire (Pearson's, two-tailed).

3.4 Results

3.4.1 Behavioural data

MDD patients showed significantly higher scores in the Body Perception Questionnaire (BPQ) when compared to healthy subjects (see Figure 3.2 and Figure 3.3).

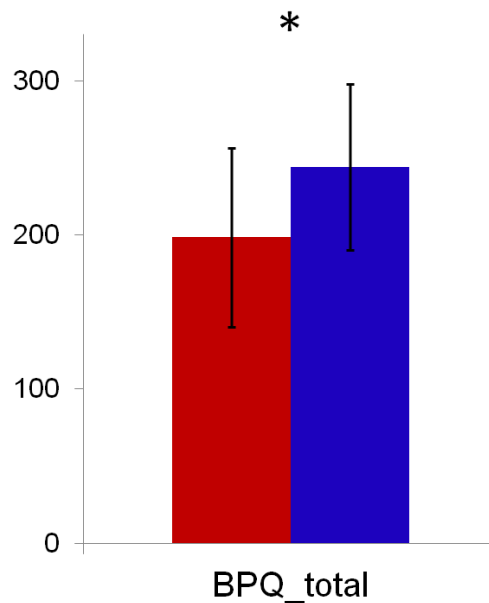


Figure 3.2: Group comparison (mean \pm SD) of the total score of the Body Perception Questionnaire (BPQ_total). Healthy (red bar) and depressed participants (blue bar) differ significantly. * $P \leq 0.05$

This is true for the total score (t-test $P = 0.03$, Figure 3.2), as well as the subscores for stress response (S) (t-test $P = 0.001$), autonomic nervous system reactivity (ANSR) (t-test $P = 0.0001$) and stress style (SS) (t-test $P = 0.0001$) (see Figure 3.3). MDD patients did not differ significantly from healthy subjects in the BPQ subscore for awareness (A). The BPQ stress style subscale scores correlated positively with total BDI scores ($r = 0.61$, $P \leq 0.05$). The higher the BPQ for stress style is, the higher the BDI scores and hence depression severity.

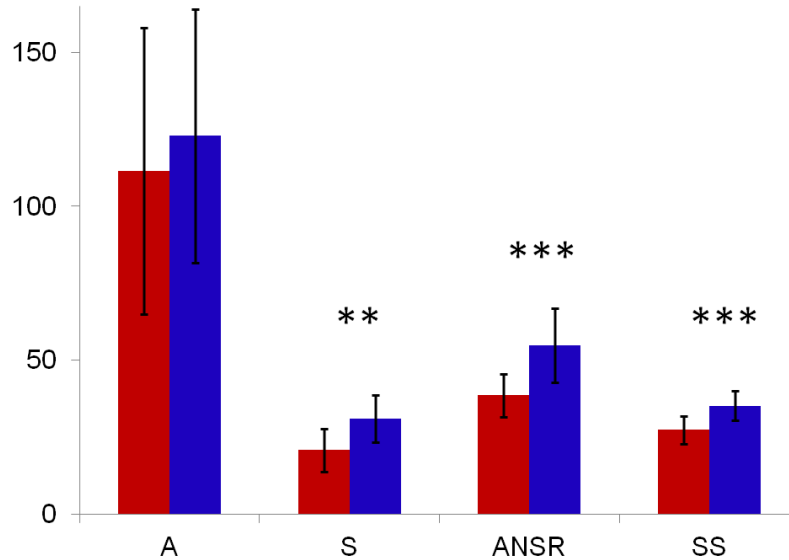


Figure 3.3: Comparison of the four subscores of the Body Perception Questionnaire. A = Awareness; S = Stress Response; ANSR = Autonomic Nervous System Reactivity; SS = Stress Style (1+2); total = total score.

3.4.2 Signal changes during intero- and exteroceptive processing and rest in the insula

In a first step, we identified the bilateral anterior and middle insula as being involved in interoception by investigating signal changes from the comparison between intero- and exteroceptive awareness in the contrast (count heartbeat > count tones) in all subjects, healthy and depressed ($n = 34$), as described in the methods part above. This is in accordance with the regions obtained from the same contrast by Critchley [Critchley et al., 2004], suggesting that our modified paradigm can be considered to be valid. Using the bilateral anterior and middle insula as functional localisers, we determined signal changes in these regions during intero- and exteroceptive awareness and rest (fixation cross), and compared them between the two groups. Signal changes during interoceptive processing, e.g., the heartbeat perception task, did not differ significantly between groups in the two relevant parts of the insula (Figures 3.4, 3.5, and 3.6). This was independent of whether interoceptively-associated signal changes were analyzed in relation to the preceding rest period or not (Table 3.1).

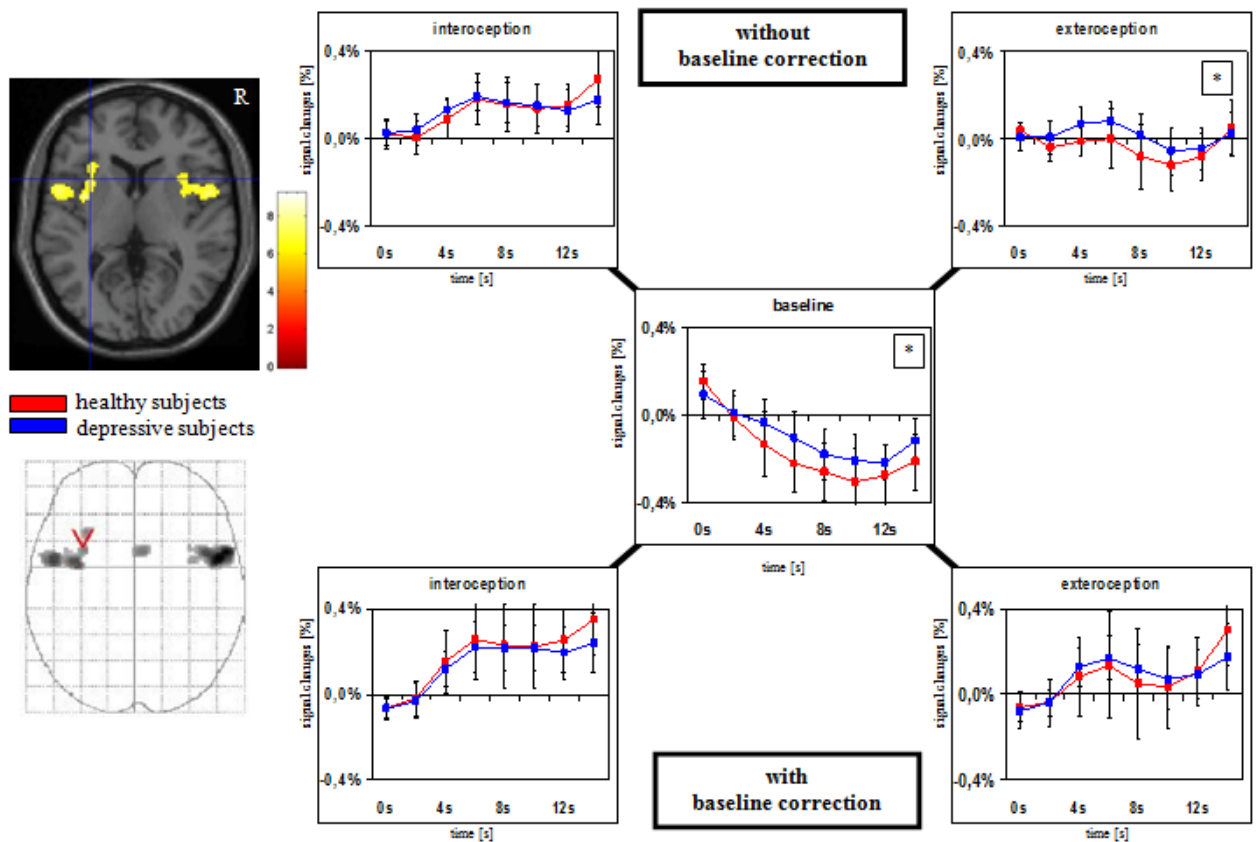


Figure 3.4: **Comparison of interoceptive insular activity (SPM images) during intero- and exteroception (with and without baseline correction) and baseline between healthy (red lines) and depressed participants (blue lines).** SPM images show the comparison between interoceptive and exteroceptive awareness by the contrast (count heartbeat > count tones), $P \leq 0.01$, FWE corrected, $k \geq 10$, $n = 34$ subjects (17 healthy and 17 depressive subjects). BOLD curves (x axis: time in seconds, y axis: percent signal changes) are based upon regions of interest (ROIs) that are derived from this contrast. These are plotted separately for healthy (red lines) and depressive (blue lines) subjects and show baseline-corrected (i.e., signal intensities during interoception relative to the preceding baseline) and non-baseline-corrected (i.e., signal intensities during interoception independent of the preceding baseline) time courses for interoception and exteroception, as well as for rest periods. Figure 3.4 shows the results for the left anterior insula, Figure 3.5 for the right anterior insula, Figure 3.6 for the left middle insula and Figure 3.7 for the right middle insula. Significant differences between both groups were obtained for exteroception without baseline-correction in the left and right anterior insula ($* P \leq 0.05$), while this difference was no longer seen when baseline-correction was done. Shown here: activation of **left anterior insula** (x, y, z: -32, 14, 6) in healthy and depressed participants ($n = 34$).

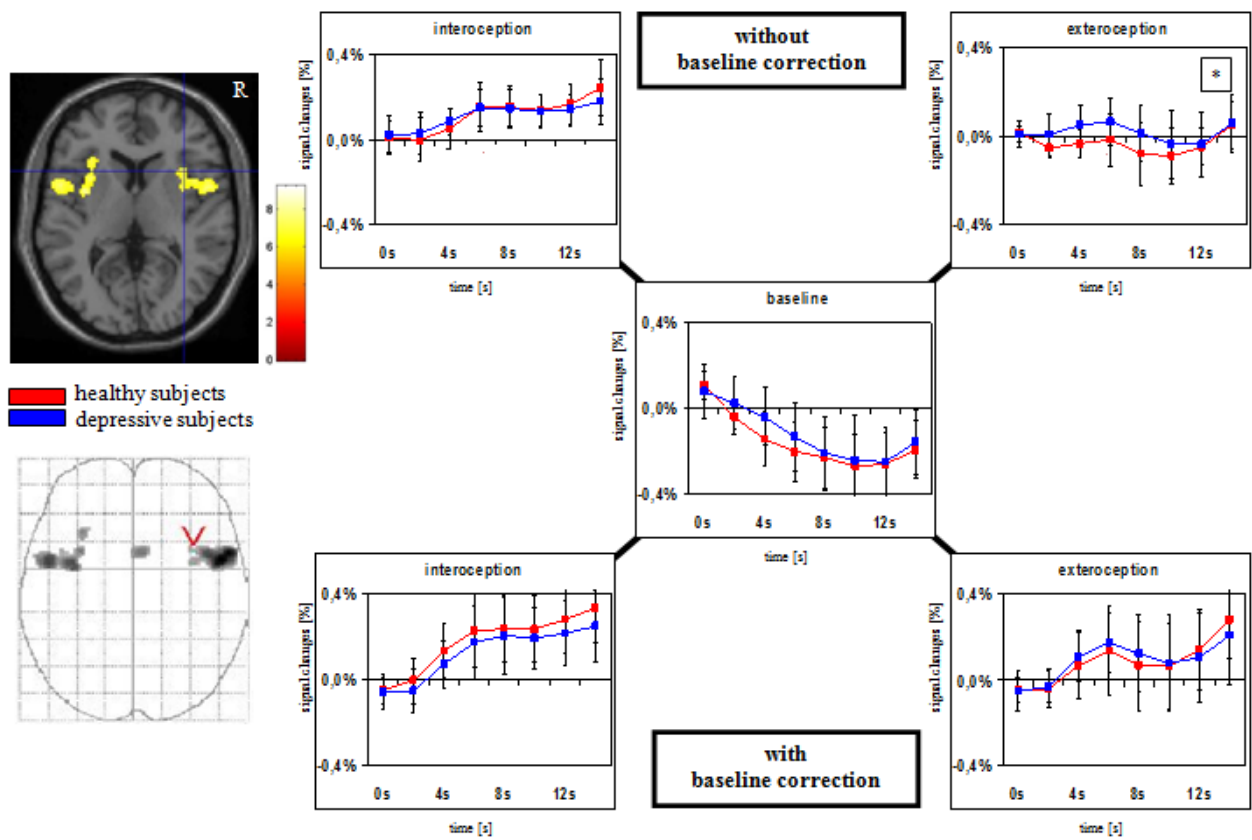


Figure 3.5: Activation of the **right anterior insula** (x, y, z: 36, 16, 6) in healthy and depressed participants (n = 34).

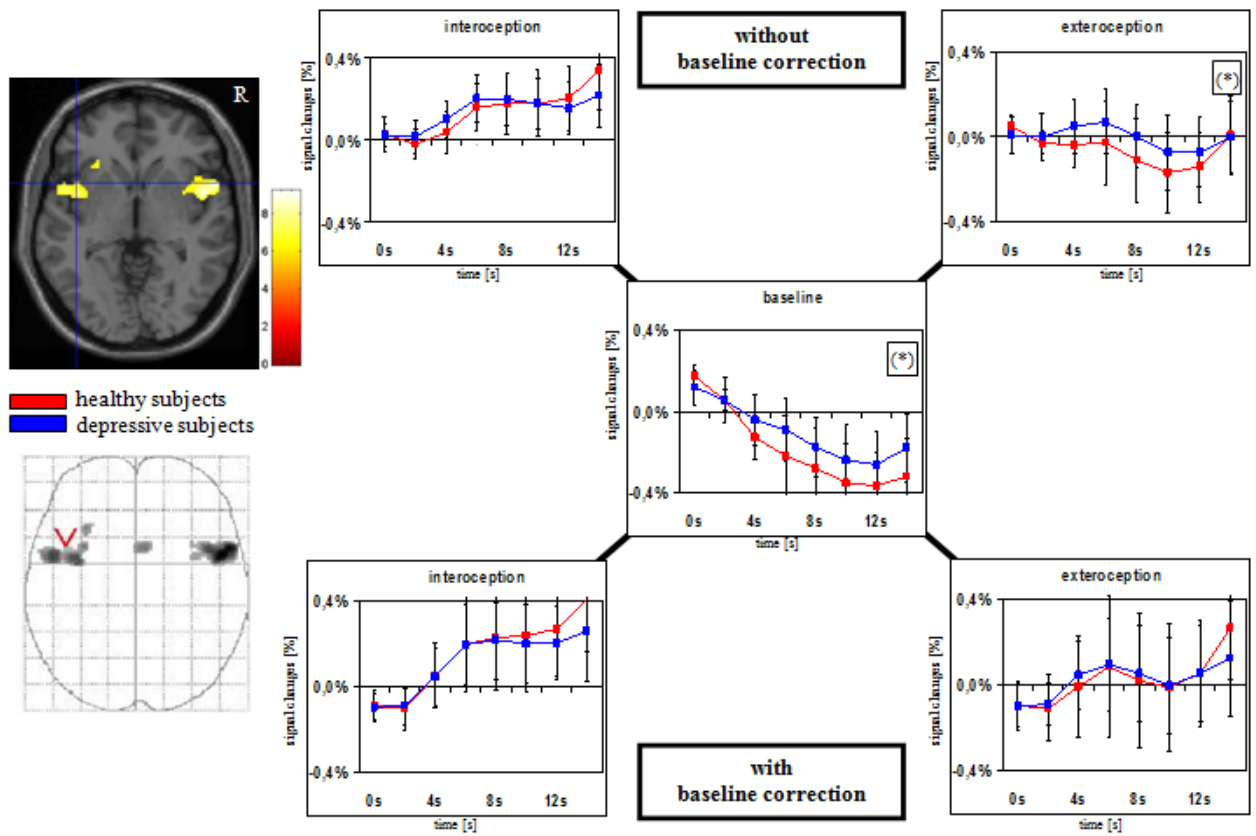


Figure 3.6: Activation of the **left middle insula** (x, y, z: -42, 12, -2) in healthy and depressed participants (n = 34).

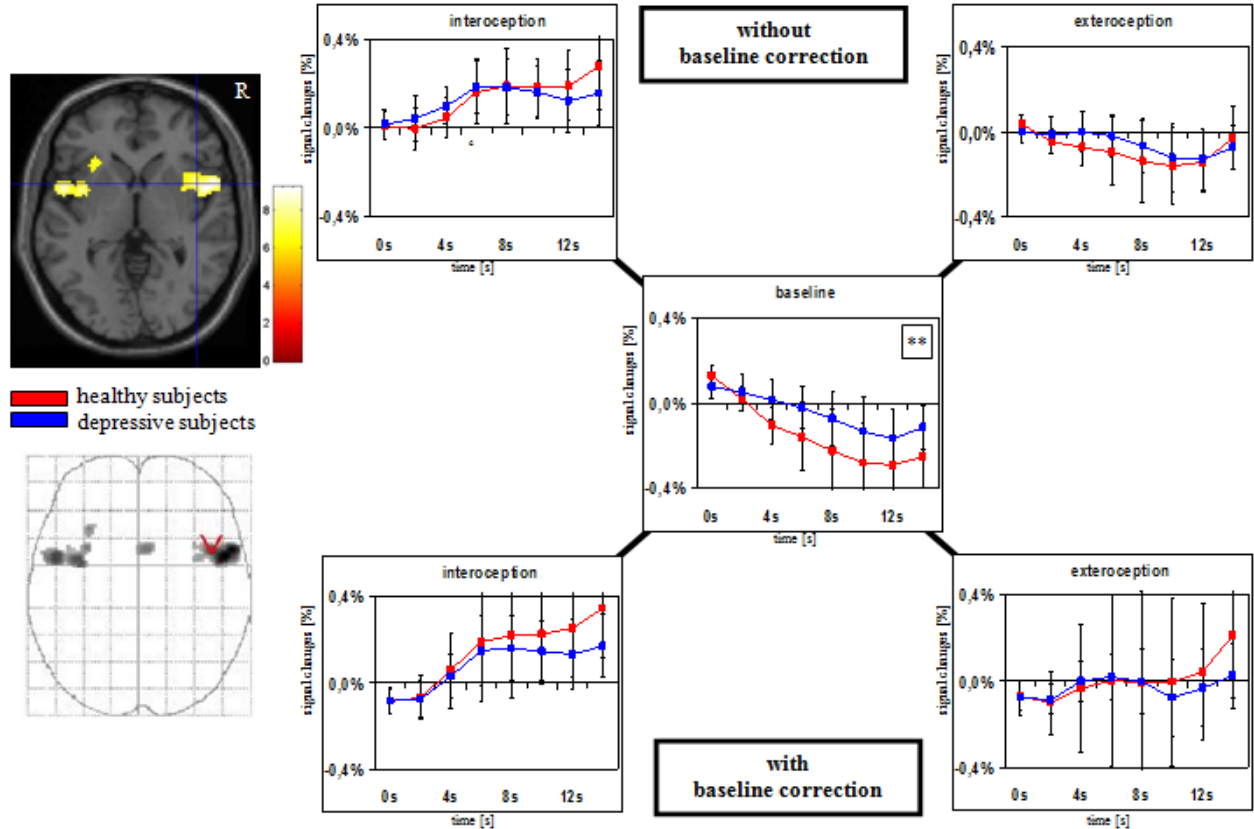


Figure 3.7: Activation of the **right middle insula** (x, y, z: 43, 8, 0) in healthy and depressed participants (n = 34).

In contrast to interoceptive signal changes, signal changes during exteroceptive processing, the tone perception task, did differ significantly between both groups. Depressed participants showed significantly reduced signal changes, with lower deactivation (i.e. smaller negative BOLD response), or even activation (i.e. switching to a positive BOLD response), in the left and right anterior insula when compared to healthy participants (see Table 3.1). However, it cannot be excluded that such altered signal changes during exteroceptive processing might also be due to higher signal changes during the preceding rest period, e.g., the fixation cross period, that was rather long in our case (see above in the methods). This in turn might enhance the signal changes

that are induced by subsequent exteroceptive stimulation. We therefore conducted a second analysis of the same data where we calculated exteroceptive signal changes as dependent on the level of signal change in the respectively preceding rest period (i.e. the fixation cross) for both healthy and depressed patients. When these signal changes were then compared, depressed participants no longer showed any significant difference from healthy participants in the anterior and middle insula during exteroceptive processing (see Table 3.1 and Figures 3.4, 3.5, 3.6). This suggests that the higher signal changes during exteroceptive processing yielded in the first analysis may be due to increased signal changes during rest periods. Since the preceding rest period was shown to most likely affect signal changes during exteroceptive processing, we compared these signal changes themselves between both groups in the two relevant insula regions. MDD patients showed significantly lower deactivation (i.e. a reduced negative BOLD response) in the left anterior and middle (only marginally significant) insula, as well as in the right middle insula (see Figures 3.4, 3.5, 3.6 and Table 3.1).

Taken together, our findings show abnormally reduced activity changes, i.e., a lower deactivation, during rest periods in the insula in MDD patients when compared to healthy participants. In contrast, depressed patients showed no abnormalities in intero- and exteroceptive processing in the insula independent from rest periods.

	healthy	MDD	P-value
Anterior Insula, L			
Int. without base corr.	-	-	-
Ext. without base corr.	-0.054 ± 0.11	0.028 ± 0.08	0.02*
Rest	-0.231 ± 0.12	-0.13 ± 0.1	0.013*
Int. with base corr.	-	-	-
Ext. with base corr.	-	-	-
Anterior Insula, R			
Int. without base corr.	-	-	-
Ext. without base corr.	-0.057 ± 0.11	0.024 ± 0.097	0.03*
Rest	-	-	-
Int. with base corr.	-	-	-
Ext. with base corr.	-	-	-
Middle Insula, L			
Int. without base corr.	-	-	-
Ext. without base corr.	-0.085 ± 0.158	0.011 ± 0.123	0.055(*)
Rest	-0.242 ± 0.164	-0.137 ± 0.171	0.076(*)
Int. with base corr.	-	-	-
Ext. with base corr.	-	-	-
Middle Insula, R			
Int. without base corr.	-	-	-
Ext. without base corr.	-	-	-
Rest	-0.192 ± 0.132	-0.053 ± 0.111	0.002**
Int. with base corr.	-	-	-
Ext. with base corr.	-	-	-

Table 3.1: Percent signal changes (mean ± SD) in the anterior and middle insula for healthy (n = 17) and depressed (n = 17) participants. Interoceptive (Int.) and exteroceptive (Ext.) processes were analyzed in relation to the preceding rest period (with base correction) or not (without base correction). ** $P \leq 0.005$; * $P \leq 0.05$; (*) $P \leq 0.1$; - $P > 0.1$

3.4.3 Relationship between signal changes in the insula and body perception

Utilising the same regions of the insula as described above, we correlated signal changes during rest and intero- and exteroceptive processing with the scores in the BPQ (Body Perception Questionnaire) in healthy and depressed participants.

Healthy participants showed significantly positive correlations of rest signal changes in the right anterior insula with the BPQ total, BPQ awareness and BPQ stress response scores (see Figure 3.8 and Table 3.2). The less deactivation during the rest periods in the right anterior insula, the higher the BPQ scores indicating abnormal body perception. This relationship was not obtained in MDD patients, where decreased deactivation in the insula was no longer related to body perception, i.e., BPQ scores (see Figure 3.8).

	A	S	ANSR	SS	Total
Anterior Insula, L					
Rest, Healthy	-	r=0.5	-	r=0.42	-
P-value	-	0.044*	-	0.097(*)	-
Rest, MDD	-	-	r=-0.51	-	-
P-value	-	-	0.054(*)	-	-
Anterior Insula, R					
Rest, healthy	r=0.53	r=0.54	-	-	r=0.56
P-value	0.028*	0.027*	-	-	0.019*
Rest, MDD	-	-	-	-	-
P-value	-	-	-	-	-
Middle Insula, L					
Rest, healthy	-	r=0.45	r=0.47	r=0.43	-
P-value	-	0.068(*)	0.057(*)	0.087(*)	-
Rest, MDD	-	-	-	-	-
P-value	-	-	-	-	-
Middle Insula, R					
Rest, healthy	-	-	-	-	-
P-value	-	-	-	-	-
Rest, MDD	-	-	-	-	-
P-value	-	-	-	-	-

Table 3.2: Results of correlational analysis between signal changes in rest periods in different insular regions and subscores of the Body Perception Questionnaire (BPQ). white: healthy subjects, grey: depressive subjects. * $P \leq 0.05$; (*) $P \leq 0.1$; - $P > 0.1$.

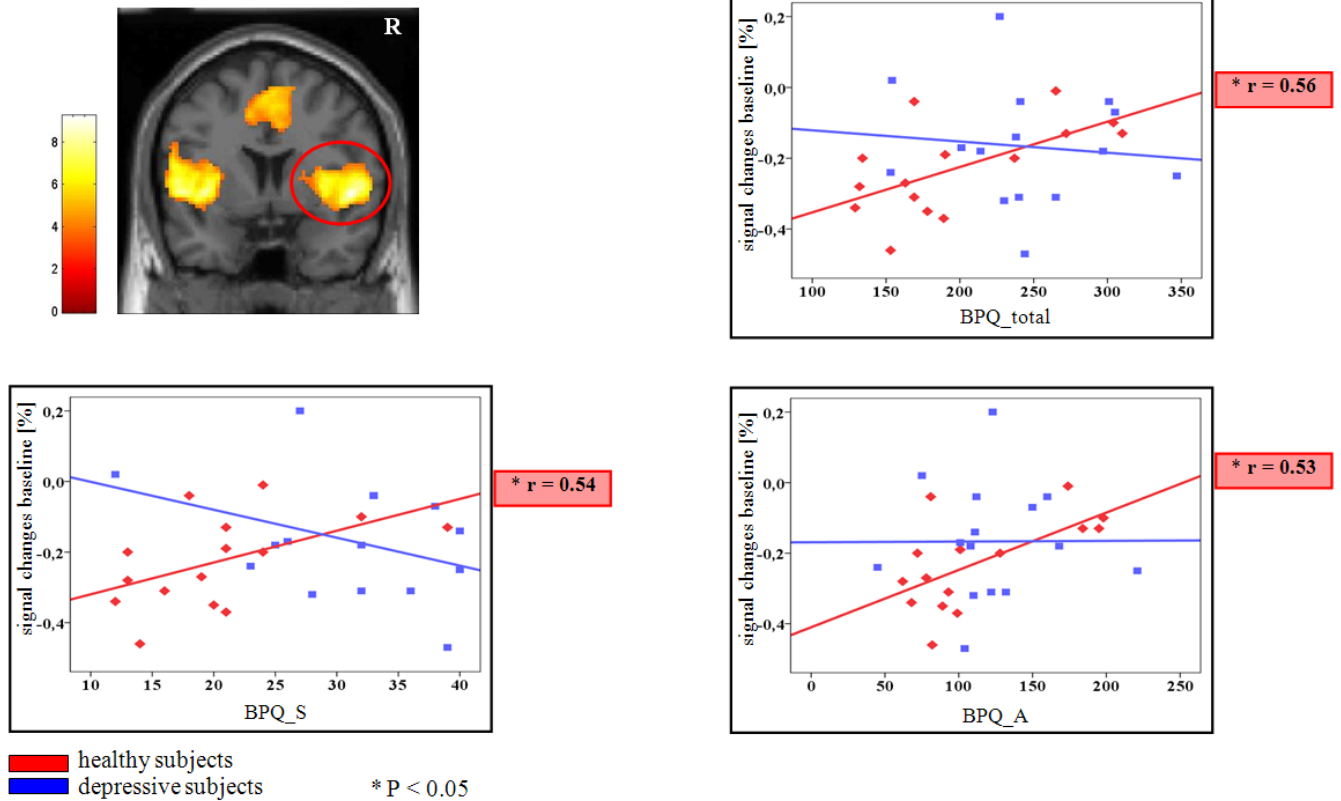


Figure 3.8: Correlation between baseline activations in right anterior insula and BPQ. Healthy subjects ($n = 17$, red lines) show significant correlations of the baseline signal changes in the right anterior insula with the total score of the BPQ (BPQ_total), awareness (BPQ_A) and stress response (BPQ_S) ($* P \leq 0.05$). MDD patients ($n = 15$, blue lines), in contrast, showed no correlations between the BPQ in the right anterior insula.

Signal changes during rest periods in the left anterior insula were also significantly positively correlated with BPQ stress response in healthy participants; this no longer being the case in MDD patients (see Figure 3.9 and Table 3.2). Instead, the reduced signal changes during rest periods correlated significantly with depression severity as measured with the BDI ($r = 0.57$, $P \leq 0.05$). The less deactivation during rest in the left anterior insula, the more severely patients experience their depressive symptoms (see Figure 3.9). No significant correlation of BDI was observed with either the right anterior or middle insula.

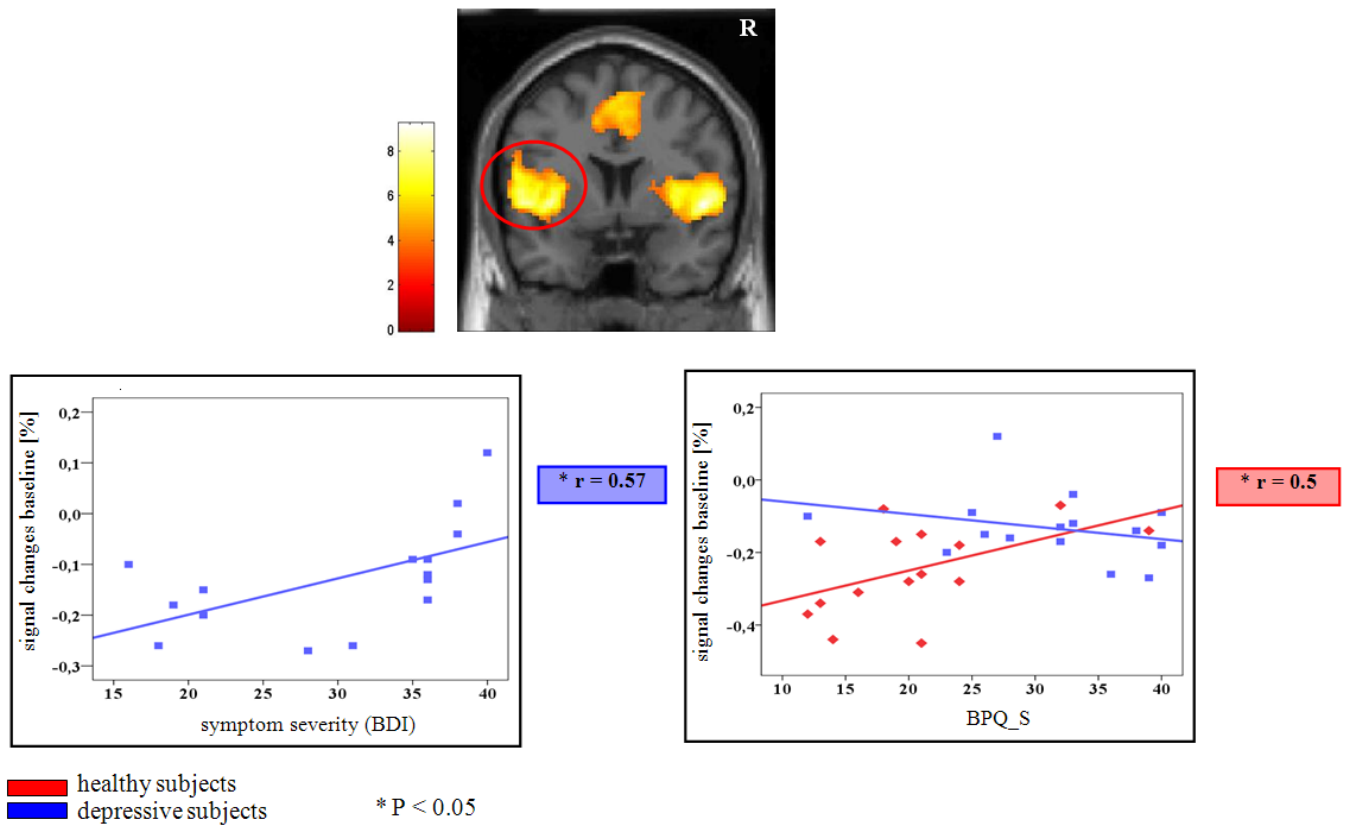


Figure 3.9: Correlation diagrams between left anterior insula activity during rest, Body Perception Questionnaire (BPQ) and Beck Depression Inventory (BDI) in healthy ($n = 17$, red lines) and depressed participants ($n = 15$, blue lines). The SPM image shows the comparison between interoceptive and exteroceptive awareness (count heartbeat > count tones, $n = 34$). The threshold of significance is set to $P \leq 0.01$ (FDR corrected, $k \geq 10$). The diagrams show the correlation curves between percent signal changes of the left anterior insula during rest (y axis) and the scores of the Body Perception Questionnaire (BPQ, x axis). Baseline signal changes in the left anterior insula show a significant correlation with stress response (BPQ_S) in healthy subjects, while the same region correlated with depression severity in depressed participants ($* P \leq 0.05$). The higher the signal changes in the left anterior insula during rest, the more severe subjects scored their depressive symptoms.

3.5 Discussion

We here investigated body perception and neural activity in the insula as behavioural and neural measures of abnormal interoceptive awareness in depression. MDD patients showed significantly higher body perception scores and lower signal changes during rest periods (i.e. reduced negative BOLD response) in the anterior and middle insula when compared to healthy participants. It should be noted that a reduced negative BOLD-response may be due to either higher activity during rest periods or decreased neural activity. In contrast to healthy participants, signal changes during rest periods in the anterior insula were no longer parametrically related to body perception scores in MDD. Most interestingly, both abnormal body perception scores and reduced signal changes during rest periods in the left anterior insula correlated with depression severity, as measured with the Beck Depression Inventory (BDI) [Beck et al., 1961]. Taken together, our findings demonstrate abnormal body perception and modulation of exteroceptive processing by the activity during rest in the anterior insula in MDD, mirroring these patients' abnormal "material me".

MDD patients showed significantly higher scores in body perception, as measured with the BPQ. Our observation of abnormal body perception is in accordance with previous findings of altered sensitivity and awareness of vegetative bodily changes in MDD [Stewart et al., 2001, Dunn et al., 2007, Strigo et al., 2008a,b]. We were able to extend these findings by showing that different dimensions of body perception, such as stress response, autonomic nervous system reactivity and stress style, seem to be abnormally increased in depressed patients. This indicates abnormal body perception; although this may not concern awareness itself as we did not observe a significant difference in the awareness subscale of the BPQ. Future investigations of depressive subgroups, such as anxiety-dominated MDD patients, may be needed to further detail the relationship with bodily awareness.

Moreover, abnormal body perception correlated with depression severity as measured with the BDI. The more abnormally high body perception was, the more intense and severe patients experience their depressive symptoms. This yields strong empirical support to the often made clinical observations of somato-vegetative symptoms, and of abnormal interoceptive awareness being an indicator of depressive symptoms and depression severity [[Kirmayer, 2001](#), [Garcia-Cebrian et al., 2006](#), [Nyboe Jacobsen et al., 2006](#), [Tylee and Gandhi, 2005](#)].

MDD patients showed significantly reduced signal changes during rest in the insula, predominantly in the left anterior and middle insula. This is in accordance with early studies in MDD concerning rest periods that, using PET, also observed increased activity during rest in the insula [[Mayberg, 2002, 2003](#), [Philips et al., 2003](#), [Fitzgerald et al., 2008](#)]. In contrast, MDD patients did not show any abnormalities in this region during either intero- or exteroceptive stimulation when compared to healthy participants. We were here able to extend these early observations by showing no changes during either intero- or exteroceptive stimulation independent of changes during rest periods. Although we did observe some abnormalities in the insula during the exteroceptive task, these could most likely be traced back to the reduced activity during rest rather than the exteroceptive stimulation itself, as revealed in our baseline corrected analysis. This underlines the proposed abnormal rest-stimulus interaction in depressed patients, with, it is suggested, an abnormally high activity during rest periods leading to a reduced stimulus-induced change in activity.

Furthermore, reduced neural changes during rest periods in the left anterior insula correlated with depression severity. The smaller the deactivation during rest was, the more severely MDD patients experienced their depressive symptoms. This is in accordance with previous findings concerning both the insula and other regions, such as the ventro- and dorsomedial prefrontal cortex [[Paulus and Stein, 2006](#), [Grimm et al., 2009a,c](#), [Brody et al., 2001](#), [Milak et al., 2005](#), [Périco et al., 2005](#), [Simmons et al.,](#)

2006, Stein et al., 2007]. Taken together, our findings provide strong evidence of reduced activity during rest periods in the left anterior insula and the relation of this to depressive symptoms.

Most importantly, our findings indicate decoupling of body perception from neural activity changes in the insula in MDD. In accordance with Craig's hypothesis of the right anterior insula mediating the "material me", rest activity in this region correlated with body perception, as measured with the BPQ, in healthy participants. This was no longer the case in depressed participants, where activity during rest periods in both right and left anterior insula no longer correlated with BPQ scores. Body perception and activity during rest thus seem to be dissociated or, better, decoupled from each other in MDD. MDD patients' abnormal body perception and its relation to altered activity in the insula may be interpreted as the inability of depressed participants to shift their focus of perception/ awareness from the own body to their environment. This could lead to increased interoceptive awareness, mirroring the abnormal "material me" of MDD patients.

Several limitations of our study need to be considered. Our patients were all medicated and therefore we cannot exclude medication effects. Hence, the same study may need to be conducted again in unmedicated MDD patients. One may criticize that we did not include a true resting state period with scanning for about 5-10 minutes in the mere resting state. Instead, we only included 4-10 seconds long periods with fixation cross. This was done because our main purpose was to clearly separate signal changes associated with rest from those related to intero- and exteroceptive processing within the regions of interest. In order to do this we analysed the relative signal changes induced by intero- and exteroceptive processing in relation to the respectively preceding rest period, something that is not possible with a separate, long rest period. Future studies with a separate and longer resting state period will be necessary to investigate fully

the relationship between the resting state network, the default-mode network [Raichle et al., 2001, Raichle and Gusnard, 2005], and the interoceptive network and body perception. One may also argue that body perception itself does not account for what is called the “material self”. The “material self” could only be investigated by explicitly testing for self-relatedness of one’s body, which we did not do here. Hence, future studies are necessary that include both body perception and self-relatedness as implicit and explicit measures of the self with regard to the (inner and outer) body.

In conclusion, we here demonstrate the crucial relevance of the anterior insula to abnormal body perception and depression severity in MDD. MDD patients showed differing body perception scores and reduced activity during rest periods in the anterior insula specifically. Signal changes during rest in the anterior insula no longer correlated with BPQ scores in MDD patients, while they were related to depression severity. Taken together, our findings demonstrate abnormal body perception and reduced activity in the insula during rest periods, with the latter being decoupled from the former. This may account for the often observed somato-vegetative symptoms in MDD patients.

3.6 Acknowledgements

The work was made possible by financial contributions from the Salus Foundation and Lilly Germany.

We thank the staff from the state hospital of Uchtspringe, the Department of Neurology II and Lilly Germany for their skilful assistance as well as Björn Enzi for his helpful comments on the manuscript.

Chapter 4

Neural response to interoceptive awareness in the insula as state marker for depression - an fMRI study investigating healthy, depressed and remitted participants

4.1 Abstract

Interoceptive awareness, the awareness of stimuli originating inside of the body, plays an important role in human emotions and psychopathology. The insula has been described as a brain structure particularly involved in neural processes underlying interoceptive awareness. The aim of the present study was to investigate neural differences in functional subregions of the insula during interoceptive awareness between depressed, remitted, and healthy participants.

Using fMRI, a well established paradigm to study intero- and exteroceptive awareness (heartbeat and tone counting) was used in 22 patients suffering from major depression, as well as 10 participants after remission from depression and 30 healthy participants. Neural activity in *a priori* defined functional subdivision of the insula was compared between these independent groups of depressed, remitted, and healthy individuals.

Significant group effects occurred mainly during interoceptive awareness in anterior regions of the insula, whilst the posterior insula showed a group effect in exteroceptive awareness conditions. Depressed patients showed neural hypo-responses during interoceptive awareness, as compared to both remitted and healthy participants. Moreover, the right dorsal anterior insula showed the strongest neural activity during interoceptive awareness across groups, whilst depressed patients showed no differential activation in this region when compared to exteroceptive awareness or rest. Correlations with scores for hopelessness revealed negative relationships with neural activity during interoceptive awareness and rest in the dorsal anterior insula in healthy participants, as well as negative relationships with neural activity during exteroceptive awareness and rest in the posterior insula.

This is the first study comparing neural activity in the insula in depressed patients to that of healthy and remitted participants in an encompassing study designed to explore intero- and exteroceptive awareness. The results suggest that group differences were due to a neural hypo-response across insula regions in the depressed group. This effect normalizes after remission from depression, implying a dynamic mechanism. The lack of differential processing in the depressed group in the dorsal anterior insula might account for their altered external and internal focus. In order to support the regeneration of neural activity especially during interoceptive awareness and accordingly improve depressive symptoms, therapies like biofeedback or mindfulness based therapies may lead to a faster recovery.

4.2 Introduction

The insula has been described as a brain region serving as an interface between stimuli originating constantly from the external environment, i.e. outside the body, and stimuli originating internally, i.e. inside the body [Craig, 2009, Farb et al., 2012a, Craig, 2011]. Becoming a prominent target of neuroimaging studies over the past decade, this multimodal character of the insula has been explored in further detail by functional connectivity and resulting parcellation [Eckert et al., 2009, Cauda et al., 2011, Deen et al., 2011, Chang et al., 2012, Kelly et al., 2012], cytoarchitectonic mapping [Mesulam and Mufson, 1982, Kurth et al., 2010], diffusion imaging-based tractography [Nanetti et al., 2009, Cerliani et al., 2012], neurochemical studies [Wiebking et al., 2012b, Dupont et al., 2003] and task-related functional magnetic resonance imaging (fMRI) [Critchley et al., 2004, Pollatos et al., 2007c, Farb et al., 2012a, Zaki et al., 2012]. The latter mentioned fMRI studies investigated, amongst others, the involvement of the insula in interoceptive awareness (IA) – becoming aware of the processing of stimuli originating inside of the own body - by using a heartbeat detection task [Critchley et al., 2004, Pollatos et al., 2007c]. The insula has been reliably identified as brain structure sensitive to IA, next to other regions like the cingulate cortex and prefrontal cortices, a finding that is supported also by functional connectivity studies and structural investigations [Nanetti et al., 2009, Deen et al., 2011].

In line with former research and prominent theories of emotional processing, the insula has been suggested to play a key role in the connection between IA and affective experience [Damasio, 1999b, Bechara and Naqvi, 2004, Wiens, 2005, Lamm and Singer, 2010] as well as an important brain structure for the conscious perception of internal body states [Craig, 2002, 2011, Bechara and Naqvi, 2004]. EEG studies, although limited in spatial resolution, have shown a correlation between emotional processing and

IA [[Herbert et al., 2007](#), [Pollatos et al., 2007a](#)], whilst fMRI studies showed a correlation between the neural response to IA and negative emotions specifically in the right insula [[Critchley et al., 2004](#)] as well as a neural co-activation of IA and emotional processing in the insula [[Zaki et al., 2012](#)].

This connection within the insula between neural IA related activity and emotional processing is suggestive of an involvement of the insula in mood disorders, such as anxiety or major depressive disorder (MDD), which are characterized by negative affect. This assumption is supported by findings in healthy participants showing an association in the insula to stress or anxiety [[Paul et al., 2012](#), [Terasawa Y, Shibata M, Moriguchi Y, 2012](#)]. In addition, altered insula function in depression has been reported on several different levels of research: on the structural level showing reduced insula cortex grey matter volume [[Sprengelmeyer et al., 2011](#)]; on the biochemical level showing a decreased metabolism in the insula [[Brooks et al., 2009](#)] as well as an association between depression severity and serotonin in the insula [[Lothe et al., 2008](#)]; and also impaired regional homogeneity in the left [[Guo et al., 2011](#)] and right insula [[Liu et al., 2010](#)] when compared to healthy participants. Recent findings on the behavioural level suggest impaired body perception in depression in combination with reduced heartbeat-evoked potentials in EEG [[Terhaar et al., 2012](#)] and altered activity during rest in fMRI [[Wiebking et al., 2010](#)].

Taken together, research suggests impaired insula functioning in combination with impaired emotional and interoceptive processing in MDD. Assuming main abnormalities in regards to IA related activity in the insula in MDD as well as an effect of normalization after remission [[Schaefer et al., 2006](#)], we investigated IA in the insula in depressed patients and compared it to those in healthy participants as well as participants remitted from MDD. Considering the functionally different sub-regions of the insula, as revealed by functional connectivity [[Deen et al., 2011](#), [Chang et al., 2012](#), [Kelly et al.,](#)

2012], *a priori* defined regions of interest in the bilateral insula were applied, which emerged from parcellation and were kindly provided by B. Deen [Deen et al., 2011]. Carefully controlling for physiological noise artifacts, a well established fMRI paradigm to study intero- and exteroceptive awareness (heartbeat counting and tone counting) was applied. In addition, fixation periods were included in the paradigm. These three conditions were used to investigate neural task differences within the different subject groups in IA sensitive regions, assuming impaired differentiation between conditions in depressed participants.

4.3 Materials and methods

4.3.1 Participants

Using functional magnetic resonance imaging (fMRI), a total of 62 data sets were acquired for this study. These split up into 30 healthy participants (n = 15 female, mean age: 33.7 ± 11.6 SD, min: 22, max: 60), a total of 22 participants in an acute state of major depression (13 female, mean age: 40.1 ± 12.4 SD, min: 21, max: 58) and 10 participants after remission from MDD (n = 7 female, mean age: 37.9 ± 10.1 SD, min: 26, max: 54). In order to avoid a potential confounding influence of repeated use of the same subjects by using independent groups, ten depressed participants which were measured in remitted state were discarded from further analysis, leaving 12 participants in an acute state of major depression (n = 6 female, mean age: 42.0 ± 14.2 SD, min: 21, max: 58) (see Suppl. table B.1). The healthy control group had no psychiatric, neurological, or other diseases as assessed using a custom-made semi-structured clinical questionnaire. The healthy group had an intelligence score (mean of verbal and nonverbal testing) of $116.6 (\pm 12.0$ SD, 1 missing value), the MDD group of $109.4 (\pm 8.5$ SD, 4 missing values) and the remitted group of $110.2 (\pm 10.7$ SD).

An ANOVA showed no differences ($P \geq 0.1$) between groups for age or intelligence (Suppl. table B.1). Healthy participants were recruited from the Otto-von-Guericke University (Magdeburg, Germany) and the local community. The study was approved by the local ethics committee. All participants gave their written informed consent before participating in this study. Healthy participants were financially compensated.

Psychiatric in-patients and remitted participants were recruited from either the Department of Psychiatry (University of Magdeburg, Germany) or from the state hospital of Uchtspringe. Major depressive disorder was diagnosed according to DSM-IV (Diagnostic and Statistical Manual of Mental Disorders, [American Psychiatric Association, 1994]). Evaluation of acute and remitted stage of MDD was made by the participants' treating psychiatrist. General exclusion criteria involved major medical illnesses, histories of seizures, metallic implants, a history of substance dependence, head trauma with loss of consciousness, pregnancy and criteria for any psychiatric disorder other than MDD.

Mean BDI scores, not available for healthy participants, differed significantly ($P \leq 0.05$) between depressed (28.6 ± 10.3) and remitted (17.4 ± 4.3) participants ($n = 7$ in both groups available). Mean BHS scores, not available for remitted participants, differed significantly ($P \leq 0.001$) between healthy (4.6 ± 3.9) and depressed (10.9 ± 4.6).

4.3.2 Paradigm

The event related fMRI design was based on a paradigm introduced by Pollatos and Critchley [Critchley et al., 2004, Pollatos et al., 2007c], which involves participants counting their own heartbeat – a stimuli originating from their own body and hence defined as interoceptive awareness (IA) – and counting external applied tones (i.e., exteroceptive awareness (EA)). The paradigm was altered from the form originally described by Pollatos and Critchley in order to make it more suitable for use with a de-

pressed population. In order to make the paradigm less complicated and to reduce the scanning time for patients, the presence or absence of a feedback delay and a modulated tone were excluded. Instead, three simple symbols were used as task type indicators to show start and duration of a task.

Three separate experimental conditions and three simple symbols were presented: an interoceptive task, an exteroceptive task, and fixation periods in a pseudo-randomized order. During IA conditions, participants were asked to silently count their own heartbeat without any manipulation, as for example holding their breath or evaluating their pulse at the radial artery. A dark coloured heart on a light background (9–13 s) indicated onset and duration of heartbeat counting. Afterwards, the number of counted heartbeats was reported via a visual analogue scale (4 s). The indicator on the scale was moved by the subject to the labelled position representing the number of beats that they counted (left and right button presses corresponding to moving left and right on the scale). This feedback component allowed subject's attendance to the task to be monitored. EA conditions were indicated by a dark coloured musical note symbol on a light background (9–13 s). During such tasks individuals had to silently count the number of tones heard during the period that the indicator was visible on the screen. Two different tones were presented, alternating with each of the four scanning sessions, each with a duration of 200 ms; a length that is comparable to the average duration of the sound of a heartbeat. In order to make the difficulty of both the IA and EA tasks closely comparable, tones were presented at an individually determined volume that meant they were, like the heartbeat, just audible. Controlling for habituation effects, the volume was individually changed, if necessary, before each of the four sessions. The general presentation frequency of the tones was adapted to correspond to each subject's pulse-rate, with the individual onset time of the tones being jittered by 200 ms from this general frequency in order to control for habituation effects. As with the IA task, participants reported the number of tones heard via a visual analogue scale (4

s). Rest conditions were indicated by a dark Fixation cross on light background (9–13 s). Participants were instructed to relax and reduce any cognitive work during these periods.

The total experiment consisted of 4 sessions of 9.6 min (290 volumes). Each condition was repeated 48 times in total, which guaranteed a sufficient statistical effect in subsequent statistical parametric mapping analyses. The paradigm was executed on an ordinary desktop personal computer running the software package “Presentation” (Neurobehavioral Systems, <http://www.neurobs.com>). Visual stimuli were projected via an LCD projector onto a screen visible through a mirror mounted on the headcoil. Auditory stimuli were presented via the scanner loudspeaker.

4.3.3 fMRI data acquisition and analysis

Functional measurements were performed on a 3-Tesla whole body MRI system (Siemens Trio, Erlangen, Germany) with echo planar imaging (EPI) using an eight channel head coil. The slices were acquired parallel to AC–PC plane in an odd-even interleaved acquisition order. Thirty-two T_2^* -weighted echo planar images per volume with blood oxygenation level-dependent (BOLD) contrast were obtained with following settings: matrix 64 x 64; 32 slices per volume; FoV: 224 x 224 mm²; spatial resolution: 3.5 x 3.5 x 4 mm³; $T_E = 30$ ms; $T_R = 2000$ ms; flip angle = 80°. Functional data were recorded in four scanning sessions, each containing 290 volumes. One MDD participant is missing one out of the four sessions.

The fMRI data were pre-processed and statistically analyzed according to the general linear model approach [Friston et al., 1995] using the SPM8 software package (<http://www.fil.ion.ucl.ac.uk>) running on MATLAB 7.11 (The Mathworks Inc., Natick, MA, USA). All functional images were slice time corrected with reference to the first acquired slice, corrected for motion artifacts by realignment to the mean functional image, and

spatially normalized to a standard T_1 -weighted SPM template [Ashburner and Friston, 1999]. The normalization was generated by warping the coregistered anatomical image to the MNI T_1 -template and applying these parameters to all functional images. The images were resampled to $2 \times 2 \times 2 \text{ mm}^3$ and smoothed with an isotropic 6 mm full-width half-maximum (FWHM) Gaussian kernel. The time-series fMRI data were filtered using a high pass filter (threshold 128 s). A statistical model for each subject was computed by applying a canonical response function [Friston et al., 1998].

Since structured noise still remains in the fMRI data after traditional steps of pre-processing, an independent component analysis (ICA) was applied to remove noise and hence improve the sensitivity and specificity of the results. Using Probabilistic Independent Component Analysis, which is implemented in the MELODIC toolbox [Beckmann and Smith, 2004] of FSL (FMRIB's Software Library, <http://www.fmrib.ox.ac.uk/fsl/>) [Smith et al., 2004, Woolrich et al., 2009], a group ICA was performed on all pre-processed fMRI data, which were temporally concatenated across individuals. ICA separates the different spatiotemporal components by assuming statistical independence. Due to their different time-course, each component represents afterwards a different pattern of activation (signals of interest) or artefact (signals of noise). Noise or signals of interest were distinguished according to a detailed description of an operationalized denoising procedure [Kelly et al., 2010]. In particular, components were considered as noise and removed through linear regression when they showed a ring-like pattern in the periphery of the brain and tightly clustered areas in the frontal regions [McKeown et al., 1998], clusters with a location in the white matter/ CSF or an association with blood vessels [Sui et al., 2009, Zou et al., 2009], spotted patterns diffusely spread over the brain, and time courses showing a saw-tooth pattern or spikes [McKeown et al., 1998]. After removing non-brain voxels using BET (Brain Extraction Tool, [Smith, 2002]), all three conditions (IA, EA, Fix) were included in the SPM model as separate events including their feedback phases. Movement parameters were included as nuisance variables.

4.3.4 Definition of insula regions and statistical analysis

Regions of interest (ROIs) were taken over from Deen et al. [Deen et al., 2011]. Here, cluster analysis identified three bilateral subregions of the insula: the left (L) and right (R) dorsal anterior to middle insula (dAI), ventral anterior insula (vAI) and the posterior insula (PI) (see Figure 4.1 A). These subregions were identified due to their distinct connectivity patterns. In particular, dAI connected primarily with the dorsal anterior cingulate cortex, vAI with pregenual anterior cingulate cortex and PI was functionally connected with primary and secondary somatomotor cortices [Deen et al., 2011].

The Marseille Region of Interest Toolbox software package (MarsBaR, [Brett et al., 2002], <http://www.sourceforge.net/projects/marsbar>) was used to extract time courses from voxels within the aforementioned ROIs. The maximum of the time course of the estimated event for a specific condition (IA, EA, and Fixation) was calculated by MarsBaR, divided by the mean signal across the time course of the whole session and multiplied by 100. This value, the percent signal change, represents an individual value for each subject and each condition within a certain ROI. Values for each condition and each ROI were averaged across the four sessions. Percent signal changes for healthy, depressed and remitted participants were entered into SPSS 20.0 (SPSS inc., Chicago, IL). Extreme values, which were farther than three interquartile ranges away from the first or third quartile, were defined as outliers and excluded from the analysis. In detail, this affected averaged signal change values of single conditions for three healthy participants. No values of the depressed or remitted group were affected.

To determine an effect of group, multivariate analysis of variance (MANOVA) was performed [Himmelbach et al., 2007]. The three different treatment groups were defined as between-subjects factor, while the percent signal changes of the three conditions (IA, EA, and Fixation) in each ROI were entered as dependent within-subjects variables.

In order to reduce type I errors, the most conservative method for post-hoc testing, Bonferroni correction, was used.

Based on the results of the MANOVA, a paired T-Test was performed on IA related signal changes comparing right and left hemispheric ROIs within groups. Moreover, differentiations between the three conditions in each group within the R-dAI and L-dAI were identified by using the three conditions as between-subjects factor and the signal changes of each group as within-subjects variables. Post-hoc tests were Bonferroni corrected as well. Since unequal sample sizes can affect the homogeneity of variances, only results showing a significance value above 0.1 ($P \geq 0.1$) in the test of homogeneity of variances (Levene statistic) were considered for analysis.

In a last step, signal changes were used for correlation (Pearson, two-tailed) with behavioural markers of depression, i.e., the Beck Hopelessness Scale (BHS) [Beck et al., 1974] and Beck Depression Inventory (BDI) [Beck et al., 1961].

4.4 Results

4.4.1 Results in insula regions (Figure 4.1)

As determined by MANOVA, there was a statistically significant difference between the three different groups (F (hypothesis df: 36, error df: 58) = 1.7, $P < 0.05$; Wilk's $\lambda = 0.24$, partial $\epsilon^2 = 0.5$).

Significant differences occurred in IA conditions in the R-dAI (F (2, 46) = 6.6; $P = 0.007$; partial $\epsilon^2 = 0.22$), L-PI (F (2, 46) = 3.8; $P = 0.03$; partial $\epsilon^2 = 0.14$), R-PI (F (2, 46) = 5.23; $P = 0.009$; partial $\epsilon^2 = 0.19$) and R-vAI (F (2, 46) = 6.02; $P = 0.005$; partial $\epsilon^2 = 0.21$) (Suppl. table B.2). EA conditions, on the other hand, showed a single significant group difference in the R-PI (F (2, 46) = 3.86; $P = 0.028$; partial $\epsilon^2 = 0.14$) and a marginal effect in the R-dAI (F (2, 46) = 2.67; $P = 0.08$; partial $\epsilon^2 = 0.10$). No group

effects occurred regards the Fixation condition. Hence, the statistical group effect was mainly due to differences in the IA conditions.

The results of the Bonferroni post-hoc tests, used to determine which groups differ from each other in which region, are illustrated in Figure 4.1 and listed in Suppl. table B.2. Neural activity during IA in the R-dAI of depressed individuals (mean \pm SD: 0.01 ± 0.03) was significantly lower compared to both healthy (0.05 ± 0.03 , $P = 0.003$) as well as remitted participants (0.05 ± 0.03 , $P = 0.037$) (orange line, Figure 4.1 B). There were no statistically significant differences between the healthy and remitted groups ($P = 1$). A similar pattern for IA occurred in the R-vAI (red line, Figure 4.1 B): values for neural activity during IA in depressed participants (-0.02 ± 0.04) were significantly decreased compared to those in healthy (0.02 ± 0.03 , $P = 0.004$) and marginal decreased compared to remitted participants (0.01 ± 0.03 , $P = 0.09$). Values between healthy and remitted participants did not differ ($P = 1$) (see also Suppl. table B.2).

In addition, depressed participants showed significant differences to healthy participants in the bilateral PI during IA (L: $P = 0.026$; R: $P = 0.008$). In both regions, depressed participants showed lower signal changes (L: -0.001 ± 0.03 ; R: -0.04 ± 0.02) compared to healthy participants (L: 0.03 ± 0.03 ; R: 0.001 ± 0.03). Significant differences occurred neither between remitted (L: 0.02 ± 0.03 ; R: -0.02 ± 0.04) and healthy (L: $P = 1$; R: $P = 0.40$) nor between remitted and depressed participants (L: $P = 0.21$; R: $P = 0.67$). The purple line in Figure 4.1 B illustrates the results for the L-PI; the yellow line illustrates results for the R-PI. The two remaining regions on the left side, the dAI (blue line, Figure 4.1 B) and the vAI (cyan line, Figure 4.1 B), showed no significant differences. In summary, predominantly IA conditions in right insula regions showed significant differences in depressed participants when compared to remitted as well as to healthy participants.

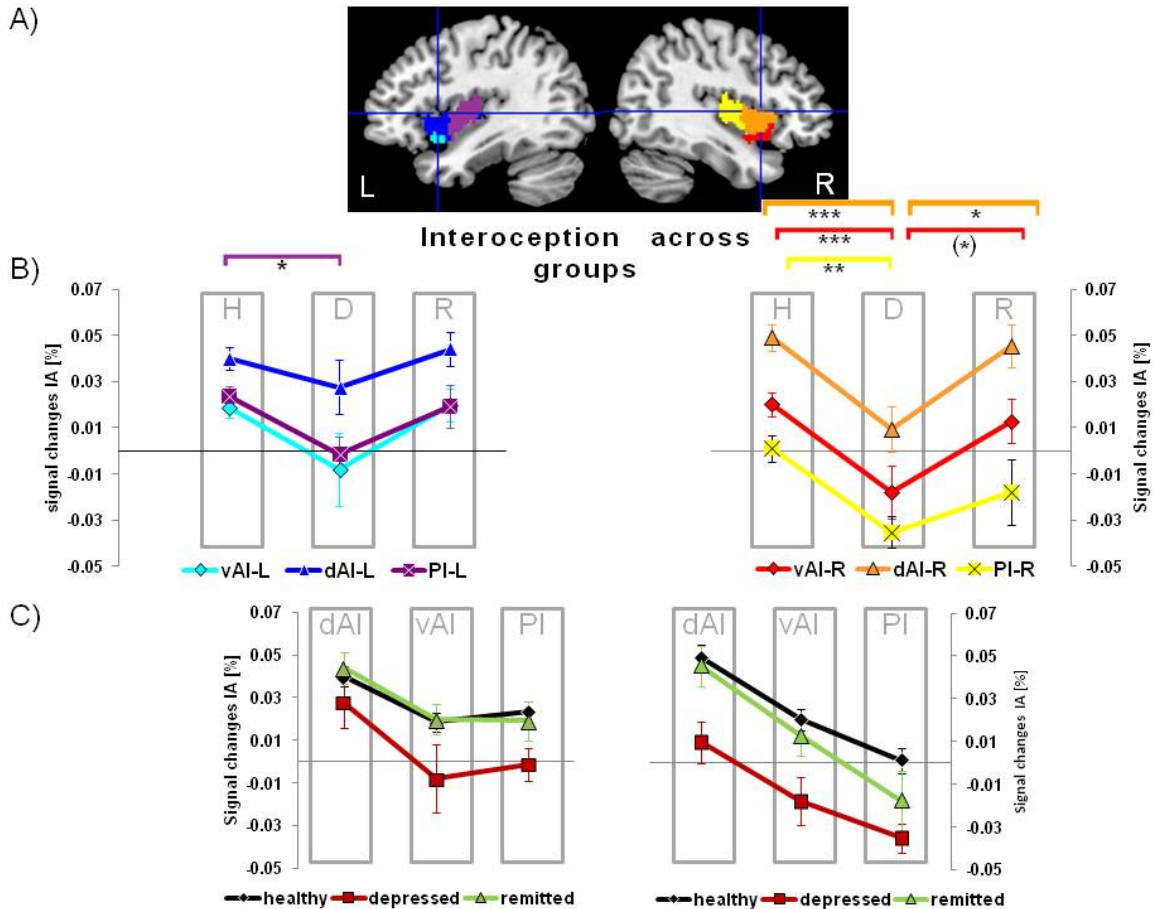


Figure 4.1: Neural activity for interoceptive awareness (IA) in the left (L) and right (R) dorsal anterior insula (dAI), ventral anterior insula (vAI) and the posterior insula (PI) in independent groups of healthy (H), depressed (D) and remitted (R) participants.

A) Regions of interest in the left (L) and right (R) insula (L-dAI: blue, L-vAI: cyan, L-PI: purple, R-dAI: orange, L-vAI: red, L-PI: yellow) (provided by [Deen et al., 2011]).

B) Neural activity of interoceptive awareness (mean \pm SEM) across groups within insula regions. On the left side, significant results between healthy and depressed groups were seen in the PI (purple). On the right side, the depressed group differed across all regions to the healthy group, whereas differences to the remitted group occurred in the dAI (orange) and vAI (red) as revealed by MANOVA. Healthy and remitted groups showed no differences. IA across left and right regions showed significantly lower activity on the right side for depressed subjects. [*** $P < 0.005$, ** $P < 0.01$, * $P < 0.05$, (*) $P < 0.1$, post-hoc Bonferroni]

C) Results shown in A) across groups are shown here across regions within treatment groups. Interestingly, all groups showed a similar activity pattern across the different regions, whilst the overall pattern of the depressed group was attenuated.

This was confirmed by a paired t-test, which compared right and left hemispheric IA-related activity within groups. Neural activity during IA differed between left and right hemispheric ROIs in the group of depressed participants ($t(70) = 2.151$, $P = 0.035$), with significantly lower activity on the right side (R: -0.015 ± 0.04 , L: 0.006 ± 0.04). No significant differences were seen in the healthy ($t(163) = 0.652$, $P = 0.516$) or remitted group ($t(49) = 1.526$, $P = 0.134$).

4.4.2 Results in the dAI (Figure 4.2)

Following our hypothesis of an impaired differentiation between conditions in depressed participants in regions specifically sensitive to IA, we investigated next the pattern of BOLD responses during EA and Fixation in the dAI. This region was chosen because of two reasons: first, the dAI showed the highest BOLD responses to IA across the three groups (see Figure 4.1 C), indicating a high specificity to IA. Second, the depressed group showed in the R-dAI the most distinct differences to both healthy and remitted groups, (see Figure 4.1 B), an indicator for an altered pattern of activity in depression that recovers after remission.

As hypothesized, the depressed group showed no differentiation between conditions in the right or left dAI (L-dAI: $F(2,33) = 1.459$, $P = 0.247$, R-dAI: $F(2,33) = 0.853$, $P = 0.435$) (Figure 4.2 A). In contrast, discriminations between the three conditions within the dAI occurred in healthy (L-dAI: $F(2,86) = 8.765$, $P < 0.0005$, R-dAI: $F(2,86) = 14.166$, $P < 0.00001$) as well as remitted participants (L-dAI: $F(2,27) = 5.777$, $P = 0.008$, R-dAI: $F(2,27) = 5.408$, $P = 0.011$).

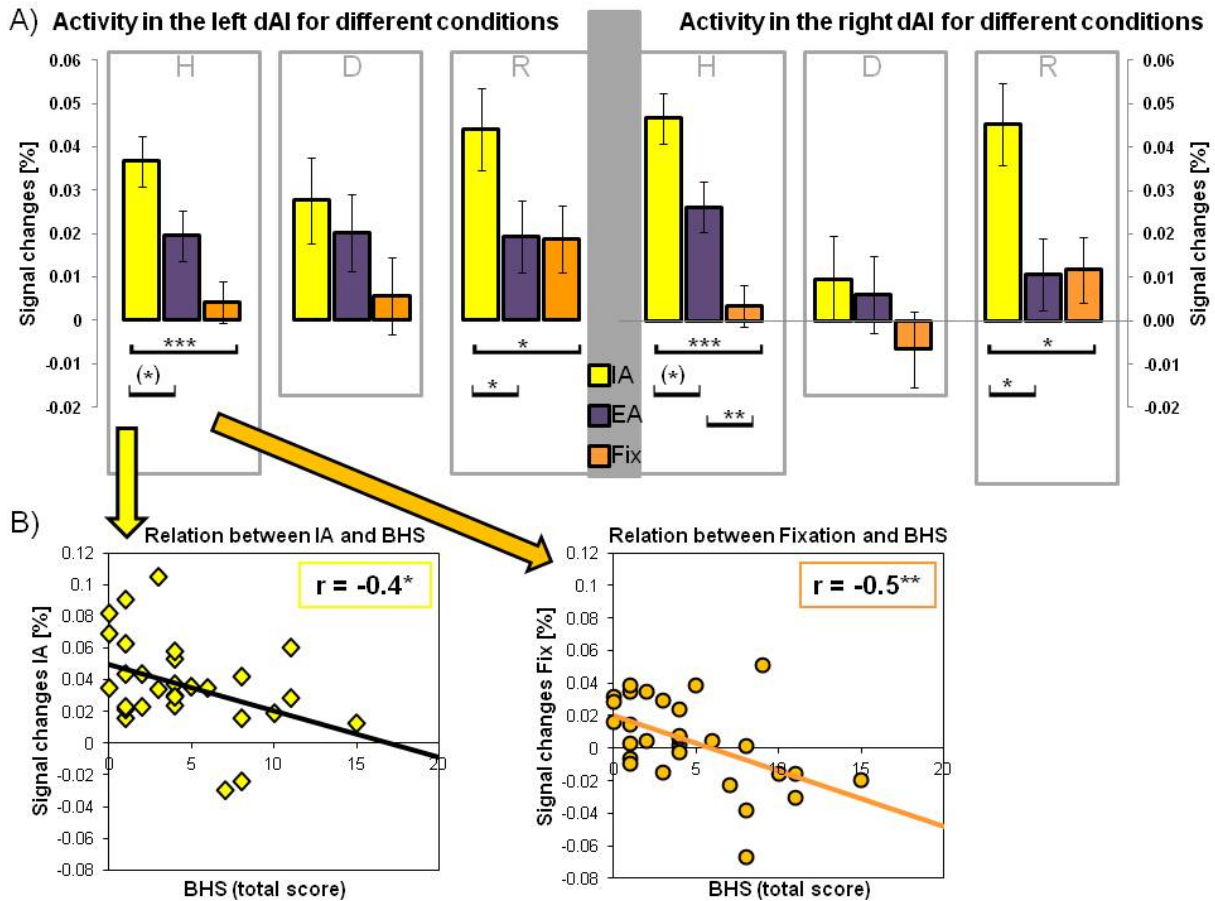


Figure 4.2: Neural activity (mean \pm SEM) for different conditions in healthy (H), depressed (D), and remitted (R) participants in the left and right dorsal anterior insula (dAI). Interoceptive awareness (IA) is marked in yellow, exteroceptive awareness (EA) is marked in purple and Fixation (Fix) in orange.

A) Healthy and remitted participants show a clear distinction between IA and specifically Fixation in both regions. Additionally, IA differed to EA in both groups and regions, whereas the R-dAI revealed also a differentiation between EA and Fixation in the healthy group. Depressed participants showed no differentiation in both regions between any of the three conditions. [*** $P < 0.0005$, ** $P < 0.01$, * $P < 0.05$, (*) $P \leq 0.1$, post-hoc Bonferroni]

B) The Beck Hopelessness Scale (BHS), a behavioural measure for depression, correlated negatively (Pearson, two-tailed) with signal changes for IA and Fixation in healthy participants. No relation was seen in depressed or remitted participants.

Bonferroni post-hoc tests revealed the same pattern of distinction between conditions in the L-dAI for healthy and remitted individuals. As such, IA in both groups differed to EA (healthy: $P = 0.09$, remitted: $P = 0.02$) as well as to Fixation (healthy: $P \leq 0.0005$, remitted: $P = 0.02$), whilst EA and Fixation did not differ among each other (healthy: $P = 0.15$, remitted: $P = 1$). Descriptive statistics revealed the most positive values for IA (healthy: 0.04 ± 0.03 ; remitted: 0.04 ± 0.02) and the least estimates for Fixation (healthy: 0.004 ± 0.03 ; remitted: 0.02 ± 0.02) (descriptive Suppl. table B.3, left side of Figure 4.2 A & Suppl. figure B.1). The same differentiation of IA compared to EA and Fixation occurred in both the healthy and remitted group in the R-dAI. In detail, IA differed to EA (healthy: $P = 0.09$, remitted: $P = 0.02$) as well as to Fixation (healthy: $P \leq 0.0005$, remitted: $P = 0.03$). Healthy participants showed an additional significant difference between EA and Fixation ($P = 0.009$). Again, IA was identified showing the most positive values (healthy: 0.045 ± 0.03 ; remitted: 0.045 ± 0.03) and the least estimates for Fixation (healthy: 0.003 ± 0.03 ; remitted: 0.02 ± 0.02) (see also right side of Figure 4.2 A & Suppl. figure B.1).

In a last step, signal changes for IA, EA, and Fixation were correlated with behavioural measures of depression (BHS and BDI) (Suppl. table B.4). Interestingly, the healthy group showed significant negative correlations between BHS and signal changes for both IA ($r = -0.39$, $P = 0.035$) and Fixation ($r = -0.51$, $P = 0.004$) in the L-dAI (see Figure 4.2 B). Of note is that these two conditions differed among each other within the healthy group (Figure 4.2 A).

4.4.3 Results in the PI (Figure 4.3)

As mentioned beforehand, MANOVA revealed one significant group difference during EA conditions in the R-PI (region illustrated in Figure 4.3 A). Bonferroni post-hoc tests revealed lower signal changes in the depressed group (-0.02 ± 0.03) when compared to the healthy group (0.003 ± 0.03 , $P = 0.034$) (Figure 4.3 B). Significant differences occurred neither between remitted (-0.01 ± 0.03) and healthy ($P = 0.352$) nor depressed participants ($P = 1$). Although no condition differences were shown within groups in this region, healthy participants showed negative correlations between BHS and EA ($r = -0.55$, $P = 0.002$, see Figure 4.3 C) as well as Fixation ($r = -0.49$, $P = 0.006$) (Suppl. table B.4).

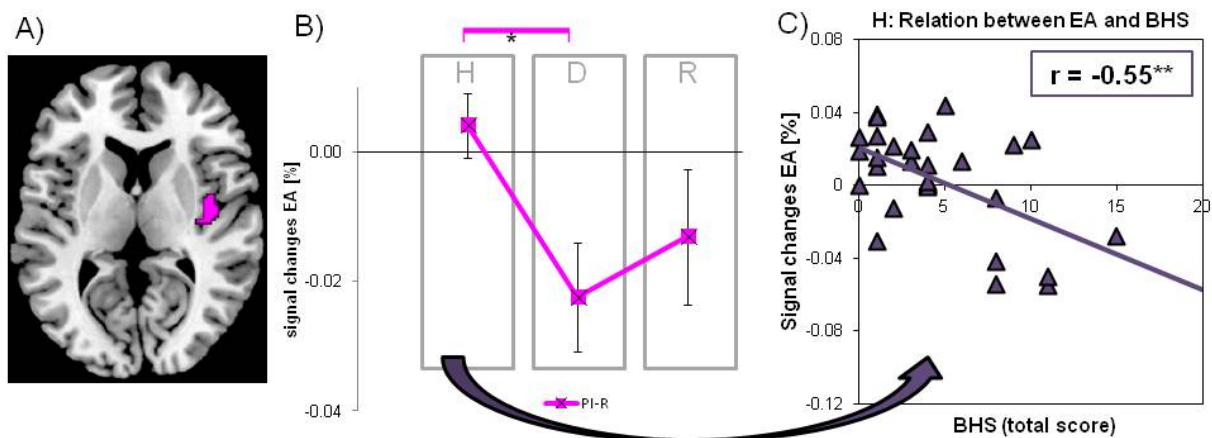


Figure 4.3: Neural activity for exteroceptive awareness (EA) in the right posterior insula in independent groups of healthy (H), depressed (D) and remitted (R) participants and its relation to BHS.

A) Right posterior insula region of interest.

B) EA (mean \pm SEM) showed a differentiation between healthy and depressed participants in the R-PI. $*P < 0.05$

C) The Beck Hopelessness Scale (BHS) correlated negatively (Pearson, two-tailed) with signal changes for EA in healthy participants. $**P < 0.01$

4.5 Discussion

Following a region-of-interest approach, neural activity during intero- and exteroceptive awareness (IA and EA) and fixation periods was investigated in three independent groups of healthy, depressed and remitted subjects. Group differences occurred predominantly during IA conditions. This finding is in concordance with our first hypothesis, the assumption of a deficit in interoceptive processing in MDD. Whilst healthy and remitted participants do not differ among each other during IA or any other condition, IA related activity in MDD patients is reduced throughout the insula cortex. This supports our assumption of an impaired differentiation between different conditions in depressed participants in regions sensitive to IA. The results show for the first time deficits in neural processing of IA in anterior insula regions and its normalization after symptom remission. This has important implications for both diagnosis and therapy of MDD.

Prior results in healthy subjects support the idea of the insula acting as a bridging factor between IA and EA networks [Farb et al., 2012a]. Nevertheless, the anterior regions, specifically the right side, are often reported to be more engaged in heartbeat monitoring tasks and show the highest BOLD responses during IA [Critchley et al., 2004, Zaki et al., 2012]. This finding can be confirmed as well as expanded by this study. Here, the dAI shows the highest activity during IA across regions and groups, whilst the activity particularly in the right dAI linearly decreases to the vAI and finally the PI. At this juncture, especially the IA activity of right-hemispheric insula regions seems to be impaired in depressed participants. They show significant activity reductions compared to left insula regions, which might be seen as main factor in causing the differences to healthy and remitted subjects. This is also consistent with lateralisation findings [Kotani et al., 2009] and hypothesis of interoceptive processes in healthy subjects, postulating a major influence of the right insula [Craig, 2002, 2003, 2004].

Interestingly, the relative pattern of IA activity across insula regions is the same for all groups. The results of the present study imply that MDD patients also show the same pattern, but a general hypo-response across insula regions during IA, an effect that returns to the level of healthy participants after remission. This finding is supported by an fMRI study (using emotional and neutral picture viewing) showing recovery of neural activity, also in the insula, as response to remission [[Schaefer et al., 2006](#)]. Our results argue against a selective deficit of a particular insula subregion. Instead, a more basic processing deficit in MDD can be assumed that spans throughout the whole insula.

The findings described in this paper concerning the absence of differences between internal- and external stimuli in a region highly affected by interoceptive input in MDD might also be interpreted in the light of altered activity during rest in MDD [[Northoff et al., 2010b](#)]. It was shown that reduced negative BOLD responses during rest need to be considered as an influencing factor regards stimulus induced activity in the insula [[Wiebking et al., 2010](#)]. Although no group differences can be seen here during task-induced fixation periods, altered neural activity during rest [[Wiebking et al., 2010](#), [Northoff et al., 2010b](#)] as well as an overall hypo-metabolism in MDD [[Brooks et al., 2009](#)] might be considered as underlying processing deficits in MDD. This remains unclear at this point and might be addressed in future studies measuring longer periods of rest and integrate this overall activation level in following analysis of task-induced activity.

Breaking down the neural activity into different conditions in the dAI, the region with the highest BOLD responses across regions and groups for IA, it is apparent that healthy subjects show a clear distinction between different conditions, especially between IA and Fixation. The same, but less distinct pattern can be seen for remitted subjects, whilst MDD patients do not show any differentiation between the different task conditions. This is the first study, to the best of our knowledge, which demonstrates a lack

of differentiation between different intero- and exteroceptive stimuli in anterior insula regions in depressed subjects; whilst at the same time the distinction rises in remitted and healthy participants. These results confirm our hypothesis and can be interpreted especially in line with hypo-metabolism in MDD [Brooks et al., 2009], which tends to normalize after remission from MDD [Schaefer et al., 2006]. A general hypo-metabolism in MDD may lead to reduced energetic resources and hence limitations in the neural activity level of IA in the insula. This needs to be investigated in future studies, for example by combining FDG-PET and fMRI.

In addition, neural activity during IA as well as Fixation was correlated with scores for depression in the healthy group, as measured by the Beck Hopelessness Scale (BHS). Whilst both conditions (IA and Fixation) differ significantly from each other in the left dAI, they show a negative association with BHS. Although group differences between healthy and depressed participants are lacking regards IA in the left dAI, the negative association between IA and BHS in the left insula confirms results from an independent study in healthy subjects, that applied the same fMRI paradigm in addition to MRS [Wiebking et al., 2012b]. Hence, healthy individuals with higher depression scores show lower activity during IA in the left dAI. Having shown a general hypo-activation of depressed during IA, one might assume that depressed participants can be considered to be at the lower extreme end of a continuous relationship between interoception and depression. This concrete hypothesis needs to be tested in future studies.

A group effect between depressed and healthy participants can also be seen during EA in the right PI. Taking into account the co-activation of the insula during IA and EA as well as depressed subjects having been described to be restricted in shifting their awareness from their own body – interoceptive awareness - to their environment, i.e., external awareness [Wiebking et al., 2010], this makes also the posterior regions inter-

esting for exploring MDD symptoms. Whilst no differences occur within groups between the different task conditions, the healthy group showed again strong negative correlations between BHS and EA (as well as Fixation) (Suppl. table B.4). This correlation might be interpreted as a necessary feature to be able to relate to external stimuli. The more depressed a person is, the lower is the neural activity during EA (or Fixation) in posterior regions of the insula. This might lead to an inability to relate to cues of the external environment, which has been described as decreased environment-focus [Northoff et al., 2011b].

Several limitations of this study need to be discussed. Firstly, the heartbeat monitoring task has been measured twice in remitted participants (once during acute depression and once in remission; remitted subjects were not included in the depressed group). One might argue that their higher positive BOLD responses compared to depressed patients in insula regions during IA is caused by a training effect. This can further be explored by measuring healthy participants twice or by measuring depressed participants twice during the acute phase of depression. Another possibility would be additional recruitment of remitted subjects, which have not been scanned during the acute phase of depression.

Secondly, the number of subjects across groups can be criticized. This result is due to the difficulty in recruitment for such a time-intensive study. Low sample sizes - 12 in the depressed group and 10 in the remitted group - are comparable to similar studies investigating pre- and post-depression [Schaefer et al., 2006]. Although this sample size can be considered as sufficient to present first results and confirm related hypothesis, confirmation through a larger scaled study would be worthwhile. In an ideal case, unmedicated MDD patients would be assigned to constitute a fourth study group. In the present study, all patients were medicated. Since also remitted patients were taking medications, a significant medication effect between these groups can be diminished,

but not excluded regards healthy subjects. Hence, the results need to be confirmed also in unmedicated depressed as well as unmedicated remitted participants. These would then form the fourth and fifth independent group of such a study, indicating the requirements of a sufficient subject number in order to perform reliable group comparisons and raising the issue of practicality.

Taken together, this is the first study comparing neural activity in the insula in depressed patients to that of healthy and remitted participants in an encompassing study designed to explore intero- and exteroceptive awareness. *A priori* defined regions of interest in the bilateral insula showed group effects particularly during IA conditions, which were due to neural hypo-response across insula regions in the MDD group. This effect remits after remission from MDD, implying a dynamic and flexible mechanism. Since all groups showed comparable activation patterns among each other across insula regions, specifically in the right hemisphere, impairments of depressed subjects during IA can be traced back to an overall attenuation effect of neural activity rather than disruptions in stimuli processing from posterior to anterior regions of the insula.

Supporting the hypothesis of a reduced signal differentiation in depression, the MDD group reveals no differences between different conditions in the dAI, the region showing the highest BOLD activity during IA across groups. Moreover, differences between healthy and depressed participants during EA in the right PI together with an association between EA and BHS in healthy subjects might account for the inability of depressed subjects to relate to external stimuli.

Our results have implications for diagnosis and treatment of MDD. In order to support the regeneration of neural activity especially during IA, therapies like biofeedback or mindfulness based therapies can possibly lead to a faster recovery.

It has been shown already that mindfulness based therapies lead to an increase in

neural activity during IA in healthy subjects [[Farb et al., 2012b](#)], although such an effect has to be established in patients with major depressive disorder.

4.6 Acknowledgements

The authors would like to thank Ben Deen (Yale Child Study Center, Yale University School of Medicine, New Haven) for providing the insula masks (Deen et al., 2011), the Department of Neurology and the staff from the state hospital of Uchtspringe for the good cooperation, Niall W. Duncan for reviewing the manuscript and computational support, David J. Hayes for statistical advice, and the patients for their participation in this study.

The work was made possible by financial contributions from Lilly Germany, the Salus Foundation, the Hope of Depression Research Foundation and the German Research Foundation (DFG, Sonderforschungsbereich 779-A6).

The authors declare no conflict of interests.

Chapter 5

External awareness and GABA – A multimodal imaging study combining fMRI and [¹⁸F]flumazenil-PET

Human Brain Mapping 2012 Sep

<http://dx.doi.org/10.1002/hbm.22166>

5.1 Abstract

Awareness is an essential feature of the human mind that can be directed internally, that is, toward our self, or externally, that is, toward the environment. The combination of internal and external information is crucial to constitute our sense of self. Although the underlying neural networks, the so-called intrinsic and extrinsic systems, have been well-defined, the associated biochemical mechanisms still remain unclear. We used a well-established functional magnetic resonance imaging (fMRI) paradigm for internal (heartbeat counting) and external (tone counting) awareness and combined this technique with [¹⁸F]FMZ-PET imaging in the same healthy subjects. Focusing on cortical midline regions, the results showed that both stimuli types induce negative BOLD responses in the mPFC and the precuneus. Carefully controlling for structured noise in fMRI data, these results were also confirmed in an independent data sample using the same paradigm. Moreover, the degree of the GABA_A receptor binding potential within these regions was correlated with the neural activity changes associated with

external, rather than internal awareness when compared to fixation. These data support evidence that the inhibitory neurotransmitter GABA is an influencing factor in the differential processing of internally and externally guided awareness. This in turn has implications for our understanding of the biochemical mechanisms underlying awareness in general and its potential impact on psychiatric disorders.

5.2 Introduction

Awareness is a central, if not defining, feature of the human mind. Through this faculty we can become explicitly aware of both our environment and ourselves, including our body, this having been described in neuroscience as external and internal awareness (IA) [James, 1890, Vanhaudenhuyse et al., 2011]. Whilst external awareness (EA) describes the perception of the environment, IA refers to the perception of self-related mental processes and awareness related to one's own body, including vegetative measures like one's own heartbeat.

Recent brain imaging studies using positron-emission-tomography (PET) or functional magnetic resonance imaging (fMRI) have associated IA and EA with different neuronal networks [Boly et al., 2008, 2009, Fox and Raichle, 2007, Fransson, 2005, 2006, Golland et al., 2007, 2008, Raichle and Snyder, 2007, Vanhaudenhuyse et al., 2011]. EA has been linked to regions in mainly the lateral frontal and parietal cortex, the “extrinsic system,” as they are recruited during external and goal-oriented behaviour [Boly et al., 2007, Fransson, 2005, Golland et al., 2007]. In contrast, IA, as for instance during mind-wandering or self-oriented thoughts, recruits a network located along the anterior and posterior cortical midline structures (CMS). This “intrinsic system” includes the anterior and posterior cingulate cortex, the ventro- and dorsomedial prefrontal cortex and the retrosplenial cortex [Lou et al., 2004, Northoff et al., 2010a, 2011a, Goldberg et al., 2006].

The anterior and posterior CMS are also involved in the default-mode network, a collection of regions that show high metabolic and neuronal activity during the absence of an active task [Buckner et al., 2008, Fox et al., 2005, Raichle, 2010, Raichle and Snyder, 2007, Raichle et al., 2001, Shulman et al., 2009, Vincent et al., 2007]. This network is characterized by task-induced deactivations (i.e., a decrease of neuronal activity), and accordingly negative BOLD responses (NBRs) in response to external stimuli — that is, awareness of stimuli originating from outside the body [Fransson, 2005, Gusnard and Raichle, 2001, McKiernan et al., 2003, Raichle and Gusnard, 2005]. In addition to stimuli originating from the external environment, the neuronal activity in these midline regions also encounters internal stimuli originating continuously from one's own body, with recent studies suggesting that the awareness of such internal stimuli also induces NBRs in CMS like the mPFC and the precuneus [Schilbach et al., 2012, Wiebking et al., 2011].

With both IA and EA being seen to induce NBRs within midline regions, the question arises as to whether there is a differentiation between these stimulus domains in these regions at the functional level. Gamma-aminobutyric acid (GABA), the primary inhibitory neurotransmitter in the brain, is a likely candidate to mediate task-induced activity along CMS in the brain. This hypothesis is supported by recent work [Alcaro et al., 2010, Northoff et al., 2007]; however, it concerns only comparisons between GABA and NBRs induced by goal-oriented external stimuli, meaning that details of the role of GABA in processing internal stimuli are lacking. This leaves open the possibility that, should there be a distinction between IA and EA within the CMS as assumed, such a distinction can be related to some degree to differential GABAergic function.

A growing body of literature shows that psychiatric disorders are accompanied by a common pathophysiological pattern of GABAergic deficits [Bajbouj et al., 2006, Kalueff and Nutt, 2007, Luscher et al., 2011, Möhler, 2012, Petty, 1995, Sanacora, 2010, Smith and Rudolph, 2011]. Depression, for example, is characterized by GABAergic deficits, especially in anterior CMS [Bielau et al., 2007, Levinson et al., 2010, Walter et al., 2009] and altered states of awareness (decreased environment-focus and increased self-focus [Grimm et al., 2011a, Paulus and Stein, 2010, Stewart et al., 2001, Wiersma et al., 2011], which lend support to the hypothesis that GABAergic function might be considered as an influencing factor in the distinction between internally and externally guided awareness within the regions of interest.

The aim of this study is to investigate, firstly, the neuronal response to IA and EA in anterior and posterior CMS, and secondly their relationship to the binding potential of GABA_A receptors in these regions. We performed an fMRI study in healthy subjects to define CMS showing NBRs in response to internal (counting one's own heartbeat) and external (counting tones) stimuli. Since paradigms dealing with IA are specifically sensitive to artifacts resulting from blood flow, we carefully controlled the fMRI for structured noise to improve the sensitivity and specificity of the results. Next, we performed high-resolution [¹⁸F]-labelled flumazenil (FMZ) PET imaging in the same subjects to investigate the binding potential of GABA_A receptors. fMRI results were confirmed in an independent data sample using the same paradigm. The combined results of PET and fMRI suggest that neuronal inhibition related to GABAergic function (as reflected indirectly through GABA_A receptor binding potential) is more closely associated with processes of EA, rather than IA.

5.3 Materials and methods

5.3.1 Participants

Twenty-eight healthy subjects (10 female, 18 male, mean age 22.37 years \pm 3.77 SD, ranging from 18 to 34 years) underwent fMRI and 24 subjects (9 female, 15 male, mean age 22.6 years \pm 3.79 SD, ranging from 18 to 34 years) out of this group also underwent PET scanning. All subjects had a Beck Depression Inventory [Beck et al., 1961] score of 4 and were questioned about psychiatric, neurological, or medical diseases using a custom-made semistructured clinical questionnaire. Participants were recruited mainly from McGill University in Montreal and the local community. The study was approved by the local ethics committee. All participants gave their written informed consent before participating in this study and were financially compensated for their participation. Four subjects were excluded due to structural abnormalities in their anatomical scans or due to motion artifacts (> 2 mm), leaving 24 subjects with fMRI scans (9 female, 15 male, mean age 22.71 years \pm 3.95 SD, ranging from 18 to 34 years) and 20 subjects with PET scans (8 female, 12 male, mean age 23.05 years \pm 4.14 SD, ranging from 18 to 34 years). Functional MRI data from an independent data sample of 30 healthy subjects (15 female, 15 male, mean age 33.73 years \pm 11.62 SD, ranging from 22 to 60 years) were also analyzed.

5.3.2 Paradigm

The fMRI design (Suppl. figure C.2) was based on a paradigm introduced by Critchley and Pollatos [Critchley et al., 2004, Pollatos et al., 2007c]. Subjects were presented with three separate conditions: an internal task, an external task, and fixation periods, in a pseudo-randomized order (each jittered between 6 and 10 s). During the internal task, subjects were asked to silently count their own heartbeat. Similarly, an

external stimulus in the form of a tone had to be counted during the external task. In both cases, the subjects reported the number of counted heartbeats or tones after each trial by using a visual analog scale (3.5 s). To make the difficulty of both tasks closely comparable, tones were presented at an individually determined volume (i.e., just noticeable, like the heartbeat). The general presentation frequency of the tones was adapted to correspond to each subject's pulse-rate. To control for habituation effects, the onset time of the tones was jittered by 200 ms from this general frequency. During rest conditions—indicated by a dark fixation cross on a light background—subjects were instructed to relax and reduce any cognitive work during these periods. The fMRI paradigm for the independent data sample included the same conditions for fixation, IA, and EA. For a detailed description of the paradigm, please see Chapter 3.3.2.

5.3.3 fMRI data acquisition and analysis

Functional scans were acquired on a 3-Tesla whole body MRI system (Siemens Trio, Erlangen, Germany), using a 32-channel headcoil. The settings were as follows: forty-seven T_2^* -weighted echo planar images per volume with BOLD contrast; alignment at 30° off the AC-PC plane in an odd–even interleaved acquisition order; FoV: 205 x 205 mm²; spatial resolution: 3.2 x 3.2 x 3.2 mm³; $T_E = 25$ ms; $T_R = 2.270$ ms; flip angle = 90°. Functional data were recorded in one scanning session containing 580 volumes for each subject. A high resolution T_1 -weighted 3D structural image was also acquired. The fMRI data of 24 subjects were preprocessed and statistically analyzed by the general linear model approach using the SPM8 software package (<http://www.fil.ion.ucl.ac.uk>) and MATLAB 7.11 (The Mathworks, Natick, MA). All functional images were slice-time corrected with reference to the first acquired slice, corrected for motion artifacts by realignment to the mean functional image, and spatially normalized to a standard T_1 -weighted SPM template [Ashburner and Friston, 1999].

The normalization was generated by warping the coregistered anatomical image to the MNI T₁-template, and applying these parameters to all functional images. The images were resampled to 2 x 2 x 2 mm³ and smoothed with an isotropic 6 mm full-width half-maximum (FWHM) Gaussian kernel. The time-series fMRI data were filtered using a high pass filter (threshold 128 s). A statistical model for each subject was computed by applying a canonical response function [Friston et al., 1998].

Since structured noise still remains in the fMRI data after traditional steps of pre-processing, an independent component analysis (ICA) was applied to denoise the data and hence improve the sensitivity and specificity of the results. Using Probabilistic Independent Component Analysis, which is implemented in the MELODIC toolbox [Beckmann and Smith, 2004] of FSL (FMRIB's Software Library, <http://www.fmrib.ox.ac.uk/fsl/>) [Smith et al., 2004, Woolrich et al., 2009], a group ICA was performed on the pre-processed fMRI data, which were temporally concatenated across subjects. Two independent raters (CW, NWD) visually inspected the resulting components and classified them as noise or signals of interest according to a detailed description of an operationalized denoising procedure [Kelly et al., 2010]. In particular, components were considered as noise when they showed a ring-like pattern in the periphery of the brain and tightly clustered areas in the frontal regions [McKeown et al., 1998], clusters with a location in the white matter/ CSF or an association with blood vessels [Sui et al., 2009, Zou et al., 2009], spotted patterns diffusely spread over the brain, and time courses showing a saw-tooth pattern or spikes [McKeown et al., 1998]. Thirteen components were independently identified as noise and discarded from the original fMRI data through linear regression.

After removing nonbrain voxels using brain extraction tool (BET) [Smith, 2002], all three conditions (Fixation, IA, and EA) were then included in the SPM model as separate events including their feedback phases. Regionally specific condition effects were tested by employing linear contrasts for each subject and different conditions. The resulting contrast images were submitted to a second level random-effects analysis. Here, one-sample t-tests were used on images obtained for each subject's volume set and different conditions.

To control for the multiple testing problem, a familywise error rate correction was performed. The anatomical localization of significant neural responses in the main contrast (Fixation > IA/ EA; $P \leq 0.05$, FWE-corrected, $k \geq 10$) was assessed with reference to the standard stereotactic atlas by superimposition of the SPM maps on a standard brain template provided by SPM8.

Based on the functional results, three clusters of deactivation were found along the cortical midline and defined as regions of interest (ROI_{func}). To confirm findings in ROI_{func} , additional anatomical regions (ROI_{ana}) were identified due to their proximity to ROI_{func} . Using the WFU-pickatlas (AAL atlas (automated anatomical labeling) of the Wake-Forrest University, NC), four medial regions were defined: the frontal middle orbital cortex, the frontal superior middle cortex, the anterior cingulate, and the precuneus. For each region, the left and right hemispheres were calculated separately. Percent signal changes (PSC) from these CMS were extracted using the MarsBaR toolbox (<http://www.sourceforge.net/projects/marsbar>). All data were controlled for possible outliers. Whole brain regressions using BP_{ND} of an anatomical region were inclusively masked by ROI_{ana} on the whole ($P \leq 0.005$, uncorrected, $k \geq 20$). Analysis for ROI_{func} is set to ($P \leq 0.001$, uncorrected, $k \geq 20$).

Regional specificity was tested by applying ROI_{func} and correspondent ROI_{ana} that were not located along the midline regions. Confirming fMRI results, since the physiologi-

cal basis of deactivation is still a controversial issue in the current literature [[Lauritzen et al., 2012](#)], by using an independent set of data, in line with proposed good practice [[Kriegeskorte et al., 2009](#), [Poldrack and Mumford, 2009](#), [Vul et al., 2009](#)], these three ROI_{func} were also applied to another sample (acquired at the Department of Neurology, Otto-von-Guericke University Magdeburg, Germany). Subjects in both studies performed the same tasks (IA, EA, Fix), and have been instructed by the same researcher (CW). Functional measurements of this independent data set were performed on an identical 3-Tesla whole body MRI system (Siemens Trio, Erlangen, Germany).

The headcoils differed across studies (an 8-channel headcoil compared to a 32-channel headcoil), but research has been shown that fMRI results across different imaging sites are very well comparable, even when comparing across different headcoils and scanner machines [see for example [Casey et al., 1998](#), [Gountouna et al., 2010](#), [Kaza et al., 2011](#), [Zou et al., 2005](#)].

The settings were as follows: thirty-two T_2^* -weighted echo planar images per volume with BOLD contrast; alignment parallel to the AC- PC plane in an odd–even interleaved acquisition order; FoV: 224 x 224 mm²; spatial resolution: 3.5 x 3.5 x 4 mm³; $T_E = 30$ ms; $T_R = 2.000$ ms; flip angle = 80°. A total of 1.160 volumes were recorded for each of the 30 healthy subjects. These data were processed in the exact same way (including ICA denoising) as the main data set. This was a reanalysis of a data set presented beforehand (see Chapter 2).

5.3.4 PET-Image Acquisition and Reconstruction

Twenty subjects underwent PET imaging with FMZ, a GABA antagonist that binds at the GABA_A benzodiazepine receptor. It is a common method to measure GABA_A receptor density *in vivo* in humans [Frey et al., 1991, Salmi et al., 2008]. [¹⁸F]FMZ has the advantages of a long half-life, a good affinity for the benzodiazepine site on the GABA_A receptor ($K_i = 11.6$ nM), and a short positron range, which enables the production of high-quality images. PET imaging was done randomly either before or after the fMRI (mean duration SD between both types of scans: 1.9 3.6 days). Whole-brain [¹⁸F]FMZ binding potential (BP_{ND}) values were obtained using a Siemens ECAT HRRT (High Resolution Research Tomograph) PET system (Siemens Medical Solutions, Knoxville, TN) [de Jong et al., 2007].

[¹⁸F]FMZ was synthesized as published previously, with a specific activity between 1,500 and 2,000 Ci/ mmol [Massaweh et al., 2009]. Head movement was minimized with a head-restraining adhesive band. A 6-min transmission scan (¹³⁷Cs-point source) was first acquired for attenuation correction followed by an intravenous tracer injection (over 60 s) of 260.7 MBq (± 21.24 SD) of [¹⁸F]FMZ. Subjects were instructed to close their eyes and remain awake. List-mode data were acquired for a period of 60 min and then binned into a series of 26 sequential sets of 2.209 span 9 sinograms of increasing temporal duration, ranging from 30 s to 5 min.

PET data were reconstructed using a 3D OP-OSEM algorithm (10 iterations and 16 subsets) [Hong et al., 2007, Hudson and Larkin, 1994] with full accounting for scatter, random coincidences, attenuation, decay, dead-time, and frame-based motion correction [Costes et al., 2009]. The images used had a voxel size of 1.22 x 1.22 x 1.22 mm³ (256 x 256 x 207 voxels). GABA_A BP_{ND} maps were then calculated according to the Logan plot method, using each of the pons ($BP_{ND-Pons}$) and cerebral white matter as the reference tissue region (BP_{ND-WM}) [Logan et al., 1996].

In a final step, all BP_{ND} images were aligned to MNI space. Two separate reference regions were used as each in itself has limitations in relation to the Logan method. The pons has commonly been used in [^{18}F]FMZ studies [Frankle et al., 2012, Klumpers et al., 2012, Odano et al., 2009, Pearl et al., 2009]; however, recent studies have suggested that it displays a significant degree of specific binding [Frankle et al., 2012, 2009, Klumpers et al., 2008, Millet et al., 2002]. The cerebral white matter has been proposed as an alternative reference region due to its lower degree of specific binding [Klumpers et al., 2008, la Fougere et al., 2011]. This region is not without downsides; however, specifically its location close to grey matter and CSF (leading to potential activity spill-in from these regions) and the fact that it is not clear that the level of nonspecific binding is the same in grey and white matter, an assumption inherent to the Logan method [Lammertsma and Hume, 1996].

Thus, given these independent limitations of the two reference regions, both were used and the correlation results seen to be consistent across both BP_{ND} values taken to be highly reliable. As $GABA_A$ receptors have been previously utilized as markers of neuronal density [la Fougere et al., 2011], there is the potential that any relation between BP_{ND} and PSC could be the result of the former acting as a proxy ROI neuronal volume measure. To account for this possibility, the segmented MR grey matter image, which contains voxel values between 1 and 0, was convolved with a Gaussian kernel of 2.5 mm FWHM to simulate the spatial resolution of the HRRT PET scanner. The proportion of grey matter in each ROI for each subject was calculated using FSL and included as a control variable in all analysis regarding BP_{ND} values. The individual biochemical measures for specific regions were entered into a second-level correlation analysis in SPM, using the proportion of grey matter as regressor of no interest in all calculations. Controlling for grey matter, BP_{ND} values were also correlated (two-tailed) with PSC derived from each ROI.

5.4 Results

5.4.1 Behavioural data

The mean reaction time for internal stimuli was 0.95 s (\pm 0.18 SD) and for external stimuli 0.98 s (\pm 0.23 SD). Reaction times showed no difference between stimuli types and no significant correlation with PSC or PET-BP_{ND} values in the main regions.

5.4.2 fMRI

To investigate BOLD responses in CMS during IA and EA, a well-established fMRI paradigm was used [Critchley et al., 2004, Pollatos et al., 2007c, Wiebking et al., 2010, 2011] (Suppl. figure C.2). As detailed in Figure 5.1 (see SPM images on the left side), the contrast (Fixation > IA/ EA; $P \leq 0.05$, FWE-corrected, $k \geq 10$) revealed clusters of deactivation in the left mPFC as well as in the bilateral precuneus. These functional clusters were defined as ROI_{func}:

1. Left mPFC: center of mass (x,y,z in MNI space): -6, 54, 4, volume: 688 mm.
2. Bilateral precuneus: center of mass (x,y,z in MNI space): -1, -55, 26, volume: 5.624 mm.

A third cluster was found in the medial frontal region (see also Suppl. figure C.1): the right mPFC, center of mass (x,y,z in MNI space): 9, 54, 10, volume: 96 mm. Calculating PSC in these functional clusters showed clear task-induced deactivations during both IA and EA across all regions. During fixation, small NBRs were observed in the bilateral precuneus (see bar diagram on the left side of Figure 5.1) and the right mPFC (see bar diagram in Suppl. figure C.1); a small positive BOLD response occurred in the left mPFC (Figure 5.1).

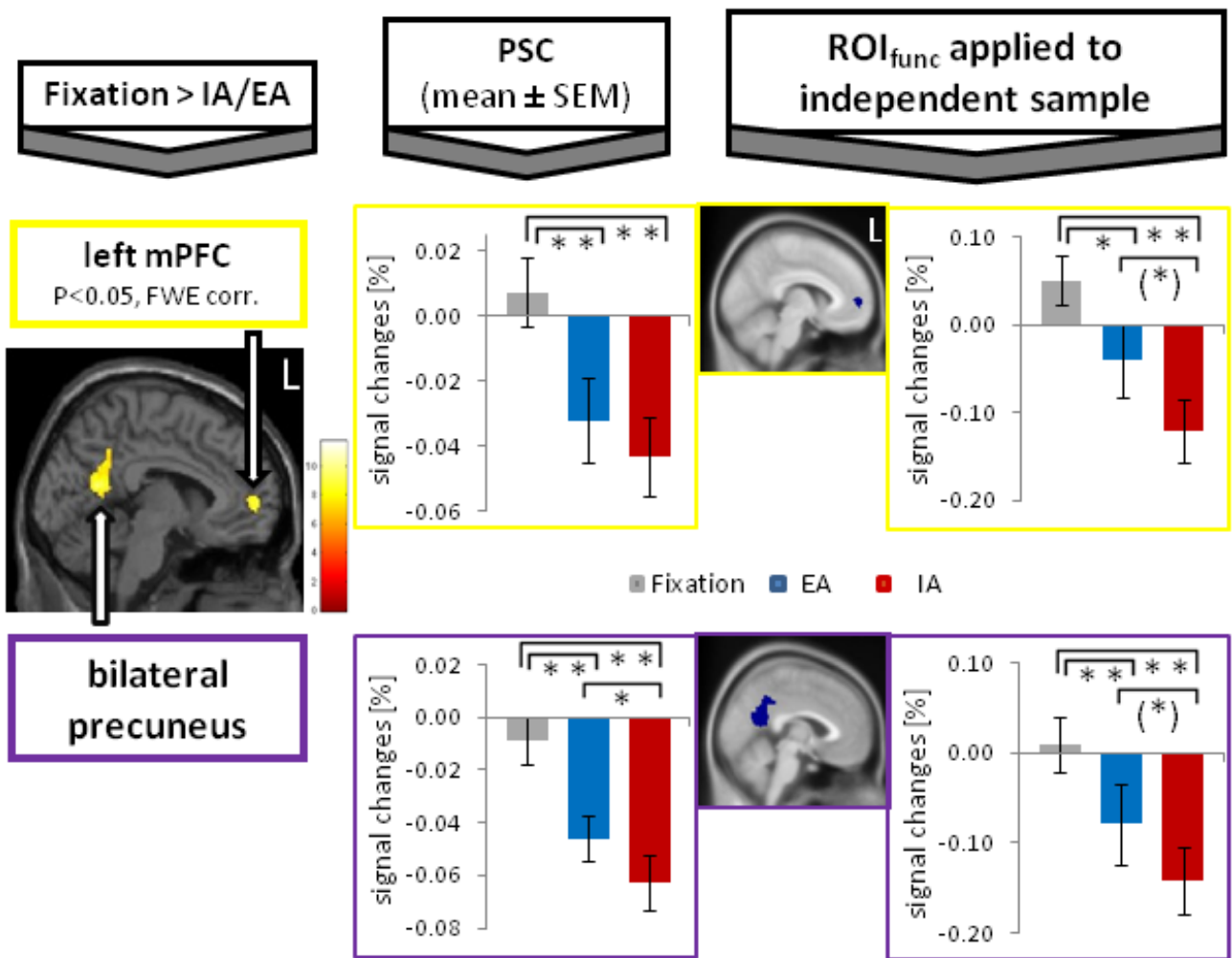


Figure 5.1: Cortical midline regions of interest (ROI_{func} , yellow colour) were defined by the contrast [Fixation > Internal (IA)/ External Awareness (EA)] ($P \leq 0.05$, FWE-corrected, $k \geq 5$, $n = 24$ subjects; see SPM images on the left side). Bar diagrams, next to the SPM images, show percent signal changes (PSC, mean \pm SEM) and accordingly negative BOLD responses (NBRs) during fixation (grey), EA (blue), and IA (red). Paired t-tests between the PSC were calculated (** $P \leq 0.005$, * $P \leq 0.05$, (*) $< P 0.1$). ROI_{func} were also applied to an independent data sample ($n = 30$ subjects), and paired t-tests between PSC were calculated.

All three regions differed significantly ($**P \leq 0.005$) when comparing fixation to IA or EA, respectively (using paired t-tests, two-tailed). The distinction between IA and EA was less pronounced across all regions, with significant differences ($*P \leq 0.05$) in the bilateral precuneus and the right mPFC and no difference in the left mPFC. To support the results of task-induced deactivations in CMS and to test for statistical independence, in line with the recommendations made by Kriegeskorte, Poldrack, and Vul [Kriegeskorte et al., 2009, Poldrack and Mumford, 2009, Vul et al., 2009], these ROI_{func} were also applied to an independent data sample that used the same fMRI paradigm and image processing. The PSC of the independent data sample (bar diagrams on the right side of Figure 5.1 and Suppl. figure C.1) showed a similar pattern between the three conditions. Signal changes for fixation differed significantly from the two conditions ($**P \leq 0.005$ or $*P \leq 0.05$), except for the right mPFC (Suppl. figure C.1), where EA showed a small positive BOLD response and hence no difference between fixation and EA. Compared to fixation, the differentiation between the signal changes for IA and EA were also less pronounced across all regions [$*P \leq 0.05$ in the right mPFC and (*) $P \leq 0.1$ in the left mPFC and bilateral precuneus].

5.4.3 PET

Having demonstrated in the two samples that both IA and EA induce reliable degrees of NBRs in the regions studied, the potential involvement of GABA_A-related function in these processes was investigated. GABA_A BP_{ND-Pons} values for each ROI_{func} (see above) were extracted from each subject's [¹⁸F]FMZ-PET scan (Figures 5.2 and 5.3 on the left side) and correlated with the signal differences between fixation and EA. Since the proportion of grey matter in each ROI was included as a control variable (see Methods; Table 5.1), the correlation graphs use the residuals of BP_{ND-Pons} and PSC.

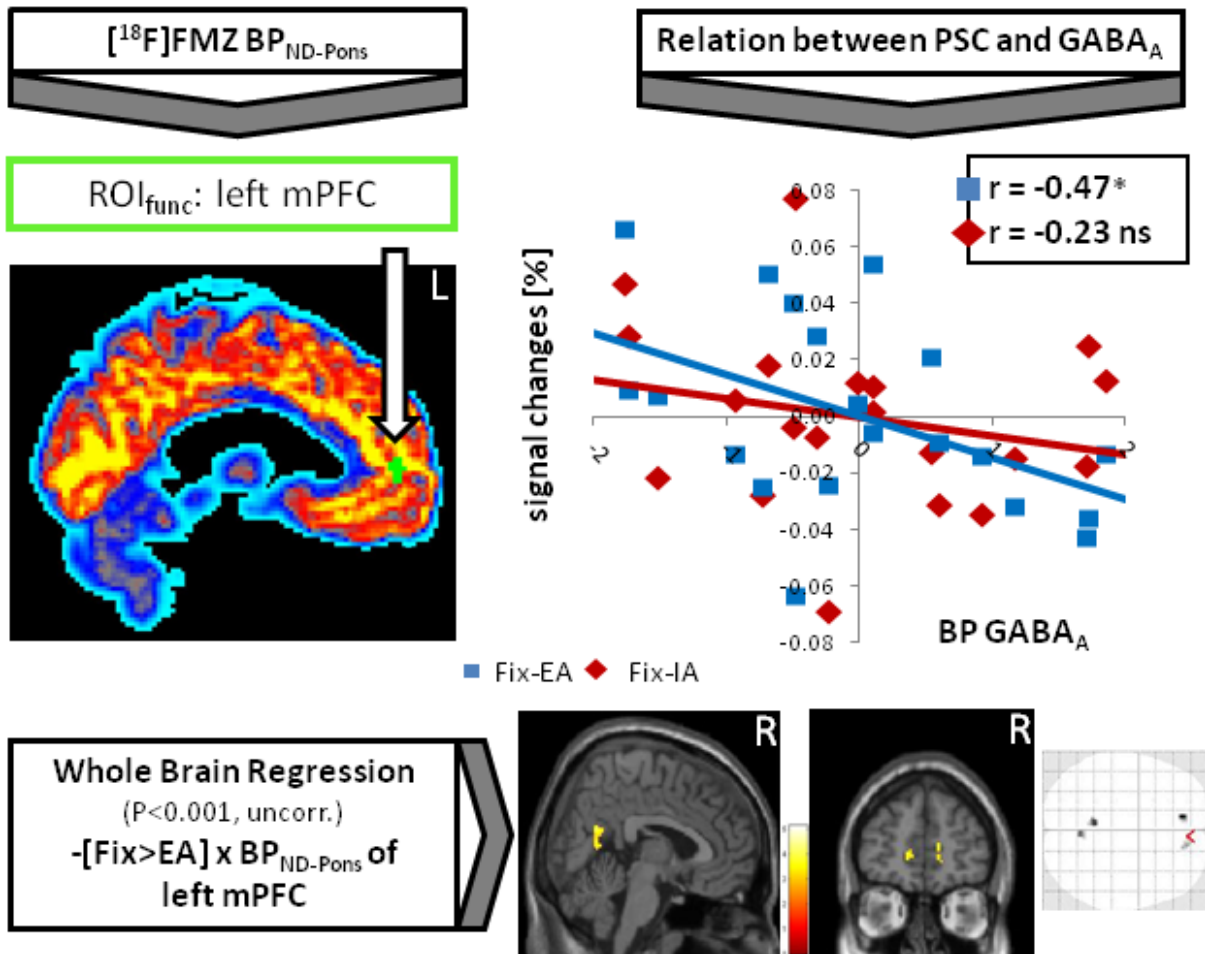


Figure 5.2: $[^{18}\text{F}]$ FMZ-PET imaging was used to calculate binding potentials ($\text{BP}_{\text{ND-Pons}}$) for GABA_A receptors, applying functional regions of deactivation (ROI_{func} , green colour) derived from the contrast [Fixation > Internal/ External Awareness] ($P \leq 0.05$, FWE-corrected, $k \geq 5$; see also Figure 5.1). These values were correlated (controlled for grey matter) with percent signal changes (PSC) of the ROIs (see partial correlation graph showing the residuals of $\text{BP}_{\text{ND-Pons}}$ and PSC, $*P \leq 0.05$, $**P \leq 0.01$). Moreover, $\text{BP}_{\text{ND-Pons}}$ values were entered into a whole brain regression analysis in SPM (controlled for the proportion of grey matter). The lower part shows a negative correlation for the contrast [Fixation > External Awareness] with $\text{BP}_{\text{ND-Pons}}$ ($P \leq 0.001$, uncorrected, $k \geq 20$). Shown here are the results for the left mPFC, Figure 5.3 shows the results for the bilateral precuneus. Results for the right mPFC can be found in Supplementary figure C.1. Calculations applying $\text{BP}_{\text{ND-WM}}$ can be found in Figure 5.4.

In all ROI_{func}, the difference in PSC between fixation and EA was found to be negatively associated with intra-regional GABA_A BP_{ND-Pons} (Figure 5.2: * $P \leq 0.05$; left mPFC, Figure 5.3: ** $P \leq 0.01$, bilateral precuneus). In contrast, no relationship was observed between BP_{ND-Pons} values and the difference between fixation and IA or other signal changes in any of the ROI_{func} (Table 5.1). Calculations using BP_{ND-WM} can confirm this pattern in the anterior midline, but not the posterior region (Table 5.1). The difference between the two correlations was significant for the bilateral precuneus ($P \leq 0.05$, one-tailed) and marginal significant ($P \leq 0.1$, one-tailed) for the right mPFC.

ROI _{func} (x,y,z)/ k/ T-value	BP _{ND-Pons}	Percent Signal Changes (PSC)			
		PSC: Fixation PSC: IA PSC: EA PSC: Fix-IA PSC: Fix-EA	Partial correlation (controlled for grey matter) between PSC and BP _{ND-Pons}	BP _{ND-WM}	Partial correlation (controlled for grey matter) between PSC and BP _{ND-WM}
Left mPFC (-4,56,6)/ 86/ 9.18	6.7±1.1	0.01±0.05	r = -0.31	9.0±1.2	r = -0.05
		-0.04±0.05	r = -0.14		r = 0.01
		-0.03±0.05	r = 0.02		r = 0.27
		0.05±0.03	r = -0.23		r = -0.10
		0.04±0.03	r = -0.47*		r = -0.49*
Right mPFC (8,56,10)/ 12/ 7.08	6.4±1.8	0.00±0.04	r = 0.05	8.1±1.9	r = -0.03
		-0.04±0.05	r = 0.10		r = -0.04
		-0.02±0.04	r = 0.29		r = 0.18
		0.04±0.03	r = -0.11		r = 0.02
		0.02±0.03	†r = -0.46(*)		r = -0.39(*)
Bilateral Precuneus (0,-48,38)/ 703/ 8.44	6.8±1.0	0.00 ±0.04	r = -0.11	9.1±1.2	r = 0.04
		-0.06±0.05	r = -0.07		r = -0.05
		-0.05±0.04	r = 0.33		r = 0.29
		0.06 ±0.02	r = -0.04		r = 0.17
		0.04 ±0.03	r = -0.59**		r = -0.34

Table 5.1: Three cortical midline regions were defined using the contrast [Fixation > IA/ EA] ($P \leq 0.05$, FWE-corrected, $k \geq 10$, $n = 24$ subjects, coordinates in MNI space).

For each region, binding potential values (BP_{ND-Pons} using the pons as reference tissue and BP_{ND-WM} using the white matter as a reference tissue) for GABA_A receptors were calculated ($n = 20$ subjects) and correlated (two-tailed, controlled for grey matter) with percent signal changes (PSC).

†Note: result for the right mPFC is due to an outlier regards extracted PSC.

* $P \leq 0.05$ ** $P \leq 0.01$

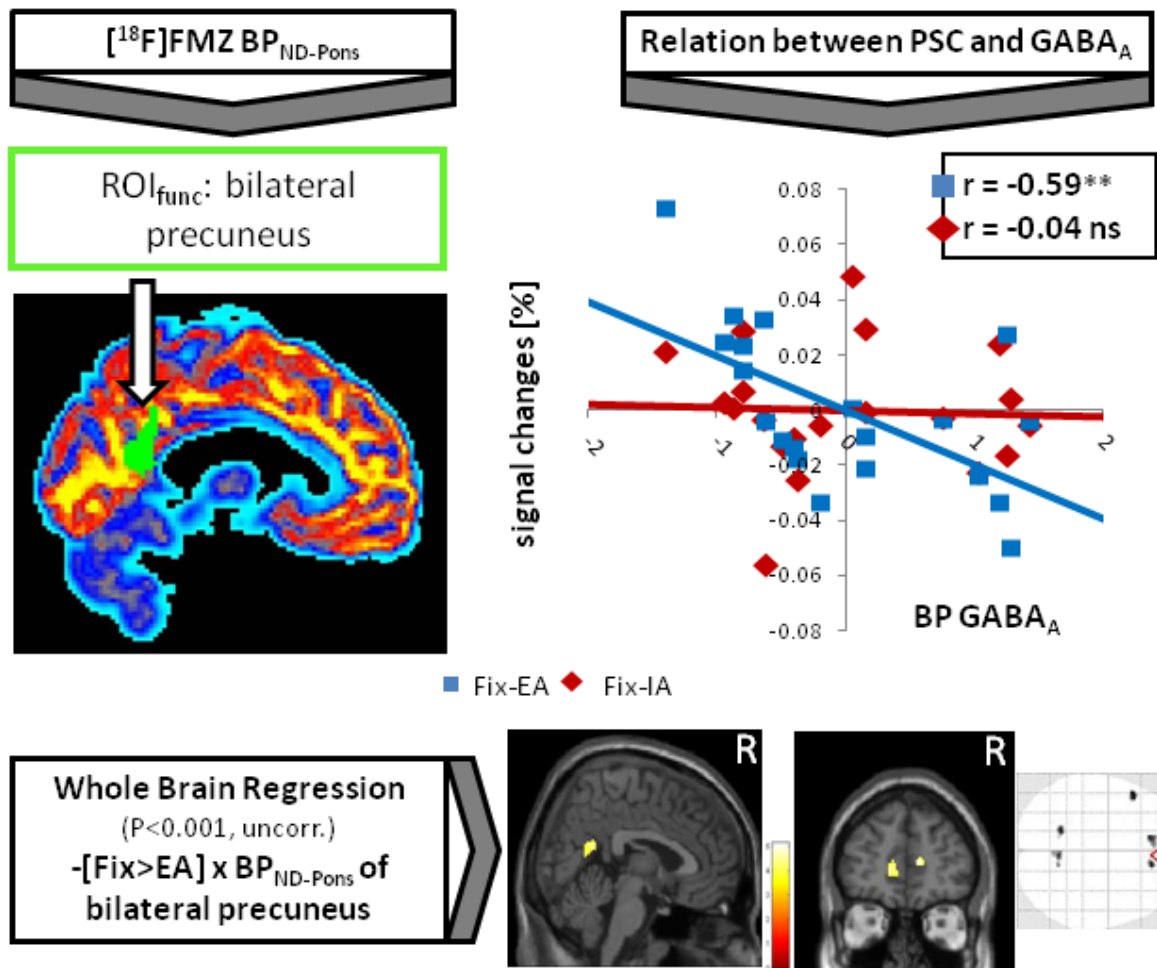


Figure 5.3: According to Figure 5.2, shown here are results for the bilateral precuneus.

The same calculations were carried out using the brain regions also derived from the main contrast, but which were not located along the cortical midline. None of these areas showed a significant relationship between BP_{ND} and PSC (Suppl. table C.1). Biochemical measures for each ROI_{func} were entered into a second-level correlation analysis in SPM. In particular, the anterior regions showed a negative correlation between BP_{ND} and the contrast containing EA [Fixation > EA]. Whole brain regressions using $BP_{ND-Pons}$ are illustrated in the lower parts of Figures 5.2 & 5.3 ($P \leq 0.001$, uncorrected, $k \geq 20$). Regressions using $BP_{ND-Pons}$ are shown in the right lower corner of Figure 5.4 (green-bordered, $P \leq 0.005$, uncorrected, $k \geq 40$).

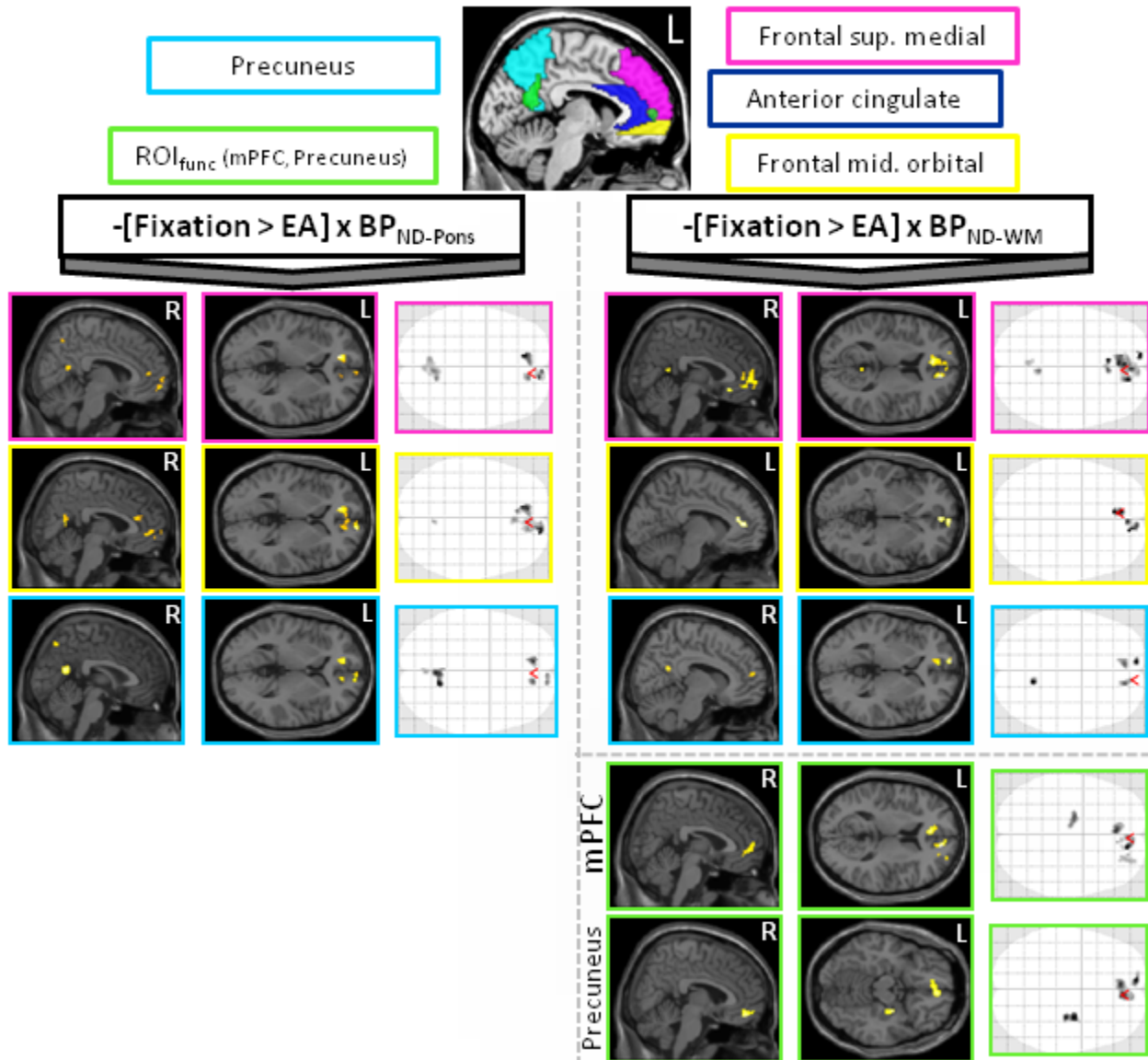


Figure 5.4: Using the WFU-pickatlas, four anatomical regions have been defined due to their proximity to ROI_{func} : the frontal middle orbital cortex (bordered yellow throughout tables and figures), the frontal superior middle cortex (pink), the anterior cingulate cortex (dark blue) and the precuneus (turquoise). For these regions, BP_{ND} values have been calculated and entered into a whole brain regression analysis in SPM (controlled for the proportion of grey matter). The left side shows negative correlations for the contrast $[Fixation > EA]$ with $BP_{ND-Pons}$, the right side shows negative correlations for this contrast using BP_{ND-WM} values ($P \leq 0.005$, uncorrected, $k \geq 20$, inclusively masked with ROI_{ana}). Detailed information about positive/ negative results of right/ left sided ROI_{ana} for the contrasts $[Fix-EA]$ and $[Fix-IA]$ is provided in Suppl. table C.2. BP_{ND} values of the anterior cingulate cortex show no correlating activity. In the lower right corner (green, $P \leq 0.005$, uncorrected, $k \geq 40$) whole brain regressions using BP_{ND-WM} values for our own activated clusters (left mPFC and precuneus) are illustrated.

No results were observed in the contrast containing IA [Fixation > IA]. Detailed results about the conducted calculations are provided in Supplementary table C.2. Again, as already shown by the previous results, it is specifically EA compared to fixation that showed a negative connection with BP_{ND} rather than IA.

Finally, to support findings in ROI_{func} , the biochemical measures ($BP_{ND-Pons}$ and BP_{ND-WM}) for anatomical-defined midline regions (ROI_{ana}) were calculated and partial correlated with signal differences (see Table 5.2) as well as entered into a second-level correlation analysis in SPM (Figure 5.4). Results in Table 5.2 focus on reporting the central values, namely, the signal differences [Fix-IA] and [Fix-EA], since signal changes for fixation, IA, or EA showed no correlation with BP_{ND} . Specifically the anterior midline regions, the frontal middle orbital cortex and the frontal superior middle cortex, showed consistent negative correlations between BP_{ND} and [Fix-EA] (see Table 5.2). Correlation analysis in SPM confirmed this pattern along CMS between BP_{ND} and [Fix-EA] (Figure 5.4). Also in accordance to ROI_{func} (Table 5.1), the posterior region of the precuneus revealed not a clear pattern. BP_{ND} values of the anterior cingulate cortex did not lead to significant results in neither [Fix-EA] nor [Fix-IA] as well as nonmedial ROI_{ana} , like the amygdala and hippocampus (see Suppl. table C.2).

ROI _{ana}	Size (mm)	BP _{ND-Pons}	BP _{ND-WM}	Partial correlation (controlled for grey matter)			
				BP _{ND-Pons}		BP _{ND-WM}	
				PSC: Fix-IA PSC: Fix-EA r-value	P-value	PSC: Fix-IA PSC: Fix-EA r-value	P-value
Front. Mid. Orb. Cortex, R	6848	5.1±0.7	7.2±0.9	r = -0.4 r = -0.5*	P = 0.1 P = 0.02	r = -0.2 r = -0.5*	P = 0.5 P = 0.03
Front. Mid. Orb. Cortex, L	5752	5.7±0.9	7.5±1.1	r = 0.05 r = -0.3(*)	P = 0.8 P = 0.1	r = -0.01 r = -0.5*	P = 0.9 P = 0.04
Front. Sup. Mid. Cortex, R	17072	5.0±0.9	6.8±1.0	r = -0.4(*) r = -0.5*	P = 0.05 P = 0.02	r = -0.2 r = -0.6**	P = 0.4 P = 0.01
Front. Sup. Mid. Cortex, L	23936	4.9±0.9	6.9±1.1	r = -0.05 r = -0.4(*)	P = 0.8 P = 0.05	r = 0.2 r = -0.4(*)	P = 0.4 P = 0.06
Anterior Cingulate, R	10504	4.5±0.7	6.7±0.7	r = -0.4(*) r = -0.4(*)	P = 0.09 P = 0.1	r = -0.1 r = -0.1	P = 0.8 P = 0.8
Anterior Cingulate, L	11192	5.5±0.9	8.0±0.8	r = -0.2 r = -0.6*	P = 0.4 P = 0.01	r = -0.1 r = -0.3	P = 0.8 P = 0.2
Precuneus, R	26120	4.7±0.8	6.7±0.8	r = -0.01 r = -0.3	P = 0.9 P = 0.2	r = 0.0 r = -0.2	P = 0.9 P = 0.5
Precuneus, L	28224	4.8±0.8	6.8±0.8	r = -0.1 r = -0.5*	P = 0.7 P = 0.02	r = 0.0 r = -0.3	P = 0.9 P = 0.2

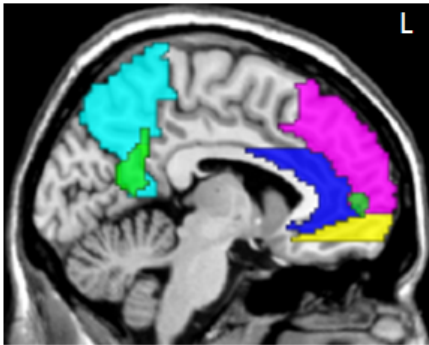


Table 5.2: BP_{ND} values (BP_{ND-Pons} as well as BP_{ND-WM}) were calculated for four anatomical regions (ROI_{ana}), defined by the WFU-pickatlas (AAL atlas of the Wake-Forrest University, NC, US). Both values were partial correlated (two-tailed, controlled for grey matter) with signal differences for (Fixation-IA) and (Fixation-EA, grey shaded).

Results for ROI_{func} (mPFC, precuneus) are listed in Table 5.1.

5.5 Discussion

The fMRI data from this study demonstrated the induction of NBRs during both IA and EA in anterior and posterior CMS (mPFC and precuneus) when compared to fixation periods (i.e., the absence of specific external stimuli). Whilst the induction of NBRs during external stimuli is in accordance with previous studies focusing on different kinds of external stimuli or goal-oriented tasks [[Gusnard et al., 2001](#), [Raichle and Snyder, 2007](#), [Simpson Jr. et al., 2001](#)], the present study extends these findings by showing the induction of NBRs also during IA. This was suggested by a previous exploratory fMRI study [[Wiebking et al., 2011](#)] (see Chapter 2), and is in accordance with a specific re-analysis of this data set, as well as with a recent meta-analysis [[Schilbach et al., 2012](#)].

Combining fMRI with biochemical measures derived from PET imaging, this study also investigated a possible differential association between the availability of GABA_A receptors (as reflected by the binding potential) and NBRs in CMS. BP_{ND} values in the anterior cortical regions, such as the mPFC (ROI_{func}), frontal superior medial cortex, and frontal middle orbital cortex (both ROI_{ana}) showed a negative relationship to NBRs induced by EA rather than IA when compared to fixation. Since correlation results across both BP_{ND} values are closely comparable, especially in the anterior cortical regions, our results can be considered as valid and not due to advantages or disadvantages of one or the other reference tissue regions for the BP_{ND} calculations. However, results concerning posterior regions were less stringent and need to be interpreted with caution.

Of note was the absence of correlating brain regions when BP_{ND} values of the anterior cingulate were applied. This can potentially be explained by the size of the anatomical region, which includes both the task-negative pgACC (perigenual anterior cingulate cortex) and the task-positive sgACC (supragenual anterior cingulate cortex) [see for ex-

ample [Duncan et al., 2011](#)]. The opposite neuronal behaviour of these regions might lead to a nonresult in the SPM analysis. These findings indicate that GABA_A receptor availability within the regions studied is more closely associated with the processing of external, rather than internal, stimuli when compared to fixation in the context of the task used. Since there is evidence that NBRs can be mediated, at least in part, by GABA [[Northoff et al., 2007](#)], the processing of internal stimuli might have a more complex relationship with GABA that is not captured by the methods employed here.

Our findings in healthy subjects might help to form concepts about pathophysiological mechanisms of altered states of awareness as observed in psychiatric disorders. Although speculative at this point, the GABAergic deficit hypotheses of anxiety and depression [[Kalueff and Nutt, 2007](#), [Levinson et al., 2010](#), [Mohler, 2011](#), [Pilc and Nowak, 2005](#), [Sanacora, 2010](#)] might in future research be linked to their altered awareness states [[Grimm et al., 2011a](#), [Paulus and Stein, 2010](#), [Wiersma et al., 2011](#)].

Several limitations of the study should be noted. Firstly, a linear relationship between the BP_{ND} of GABA_A receptors and the degree of neuronal inhibition obtained in fMRI remains speculative at this point [for more details see [Donahue et al., 2010](#), [Shmuel et al., 2002](#)]. This assumption needs to be confirmed in future studies in animals and humans, as does how GABA_A receptor availability is exactly related to intracellular and extracellular concentrations of GABA.

Secondly, apart from reaction time during fMRI, no other measures concerning the degree of awareness were recorded. Whilst reaction time was not related to either the degree of induced NBR or the GABA_A receptor BP_{ND}, further studies need to provide a more extensive and detailed monitoring during fMRI (e.g., heart rate or galvanic skin response). One may argue that our measurement of IA still requires a lot of EA. To underline our result that GABA BP_{ND} is more closely associated with mediating EA

rather than IA, the inclusion of different types of IA, for example, mind wandering, should be considered in future experiments.

Moreover, we defined a default-mode of the brain as the neuronal activity during the absence of an active task [Shulman et al., 2009], which was operationalized using the fixation cross period. Even viewing this cue may, however, induce some relevant activity, thus precluding what has been described as a “pure” default-mode [Logothetis et al., 2009]. Since we were interested in the induction of positive and negative BOLD responses in CMS during the conditions of interest, the fixation periods used were rather short. We are aware that our results must be replicated for longer rest periods in order to be sure that they are not due to overlapping BOLD responses from preceding activation periods.

Finally, the fact that IA-induced NBRs did not correlate with the BP_{ND} for $GABA_A$ leaves open the exact underlying differential mechanism, which ties into the point that a linear relationship between BP_{ND} and neuronal responses in fMRI is tentative. Also, the exact physiological mechanism underlying the BOLD signal, and especially the NBRs, remains unclear [Lauritzen et al., 2012, Logothetis, 2008]. As such, future investigations may wish to test for the distinction between IA and EA by measuring single unit activity and local field potentials during, for instance, GABAergic modulation.

In addition, future ideas to investigate the relationship between changes in BOLD signal in CMS in response to IA and EA and changes in $GABA_A$ BP_{ND} may wish to include a challenge study [e.g., with tiagabine Frankle et al., 2012]. Conceivably, even a behavioural paradigm during [^{18}F]flumazenil PET scans can be applied, as changes in BP_{ND} would represent a more dynamic component of the GABAergic system.

In conclusion, this study demonstrates that both IA and EA induce NBRs in anterior and posterior midline regions. Moreover, IA and EA, when taken in comparison to fixation, each show a different association pattern to the BP_{ND} of $GABA_A$ receptors. Hence,

GABAergic receptor availability, and thus potentially GABAergic activity, may be considered as an influencing factor in the mediation of a distinction between external, as compared to internal, processing in CMS. This might have implications for psychiatric disorders like MDD, which show a combination of altered awareness and GABAergic function.

5.6 Acknowledgements

The authors thank the staff from the MNI for their excellent technical support as well as K. Dedovic and A. Perna for helping with the subjects' recruitment and screening procedures. Financial contributions are acknowledged from the Hope of Depression Research Foundation (HDRF), the Canadian Institutes of Health Research (CIHR) and the EJLB-Michael Smith Foundation (CIHR-EJLB) to GN. Financial Disclosures: The authors declare no conflicting financial interest in relation to the work described.

Chapter 6

GABA in the insula – a predictor of the neural response to interoceptive awareness

6.1 Abstract

The insula has been identified as a key region involved in interoceptive awareness. Whilst imaging studies investigated the neural activation patterns in this region involved in intero- and exteroceptive awareness, the underlying biochemical mechanisms still remain unclear. Combining MRS in the left insula with a well-established fMRI task for interoceptive awareness in the same healthy individuals, we demonstrated that GABA concentration in a region highly involved in interoceptive processing is specifically modulating neural responses to interoceptive stimuli. In addition, both GABA and interoceptive signal changes in the insula predicted the degree of depressed affect, as measured by a hopelessness scale. On the one hand, the GABAergic modulation shown in this study provides novel insight into the biochemical underpinnings of insula function and interoception. On the other hand, through the additional association of both GABA and neural activity during interoception with depressed affect, these data bear also important implications for psychiatric disorders like depression and anxiety, where GABAergic deficits, altered insula function and abnormal affect coincide.

6.2 Introduction

A growing body of research has suggested that the insula cortex integrates the processing of various stimulus types [Craig, 2009]. This includes stimuli that originate from both internally and externally to the body. Processing of such stimuli has been located within the insula and has been suggested to underlie our ability to be aware of our internal states [Craig, 2002], termed interoceptive awareness (IA). Imaging studies in humans of the insula have provided details of task-specific subdivisions within the region [Chang et al., 2012, Simmons et al., 2012], highlighting, for example, distinctions between the anterior and posterior insula [Farb et al., 2012a]. In addition, functional connectivity analysis have been used to identify networks of regions in the brain that have patterns of spontaneous activity that are correlated with that in the insula [Cauda et al., 2011, Deen et al., 2011]. What remains unclear, however, is the neurochemistry that underlies task-induced activity in the insula in humans.

Studies regarding regions of the brain other than the insula have revealed links between task-evoked neural responses and a number of different neurotransmitters in humans. Concentrations of GABA (gamma-aminobutyric acid) – the main inhibitory transmitter in the brain – in the visual cortex have been shown in a number of studies to be correlated with both the amplitude of the BOLD response to visual stimuli and with the particular dynamic properties of this response (i.e., the latency and width) [Muthukumaraswamy et al., 2009, 2012, Donahue et al., 2010].

Similarly, GABA concentrations in the medial prefrontal cortex (mPFC) also correlate with BOLD responses to stimuli [Northoff et al., 2007]. At the same time, concentrations of glutamate – the primary excitatory transmitter – as measured in areas of the anterior cingulate have been shown to correlate with task-induced activity changes in multiple other brain regions during different tasks [Duncan et al., 2011, Falkenberg et al., 2012].

Taken together, these prior results suggest that GABA and glutamate concentrations may be related to IA-related responses in the insula.

Under a prominent theory of emotions that views them as arising, in part, from bodily states, IA is linked closely to affective experience [Lamm and Singer, 2010]. Support for this link comes from a growing body of research, including studies that show an anatomical overlap in the insula between emotional and interoceptive processing [Kelly et al., 2012, Zaki et al., 2012] and work that demonstrates a correlation between quality of emotional experience and bodily awareness [Wiens, 2005, Herbert et al., 2007, Pollatos et al., 2007c, Dunn et al., 2010b].

The link between IA activity in the insula and emotional experience suggests a role for the region in mood disorders, such as major depressive disorder (MDD), that are characterised by negative affect. Such an involvement of the insula in depression is supported by findings of altered functional responses in the region [Liotti et al., 2002, Paulus and Stein, 2010], as well as structural changes [Sprengelmeyer et al., 2011] and deficits in IA [Terhaar et al., 2012]. In addition to such changes, MDD is associated with altered GABAergic and glutamatergic function in multiple brain regions [Alcaro et al., 2010, Zhao et al., 2012], whilst drugs acting on these systems have an antidepressant effect [Möhler, 2012, Sanacora et al., 2012]. These combined factors suggest that IA in the insula may be related to depressive symptoms of negative affect and that this association is related to glutamate or GABA in the region. This remains to be investigated, however.

Based on these combined strands of IA, insula neurochemistry, and the relation between the insula and depressive symptoms, we examined whether the concentrations of GABA or glutamate and glutamine (Glu + Gln = Glx) can be related to neural activity in the insula during IA and to depressed affect. A well-established paradigm for func-

tional magnetic resonance imaging (fMRI) was used [Wiebking et al., 2010, 2011] (see Chapters 3 and 2), that consisted of a target task to induce IA (heartbeat counting), a closely matched control task to induce exteroceptive awareness (EA, tone counting), and fixation periods. In a separate session, measures of GABA and Glx concentrations from a voxel located in the target region, the left insula, were obtained in the same healthy participants using magnetic resonance spectroscopy (MRS). A control voxel was placed in the mPFC. It was hypothesised that BOLD responses in the insula would be correlated with GABA concentrations in the same region and that these responses would be further correlated with depressed affect, as measured using the Beck Hopelessness scale (BHS) [Beck et al., 1974].

6.3 Materials and Methods

6.3.1 Participants

28 healthy participants (10 females, mean age 22.37 years \pm 3.77 SD, 18-34 years) underwent fMRI and 27 out of this group participated in MRS scanning (10 females, 22.37 \pm 3.85 years, days between scans 3.7 \pm 2.7). All participants had a Beck Depression Inventory (Beck et al., 1996) score \leq 4 and were questioned about psychiatric, neurological, or other diseases. Participants were recruited from the McGill University (Montréal) student body and the local community. The study was approved by the local ethics committee. All participants gave their written informed consent and were financially compensated.

Four participants were excluded due to anatomical abnormalities or motion artefacts (\geq 2 mm) (n = 24 participants, 9 females, 22.71 \pm 3.95 years). Further quality control of the MRS data resulted in the following analysis groups: GABA/NAA: n = 15 in the insula (5 females, 23.13 \pm 4.45 years), n = 9 in the mPFC (4 females, 21.11 \pm 2.98 years);

Glx/ NAA: $n = 14$ in the insula (4 females, 23.29 ± 4.58 years), $n = 18$ in the mPFC (9 females, 22.33 ± 3.51 years).

6.3.2 fMRI paradigm

A well established fMRI design for investigating intero- and exteroceptive awareness was used in the study, based on a paradigm introduced by Critchley and Pollatos [Critchley et al., 2004, Pollatos et al., 2007c, Wiebking et al., 2010]. This consists of three independent conditions presented in pseudo-randomised order for 6-10 seconds each. These were: a task for internal awareness (IA); a task for external awareness (EA); and fixation periods.

Participants were carefully familiarized with the tasks immediately before the scan. In order to limit cognitive processes other than intero- or exteroception, simple visual stimuli were used to indicate the task type. In case of IA, a dark coloured heart on a light background was presented and indicated onset and duration of the task. As long as the task type indicator was visible on the screen, participants were asked to silently count their own heartbeat. Any kind of manipulation, such as holding their breath or evaluating their pulse at the radial artery, was not allowed.

In case of EA, a symbol of a dark coloured musical note - of the same size as the heart symbol - was presented on the same light background. During such tasks individuals silently counted the number of tones played through headphones attached to the scanner. Participants reported the number of counted heartbeats or tones after each trial using a visual analogue scale (3.5 s). In order to make the difficulty of the IA and the EA tasks comparable, tones were presented at an individually determined volume. Participants were instructed to adjust the volume of the tone to the same difficulty level as that of counting their own heartbeat. This was done using an interactive screen at the beginning of each scan (i.e., with the scanner acquiring images to also account for

scanner noise). Here, subjects had the possibility to adjust the volume of the presented tone by using left and right button presses corresponding directly to a decrease or increase in tone volume. To control for habituation effects, the same interactive inquiry was presented a second time in the middle of the scan. In addition, the presentation frequency of the tones was adapted to correspond to each subject's pulse-rate. The onset time of the tones was jittered by 200 ms to avoid habituation.

Fixation periods were indicated by a dark cross (of the same size and colour as the IA and EA symbols) on a light background. Participants were instructed to relax and minimise any cognitive work during these period.

6.3.3 fMRI data acquisition and analysis

Functional scans were acquired on a 3-Tesla whole body MRI system (Siemens Trio, Erlangen, Germany), using a body transmit and 32-channel receive headcoil at the MNI (McGill University, Montréal, Canada). The settings were as follows: forty-seven T_2^* -weighted echo planar images per volume with BOLD contrast; alignment at 30° off the AC-PC plane in an odd-even interleaved acquisition order; FoV: $205 \times 205 \text{ mm}^2$; spatial resolution: $3.2 \times 3.2 \times 3.2 \text{ mm}^3$; $T_E = 25 \text{ ms}$; $T_R = 2270 \text{ ms}$; flip angle = 90° . Data were recorded in one scanning session containing 580 volumes per participant. A high resolution T_1 -structural 3D image was also acquired.

The fMRI data from 24 subjects were pre-processed and statistically analyzed using the general linear model approach in SPM8 (<http://www.fil.ion.ucl.ac.uk>) and MATLAB 7.11 (The Mathworks Inc., Natick, MA, USA). All functional images were slice time corrected with reference to the first acquired slice, corrected for motion artefacts by realignment to the mean image, and spatially normalized to the SPM standard T_1 -template [Ashburner and Friston, 1999]. The normalization parameters were generated by warping the coregistered anatomical image to the MNI T_1 -template and applying these parame-

ters to all functional images. Images were resampled to $2 \times 2 \times 2 \text{ mm}^3$, smoothed with an isotropic 6 mm full-width half-maximum (FWHM) Gaussian kernel. The time-series fMRI data were filtered using a high pass filter (threshold 128 s).

Since structured noise still remains in the fMRI data after traditional steps of pre-processing, an independent component analysis (ICA) was applied to denoise the data and hence improve the sensitivity and specificity of the results. Using Probabilistic Independent Component Analysis (Beckmann and Smith, 2004), which is implemented in the MELODIC toolbox in the FSL Software Library, (<http://www.fmrib.ox.ac.uk/fsl/>) [Smith et al., 2004, Woolrich et al., 2009], a group ICA was performed on the pre-processed fMRI data, which were temporally concatenated across subjects. Two independent raters (CW, NWD) visually inspected 40 components and classified them as noise or signals of interest, according to a detailed description of an operationalized denoising procedure [Kelly et al., 2010]. In particular, components were considered as noise when they showed a ring-like pattern in the periphery of the brain and tightly clustered areas in the frontal regions [McKeown et al., 1998], clusters with a location in the white matter/ CSF or an association with blood vessels [Sui et al., 2009, Zou et al., 2009], spotted patterns diffusely spread over the brain, and time courses showing a saw-tooth pattern or spikes [McKeown et al., 1998]. Components were independently identified as noise and removed from the original fMRI data through linear regression.

All conditions were included in the SPM model as separate events including their feedback phases. The statistical model for each subject was created by convolving trial onsets with a canonical hemodynamic response function [Friston et al., 1998]. Movement parameters were included as nuisance variables. Regionally specific condition effects were tested by employing linear contrasts for each subject and different conditions. The resulting contrast images were submitted to a second level random-effects analysis. Here, one-sample t-tests were used on images obtained for each subject's volume set and different conditions.

The individual biochemical measures for each region as well as behavioural scores from the Beck Hopelessness Scale (BHS) were entered into a second-level correlation analysis in SPM, using the proportion of grey matter as regressor of no interest in all calculations. Controlling for grey matter, biochemical concentrations and BHS scores were also correlated (two-tailed) with percent signal changes derived from each region. Percent signal changes were extracted using the MarsBaR toolbox (<http://www.sourceforge.net/projects/marsbar>). All data were controlled for possible outliers. The proportion of grey matter in each MRS voxel was calculated using FSL and included as a control variable in all analysis regarding MRS values.

The anatomical localization of significant neural responses was assessed with reference to the standard stereotactic atlas by superimposition of the SPM maps on a standard brain template provided by SPM8. Results of the regression analysis were small volume corrected by the respective MRS voxel. Whole brain results were inclusively masked by a grey matter mask. All results were set to a threshold of $P \leq 0.005$ (uncorrected, $k \geq 25$ for insula results and $k \geq 15$ for mPFC results). Peaks of the whole brain regression, using GABA/NAA from the left insula as a regressor, were assigned to the most probable brain area by using the SPM Anatomy Toolbox [[Eickhoff et al., 2007](#)].

6.3.4 MRS acquisition and analysis

Single voxel edited ^1H MR spectra were acquired using MEGA-PRESS [[Mescher et al., 1998](#), [Marjanska et al., 2007](#)] on a 3-Tesla MRI system (Siemens Trio, Erlangen, Germany) equipped with a 12-channel headcoil at the University of Montréal. Utilizing a high resolution T_1 -image (MPRAGE; FOV = 205 x 205 mm²; spatial resolution = 1 x 1 x 1 mm³; $T_E = 3.02$ ms; $T_R = 2000$ ms; flip angle = 5°), voxels were placed in the left insula and the mPFC. In order to achieve consistent volume of interest (VOI) positioning, placement was done by the same investigator for all subjects according to easily

identifiable anatomical landmarks: left insula voxels (23 x 48 x 27 mm³) were aligned with the line of the insula cortex in an anterior-posterior direction with the most anterior edge of the VOI aligned to the anterior limit of the insula; mPFC voxels (48 x 21 x 21 mm³) were placed anterior to the genu of the corpus callosum, parallel to the AC-PC plane.

First- and second-order shim terms were adjusted using FAST(EST)MAP [Gruetter and Tkáč, 2000]. MRS data were acquired using a MEGA-PRESS sequence [Mescher et al., 1998] with double-banded pulses used to simultaneously suppress water signal and edit the γ -CH₂ resonance of GABA at 3 ppm. Additional water suppression using variable power with optimized relaxation delays (VAPOR) and outer volume suppression (OVS) techniques [Tkáč et al., 1999] was optimized for the human 3-T system and incorporated prior to MEGA-PRESS. The final spectra were obtained by subtracting the signals from alternate scans with the selective double-banded pulse applied at 4.7 ppm and 7.5 ppm ('EDIT OFF') and the selective double-banded pulse applied at 1.9 ppm and 4.7 ppm ('EDIT ON'). MEGA-PRESS data were acquired in four interleaved blocks of 32 ('EDIT OFF', 'EDIT ON') scans each with frequency drift correction between each block. Free induction decays (FIDs) were stored separately in memory for individual frequency and phase correction using the tCr signal at 3.03 ppm, as well as correction for residual eddy-current using unsuppressed water signal obtained from the same voxel.

Difference spectra were analyzed with LCModel 6.2-1A [Provencher, 1993, 2001] using the basis set which included an experimentally measured metabolite-nulled macromolecular spectrum (average from 10 participants) and experimentally measured spectra from 100 mM phantoms of NAA, creatine, GABA, Glu, and Gln with pH adjusted to 7.2 and at 37°C. The LCModel fitting was performed over the spectral range from 0.5-4.0 ppm. No baseline correction, zero-filling, or apodization functions were applied to the *in vivo* data prior to LCModel analysis.

Only results with the Cramer-Rao lower bounds (CRLB) $\leq 20\%$ were included in the analysis. Concentrations with CRLB $> 20\%$ were classified as not detected. A representative spectrum is shown in Supplementary figure [D.1](#). LCModel metabolite concentrations, CRLB values, and correlation coefficients between Glu/ Gln are given in Supplementary table [D.1 A](#). Metabolite of interest concentrations as a ratio to NAA were used in subsequent steps.

6.4 Results

6.4.1 GABA and interoceptive awareness

For the investigation of a relationship between IA neural activity and GABA/NAA in the insula, a well-established fMRI paradigm was applied [[Critchley et al., 2004](#), [Pollatos et al., 2007c](#), [Wiebking et al., 2010](#)]. Firstly, BOLD responses in the insula MRS voxel (Figure [6.1 A](#)) were explored. As shown in Figure [6.1 B](#), IA induced significantly higher positive BOLD responses in the insula when compared to EA ($P \leq 0.001$) (Suppl. table [D.1 B](#)). In contrast, the mPFC (Figure [6.2 A](#)) showed task induced negative BOLD responses during both conditions (Figure [6.2 B](#) & Suppl. table [D.1 B](#)).

Having demonstrated that both IA and EA induce reliable BOLD responses, neurochemical correlates of IA were investigated. This was done by using the individual neurotransmitter concentrations (quantified in relation to NAA, see Suppl. table [D.1 A](#) for details) as regressors in IA-specific contrasts (i.e., [IA-Fixation] and [IA-EA]). GABA/NAA showed in both contrasts a significant positive correlation in the left insula (Figure [6.1 C](#), Suppl. table [D.2](#) & [D.3](#)). No other correlations were observed in the insula when comparing GABA/NAA to the EA contrast [EA-Fix], nor when comparing IA-specific contrasts with other MRS values (Glx, Glu, Gln) (see Suppl. table [D.2](#)).

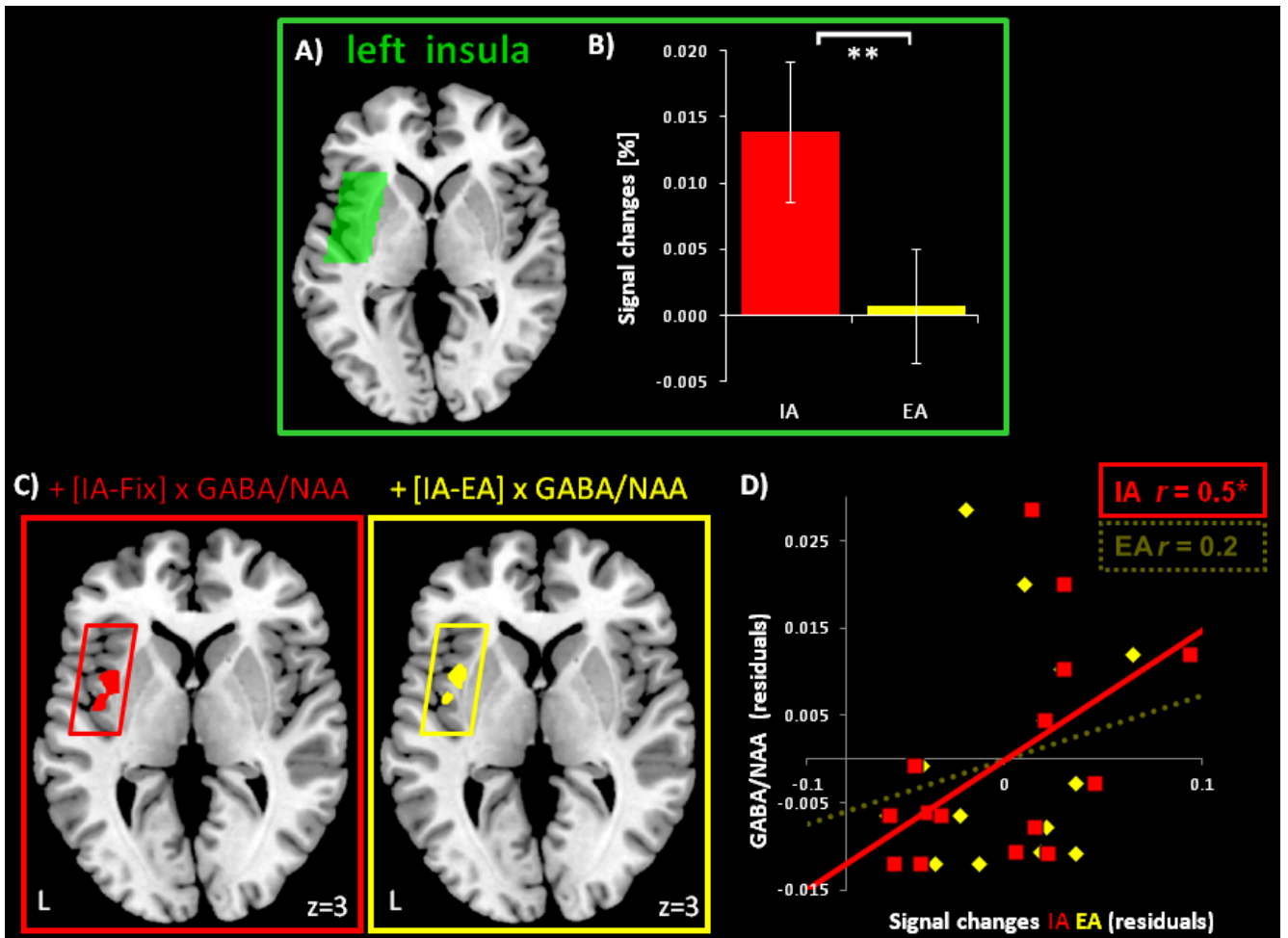


Figure 6.1: A) Placement of the left insula MRS voxel.

B) Bar diagram shows differences ($**P \leq 0.001$) between signal changes for IA (red) and EA (yellow) against Fixation (mean \pm SEM, $n = 15$ participants) (see also Suppl. table D.1 B).

C) Voxel-wise regressions within the MRS voxel show a positive relationship between GABA/NAA and [IA-Fixation] (red, cluster P FWE ≤ 0.003) and [IA-EA] (yellow, cluster P unc. ≤ 0.06) (see also Suppl. table D.2). The amount of grey matter in the MRS voxel was included as regressor of no interest.

D) Specifically IA (red) correlates with GABA/NAA. The scatter plot shows residuals for GABA/NAA, IA and EA (mean of regions revealed by C) following grey matter correction ($*P \leq 0.05$) (Table 6.1 A).

At the same time, correlations between task contrasts and neurochemical concentrations in the mPFC (Suppl. table D.1 B) revealed an exclusive negative relationship between GABA/NAA and [EA-Fixation] (Figure 6.3 C & Suppl. table D.3).

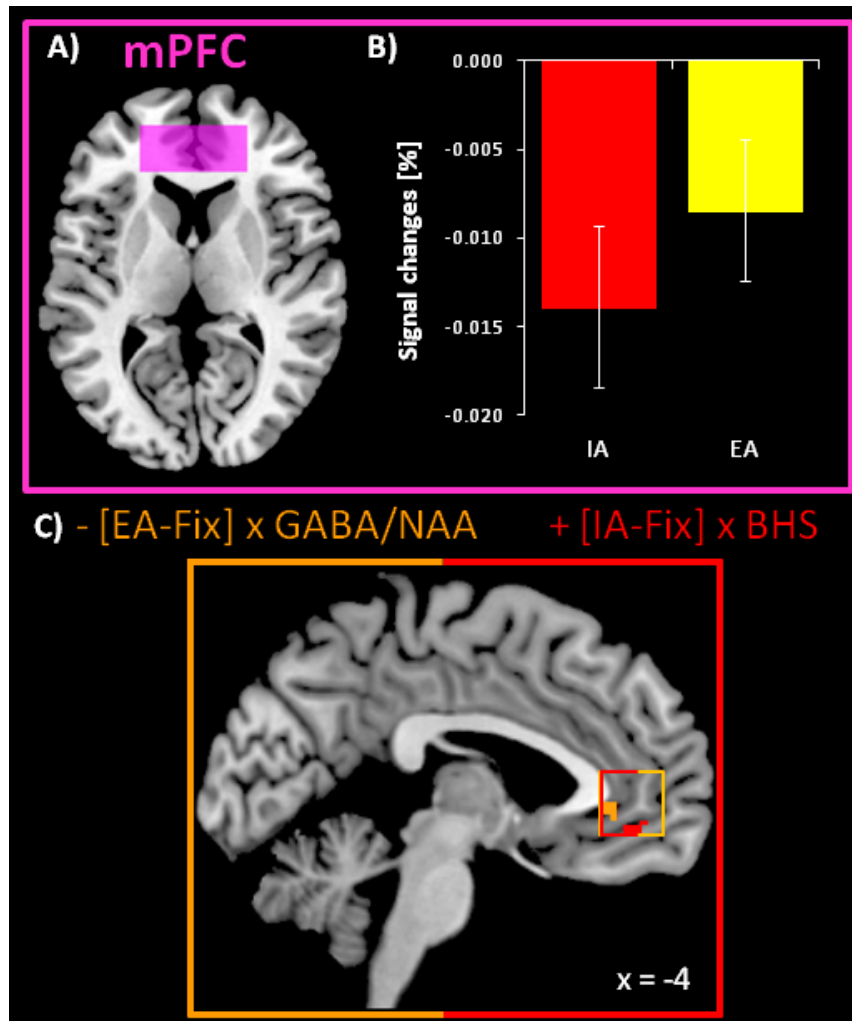


Figure 6.2: A) Placement of the mPFC MRS voxel.

B) Bars show no difference between signal changes for IA (red) and EA (yellow) against Fixation (mean \pm SEM, $n = 9$ participants) (Suppl. table D.3).

C) Voxel-wise regressions within the MRS voxel show a negative relationship between GABA/NAA and [EA-Fix] (orange, $n = 9$, cluster P FWE ≤ 0.008). BHS is positively associated with [IA-Fix] (red, $n = 24$, cluster P unc. ≤ 0.08 , Suppl. table D.1 B).

Since contrasts use the difference between two conditions (for example IA minus EA), we explored next if IA alone was the driving factor in the relation seen in IA-specific contrasts with GABA/NAA. For this, estimated mean signal changes for each *separate* condition (IA, EA, Fixation) were extracted from the correlating regions revealed by [IA-Fixation] x GABA/NAA as well as [IA-EA] x GABA/NAA.

Since the proportion of grey matter in the MRS insula voxel was included as a control variable, the correlation graphs in Figure 6.1 D use the residuals of signal changes as well as GABA/NAA. A positive relationship was found between GABA/NAA and IA ($*P \leq 0.05$). In contrast, no relationship was observed between EA or Fixation and GABA/NAA (Table 6.1 A). Calculations using the extracted single conditions of the mPFC region revealed by [EA-Fixation] x GABA/NAA (Figure 6.1 C) showed no specific relation to GABA or other biochemical values (Table 6.1 B).

A) Insula

	GABA₁₅/NAA	Glx₁₄/NAA	Glu₁₄/NAA	Gln₁₄/NAA	BHS₁₅	BHS₂₄
IA	0.52*	0.04	0.13	-0.13	-0.59*	-0.50*
EA	0.21	-0.11	-0.04	-0.20	-0.38	-0.36(*)
Fix	0.00	-0.10	-0.03	-0.19	-0.23	-0.32
GABA₁₅/NAA	/	0.51(*)	0.54*	0.23	-0.62*	-0.62*
Glx₁₄/NAA	0.51(*)	/	0.92**	0.72**	-0.14	-0.14
Glu₁₄/NAA	0.54*	0.92**	/	0.38	-0.14	-0.14
Gln₁₄/NAA	0.23	0.72**	0.38	/	-0.08	-0.08
BHS₁₅	-0.62*	-0.14	-0.14	-0.08	/	0.99**

B) mPFC

	GABA₉/NAA	Glx₁₈/NAA	Glu₁₈/NAA	Gln₁₈/NAA	BHS₁₈	BHS₂₄
IA	-0.33	0.12	0.01	0.16	-0.04	-0.08
EA	-0.48	-0.05	-0.14	0.12	-0.26	-0.22
Fix	0.05	0.10	0.14	-0.03	-0.36	-0.37(*)
GABA₉/NAA	/	0.22	0.79*	-0.32	-0.28	-0.28
Glx₁₈/NAA	0.23	/	0.74**	0.47(*)	0.55*	0.55*
Glu₁₈/NAA	0.79*	0.74**	/	-0.25	0.29	0.29
Gln₁₈/NAA	-0.32	0.47(*)	-0.25	/	0.41(*)	0.41(*)
BHS₁₈	0.15	0.55*	0.29	0.41(*)	/	1**

Table 6.1: R-values for correlations between residuals for MRS metabolites, BHS and signal changes for single conditions.

Subscripted numbers indicate number of participants.

Colour code as in corresponding Figure 6.1: red = interoceptive awareness (IA); yellow = exteroceptive awareness (EA); orange = Fixation (Fix).

A) Results for the left insula.

Residuals for IA, EA, and Fix refer to signal changes from regions found in the [IA-Fixation] x GABA and [IA-EA] x GABA regressions (Figure 6.1 C).

B) Results for the mPFC. Residuals for IA, EA, and Fix refer to signal changes extracted from the [EA-Fixation] x GABA regression (Figure 6.3 C).

* $P \leq 0.05$, ** $P \leq 0.01$

6.4.2 GABA and depressed affect

Finally, considering a probable involvement of the insula in depressed affect, GABA/NAA was correlated with scores of the Beck Hopelessness Scale (BHS), a behavioural measure for depressed affect. This revealed a negative relationship between BHS and GABA/NAA (Figure 6.3 A & Table 6.1 A).

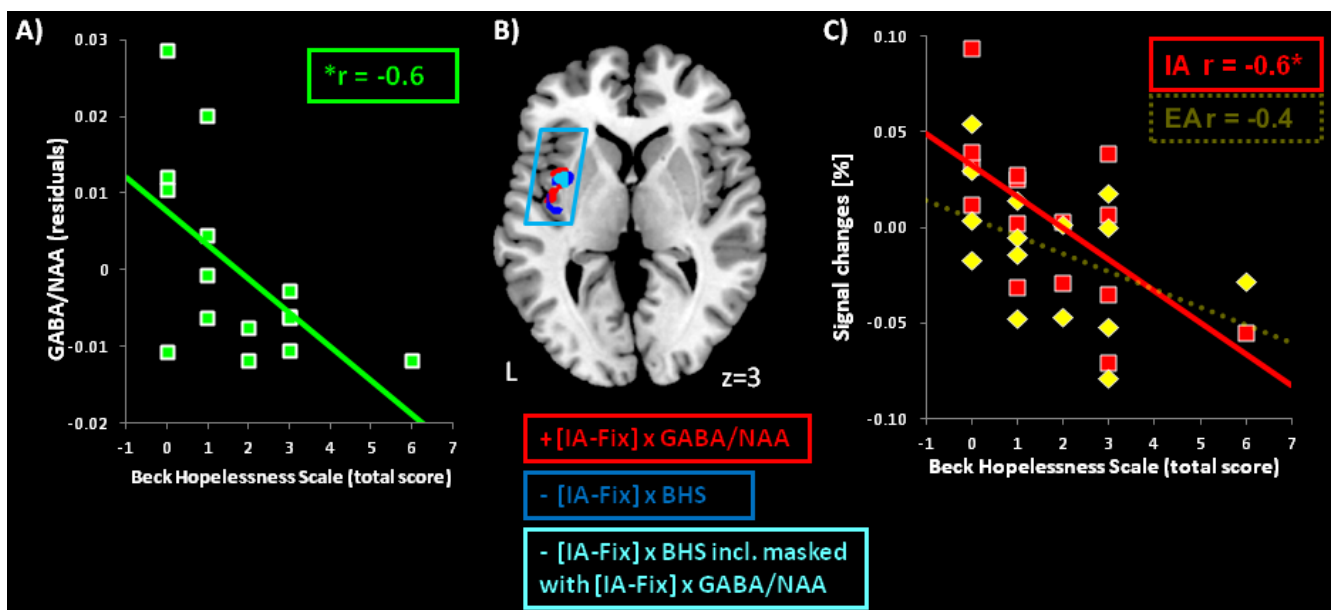


Figure 6.3: A) Scatter plot shows the negative relationship between BHS and GABA/NAA in the left insula ($*P \leq 0.05$, $n = 15$) (Table 6.1 A).

B) Voxel-wise regressions show in red the positive regression [IA-Fixation] x GABA/NAA (as in Figure 6.1 B, cluster P FWE ≤ 0.003), in blue the negative regression [IA-Fixation] x BHS (cluster P FWE ≤ 0.002) (Suppl. table D.2), and in cyan the overlap. All regressions included the amount of grey matter as control variable.

C) Specifically IA (red) is negatively associated with BHS ($*P \leq 0.05$). Signal changes were extracted from the region of activity defined by the [IA-Fixation] x GABA/NAA regression (B, red area).

As described above for GABA/NAA, the individual measures for BHS were entered into a second-level correlation analysis in SPM. Both contrasts showed a negative relation to BHS (Suppl. table D.3 & Figure 6.3 B, where the more robust result for [IA-Fixation] x BHS is illustrated). Overlaying both voxel-wise regressions, i.e., the positive [IA-Fixation] x GABA/NAA result (as in Figure 6.1 C) and the negative [IA-Fixation] x BHS result, showed a shared region in the middle of the left insula (Figure 6.3 B in cyan). Signal changes for each condition were then extracted from the region of activity defined by the [IA-Fixation] x GABA/NAA regression. Again, signal changes for the single IA condition were significantly correlated with BHS (in a negative direction), whilst EA and Fixation showed no association to BHS in the insula (Figure 6.3 C & Table 6.1 A). The inter-relationship between GABA/NAA concentrations, IA related signal changes, and depressed affect are illustrated in Figure 6.4. In addition, the mPFC showed – in this case a positive – voxel-wise regression between [IA-Fixation] and BHS (Figure 6.2 C & Suppl. table D.3). Estimated signal changes of single conditions showed no relation to BHS. Instead, BHS was positively correlated with mPFC Glx/ NAA (Table 6.1 B).

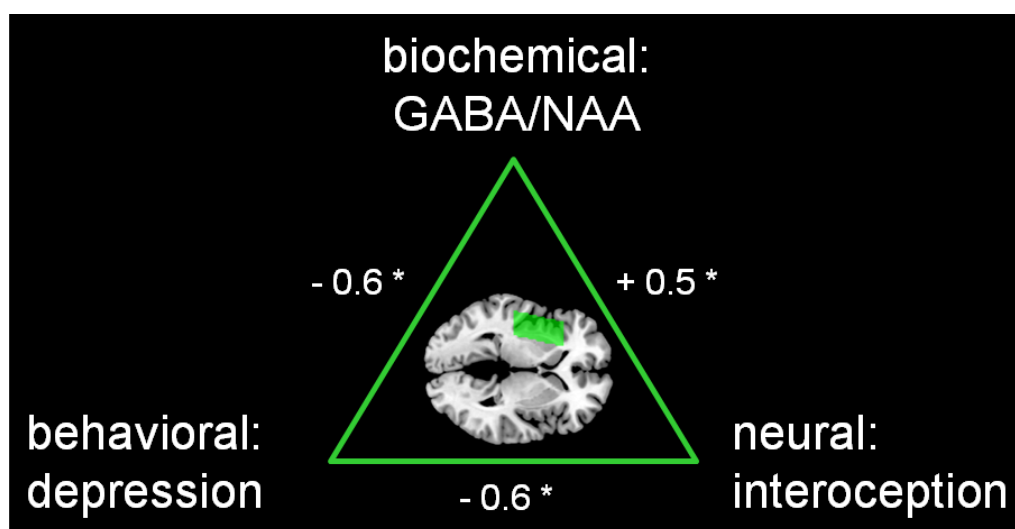


Figure 6.4: Overview showing the inter-relationship between the neurochemical level by GABA/NAA concentration, the neural level by signal changes for interoception, and the behavioural level of depression as assessed by the Beck Hopelessness Scale.

6.5 Discussion

The BOLD responses seen in the main MRS voxel in the left insula and the control MRS voxel in the mPFC are in accordance with previous studies. In detail, IA induced significantly higher positive BOLD responses in the insula when compared to EA, which is a well-documented response [[Critchley et al., 2004](#), [Pollatos et al., 2007c](#), [Zaki et al., 2012](#)] and underlines the reliability of the heartbeat monitoring task used here. In contrast, the mPFC showed task induced negative BOLD responses during both conditions. As part of the default-mode network, this finding is conform with studies investigating effects of external stimuli along this network [[Raichle, 2009](#)], as well as with a previous exploratory fMRI study of IA [[Wiebking et al., 2011](#)].

Combining fMRI with biochemical measures derived from MRS imaging, we investigated a possible influence of GABA (and Glx) on IA-related activity in the insula. This region is highly involved in these processes and hence likely to be influenced by one of the common inhibitory (GABA) or excitatory (Glx) neurotransmitters. GABA/NAA values in the insula showed positive correlations in IA-specific contrasts ([IA-Fixation] and [IA-EA]). No correlation was seen between GABA/NAA values and EA-related signal changes, nor was there any correlation between IA or EA signal changes and insula glutamatergic measures (i.e., Glx, Glu, or Gln). In the mPFC, a negative correlation was seen between GABA/NAA values and the [EA-Fixation] contrast. No other correlations were seen in this region. This result corresponds well with prior results suggesting a closer link between GABAA receptor availability and EA rather than IA in cortical midline structures [[Wiebking et al., 2012a](#)]. In addition, it is in line with a previously described negative correlation between GABA concentrations and signal changes in the mPFC evoked by an external stimulus [[Northoff et al., 2007](#)].

The positive correlation between GABA/NAA values and insula IA-related signal changes contrasts with the negative correlation seen in studies of the visual cortex [Donahue et al., 2010, Muthukumaraswamy et al., 2012]. A potential explanation for this is that the task used here involves the shifting of attention between competing stimuli (the heartbeat and the tone) whereas the tasks used in the visual cortex studies only involve a single stimulus that is switched on and off. With competing stimuli, it has been suggested that GABAergic inhibition is involved in suppressing activity related to the distractor stimulus, promoting target stimulus activity [Sumner et al., 2010]. In this case EA activity may be being suppressed by GABAergic inhibition, promoting IA-related activity. More work is required to confirm such a hypothesis, however. Also to be noted is the lack of correlations between regional signal changes and glutamatergic measures. This does, however, fit with previous glutamate imaging studies where correlations are mostly seen between glutamate concentrations and signal changes in regions other than that in which glutamate is measured [Duncan et al., 2011, Falkenberg et al., 2012]. This suggests that MRS measures of glutamate are more related to inter-regional effects than to signal changes within regions.

Previous studies have suggested that relationships between activity and GABA concentrations may be regionally specific (i.e., that, in general, concentrations in one region are unrelated to activity in another) [Sumner et al., 2010]. The current results fit with this view in two respects. Firstly, GABA/NAA values in the left insula and mPFC were not correlated with each other ($r = -0.37$, $P = 0.47$, $n = 6$). Similarly, GABA concentrations in one region do not correlate with signal changes in the other (insula GABA/NAA vs mPFC: IA – $r = 0.06$, $P = 0.91$; EA – $r = 0.244$, $P = 0.64$; fixation – $r = 0.44$, $P = 0.39$; $n = 15$; mPFC GABA/NAA vs insula: IA – $r = 0.05$, $P = 0.92$; EA – $r = 0.62$, $P = 0.19$; fixation – $r = 0.13$, $P = 0.81$; $n = 9$). Secondly, GABA concentrations were correlated with opposing conditions in the two regions studied – IA in the insula and EA in the mPFC – further suggesting specificity in each region.

The findings of the present study represent strong evidence for a coupling of GABAergic function and neural activity during IA in the insula. In depressed subjects both of these factors have been shown to be disrupted. On the one hand a GABAergic deficit in depressed patients has been reported [[Croarkin et al., 2011](#), [Möhler, 2012](#)], whilst on the other deficits in IA on the neural and behavioural level have been reported [[Paulus and Stein, 2010](#), [Grimm et al., 2011a](#), [Terhaar et al., 2012](#)].

We thus considered a probable involvement of the insula in depressed affect by, firstly, correlating insula GABA/NAA values with scores from the Beck Hopelessness Scale (BHS). This revealed a negative relationship between GABA and depressed affect. At the same time, IA-specific contrasts in the insula showed a negative correlation with BHS scores. Signal changes in this region for the single IA condition also correlated negatively with BHS, whilst the mPFC showed a positive relationship between BHS and [IA-Fixation]. The overall pattern of relationships fits well with the evidence of GABAergic and IA deficits in depression, demonstrating that even in non-clinical subjects, a consistent relationship between the three measured factors can be seen. This interaction between neurochemistry, interoception, and depressive symptoms presents a promising line of research for future studies in depressed patients.

A number of limitations of this study should be noted. Firstly, heatbeat perception was used as the IA task; repetition with different forms of interoception, such as breath monitoring [[Farb et al., 2012a](#)], should also be investigated to underline the role of GABA/NAA in the insula during interoceptive processing. Secondly, a more direct involvement of the right insula in interoception has been proposed [[Craig, 2002, 2009](#)]. As the left insula was used in the current study, it may be useful to repeat the experiment using MRS from the right insula to support the current findings and underline the role of the insula in interoception. Along similar lines, the anterior insula has been proposed to be more involved in the processing of internal stimuli [[Craig, 2009](#), [Lamm and](#)

[Singer, 2010](#), [Price and Drevets, 2012](#)]; we were, however, only able to acquire MRS data from the whole insula due to technical limitations. With improvements in MRS techniques, future studies might aim to investigate in more detail regional differences in neurochemistry across the insula subregions.

Finally, one might criticize that measurements of fMRI and MRS did not, for logistical reasons, take place on the same day. Although several studies have shown reasonable reliability over time of MRS measures [[Geurts et al., 2004](#), [O’Gorman et al., 2011](#)], repetition of the current results with data acquired at the same time is required.

In conclusion, this study demonstrates that GABA/NAA concentration in the left insula is specifically associated with neural activity during interoception, as compared to exteroception. Moreover, both GABA/NAA and neural activity during interoception are related to measures of depressed affect.

The findings thus support a triangular relationship between GABA/NAA, depressed affect and interoceptive processing in the left insula. This may have implications for psychiatric disorders, such as depression, in which alterations to all three aspects of this triangle – GABA levels, IA-related activity, and depressed affect – can be observed.

6.6 Acknowledgements

The authors would like to thank O. Lyttelton and the staff from the MNI as well as from the University of Montréal for their excellent technical support. Thanks also to K. Dedovic and A. Perna for helping with participant recruitment and screening procedures. The authors thank Edward J. Auerbach, Ph.D. (Center for Magnetic Resonance Research, University of Minnesota) for implementing the MEGA-PRESS sequence on Siemens, and Romain Valabregue, Ph.D. (Centre de NeuroImagerie de Recherche, Paris, France) for developing processing tools.

MM acknowledges support from Biotechnology Research Center grant P41 RR008079 (NCRR) and P41 EB015894 (NIBIB), and NCC P30 NS057091.

GN acknowledges support from the Hope of Depression Research Foundation (HDRF), the Canadian Institutes of Health Research (CIHR) and the EJLB-Michael Smith Foundation (CIHR-EJLB).

Chapter 7

Discussion

The work presented in the preceding chapters can be used to form an integrated picture about processes underlying or involved and influenced by intero- and exteroceptive awareness (see summarizing overview in Figure 7.1). These issues have been approached from different angles, using a range of different imaging techniques. Above all, functional magnetic resonance imaging (fMRI) was used throughout. To gather information about the biochemical underpinnings of cortical midline structures and the insula, magnetic resonance spectroscopy (MRS) and positron emission tomography (PET) were employed. Briefly, it could be shown that neural activity in the insula during interoceptive awareness is modulated by GABA (Chapter 6) and is also abnormally processed during depression, linking abnormal interoceptive awareness to abnormal emotional function (Chapter 4). In addition it could be shown that neural activity in the insula during rest is abnormally processed in depressed patients and also decoupled from perception of the own body (Chapter 3). Activity during rest in anterior cortical midline structures is more closely associated with emotional function in healthy participants (Chapter 2) and in addition GABA modulates activity in this region caused by external stimuli relative to rest (Chapter 5). The work provides an integrated view of neural activity during rest and internal/ external awareness along with emotional and biochemical functions of these processes. Investigation of depressed and remitted participants in addition to healthy individuals provides novel insights into the neural and

biochemical underpinnings of depressive disorder in combination with abnormal interoceptive awareness. These insights might serve to help identify treatment targets to normalize emotional function in affective disorders.

In the first study, the neural activity in the cortical midline structures of the brain and its association with behavioural dimensions of emotional processing was investigated in a group of healthy participants. Using fMRI, it was shown that both the intero- and exteroceptive awareness tasks lead to task-induced deactivations in cortical midline structures (Figure 2.1 and Table 2.1). This finding was later replicated in an independent sample (Chapter 5, Figure 5.1 and Table 5.1) and indicates a basic mechanistic principle of these brain regions, namely a decrease in activity in reaction to a stimulus, independent of its internal or external nature. In contrast, a different pattern can be observed in regions more specialized for interoceptive awareness, such as the insula (see for example signal changes in Figure 6.1 or 4.2). Here, both tasks induce positive BOLD responses, with the interoceptive awareness condition broadly seen to induce significantly higher positive neural responses.

In addition, it was shown that neural activity during rest in the cortical midline structures, as opposed to interoception, was correlated with emotional measures, but not with scores for body perception. This suggests a closer association between rest and emotion in cortical midline structures in healthy participants, with interoception having less of an influence here. Interestingly, neural rest activity in these structures was negatively related to emotional and positively related to depression scores, as measured with the Florida Affect Battery (FAB) and Beck Hopelessness Scale (BHS) (Table 2.2). This pattern suggests that individuals with relatively high activity levels during rest perform worse in an emotional test and score higher in depression, a constellation that can be transferred to depressed patients. As described in the general introduction in Chapter 1.1, patients suffering from MDD show reduced negative BOLD response during

rest along cortical midline regions as well as deficits in emotional processing [Grimm et al., 2009a]. This altered neural activity may be due to either higher activity during rest periods or decreased overall neural activity. Assuming a higher activity during rest in cortical midline regions in depressed patients, one might assume that depressed participants can be considered to be at the upper extreme end of a continuous relationship between rest activity and emotions. This hypothesis needs to be tested in future studies.

Taking into account the significant influence of activity during rest, the second fMRI study investigated insula activity and body perception in healthy as well as depressed participants. On the behavioural level, MDD patients showed significantly higher body perception scores, which is in agreement with clinical observations. A similar behavioural study by Nyboe Jacobsen et al. [Nyboe Jacobsen et al., 2006] clearly showed that several subcategories of body awareness correlated positively with depression severity with less or no association in remission. This contrasted with other studies investigating interoceptive awareness by mental tracking of the own heartbeat [Schandry, 1981] that have shown inconsistent findings, with either decreased or normal heartbeat detection in depressed participants [Terhaar et al., 2012, Dunn et al., 2007]. These conflicting results highlight the need to carefully distinguish in future studies between 'paper and pencil tests' asking to score awareness of the own body and attention requiring tasks, such as heartbeat counting. The tendency of depressed patients to show a high self-focus and strong introspection [Grimm et al., 2009c] seems to influence the evaluation of personal statements about body awareness, leading to higher scores compared to healthy participants. On the other hand, the strong performance-oriented character of a heartbeat counting task may lead to a faster cognitive fatigue in depressed patients [Fava, 2003], causing, for example, psychomotor retardation such as slowed thinking. This can be seen as an underlying reason for decreased heartbeat perception accuracy and needs to be carefully addressed in future study designs, for

example by implementing a control task that is not body-related but has comparable difficulty to the heartbeat perception one.

On the neural level, it was further shown here that activity in the bilateral insula during rest was reduced in MDD and at the same time influenced neural activity related to other tasks, specifically the exteroceptive component. Interestingly, in contrast to healthy subjects, behavioural body perception scores no longer correlated with activity during rest periods in the bilateral insula in MDD patients. This indicates a decoupling of body perception from neural activity changes in the insula in MDD and can be interpreted as the inability of depressed participants to switch awareness from the own body to the external world, which again supports the hypothesis of increased self-focus. In addition, reduced signal changes during rest periods in the left anterior insula correlated positively with BDI scores in MDD (Figure 3.9), whilst a negative relationship between rest and BHS was seen in healthy participants in the third study (Chapter 4, Figure 4.2). The two results deal with different questionnaires, but could possibly be interpreted as measuring an underlying theme of depression severity. A comparison and interpretation of these independent findings is difficult, though, as regions of the insula in the second study show deactivation during periods of rest (Table 3.1) in both healthy as well as depressed participants, whilst the *a priori* defined left dorsal anterior insula region showed positive signal changes during rest in both groups (Figure 4.2).

Moreover, the distribution and variability of data points, especially in the depressed group, needs to be further investigated. Differences within groups of depressed patients (e.g. moderately versus severely depressed) need to be considered [Horn et al., 2010]. Figure 3.9 suggests indeed a genuine split between five moderately depressed participants (ranging from a BDI of 16 to 21) and eight severely depressed individuals (scoring 34 to 40). This needs to be considered in future analysis and complicates the

comparison between healthy and depressed participants regarding opposing correlations between neural activity during rest in the insula and depression severity.

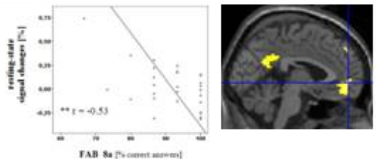
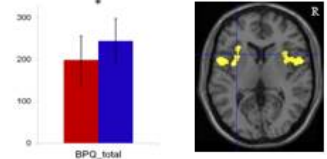
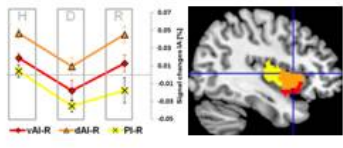
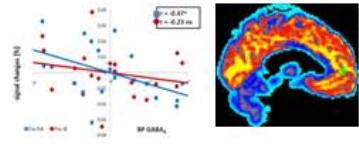
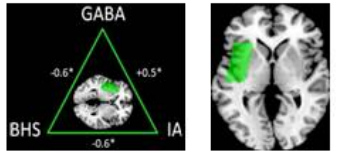
group	contrast	region technique	main findings
healthy	Fixation >IA/EA	CMS fMRI+ behav.	◦ Fixation negative related to emotional tests 
MDD healthy	Fixation >IA/EA	insula fMRI+ behav.	◦ MDD: abnormal body perception ◦ MDD: reduced NBR (Fixation) ◦ MDD: body perception & Fixation decoupled 
MDD healthy remitted	single conditions	insula sub- regions fMRI+ behav.	◦ MDD: reduced IA ◦ normalizes after remission ◦ MDD: no stimuli differentiation 
healthy	Fixation >IA/EA	CMS fMRI+ PET	◦ GABA modulates activity during EA (Fixation-EA) 
healthy	IA>EA x GABA IA>Fix x GABA single conditions	insula MRS box fMRI+ MRS+ behav.	◦ IA positive related to GABA ◦ IA negative related to BHS ◦ BHS negative related to GABA 

Figure 7.1: Overview showing the results presented in this work.

From top to bottom: fMRI based results of Chapter 2, Chapter 3, Chapter 4, and biochemical results of Chapter 5 and 6.

The next study investigated the insula region in detail, considering three functionally different subregions. Comparing healthy, depressed and remitted participants, neural activations during rest did not – as one might expect depending on results in Chapter 3 – differ between groups. Instead, group differences occurred particularly during conditions of interoceptive awareness. This approach, using *a priori* defined regions of interest that show functional differences, might be considered a more appropriate way to investigate group differences. In Chapter 3, both groups of healthy and depressed subjects were combined into one group. Hence, the functional contrast to investigate interoceptive awareness (heartbeat counting > tone counting) and the resulting regions of neural activity reflected the results of a combined group of healthy and depressed participants. This was done to ensure that neither of the groups had a dominant influence on the region of interest selection (see [Goldstein et al., 2007] and Methods 3.3.4), but might have led to differential results (i.e., no differences during interoceptive conditions between healthy and depressed participants).

Using functional sub-regions of the insula revealed interesting insights into several of its aspects. Firstly, anterior insula regions were identified as the regions showing the highest neural activity during interoceptive awareness [Zaki et al., 2012, Critchley et al., 2004]. Expanding these findings, a linear decrease of neural activity was seen comparing dorsal, ventral and posterior insula (Figure 4.1 C), with the dorsal anterior insula showing the highest activity across groups. Of note is the same pattern of decreasing neural activity during interoception across these regions for all three treatment groups, indicating that MDD patients show a general hypo-response to interoceptive stimuli instead of deficits in processing the neural signal across different insular regions. The results of this study are highly interesting since they show a hypo-responsiveness towards interoception in the dorsal anterior insula in the MDD group compared to both healthy as well as remitted participants. Neural activity normalizes after remission from MDD,

suggesting potential benefits of therapies like biofeedback. Here, individuals learn to become aware and eventually control their own bodily processes, such as heart rate, which has been shown to increase interoceptive activity in the insula in healthy subjects [Farb et al., 2012b]. Hence, a role for biofeedback and related therapy strategies in MDD should be investigated in future studies.

The final two studies reveal details of biochemical underpinnings of the two main brain areas described in the preceding chapters – the cortical midline structures and the insula. Using the same paradigm in fMRI and the same functional contrast (Fixation > Task) as described in Chapter 2, the addition of PET imaging gave significant information about the association between neural activity in cortical midline structures and GABA_A receptor density. This third study showed that GABA_A receptor binding potential within cortical midline structures was correlated with neural activity changes during external but not internal awareness. These data provide evidence that the inhibitory neurotransmitter GABA is an important influencing factor in the differential processing of internal and external awareness. Since depression is characterized by a common pathophysiological pattern of GABAergic deficits [Bajbouj et al., 2006, Luscher et al., 2011, Möhler, 2012, Smith and Rudolph, 2011], especially in anterior cortical midline structures [Bielau et al., 2007, Levinson et al., 2010, Walter et al., 2009], and altered states of external and internal awareness [Grimm et al., 2011b, Paulus and Stein, 2010, Wiebking et al., 2010], future research should aim to provide further evidence for a connection between these factors.

By measuring the concentration of GABA rather than the receptor binding potential using MRS, a closer look at the biochemical underpinnings of interoceptive awareness in the left insula showed that neural activity during interoceptive awareness is more closely associated to GABA in this region. The results of Chapter 6 in healthy partic-

ipants demonstrate for the first time that GABA modulates neural activity induced by interoceptive awareness, rather than exteroceptive awareness, in a region particularly sensitive to interoception. Moreover, both GABA and neural signal changes during interoceptive awareness were related to the degree of depressed affect (Figure 6.3). This interconnects neurochemical modulation with neural and behavioural function in the insula in a novel way and needs to be further confirmed by future studies in depressed patients. With the development of enhanced MRS imaging techniques, future studies should aim to measure neurotransmitter levels in sub-regions of the region in its entirety.

Taken together, the work presented here provides valuable information about the interplay between internal and external awareness, along with rest, in combination with emotional processes. Healthy, depressed and remitted participants were investigated, and moreover the use of a number of different imaging techniques allowed also the examination of the neurochemical underpinnings of these processes. The results give interesting clues for neural underpinnings as well as treatment of psychiatric disorders.

Chapter 8

Perspectives

The work presented in the former chapters will be the foundation of future studies investigating further details of the connection between intero-/ exteroceptive awareness, rest, and behavioural processes like emotional function or body perception. It is of advantage to investigate altered functions and shifted connections between these processes by studying psychiatric populations. Determining alterations on the behavioural level and trying to link them to individual neural responses through an appropriate designed task, e.g. as described here in fMRI, can lead to further conclusions about functionally abnormal involved brain structures and their influence on altered behaviour.

The results described in Chapter 4 regards a neural hypo-response of depressed individuals during interoceptive awareness and its normalization after remission from depression imply promising treatment results through biofeedback therapy. This approach aims to improve awareness of physiological functions by utilizing information about different physiological functions of an individual, such as heart rate or neural activity. These constantly changing measures are recorded and immediately played back to the user in an easy understandable way, for example in form of increasing or decreasing thermometer bars. Through this setup a person is now able to gain control and voluntarily up- or downregulate their own physiological responses in order to evoke the desired physiological changes. Eventually, these changes can endure and lead to improvement of bodily and mental well-being.

In order to successfully manipulate and improve neural activity of a certain brain area like the insula, fMRI-based neurofeedback can be applied. While in an MRI machine, participants are continuously updated about their neural insula activity by displaying its in- or decreasing activity on a screen that the subject can see through a mirror mounted on the headcoil, as in usual fMRI experiments [Caria et al., 2007]. Since this neurofeedback is done in real time, the technique has been described as real-time fMRI (rtfMRI). The study by Caria [Caria et al., 2007] showed that self-regulation of neural activity in the anterior insula during rtfMRI is possible. Healthy participants were able to upregulate neural activity in this region by using cognitive strategies like recall of positive events. As discussed, their results can be seen in the light of increased interoceptive awareness during subjective emotional responses. A recent study by Linden [Linden et al., 2012] showed that neurofeedback in a group of depressed patients is more effective and leads to improvement of depression severity and treatment effects. Neurofeedback through rtfMRI has several important advantages as it combines the principles of cognitive-behavioural therapy with physical brain stimulation and might lead to more stable long-term effects in the treatment of depression and other mental disorders, which has to be proven in future studies. However, this approach is seen as having big potential to be a possible first therapeutic application of functional imaging in the area of mental health research.

Since other studies have shown increased neural activity in the insula after mindfulness-based training [Farb et al., 2012b], i.e. the development and improvement of interoceptive awareness, this technique might lead in combination with rtfMRI to a more effective result to improve depressed symptoms. Whilst it might be difficult for depressed individuals to mentally engage in positive situations and in addition maintain this strategy without the actual neural feedback, the approach using interoceptive awareness might be more effective. Moreover, the learned interoceptive strategies can be easier to main-

tain for depressed patients, since local communities offer similar programs. Future studies in this area need to further investigate the emotional component of interoceptive awareness or the interoceptive component of emotional processes, respectively, to further understand their relationship and eventually the neural and cognitive processes that underlie depression.

Besides major depression, anxiety disorders represent an interesting study group, as for example Critchley showed correlations between anxiety scores and neural insula activity in healthy participants [Critchley et al., 2004]. Chapter 8.1 describes a new research study, which just started with a very first fMRI run at the Civic Hospital and the Institute of Mental Health Research, Ottawa, Canada. Basing on the intero-/ exteroceptive paradigm described in the previous chapters, it will be used here to acquire fMRI data in adolescent anxiety patients. Application of the fMRI paradigm as described in the previous chapters is an interesting study approach on its own in this patient group. However, adolescent anxiety patients show similarities to what has been described as an altered self-focus in Chapter 3, and so the paradigm has been modified to, in addition, investigate effects of self-relatedness.

8.1 Neural mechanisms underlying abnormal arousal and body perception in adolescent anxiety patients

8.1.1 Introduction

Anxiety disorders are the most common mental illnesses of adolescence, with an overall prevalence ranging from 8% to 27% [Costello et al., 2005]. Six- to 12-month prevalence has been estimated at 0.6 to 2.4% for separation anxiety disorder [Bowen et al., 1990, Kashani and Orvaschel, 1988], 2.4 to 4.6% for overanxious disorder (the DSM-III-R pe-

diatric equivalent of generalized anxiety disorder) [Bowen et al., 1990, Fergusson et al., 1993] and up to 6.3% for social phobia [Verhulst et al., 1997].

Anxiety disorder patients experience amongst affective and cognitive deficits also severe vegetative symptoms [Ollendick and Hirshfeld-Becker, 2002], which is a comparable mixture of symptoms as described for major depression (see Chapters 3 and 4). Similar to their adult counterparts, anxious youth suffer from an abnormally increased arousal, with autonomic symptoms such as increased heartbeat and breathing rates, blushing, and abnormal sweating [Boyce et al., 2001, Kagan et al., 1987, Middleton and Ashby, 1995]. Anxious youths are overly attentive to their internal states, and show heightened sensitivity and increased threat reaction to bodily sensations [Eley et al., 2004, Weems et al., 2002]. This appears to be similar to what has been described for patients suffering from major depression, especially regards an increased self-focus (see Chapter 3). This is also supported by studies showing that all three types of anxiety disorders (separation anxiety, social phobia, generalized anxiety) show similar relationships with adult anxiety and depressive disorders [Fyer et al., 1995, Last et al., 1991]. Moreover, they respond to similar psychosocial and pharmacological treatments (e.g., cognitive behavioural therapy) [Barrett, 1998, Kendall, 1994, Kendall et al., 2001]. Hence, the characteristics of this disorder mirror an ideal study population to further investigate neural abnormalities underlying abnormal body perception and associated emotional processing.

Of all the psychosocial approaches that have been used for treating anxiety disorders in youth, cognitive-behavioural treatment is the only one whose efficacy is supported by data from randomized controlled trials [Compton et al., 2004, Prins and Ollendick, 2003]. Follow-up studies have indicated that early diagnosis and treatment of an anxiety disorder may have a positive impact on long-term outcomes, including chronic anxiety,

depression and substance abuse [Kendall et al., 2005]. Nevertheless, fundamental research questions remain regarding treatment processes and underlying mechanisms of change [Prins and Ollendick, 2003].

As discussed in Chapter 4, imaging results in healthy participants after mindfulness based therapy describe an increase of neural activity in the insula during interoceptive awareness [Farb et al., 2012b]. A similar effect might occur after successful cognitive-behavioural treatment, which has to be demonstrated. Although the recruitment of patients in pre- and post-treatment phases is a difficult and time-intensive process (see section 4.5), the current project seeks to identify specific areas of the brain associated with anxiety in young people and to document their changes following treatment.

8.1.2 Imaging studies in adolescent anxiety disorders

So far, imaging studies of anxiety disorders in adolescents have focused predominantly on the neural correlates of emotions [Pine, 2007, Pine et al., 2008]. A recent study [Beesdo et al., 2009] presented facial expressions in different attentional conditions (afraid, hostility, passive viewing) to adolescent patients with anxiety and/ or depression, demonstrating abnormal activation in the amygdala, predominantly an increase, in response to fearful faces. Another imaging study presented masked emotional (happy or angry) and neutral faces to adolescents with generalized anxiety disorder [Monk et al., 2008] and showed abnormal hyperactivation in the right amygdala, that also correlated with anxiety disorder severity. Connectivity of the right amygdala to the right ventrolateral prefrontal cortex was abnormally weakened, indicating decreased cognitive-emotional top-down modulation.

A study by Guyer [Guyer et al., 2008] also showed amygdala hyperactivation in patients with generalized anxiety disorder and/ or social phobia. Moreover, neural activity in

the amygdala was associated with symptom improvement, a similar pattern as seen in adults [McClure et al., 2007]. Similarly, the connectivity and interaction of the amygdala to the ventrolateral prefrontal cortex was abnormal in patients compared to healthy subjects. These results concerning the amygdala are well in accordance with an earlier study in healthy adolescents, in which high amygdala activity was observed during presentation of fearful and happy faces; this correlated with several social (but not non-social) dimensions of anxiety [Killgore and Yurgelun-Todd, 2005].

Imaging studies of the effects of cognitive therapy in adolescent anxiety disorders have not been reported yet. In addition to imaging studies probing cognitive-emotion regulation strategies [Goldin et al., 2009, Ochsner et al., 2004] including the effects of cognitive therapy, the changes in the neural networks underlying abnormal arousal and interoceptive awareness also remain to be investigated in adolescent anxiety disorders.

8.1.3 fMRI paradigm (in developmental phase)

A self-designed questionnaire is used to acquire personal information about the participant and about a friend. These items will be used as primers ('self priming' or 'other priming') and shown immediately before the task for fixation or internal/ external awareness (see Figure 8.1). Currently, the fMRI paradigm consists of three runs. Each run shows 27 repetitions of self as well as other primed tasks (internal/ external awareness and fixation). In addition, the three tasks are also shown 27 times without preceding primer.

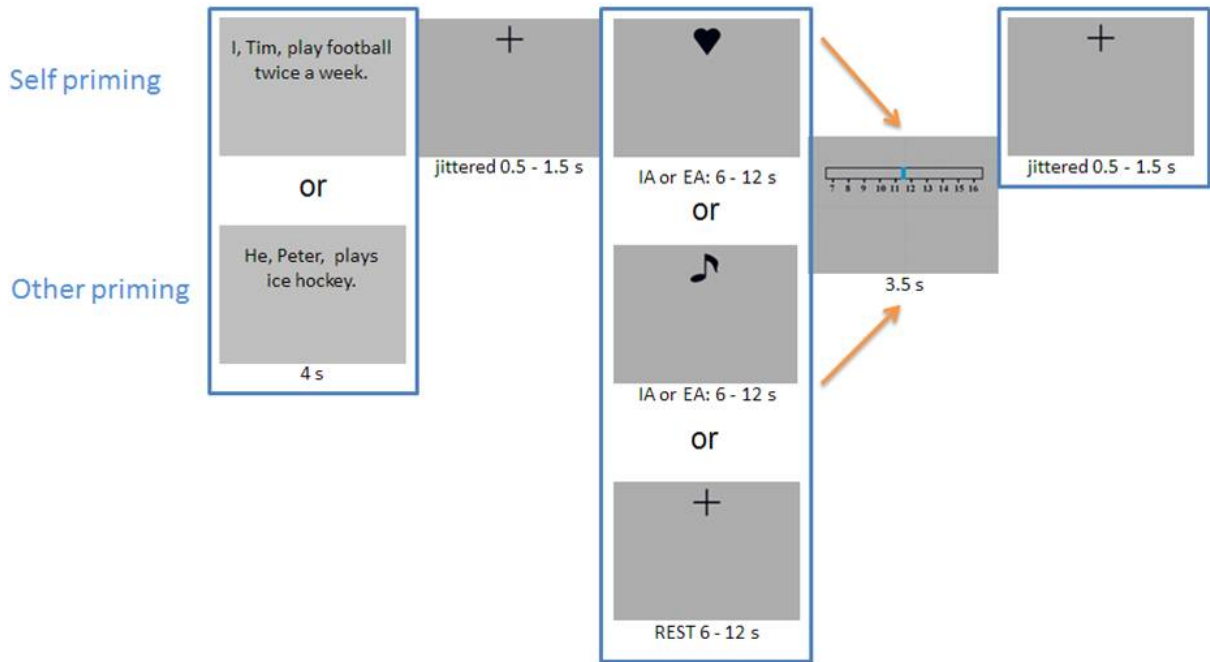


Figure 8.1: FMRI paradigm for a new study in adolescent anxiety patients.

Diagnostic and clinical assessment includes several questionnaires, e.g.: Anxiety Disorders Interview Schedule for DSM-IV, Research and Lifetime Versions for Child and Parent [Silverman, 1987, Silverman and Albano, 1997], Response to Stress Questionnaire [Connor-Smith et al., 2000], Clinical Global Impression–Severity of Illness and Improvement scales [Guy, 1976] as well as scales used in prior studies like the Beck Depression Inventory-II [Beck et al., 1996, 1961], the Beck Hopelessness Scale [Beck et al., 1974] and the Body Perception Questionnaire [Porges, 1993].

8.1.4 Aims and hypotheses

The general aim of our study is to investigate the changes in the neural network of interoception in adolescents with anxiety disorders, before and after cognitive behavioural therapy.

The specific aims and hypotheses are as follows:

The first aim is to investigate the changes in the neural network underlying interoceptive awareness in adolescent patients with anxiety disorders using fMRI. We hypothesize that the adolescent anxiety disorder patients will show altered signal changes, especially in the bilateral anterior insula, the thalamus and the anterior cingulate cortex (ACC), when compared to age- and sex-matched healthy controls. Though no data are available in adolescent anxiety patients, this hypothesis is based upon findings in adult anxiety subjects [[Paulus and Stein, 2006](#)].

The second aim is to investigate the effects of a standardized cognitive behavioural therapy on the neural measures of interoceptive awareness using fMRI. We hypothesize that the abnormal findings in neural activity seen in the anxiety disorder patients will normalize, particularly in those subjects showing strong therapeutic effects after cognitive behavioural therapy.

The third aim is to acquire data about the influence of self-referential processing on the three main tasks (internal/ external awareness, fixation periods) that comprise the paradigm.

8.1.5 Pilot data

Data have been acquired on a 3-Tesla MRI system (Siemens Trio, Erlangen, Germany), using a body transmit and 32-channel receive headcoil at the Civic Hospital (Ottawa, Canada). The settings were as follows: 47 T_2^* -weighted echo planar images per volume with BOLD contrast; alignment at 30° off the AC-PC plane in an odd-even interleaved acquisition order; FoV: $205 \times 205 \text{ mm}^2$; spatial resolution: $3.2 \times 3.2 \times 3.2 \text{ mm}^3$; $T_E = 25 \text{ ms}$; $T_R = 2270 \text{ ms}$; flip angle = 90° . A single subject was scanned using the above described fMRI paradigm. Three runs were recorded, each containing 455 volumes. A high resolution T_1 -structural 3D image was also acquired.

The fMRI data were preprocessed and statistically analyzed by the general linear model approach using the SPM8 software package (<http://www.fil.ion.ucl.ac.uk>) and MATLAB 7.11 (The Mathworks, Natick, MA). The detailed steps of processing are taken over from prior analysis (see for example Chapter 3.3.4).

The results in Figure 8.2 demonstrate that the modified paradigm can be considered to be valid, as common brain areas like the bilateral insula show increased activity during interoceptive awareness (IA) when compared to fixation periods (Fix).

Hence, recruiting of adolescent anxiety patients and healthy controls for further fMRI scans is currently starting.

Although these are preliminary data from a single subject, also the contrast investigating self-related processing [self prime > other prime] suggests promising results of the future study, as regions showing increased neural activity (anterior, caudal, and posterior parts of the cingulate cortex) can be compared with other work studying self-related processing [Qin et al., 2010].

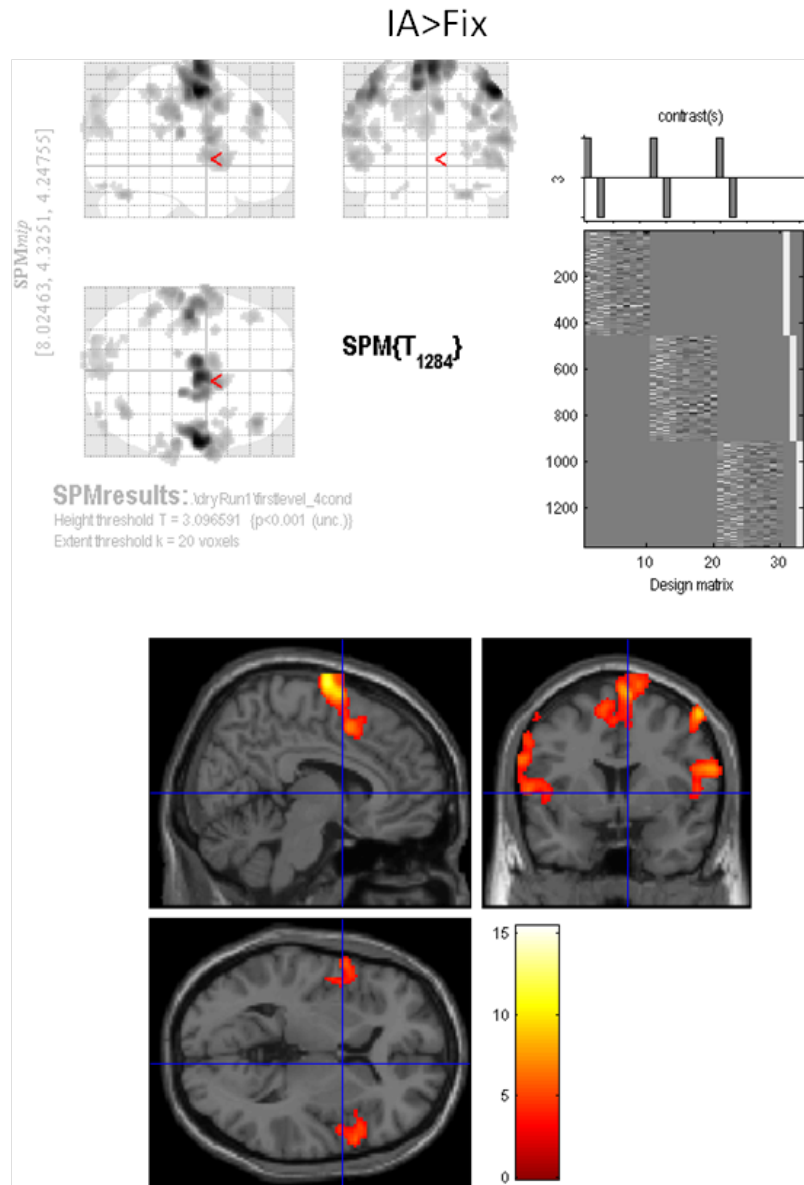


Figure 8.2: Pilot data from a single participant, using a modified fMRI paradigm. The picture shows neural activity for the contrast interoceptive awareness versus Fixation [IA > Fix] ($P \leq 0.001$ uncorrected, $k \geq 20$).

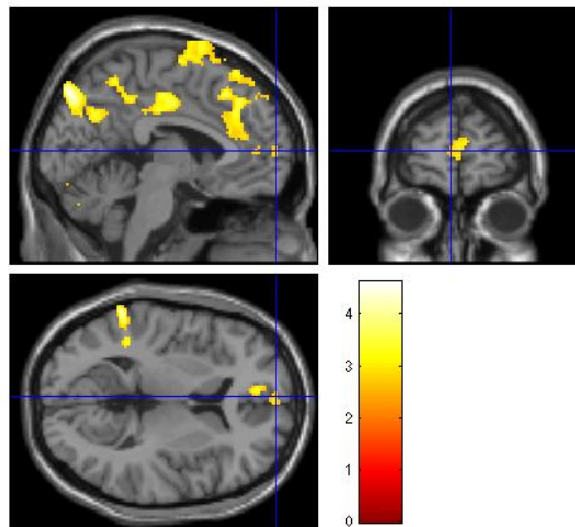
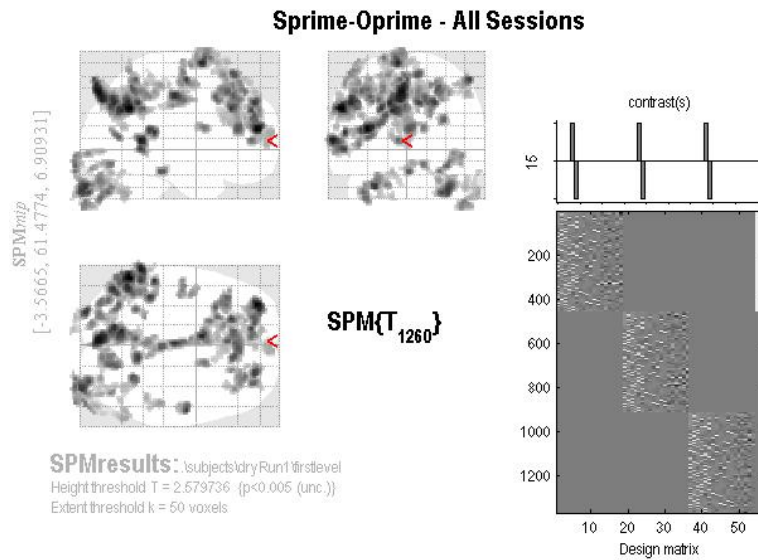


Figure 8.3: Pilot data from a single participant, using a modified fMRI paradigm. The picture shows neural activity for the contrast self prime versus other prime [Sprime > Oprime] ($P \leq 0.005$ uncorrected, $k \geq 50$).

Chapter 9

Abstracts

Abstract (English)

Interoceptive awareness, the awareness of stimuli originating inside the body, plays an important role in theories of human emotions. Pushed forward by the emergence of new brain imaging techniques, our understanding of the neural substrates underlying interoceptive awareness continues to increase. The insula, a bilateral brain structure located within the Sylvian fissure, has been identified as a key region involved in interoceptive awareness in neurotypical individuals. Emotional functions in turn have been associated with interoceptive awareness and with activity during rest in cortical midline structures, whose anterior parts are functionally connected with insula activity.

That said, this dual association of emotions with activity during rest and interoception remains to be investigated. In addition, to date, little has been established regarding the biochemical underpinnings of interoceptive awareness. Similarly, its role in affective disorders like major depression has been suggested but remains unclear.

In order to investigate these points, imaging techniques including functional magnetic resonance imaging (fMRI), positron emission tomography (PET) and magnetic resonance spectroscopy (MRS) were combined in studies on healthy, depressed and remitted participants. A well established fMRI paradigm to investigate neural activity during intero- and exteroceptive awareness (heartbeat counting and external tone counting)

as well as during rest was used in combination with behavioural tests.

Firstly, it was shown that neural activity in anterior cortical midline regions during rest, rather than during interoceptive awareness, is associated with emotional scores in a group of healthy participants. In a second study, it was shown that neural activity in the insula during rest is abnormally processed in depressed patients. Moreover, activity during rest was decoupled from perception of one's own body in the depressed group as well as positively related to depression severity. Thirdly, it was shown that group differences between healthy, depressed and remitted participants occurred particularly in the dorsal anterior part of the insula during interoceptive awareness. This region showed hypo-responsiveness in depressed participants, which normalized after remission. In addition, the depressed group showed no differential activity in this region between rest and intero-/exteroceptive awareness. Finally, biochemical investigations in healthy participants in the areas of interest (insula and cortical midline structures) revealed that i) the inhibitory neurotransmitter GABA within cortical midline structures is an important influencing factor in the differential processing of intero- and exteroceptive awareness and ii) GABA modulates neural activity induced by specifically interoceptive awareness in the insula, with this link not seen in cortical midline structures. Moreover, both GABA and neural signal changes during interoceptive awareness were related here to the degree of depressed affect.

Taken together, the results presented in this work provide on the one hand initial biochemical links to neural processes induced by interoceptive awareness in the insula as well as neural processes induced by exteroceptive awareness in cortical midline regions. On the other hand, they provide valuable information about the interconnections between rest, and intero- and exteroceptive awareness in combination with behaviour (emotions and body perception). By investigating individuals suffering from depression, novel insights into the neural underpinnings of interoceptive awareness and its link to abnormal behaviour was provided.

Abstract (German)

Die Fähigkeit, körperliche Vorgänge wahrzunehmen, wird als interozeptive Aufmerksamkeit bezeichnet und spielt eine wichtige Rolle in Theorien menschlicher Emotionsverarbeitung. Moderne, bildgebende Verfahren haben sich zu einem populären Instrument der neurowissenschaftlichen Forschung entwickelt und dazu beigetragen, unser Verständnis der zu Grunde liegenden neuronalen Substrate interozeptiver Aufmerksamkeit ständig zu erweitern. Vor allem die Insula, eine in der Tiefe der Sylvischen Furche gelegene bilaterale Hirnstruktur, ist in aktuellen Forschungsarbeiten zur interozeptiven Aufmerksamkeit in den Mittelpunkt gerückt. Emotionsverarbeitung wiederum steht in engem Zusammenhang mit interozeptiver Aufmerksamkeit sowie mit neuronaler Ruheaktivität in den kortikalen Mittellinienstrukturen, deren anteriore Bereiche funktionell mit neuronaler Aktivität in der Insula gekoppelt sind.

Allerdings bleibt diese zweifache Assoziation von Emotionen - zum einen mit neuronaler Ruheaktivität und zum anderen mit Interozeption - Gegenstand aktueller Forschung. Darüber hinaus ist zur Zeit wenig bekannt über die biochemischen Grundlagen der interozeptiven Aufmerksamkeit. Ebenso bleibt die Rolle bei affektiven Erkrankungen wie der Major Depression unklar.

Um diese Zusammenhänge zu untersuchen, wurden bildgebende Verfahren wie die funktionelle Magnetresonanztomographie (fMRT), Positronen-Emissions-Tomographie (PET) und Magnetresonanzspektroskopie (MRS) angewandt. Es wurden hierfür sowohl gesunde Probanden als auch Patienten mit Major Depression und remittierte Patienten (nach Abklingen der depressiven Symptomatik) rekrutiert. Die neuronale Aktivität während intero- und exterozeptiver Aufmerksamkeit (durch internes Zählen des eigenen Herzschlages und eines extern applizierten Tones) sowie während einer Ruhebedingung wurde mittels eines etablierten fMRT-Paradigmas untersucht und mit behavioralen Tests kombiniert.

Zunächst konnte in einer Gruppe von gesunden Probanden gezeigt werden, dass behaviorale Werte der Emotionsverarbeitung mit neuronaler Ruheaktivität in anterioren kortikalen Mittellinienstrukturen korreliert waren und nicht mit interozeptiver Aufmerksamkeit. In einer zweiten Studie wiesen depressive Patienten im Vergleich zu einer gesunden Probandengruppe eine abnorme neuronale Ruheaktivität in der Insula auf. Zudem zeigten depressive Patienten keine Korrelation zwischen neuronaler Ruheaktivität in der Insula und Körperwahrnehmung, so wie es in der gesunden Gruppe zu beobachten war. Die abweichende Ruheaktivität war außerdem mit der Depressionsschwere assoziiert.

In einer dritten Studie konnte dargelegt werden, dass Gruppenunterschiede zwischen gesunden, depressiven sowie remittierten Probanden vor allem im dorsalen anterioren Teil der Insula während interozeptiver Aufmerksamkeit auftraten. Depressive Patienten wiesen hier neuronale Hypoaktivierung auf, welche sich nach Abklingen der Symptomatik normalisierte. Darüber hinaus fanden sich in der depressiven Gruppe keine Aktivitätsunterschiede zwischen den verschiedenen Bedingungen (intero- und exterozeptive Aufmerksamkeit sowie Ruhebedingung).

Zum Schluss zeigten biochemische Untersuchungen in den hier primär untersuchten Gehirnbereichen (Insula und kortikale Mittellinienstrukturen) gesunder Probanden, dass i) der inhibitorische Neurotransmitter GABA eine wichtige Rolle in kortikalen Mittellinienstrukturen bei der differentiellen Verarbeitung von intero- und exterozeptiver Aufmerksamkeit spielt und ii) dass GABA die neuronale interozeptive Aktivität in der Insula moduliert, welches nicht in kortikalen Mittellinienstrukturen beobachtet wurde. GABA und neuronale Signalveränderungen während interozeptiver Aufmerksamkeit korrelierten außerdem mit behavioralen Depressionswerten.

Zusammenfassend kann gesagt werden, dass die hier vorgestellten Ergebnisse erste biochemische Grundlagen interozeptiver Aufmerksamkeit in der Insula sowie exterozeptiver Aufmerksamkeit in kortikalen Mittellinienstrukturen aufzeigen. Darüber hinaus liefern die Ergebnisse wertvolle Informationen über die Verbindungen zwischen Ruheaktivität und intero-/ exterozeptiver Aufmerksamkeit in Kombination mit Verhaltensvariablen (Emotionen und Körperwahrnehmung). Die Untersuchung depressiver Patienten liefert neue Einblicke in neuronale Grundlagen interozeptiver Aufmerksamkeit in Verbindung mit Verhaltensauffälligkeiten.

Bibliography

A Alcaro, J Panksepp, J Witczak, D J Hayes, and G Northoff. Is subcortical-cortical midline activity in depression mediated by glutamate and GABA? A cross-species translational approach. *Neurosci Biobehav Rev*, 34(4):592–605, 2010. URL http://www.ncbi.nlm.nih.gov/entrez/query.fcgi?cmd=Retrieve&db=PubMed&dopt=Citation&list_uids=19958790.

American Psychiatric Association. *American Psychiatric Association (APA). Diagnostic and Statistical Manual of Mental Disorders*. Washington, DC, 4th editio edition, 1994.

J Ashburner and K J Friston. Nonlinear spatial normalization using basis functions. *Hum Brain Mapp*, 7(4):254–266, 1999. doi: 10.1002/(SICI)1097-0193(1999)7:4<254::AID-HBM4>3.0.CO;2-G[pii]. URL http://www.ncbi.nlm.nih.gov/entrez/query.fcgi?cmd=Retrieve&db=PubMed&dopt=Citation&list_uids=10408769.

D.L. Bailey, D.W. Townsend, P.E. Valk, and M.N. Maisey. *Positron Emission Tomography: Basic Sciences*. Springer, 1st editio edition, 2003. ISBN 978-1852334857.

M Bajbouj, S H Lisanby, U E Lang, H Danker-Hopfe, I Heuser, and P Neu. Evidence for impaired cortical inhibition in patients with unipolar major depression. *Biol Psychiatry*, 59(5):395–400, 2006. doi: S0006-3223(05)00925-X[pii]10.1016/j.biopsych.2005.07.036. URL <http://www.ncbi.nlm.nih.gov/pubmed/16197927>.

Karl-Jürgen Bär, Gerd Wagner, Mandy Koschke, Silke Boettger, Michael Karl Boettger, Ralf Schlösser, and Heinrich Sauer. Increased prefrontal activation during pain perception in major depression. *Biological psychiatry*, 62(11):1281–7, December 2007.

ISSN 0006-3223. doi: 10.1016/j.biopsycho.2007.02.011. URL <http://www.ncbi.nlm.nih.gov/pubmed/17570347>.

P M Barrett. Evaluation of cognitive-behavioral group treatments for childhood anxiety disorders. *Journal of clinical child psychology*, 27(4):459–68, December 1998. ISSN 0047-228X. doi: 10.1207/s15374424jccp2704_10. URL <http://www.ncbi.nlm.nih.gov/pubmed/9866083>.

A Bechara and N Naqvi. Listening to your heart: interoceptive awareness as a gateway to feeling. *Nat Neurosci*, 7(2):102–103, 2004. doi: 10.1038/nm0204-102.

A T Beck. A systematic investigation of depression. *Compr Psychiatry*, 2:163–170, 1961. URL http://www.ncbi.nlm.nih.gov/entrez/query.fcgi?cmd=Retrieve&db=PubMed&dopt=Citation&list_uids=13866251.

A T Beck, C H Ward, M Mendelson, J Mock, and J Erbaugh. An inventory for measuring depression. *Arch Gen Psychiatry*, 4:561–571, 1961. URL http://www.ncbi.nlm.nih.gov/entrez/query.fcgi?cmd=Retrieve&db=PubMed&dopt=Citation&list_uids=13688369.

A T Beck, A Weissman, D Lester, and L Trexler. The measurement of pessimism: the hopelessness scale. *J Consult Clin Psychol*, 42(6):861–865, 1974. URL http://www.ncbi.nlm.nih.gov/entrez/query.fcgi?cmd=Retrieve&db=PubMed&dopt=Citation&list_uids=4436473.

A.T. Beck, R.A. Steer, R. Ball, and W. Ranieri. Comparison of Beck Depression Inventories -IA and -II in psychiatric outpatients. *Journal of Personality Assessment*, 67(3): 588–97, 1996.

C F Beckmann and S M Smith. Probabilistic independent component analysis for functional magnetic resonance imaging. *IEEE Trans Med Imaging*, 23(2):137–152, 2004. doi: 10.1109/TMI.2003.822821. URL http://www.ncbi.nlm.nih.gov/entrez/query.fcgi?cmd=Retrieve&db=PubMed&dopt=Citation&list_uids=14964560.

M Beckmann, H Johansen-Berg, and M F Rushworth. Connectivity-based parcellation of human cingulate cortex and its relation to functional specialization. *J Neurosci*, 29(4):1175–1190, 2009. doi: 29/4/1175[pii]10.1523/JNEUROSCI.3328-08.2009. URL http://www.ncbi.nlm.nih.gov/entrez/query.fcgi?cmd=Retrieve&db=PubMed&dopt=Citation&list_uids=19176826.

Katja Beesdo, Jennifer Y F Lau, Amanda E Guyer, Erin B McClure-Tone, Christopher S Monk, Eric E Nelson, Stephen J Fromm, Michelle A Goldwin, Hans-Ulrich Wittchen, Ellen Leibenluft, Monique Ernst, and Daniel S Pine. Common and distinct amygdala-function perturbations in depressed vs anxious adolescents. *Archives of general psychiatry*, 66(3):275–85, March 2009. ISSN 1538-3636. doi: 10.1001/archgenpsychiatry.2008.545. URL <http://www.pubmedcentral.nih.gov/articlerender.fcgi?artid=2891508&tool=pmcentrez&rendertype=abstract>.

C M Bennett, G L Wolford, and M B Miller. The principled control of false positives in neuroimaging. *Soc Cogn Affect Neurosci*, 4(4):417–422, 2009. URL http://www.ncbi.nlm.nih.gov/entrez/query.fcgi?cmd=Retrieve&db=PubMed&dopt=Citation&list_uids=20042432.

H Bielau, J Steiner, C Mawrin, K Trubner, R Brisch, G Meyer-Lotz, M Brodhun, H Dobrowolny, B Baumann, T Gos, H G Bernstein, and B Bogerts. Dysregulation of GABAergic neurotransmission in mood disorders: a postmortem study. *Ann N Y Acad Sci*, 1096:157–169, 2007. doi: 1096/1/157[pii]10.1196/annals.1397.081. URL http://www.ncbi.nlm.nih.gov/entrez/query.fcgi?cmd=Retrieve&db=PubMed&dopt=Citation&list_uids=17405927.

M Boly, E Balteau, C Schnakers, C Degueldre, G Moonen, A Luxen, C Phillips, P Peigneux, P Maquet, and S Laureys. Baseline brain activity fluctuations predict somatosensory perception in humans. *Proc Natl Acad Sci U S A*, 104(29):12187–12192, 2007. doi: 0611404104[pii]10.1073/

pnas.0611404104. URL http://www.ncbi.nlm.nih.gov/entrez/query.fcgi?cmd=Retrieve&db=PubMed&dopt=Citation&list_uids=17616583.

M Boly, C Phillips, L Tshibanda, A Vanhaudenhuyse, M Schabus, T T Dang-Vu, G Moonen, R Hustinx, P Maquet, and S Laureys. Intrinsic brain activity in altered states of consciousness: how conscious is the default mode of brain function? *Ann N Y Acad Sci*, 1129:119–129, 2008. doi: 10.1196/annals.1417.0151129/1/119[pii]. URL http://www.ncbi.nlm.nih.gov/entrez/query.fcgi?cmd=Retrieve&db=PubMed&dopt=Citation&list_uids=18591474.

M Boly, L Tshibanda, A Vanhaudenhuyse, Q Noirhomme, C Schnakers, D Ledoux, P Boveroux, C Garweg, B Lambermont, C Phillips, A Luxen, G Moonen, C Bassetti, P Maquet, and S Laureys. Functional connectivity in the default network during resting state is preserved in a vegetative but not in a brain dead patient. *Hum Brain Mapp*, 30(8):2393–2400, 2009. doi: 10.1002/hbm.20672. URL http://www.ncbi.nlm.nih.gov/entrez/query.fcgi?cmd=Retrieve&db=PubMed&dopt=Citation&list_uids=19350563.

R C Bowen, D R Offord, and M H Boyle. The prevalence of overanxious disorder and separation anxiety disorder: results from the Ontario Child Health Study. *Journal of the American Academy of Child and Adolescent Psychiatry*, 29(5):753–8, September 1990. ISSN 0890-8567. doi: 10.1097/00004583-199009000-00013. URL <http://www.ncbi.nlm.nih.gov/pubmed/2228929>.

D Bowers, L X Blonder, and K M Heilman. The Florida Affect Battery Manual. *Center for Neuropsychological Studies, University of Florida, Gainesville FL*, 1991.

W T Boyce, J Quas, A Alkon, N A Smider, M J Essex, and D J Kupfer. Autonomic reactivity and psychopathology in middle childhood. *The British journal of psychiatry : the journal of mental science*, 179:144–50, August 2001. ISSN 0007-1250. URL <http://www.ncbi.nlm.nih.gov/pubmed/11483476>.

- M Brett, J L Anton, R Valabrgue, and J B Poline. Region of interest analysis using an SPM toolbox. Presented at the 8th International Conference on Functional Mapping of the Human Brain, June 2-6, 2002, Sendai, Japan. *Neuroimage*, 13:210–217, 2002. URL <http://www.sourceforge.net/projects/marsbar>.
- A L Brody, S Saxena, P Stoessel, L A Gillies, L A Fairbanks, S Alborzian, M E Phelps, S C Huang, H M Wu, M L Ho, M K Ho, S C Au, K Maidment, and L R Baxter. Regional brain metabolic changes in patients with major depression treated with either paroxetine or interpersonal therapy: preliminary findings. *Archives of general psychiatry*, 58(7):631–40, July 2001. ISSN 0003-990X. URL <http://www.ncbi.nlm.nih.gov/pubmed/11448368>.
- Evelyn Bromet, Laura Helena Andrade, Irving Hwang, Nancy A Sampson, Jordi Alonso, Giovanni de Girolamo, Ron de Graaf, Koen Demyttenaere, Chiyi Hu, Noboru Iwata, Aimee N Karam, Jagdish Kaur, Stanislav Kostyuchenko, Jean-Pierre Lépine, Daphna Levinson, Herbert Matschinger, Maria Elena Medina Mora, Mark Oakley Browne, Jose Posada-Villa, Maria Carmen Viana, David R Williams, and Ronald C Kessler. Cross-national epidemiology of DSM-IV major depressive episode. *BMC medicine*, 9:90, January 2011. ISSN 1741-7015. doi: 10.1186/1741-7015-9-90. URL <http://www.pubmedcentral.nih.gov/articlerender.fcgi?artid=3163615&tool=pmcentrez&rendertype=abstract>.
- John O Brooks, Po W Wang, Julie C Bonner, Allyson C Rosen, Jennifer C Hoblyn, Shelley J Hill, and Terence a Ketter. Decreased prefrontal, anterior cingulate, insula, and ventral striatal metabolism in medication-free depressed outpatients with bipolar disorder. *Journal of psychiatric research*, 43(3):181–8, January 2009. ISSN 0022-3956. doi: 10.1016/j.jpsychires.2008.04.015. URL <http://www.pubmedcentral.nih.gov/articlerender.fcgi?artid=3265392&tool=pmcentrez&rendertype=abstract>.
- R L Buckner, J R Andrews-Hanna, and D L Schacter. The brain's default network: anatomy, function, and relevance to disease. *Ann*

N Y Acad Sci, 1124:1–38, 2008. doi: 1124/1/1[pii]10.1196/annals.1440.011. URL http://www.ncbi.nlm.nih.gov/entrez/query.fcgi?cmd=Retrieve&db=PubMed&dopt=Citation&list_uids=18400922.

R B Buxton, E C Wong, and L R Frank. Dynamics of blood flow and oxygenation changes during brain activation: the balloon model. *Magnetic resonance in medicine : official journal of the Society of Magnetic Resonance in Medicine / Society of Magnetic Resonance in Medicine*, 39(6):855–64, June 1998. ISSN 0740-3194. URL <http://www.ncbi.nlm.nih.gov/pubmed/9621908>.

Andrea Caria, Ralf Veit, Ranganatha Sitaram, Martin Lotze, Nikolaus Weiskopf, Wolfgang Grodd, and Niels Birbaumer. Regulation of anterior insular cortex activity using real-time fMRI. *NeuroImage*, 35(3):1238–46, April 2007. ISSN 1053-8119. doi: 10.1016/j.neuroimage.2007.01.018. URL <http://www.ncbi.nlm.nih.gov/pubmed/17336094>.

B J Casey, J D Cohen, K O’Craven, R J Davidson, W Irwin, C A Nelson, D C Noll, X Hu, M J Lowe, B R Rosen, C L Truwitt, and P A Turski. Reproducibility of fMRI results across four institutions using a spatial working memory task. *Neuroimage*, 8(3):249–261, 1998. doi: S1053-8119(98)90360-3[pii]10.1006/nimg.1998.0360. URL http://www.ncbi.nlm.nih.gov/entrez/query.fcgi?cmd=Retrieve&db=PubMed&dopt=Citation&list_uids=9758739.

Franco Cauda, Federico D’Agata, Katiusia Sacco, Sergio Duca, Giuliano Geminiani, and Alessandro Vercelli. Functional connectivity of the insula in the resting brain. *NeuroImage*, 55(1):8–23, March 2011. doi: 10.1016/j.neuroimage.2010.11.049.

Leonardo Cerliani, Rajat M Thomas, Saad Jbabdi, Jeroen C W Siero, Luca Nanetti, Alessandro Crippa, Valeria Gazzola, Helen D’Arceuil, and Christian Keysers. Probabilistic tractography recovers a rostrocaudal trajectory of connectivity variability in the human insular cortex. *Human brain mapping*, 33(9):2005–34, September 2012.

ISSN 1097-0193. doi: 10.1002/hbm.21338. URL <http://www.pubmedcentral.nih.gov/articlerender.fcgi?artid=3443376&tool=pmcentrez&rendertype=abstract>.

Luke J Chang, Tal Yarkoni, Mel Win Khaw, and Alan G Sanfey. Decoding the Role of the Insula in Human Cognition: Functional Parcellation and Large-Scale Reverse Inference. *Cerebral Cortex*, March 2012. ISSN 1460-2199. URL <http://www.ncbi.nlm.nih.gov/pubmed/22437053>.

J.M. Chein and W Schneider. Designing effective fMRI experiments. In J Grafman and I Robertson, editors, *The handbook of neuropsychology*. Elsevier, Amsterdam, 2003.

K Christoff, A M Gordon, J Smallwood, R Smith, and J W Schooler. Experience sampling during fMRI reveals default network and executive system contributions to mind wandering. *Proc Natl Acad Sci U S A*, 106(21):8719–8724, 2009. doi: 0900234106[pii] 10.1073/pnas.0900234106. URL http://www.ncbi.nlm.nih.gov/entrez/query.fcgi?cmd=Retrieve&db=PubMed&dopt=Citation&list_uids=19433790.

Lauren L Cloutman, Richard J Binney, Mark Drakesmith, Geoffrey J M Parker, and Matthew a Lambon Ralph. The variation of function across the human insula mirrors its patterns of structural connectivity: evidence from in vivo probabilistic tractography. *NeuroImage*, 59(4):3514–21, February 2012. ISSN 1095-9572. doi: 10.1016/j.neuroimage.2011.11.016. URL <http://www.ncbi.nlm.nih.gov/pubmed/22100771>.

Scott N Compton, John S March, David Brent, Anne Marie Albano, Robin Weersing, and John Curry. Cognitive-behavioral psychotherapy for anxiety and depressive disorders in children and adolescents: an evidence-based medicine review. *Journal of the American Academy of Child and Adolescent Psychiatry*, 43(8):930–59, August 2004. ISSN 0890-8567. URL <http://www.ncbi.nlm.nih.gov/pubmed/15266189>.

J K Connor-Smith, B E Compas, M E Wadsworth, A H Thomsen, and H Saltzman. Responses to stress in adolescence: measurement of coping and involuntary stress

responses. *Journal of consulting and clinical psychology*, 68(6):976–92, December 2000. ISSN 0022-006X. URL <http://www.ncbi.nlm.nih.gov/pubmed/11142550>.

E Jane Costello, Helen Egger, and Adrian Angold. 10-year research update review: the epidemiology of child and adolescent psychiatric disorders: I. Methods and public health burden. *Journal of the American Academy of Child and Adolescent Psychiatry*, 44(10):972–86, October 2005. ISSN 0890-8567. doi: 10.1097/01.chi.0000172552.41596.6f. URL <http://www.ncbi.nlm.nih.gov/pubmed/16175102>.

N Costes, A Dagher, K Larcher, A C Evans, D L Collins, and A Reilhac. Motion correction of multi-frame PET data in neuroreceptor mapping: simulation based validation. *Neuroimage*, 47(4):1496–1505, 2009. doi: S1053-8119(09)00558-8[pii]10.1016/j.neuroimage.2009.05.052. URL http://www.ncbi.nlm.nih.gov/entrez/query.fcgi?cmd=Retrieve&db=PubMed&dopt=Citation&list_uids=19481154.

A D Craig. How do you feel? Interoception: the sense of the physiological condition of the body. *Nat Rev Neurosci*, 3(8):655–666, 2002. doi: 10.1038/nrn894nrn894[pii]. URL http://www.ncbi.nlm.nih.gov/entrez/query.fcgi?cmd=Retrieve&db=PubMed&dopt=Citation&list_uids=12154366.

A D Craig. Interoception: the sense of the physiological condition of the body. *Curr Opin Neurobiol*, 13(4):500–505, 2003. URL http://www.ncbi.nlm.nih.gov/entrez/query.fcgi?cmd=Retrieve&db=PubMed&dopt=Citation&list_uids=12965300.

A D Craig. Human feelings: why are some more aware than others? *Trends Cogn Sci*, 8(6):239–241, 2004. URL http://www.ncbi.nlm.nih.gov/entrez/query.fcgi?cmd=Retrieve&db=PubMed&dopt=Citation&list_uids=15165543.

A D Craig. How do you feel—now? The anterior insula and human awareness. *Nat Rev Neurosci*, 10(1):59–70, 2009. doi: nrn2555[pii]10.1038/nrn2555. URL http://www.ncbi.nlm.nih.gov/entrez/query.fcgi?cmd=Retrieve&db=PubMed&dopt=Citation&list_uids=19096369.

A D Bud Craig. Interoception and Emotion : a Neuroanatomical Perspective. In M Lewis, J M Haviland-Jones, and L F Barrett, editors, *Handbook of Emotions*, volume 06, pages 272–288. Guilford Press, New York, 3rd edition, 2008.

a D Bud Craig. Significance of the insula for the evolution of human awareness of feelings from the body. *Annals of the New York Academy of Sciences*, 1225:72–82, April 2011. ISSN 1749-6632. doi: 10.1111/j.1749-6632.2011.05990.x. URL <http://www.ncbi.nlm.nih.gov/pubmed/21534994>.

H D Critchley, S Wiens, P Rotshtein, A Ohman, and R J Dolan. Neural systems supporting interoceptive awareness. *Nat Neurosci*, 7(2):189–195, 2004. URL http://www.ncbi.nlm.nih.gov/entrez/query.fcgi?cmd=Retrieve&db=PubMed&dopt=Citation&list_uids=14730305.

H D Critchley, P Rotshtein, Y Nagai, J O’Doherty, C J Mathias, and R J Dolan. Activity in the human brain predicting differential heart rate responses to emotional facial expressions. *Neuroimage*, 24(3):751–762, 2005. URL http://www.ncbi.nlm.nih.gov/entrez/query.fcgi?cmd=Retrieve&db=PubMed&dopt=Citation&list_uids=15652310.

Paul E Croarkin, Andrea J Levinson, and Zafiris J Daskalakis. Evidence for GABAergic inhibitory deficits in major depressive disorder. *Neuroscience and Biobehavioral Reviews*, 35(3):818–25, January 2011. doi: 10.1016/j.neubiorev.2010.10.002.

A R Damasio. How the brain creates the mind. *Sci Am*, 281(6): 112–117, 1999a. URL http://www.ncbi.nlm.nih.gov/entrez/query.fcgi?cmd=Retrieve&db=PubMed&dopt=Citation&list_uids=10614073.

Antonio R Damasio. *The feeling of what happens : body and emotion in the making of consciousness*. Harcourt Brace, New York, 1st edition, 1999b. ISBN 0151003696. URL <http://www.loc.gov/catdir/description/har021/99026357.html><http://lcweb.loc.gov/catdir/toc/99026357.html>.

J S Damoiseaux, S A Rombouts, F Barkhof, P Scheltens, C J Stam, S M Smith, and C F Beckmann. Consistent resting-state networks across healthy subjects. *Proc Natl Acad Sci U S A*, 103(37):13848–13853, 2006. URL http://www.ncbi.nlm.nih.gov/entrez/query.fcgi?cmd=Retrieve&db=PubMed&dopt=Citation&list_uids=16945915.

H W de Jong, F H van Velden, R W Kloet, F L Buijs, R Boellaard, and A A Lammertsma. Performance evaluation of the ECAT HRRT: an LSO-LYSO double layer high resolution, high sensitivity scanner. *Phys Med Biol*, 52(5):1505–1526, 2007. doi: S0031-9155(07)33171-0[pii]10.1088/0031-9155/52/5/019. URL http://www.ncbi.nlm.nih.gov/entrez/query.fcgi?cmd=Retrieve&db=PubMed&dopt=Citation&list_uids=17301468.

Ben Deen, Naomi B Pitskel, and Kevin a Pelphrey. Three systems of insular functional connectivity identified with cluster analysis. *Cerebral cortex (New York, N.Y. : 1991)*, 21(7):1498–506, July 2011. ISSN 1460-2199. doi: 10.1093/cercor/bhq186. URL <http://www.pubmedcentral.nih.gov/articlerender.fcgi?artid=3116731&tool=pmcentrez&rendertype=abstract>.

M J Donahue, J Near, J U Blicher, and P Jezard. Baseline GABA concentration and fMRI response. *Neuroimage*, 53(2):392–398, 2010. doi: S1053-8119(10)00968-7[pii]10.1016/j.neuroimage.2010.07.017. URL http://www.ncbi.nlm.nih.gov/entrez/query.fcgi?cmd=Retrieve&db=PubMed&dopt=Citation&list_uids=20633664.

J Duncan and A M Owen. Common regions of the human frontal lobe recruited by diverse cognitive demands. *Trends Neurosci*, 23(10):475–483, 2000. doi: S0166-2236(00)01633-7[pii]. URL http://www.ncbi.nlm.nih.gov/entrez/query.fcgi?cmd=Retrieve&db=PubMed&dopt=Citation&list_uids=11006464.

N W Duncan, B Enzi, C Wiebking, and G Northoff. Involvement of glutamate in rest-stimulus interaction between perigenual and supragenual anterior cingulate cortex:

- a combined fMRI-MRS study. *Hum Brain Mapp*, 32(12):2172–2182, 2011. doi: 10.1002/hbm.21179. URL http://www.ncbi.nlm.nih.gov/entrez/query.fcgi?cmd=Retrieve&db=PubMed&dopt=Citation&list_uids=21305662.
- B D Dunn, I Stefanovitch, D Evans, C Oliver, A Hawkins, and T Dalgleish. Can you feel the beat? Interoceptive awareness is an interactive function of anxiety- and depression-specific symptom dimensions. *Behav Res Ther*, 2010a. doi: S0005-7967(10)00149-X[pii]10.1016/j.brat.2010.07.006. URL <http://www.ncbi.nlm.nih.gov/pubmed/20692645>.
- Barnaby D Dunn, Tim Dalgleish, Alan D Ogilvie, and Andrew D Lawrence. Heartbeat perception in depression. *Behaviour research and therapy*, 45(8):1921–30, August 2007. ISSN 0005-7967. doi: 10.1016/j.brat.2006.09.008. URL <http://www.ncbi.nlm.nih.gov/pubmed/17087914>.
- Barnaby D Dunn, Hannah C Galton, Ruth Morgan, Davy Evans, Clare Oliver, Marcel Meyer, Rhodri Cusack, Andrew D Lawrence, and Tim Dalgleish. Listening to your heart. How interoception shapes emotion experience and intuitive decision making. *Psychological Science*, 21(12):1835–44, December 2010b. doi: 10.1177/0956797610389191.
- S Dupont, V Boullieret, D Hasboun, F Semah, and M Baulac. Functional anatomy of the insula: new insights from imaging. *Surgical and radiologic anatomy : SRA*, 25(2):113–9, May 2003. ISSN 0930-1038. doi: 10.1007/s00276-003-0103-4. URL <http://www.ncbi.nlm.nih.gov/pubmed/12819943>.
- Mark a Eckert, Vinod Menon, Adam Walczak, Jayne Ahlstrom, Stewart Denslow, Amy Horwitz, and Judy R Dubno. At the heart of the ventral attention system: the right anterior insula. *Human brain mapping*, 30(8):2530–41, August 2009. ISSN 1097-0193. doi: 10.1002/hbm.20688. URL <http://www.pubmedcentral.nih.gov/articlerender.fcgi?artid=2712290&tool=pmcentrez&rendertype=abstract>.

S B Eickhoff, T Paus, S Caspers, M H Grosbras, A C Evans, K Zilles, and K Amunts. Assignment of functional activations to probabilistic cytoarchitectonic areas revisited. *Neuroimage*, 36(3):511–521, 2007. doi: S1053-8119(07)00230-3[pil]10.1016/j.neuroimage.2007.03.060. URL http://www.ncbi.nlm.nih.gov/entrez/query.fcgi?cmd=Retrieve&db=PubMed&dopt=Citation&list_uids=17499520.

Thalia C Eley, Lucy Stirling, Anke Ehlers, Alice M Gregory, and David M Clark. Heart-beat perception, panic/somatic symptoms and anxiety sensitivity in children. *Behaviour research and therapy*, 42(4):439–48, April 2004. ISSN 0005-7967. doi: 10.1016/S0005-7967(03)00152-9. URL <http://www.ncbi.nlm.nih.gov/pubmed/14998737>.

Amit Etkin, Tobias Egner, and Raffael Kalisch. Emotional processing in anterior cingulate and medial prefrontal cortex. *Trends in cognitive sciences*, 15(2):85–93, February 2011. ISSN 1879-307X. doi: 10.1016/j.tics.2010.11.004. URL <http://www.pubmedcentral.nih.gov/articlerender.fcgi?artid=3035157&tool=pmcentrez&rendertype=abstract>.

Liv E Falkenberg, René Westerhausen, Karsten Specht, and Kenneth Hugdahl. Resting-state glutamate level in the anterior cingulate predicts blood-oxygen level-dependent response to cognitive control. *Proceedings of the National Academy of Sciences of the United States of America*, pages 1–6, March 2012. doi: 10.1073/pnas.1115628109.

Norman a S Farb, Zindel V Segal, and Adam K Anderson. Attentional Modulation of Primary Interoceptive and Exteroceptive Cortices. *Cerebral cortex (New York, N.Y. : 1991)*, pages 1–13, January 2012a. ISSN 1460-2199. doi: 10.1093/cercor/bhr385. URL <http://www.ncbi.nlm.nih.gov/pubmed/22267308>.

Norman A S Farb, Zindel V Segal, and Adam K Anderson. Mindfulness meditation training alters cortical representations of interoceptive attention. *Social cognitive and*

affective neuroscience, pages nss066–, 2012b. ISSN 17495024. doi: 10.1093/scan/nss066. URL <http://www.ncbi.nlm.nih.gov/pubmed/22689216>.

Maurizio Fava. Symptoms of fatigue and cognitive/executive dysfunction in major depressive disorder before and after antidepressant treatment. *The Journal of clinical psychiatry*, 64 Suppl 1(suppl 14):30–4, January 2003. ISSN 1555-2101. URL <http://www.ncbi.nlm.nih.gov/pubmed/14658933>.

David a Feinberg and Essa Yacoub. The rapid development of high speed, resolution and precision in fMRI. *NeuroImage*, 62(2):720–5, August 2012. ISSN 1095-9572. doi: 10.1016/j.neuroimage.2012.01.049. URL <http://www.ncbi.nlm.nih.gov/pubmed/22281677>.

D M Fergusson, L J Horwood, and M T Lynskey. Prevalence and comorbidity of DSM-III-R diagnoses in a birth cohort of 15 year olds. *Journal of the American Academy of Child and Adolescent Psychiatry*, 32(6):1127–34, November 1993. ISSN 0890-8567. doi: 10.1097/00004583-199311000-00004. URL <http://www.ncbi.nlm.nih.gov/pubmed/8282656>.

P B Fitzgerald, A R Laird, J Maller, and Z J Daskalakis. A meta-analytic study of changes in brain activation in depression. *Hum Brain Mapp*, 29(6):683–695, 2008. URL http://www.ncbi.nlm.nih.gov/entrez/query.fcgi?cmd=Retrieve&db=PubMed&dopt=Citation&list_uids=17598168.

M D Fox and M E Raichle. Spontaneous fluctuations in brain activity observed with functional magnetic resonance imaging. *Nat Rev Neurosci*, 8(9):700–711, 2007. doi: nrn2201[pii]10.1038/nrn2201. URL http://www.ncbi.nlm.nih.gov/entrez/query.fcgi?cmd=Retrieve&db=PubMed&dopt=Citation&list_uids=17704812.

M D Fox, A Z Snyder, J L Vincent, M Corbetta, D C Van Essen, and M E Raichle. The human brain is intrinsically organized into dynamic, anticorrelated functional networks. *Proc Natl Acad Sci U S A*, 102(27):9673–9678, 2005. doi: 0504136102[pii]10.

1073/pnas.0504136102. URL http://www.ncbi.nlm.nih.gov/entrez/query.fcgi?cmd=Retrieve&db=PubMed&dopt=Citation&list_uids=15976020.

W G Frankle, R Y Cho, R Narendran, N S Mason, S Vora, M Litschge, J C Price, D A Lewis, and C A Mathis. Tiagabine increases [11C]flumazenil binding in cortical brain regions in healthy control subjects. *Neuropsychopharmacology*, 34(3):624–633, 2009. doi: npp2008104[pii]10.1038/npp.2008.104. URL http://www.ncbi.nlm.nih.gov/entrez/query.fcgi?cmd=Retrieve&db=PubMed&dopt=Citation&list_uids=18615011.

W G Frankle, R Y Cho, N S Mason, C M Chen, M Himes, C Walker, D A Lewis, C A Mathis, and R Narendran. [11C]flumazenil binding is increased in a dose-dependent manner with tiagabine-induced elevations in GABA levels. *PLoS ONE*, 7(2):e32443, 2012. doi: 10.1371/journal.pone.0032443PONE-D-11-19835[pii]. URL http://www.ncbi.nlm.nih.gov/entrez/query.fcgi?cmd=Retrieve&db=PubMed&dopt=Citation&list_uids=22384252.

P Fransson. Spontaneous low-frequency BOLD signal fluctuations: an fMRI investigation of the resting-state default mode of brain function hypothesis. *Hum Brain Mapp*, 26(1):15–29, 2005. doi: 10.1002/hbm.20113. URL http://www.ncbi.nlm.nih.gov/entrez/query.fcgi?cmd=Retrieve&db=PubMed&dopt=Citation&list_uids=15852468.

P Fransson. How default is the default mode of brain function? Further evidence from intrinsic BOLD signal fluctuations. *Neuropsychologia*, 44(14):2836–2845, 2006. URL http://www.ncbi.nlm.nih.gov/entrez/query.fcgi?cmd=Retrieve&db=PubMed&dopt=Citation&list_uids=16879844.

K A Frey, V A Holthoff, R A Koeppe, D M Jewett, M R Kilbourn, and D E Kuhl. Parametric in vivo imaging of benzodiazepine receptor distribution in human brain. *Ann Neurol*, 30(5):663–672, 1991. doi: 10.

1002/ana.410300506. URL http://www.ncbi.nlm.nih.gov/entrez/query.fcgi?cmd=Retrieve&db=PubMed&dopt=Citation&list_uids=1662476.

K J Friston, A P Holmes, K J Worsley, J B Poline, C Frith, and R S J Frackowiak. Statistical Parametric Maps in Functional Imaging: A General Linear Approach. *Hum Brain Mapp*, 2:189–210, 1995.

K J Friston, P Fletcher, O Josephs, A Holmes, M D Rugg, and R Turner. Event-related fMRI: characterizing differential responses. *Neuroimage*, 7(1):30–40, 1998. doi: S1053-8119(97)90306-2[pii]10.1006/nimg.1997.0306. URL http://www.ncbi.nlm.nih.gov/entrez/query.fcgi?cmd=Retrieve&db=PubMed&dopt=Citation&list_uids=9500830.

T Frodl, J Scheuerecker, J Albrecht, A M Kleemann, S Muller-Schunk, N Koutsouleris, H J Moller, H Bruckmann, M Wiesmann, and E Meisenzahl. Neuronal correlates of emotional processing in patients with major depression. *World J Biol Psychiatry*, pages 1–7, 2007. URL http://www.ncbi.nlm.nih.gov/entrez/query.fcgi?cmd=Retrieve&db=PubMed&dopt=Citation&list_uids=17965984.

A J Fyer, S Mannuzza, T F Chapman, L Y Martin, and D F Klein. Specificity in familial aggregation of phobic disorders. *Archives of general psychiatry*, 52(7):564–73, July 1995. ISSN 0003-990X. URL <http://www.ncbi.nlm.nih.gov/pubmed/7598633>.

A Garcia-Cebrian, P Gandhi, K Demyttenaere, and R Peveler. The association of depression and painful physical symptoms—a review of the European literature. *Eur Psychiatry*, 21(6):379–388, 2006. doi: S0924-9338(05)00217-8[pii]10.1016/j.eurpsy.2005.12.003. URL http://www.ncbi.nlm.nih.gov/entrez/query.fcgi?cmd=Retrieve&db=PubMed&dopt=Citation&list_uids=16797937.

C Gentili, E Ricciardi, M I Gobbi, M F Santarelli, J V Haxby, P Pietrini, and M Guazzelli. Beyond amygdala: Default Mode Network activity differs between patients with social phobia and healthy controls. *Brain Res Bull*, 79(6):409–413,

2009. doi: S0361-9230(09)00062-8[pii]10.1016/j.brainresbull.2009.02.002. URL <http://www.ncbi.nlm.nih.gov/pubmed/19559343>.

Jeroen J G Geurts, Frederik Barkhof, Jonas A Castelijns, Bernard M J Uitdehaag, Chris H Polman, and Petra J W Pouwels. Quantitative ¹H-MRS of healthy human cortex, hippocampus, and thalamus: metabolite concentrations, quantification precision, and reproducibility. *Journal of Magnetic Resonance Imaging*, 20(3):366–371, 2004. URL <http://www.ncbi.nlm.nih.gov/pubmed/15332241>.

S J Gillihan and M J Farah. Is self special? A critical review of evidence from experimental psychology and cognitive neuroscience. *Psychol Bull*, 131(1):76–97, 2005. doi: 2004-22408-006[pii]10.1037/0033-2909.131.1.76. URL http://www.ncbi.nlm.nih.gov/entrez/query.fcgi?cmd=Retrieve&db=PubMed&dopt=Citation&list_uids=15631554.

Il Goldberg, M Harel, and R Malach. When the brain loses its self: prefrontal inactivation during sensorimotor processing. *Neuron*, 50(2):329–339, 2006. doi: S0896-6273(06)00212-1[pii]10.1016/j.neuron.2006.03.015. URL http://www.ncbi.nlm.nih.gov/entrez/query.fcgi?cmd=Retrieve&db=PubMed&dopt=Citation&list_uids=16630842.

Philippe R Goldin, Tali Manber, Shabnam Hakimi, Turhan Canli, and James J Gross. Neural bases of social anxiety disorder: emotional reactivity and cognitive regulation during social and physical threat. *Archives of general psychiatry*, 66(2):170–80, March 2009. ISSN 1538-3636. doi: 10.1001/archgenpsychiatry.2008.525. URL <http://www.ncbi.nlm.nih.gov/pubmed/19188539>.

R Z Goldstein, N Alia-Klein, D Tomasi, L Zhang, L A Cottone, T Maloney, F Telang, E C Caparelli, L Chang, T Ernst, D Samaras, N K Squires, and N D Volkow. Is decreased prefrontal cortical sensitivity to monetary reward associated with impaired motivation and self-control in cocaine addiction? *Am J Psychiatry*, 164(1):43–51,

2007. URL http://www.ncbi.nlm.nih.gov/entrez/query.fcgi?cmd=Retrieve&db=PubMed&dopt=Citation&list_uids=17202543.

Y Golland, S Bentin, H Gelbard, Y Benjamini, R Heller, Y Nir, U Hasson, and R Malach. Extrinsic and intrinsic systems in the posterior cortex of the human brain revealed during natural sensory stimulation. *Cereb Cortex*, 17(4):766–777, 2007. doi: bhk030[pii]10.1093/cercor/bhk030. URL http://www.ncbi.nlm.nih.gov/entrez/query.fcgi?cmd=Retrieve&db=PubMed&dopt=Citation&list_uids=16699080.

Y Golland, P Golland, S Bentin, and R Malach. Data-driven clustering reveals a fundamental subdivision of the human cortex into two global systems. *Neuropsychologia*, 46(2):540–553, 2008. doi: S0028-3932(07)00347-8[pii]10.1016/j.neuropsychologia.2007.10.003. URL http://www.ncbi.nlm.nih.gov/entrez/query.fcgi?cmd=Retrieve&db=PubMed&dopt=Citation&list_uids=18037453.

V E Gountouna, D E Job, A M McIntosh, T W Moorhead, G K Lymer, H C Whalley, J Hall, G D Waiter, D Brennan, D J McGonigle, T S Ahearn, J Cavanagh, B Condon, D M Hadley, I Marshall, A D Murray, J D Steele, J M Wardlaw, and S M Lawrie. Functional Magnetic Resonance Imaging (fMRI) reproducibility and variance components across visits and scanning sites with a finger tapping task. *Neuroimage*, 49(1):552–560, 2010. doi: S1053-8119(09)00798-8[pii]10.1016/j.neuroimage.2009.07.026. URL http://www.ncbi.nlm.nih.gov/entrez/query.fcgi?cmd=Retrieve&db=PubMed&dopt=Citation&list_uids=19631757.

M D Greicius, B H Flores, V Menon, G H Glover, H B Solvason, H Kenna, A L Reiss, and A F Schatzberg. Resting-state functional connectivity in major depression: abnormally increased contributions from subgenual cingulate cortex and thalamus. *Biol Psychiatry*, 62(5):429–437, 2007. doi: S0006-3223(06)01193-0[pii]10.1016/j.biopsych.2006.09.020. URL http://www.ncbi.nlm.nih.gov/entrez/query.fcgi?cmd=Retrieve&db=PubMed&dopt=Citation&list_uids=17210143.

S Grimm, P Boesiger, J Beck, D Schuepbach, F Bermpohl, M Walter, J Ernst, D Hell, H Boeker, and G Northoff. Altered negative BOLD responses in the default-mode network during emotion processing in depressed subjects. *Neuropsychopharmacology*, 34(4):843–932, 2009a. doi: npp200881[pii]10.1038/npp.2008.81. URL http://www.ncbi.nlm.nih.gov/entrez/query.fcgi?cmd=Retrieve&db=PubMed&dopt=Citation&list_uids=18536699.

S Grimm, P Boesiger, J Beck, D Schuepbach, F Bermpohl, M Walter, J Ernst, D Hell, H Boeker, and G Northoff. Altered negative BOLD responses in the default-mode network during emotion processing in depressed subjects. *Neuropsychopharmacology*, 34(4):843–932, 2009b. doi: npp200881[pii]10.1038/npp.2008.81. URL http://www.ncbi.nlm.nih.gov/entrez/query.fcgi?cmd=Retrieve&db=PubMed&dopt=Citation&list_uids=18536699.

S Grimm, J Ernst, P Boesiger, D Schuepbach, D Hell, H Boeker, and G Northoff. Increased self-focus in major depressive disorder is related to neural abnormalities in subcortical-cortical midline structures. *Hum Brain Mapp*, 30(8):2617–2627, 2009c. doi: 10.1002/hbm.20693. URL http://www.ncbi.nlm.nih.gov/entrez/query.fcgi?cmd=Retrieve&db=PubMed&dopt=Citation&list_uids=19117277.

S Grimm, J Ernst, P Boesiger, D Schuepbach, H Boeker, and G Northoff. Reduced negative BOLD responses in the default-mode network and increased self-focus in depression. *World J Biol Psychiatry*, 2011a. doi: 10.3109/15622975.2010.545145. URL http://www.ncbi.nlm.nih.gov/entrez/query.fcgi?cmd=Retrieve&db=PubMed&dopt=Citation&list_uids=21247256.

Simone Grimm, Jutta Ernst, Peter Boesiger, Daniel Schuepbach, Heinz Boeker, and Georg Northoff. Reduced negative BOLD responses in the default-mode network and increased self-focus in depression. *The World Journal of Biological Psychiatry*, 12(8):627–37, December 2011b. doi: 10.3109/15622975.2010.545145.

- R Gruetter and I Tkáč. Field mapping without reference scan using asymmetric echo-planar techniques. *Magnetic resonance in medicine : official journal of the Society of Magnetic Resonance in Medicine / Society of Magnetic Resonance in Medicine*, 43(2):319–23, February 2000. ISSN 0740-3194. URL <http://www.ncbi.nlm.nih.gov/pubmed/10680699>.
- G Gründer, T Siessmeier, C Lange-Asschenfeldt, I Vernaleken, H G Buchholz, P Stoeter, A Drzezga, H Lüddens, F Rösch, and P Bartenstein. [18F]Fluoroethylflumazenil: a novel tracer for PET imaging of human benzodiazepine receptors. *European journal of nuclear medicine*, 28(10):1463–70, October 2001. ISSN 0340-6997. doi: 10.1007/s002590100594. URL <http://www.ncbi.nlm.nih.gov/pubmed/11685488>.
- Wen-bin Guo, Xue-li Sun, Ling Liu, Qiang Xu, Ren-rong Wu, Zhe-ning Liu, Chang-lian Tan, Hua-fu Chen, and Jing-ping Zhao. Disrupted regional homogeneity in treatment-resistant depression: a resting-state fMRI study. *Progress in neuro-psychopharmacology & biological psychiatry*, 35(5):1297–302, July 2011. ISSN 1878-4216. doi: 10.1016/j.pnpbp.2011.02.006. URL <http://www.ncbi.nlm.nih.gov/pubmed/21338650>.
- D A Gusnard and M E Raichle. Searching for a baseline: functional imaging and the resting human brain. *Nat Rev Neurosci*, 2(10):685–694, 2001. doi: 10.1038/3509450035094500[pii]. URL http://www.ncbi.nlm.nih.gov/entrez/query.fcgi?cmd=Retrieve&db=PubMed&dopt=Citation&list_uids=11584306.
- D A Gusnard, E Akbudak, G L Shulman, and M E Raichle. Medial prefrontal cortex and self-referential mental activity: relation to a default mode of brain function. *Proc Natl Acad Sci U S A*, 98(7):4259–4264, 2001. URL http://www.ncbi.nlm.nih.gov/entrez/query.fcgi?cmd=Retrieve&db=PubMed&dopt=Citation&list_uids=11259662.

William Guy. *ECDEU assessment manual for psychopharmacology*. U. S. Dept. of Health Education and Welfare Public Health Service Alcohol Drug Abuse and Mental Health Administration National Institute of Mental Health Psychopharmacology Research Branch, Rockville Md., rev. edition, 1976. URL <http://www.worldcat.org/title/ecdeu-assessment-manual-for-psychopharmacology/oclc/2344751>.

Amanda E Guyer, Jennifer Y F Lau, Erin B McClure-Tone, Jessica Parrish, Nina D Shiffrin, Richard C Reynolds, Gang Chen, R J R Blair, Ellen Leibenluft, Nathan A Fox, Monique Ernst, Daniel S Pine, and Eric E Nelson. Amygdala and ventrolateral prefrontal cortex function during anticipated peer evaluation in pediatric social anxiety. *Archives of general psychiatry*, 65(11):1303–12, November 2008. ISSN 1538-3636. doi: 10.1001/archpsyc.65.11.1303. URL <http://www.pubmedcentral.nih.gov/articlerender.fcgi?artid=2717208&tool=pmcentrez&rendertype=abstract>.

B J Harrison, J Pujol, H Ortiz, A Fornito, C Pantelis, and M Yucel. Modulation of brain resting-state networks by sad mood induction. *PLoS ONE*, 3(3):e1794, 2008. doi: 10.1371/journal.pone.0001794. URL http://www.ncbi.nlm.nih.gov/entrez/query.fcgi?cmd=Retrieve&db=PubMed&dopt=Citation&list_uids=18350136.

Wolf-Dieter Heiss and Karl Herholz. Brain receptor imaging. *Journal of nuclear medicine : official publication, Society of Nuclear Medicine*, 47(2):302–12, February 2006. ISSN 0161-5505. URL <http://www.ncbi.nlm.nih.gov/pubmed/16455637>.

Peter Henningsen, Thomas Zimmermann, and Heribert Sattel. Medically unexplained physical symptoms, anxiety, and depression: a meta-analytic review. *Psychosomatic medicine*, 65(4):528–33, 2003. ISSN 1534-7796. URL <http://www.ncbi.nlm.nih.gov/pubmed/12883101>.

B M Herbert, O Pollatos, and R Schandry. Interoceptive sensitivity and emotion processing: an EEG study. *Int J Psychophysiol*, 65(3):214–227, 2007. URL <http://www.ncbi.nlm.nih.gov/entrez/query.fcgi?cmd=Retrieve&db=>

PubMed&dopt=Citation&list_uids=17543405.

Marc Himmelbach, Michael Erb, and Hans-Otto Karnath. Activation of superior colliculi in humans during visual exploration. *BMC neuroscience*, 8:66, January 2007. ISSN 1471-2202. doi: 10.1186/1471-2202-8-66. URL <http://www.pubmedcentral.nih.gov/articlerender.fcgi?artid=1976416&tool=pmcentrez&rendertype=abstract>.

I K Hong, S T Chung, H K Kim, Y B Kim, Y D Son, and Z H Cho. Ultra fast symmetry and SIMD-based projection-backprojection (SSP) algorithm for 3-D PET image reconstruction. *IEEE Trans Med Imaging*, 26(6):789–803, 2007. doi: 10.1109/TMI.2002.808360. URL http://www.ncbi.nlm.nih.gov/entrez/query.fcgi?cmd=Retrieve&db=PubMed&dopt=Citation&list_uids=17679330.

Dorothea I Horn, Chunshui Yu, Johann Steiner, Julia Buchmann, Joern Kaufmann, Annemarie Osoba, Ulf Eckert, Kathrin C Zierhut, Kolja Schiltz, Huiguang He, Bharat Biswal, Bernhard Bogerts, and Martin Walter. Glutamatergic and resting-state functional connectivity correlates of severity in major depression - the role of pregenual anterior cingulate cortex and anterior insula. *Frontiers in systems neuroscience*, 4(July):1–10, January 2010. ISSN 1662-5137. doi: 10.3389/fnsys.2010.00033. URL <http://www.pubmedcentral.nih.gov/articlerender.fcgi?artid=2914530&tool=pmcentrez&rendertype=abstract>.

W Horn. LPS - Leistungspruefsystem. *Hogrefe, Goettingen*, 1983.

H M Hudson and R S Larkin. Accelerated image reconstruction using ordered subsets of projection data. *IEEE Trans Med Imaging*, 13(4):601–609, 1994. doi: 10.1109/42.363108. URL http://www.ncbi.nlm.nih.gov/entrez/query.fcgi?cmd=Retrieve&db=PubMed&dopt=Citation&list_uids=18218538.

Scott A. Huettel, Allen W. Song, and Gregory McCarthy. *Functional Magnetic Resonance Imaging*. Sinauer Associates, Inc., Sunderland, Massachusetts, USA, 2nd editio edition, 2008. ISBN 978-0878932863.

W Hunkeler, H Möhler, L Pieri, P Polc, E P Bonetti, R Cumin, R Schaffner, and W Häfely. Selective antagonists of benzodiazepines. *Nature*, 290(5806):514–6, April 1981. ISSN 0028-0836. URL <http://www.ncbi.nlm.nih.gov/pubmed/6261143>.

R E Ingram. Self-focused attention in clinical disorders: review and a conceptual model. *Psychol Bull*, 107(2):156–176, 1990. URL http://www.ncbi.nlm.nih.gov/entrez/query.fcgi?cmd=Retrieve&db=PubMed&dopt=Citation&list_uids=2181521.

Robert B Innis, Vincent J Cunningham, Jacques Delforge, Masahiro Fujita, Albert Gjedde, Roger N Gunn, James Holden, Sylvain Houle, Sung-Cheng Huang, Masanori Ichise, Hidehiro Iida, Hiroshi Ito, Yuichi Kimura, Robert A Koeppe, Gitte M Knudsen, Juhani Knuuti, Adriaan A Lammertsma, Marc Laruelle, Jean Logan, Ralph Paul Maguire, Mark A Mintun, Evan D Morris, Ramin Parsey, Julie C Price, Mark Slifstein, Vesna Sossi, Tetsuya Suhara, John R Votaw, Dean F Wong, and Richard E Carson. Consensus nomenclature for in vivo imaging of reversibly binding radioligands. *Journal of cerebral blood flow and metabolism : official journal of the International Society of Cerebral Blood Flow and Metabolism*, 27(9): 1533–9, September 2007. ISSN 0271-678X. doi: 10.1038/sj.jcbfm.9600493. URL <http://www.ncbi.nlm.nih.gov/pubmed/17519979>.

Tija C Jacob, Stephen J Moss, and Rachel Jurd. GABA(A) receptor trafficking and its role in the dynamic modulation of neuronal inhibition. *Nature reviews. Neuroscience*, 9(5):331–43, May 2008. ISSN 1471-0048. doi: 10.1038/nrn2370. URL <http://www.pubmedcentral.nih.gov/articlerender.fcgi?artid=2709246&tool=pmcentrez&rendertype=abstract>.

W James. What is an emotion? *Mind*, 9:185–205, 1884.

W James. The principles of psychology, 1890.

W James. Physical basis of emotion. *Psychol Rev*, 1:519–529, 1894.

Peter Jezzard, Paul M. Matthews, and Stephen M. Smith. *Functional MRI: An Intro-*

duction to Methods. Oxford University Press, USA, 1st editio edition, 2002. ISBN 978-0198527732.

J Kagan, J S Reznick, and N Snidman. The physiology and psychology of behavioral inhibition in children. *Child development*, 58(6):1459–73, December 1987. ISSN 0009-3920. URL <http://www.ncbi.nlm.nih.gov/pubmed/3691195>.

A V Kalueff and D J Nutt. Role of GABA in anxiety and depression. *Depress Anxiety*, 24(7):495–517, 2007. doi: 10.1002/da.20262. URL http://www.ncbi.nlm.nih.gov/entrez/query.fcgi?cmd=Retrieve&db=PubMed&dopt=Citation&list_uids=17117412.

J H Kashani and H Orvaschel. Anxiety disorders in mid-adolescence: a community sample. *The American journal of psychiatry*, 145(8):960–4, August 1988. ISSN 0002-953X. URL <http://www.ncbi.nlm.nih.gov/pubmed/3394880>.

E Kaza, U Klose, and M Lotze. Comparison of a 32-channel with a 12-channel head coil: are there relevant improvements for functional imaging? *J Magn Reson Imaging*, 34(1):173–183, 2011. doi: 10.1002/jmri.22614. URL http://www.ncbi.nlm.nih.gov/entrez/query.fcgi?cmd=Retrieve&db=PubMed&dopt=Citation&list_uids=21618334.

P A Keedwell, C Andrew, S C Williams, M J Brammer, and M L Phillips. The neural correlates of anhedonia in major depressive disorder. *Biol Psychiatry*, 58(11):843–853, 2005. URL http://www.ncbi.nlm.nih.gov/entrez/query.fcgi?cmd=Retrieve&db=PubMed&dopt=Citation&list_uids=16043128.

Clare Kelly, Roberto Toro, Adriana Di Martino, Christine L Cox, Pierre Bellec, F Xavier Castellanos, and Michael P Milham. A convergent functional architecture of the insula emerges across imaging modalities. *NeuroImage*, 61(4):1129–42, July 2012. ISSN 1095-9572. doi: 10.1016/j.neuroimage.2012.03.021. URL <http://www.ncbi.nlm.nih.gov/pubmed/22440648>.

Robert E Kelly, George S Alexopoulos, Zhishun Wang, Faith M Gunning, Christopher F Murphy, Sarah Shizuko Morimoto, Dora Kanellopoulos, Zhiru Jia, Kelvin O Lim, and Matthew J Hoptman. Visual inspection of independent components: defining a procedure for artifact removal from fMRI data. *Journal of Neuroscience Methods*, 189 (2):233–45, June 2010. doi: 10.1016/j.jneumeth.2010.03.028.

P C Kendall. Treating anxiety disorders in children: results of a randomized clinical trial. *Journal of consulting and clinical psychology*, 62(1):100–10, March 1994. ISSN 0022-006X. URL <http://www.ncbi.nlm.nih.gov/pubmed/8034812>.

P C Kendall, E U Brady, and T L Verduin. Comorbidity in childhood anxiety disorders and treatment outcome. *Journal of the American Academy of Child and Adolescent Psychiatry*, 40(7):787–94, July 2001. ISSN 0890-8567. doi: 10.1097/00004583-200107000-00013. URL <http://www.ncbi.nlm.nih.gov/pubmed/11437017>.

P. C. Kendall, J. L. Hudson, M. S. Choudhury, A. Webb, and S. Pimentel. Cognitive-behavioral treatment for childhood anxiety disorders. In E.D. Hibbs and P. S. Jensen, editors, *Psychosocial Treatments For Child And Adolescent Disorders: Empirically Based Strategies For Clinical Practice*, pages 47–73. American Psychological Association (APA), Washington, D.C., 2nd editio edition, 2005. ISBN 978-1591470922.

William D S Killgore and Deborah A Yurgelun-Todd. Social anxiety predicts amygdala activation in adolescents viewing fearful faces. *Neuroreport*, 16(15):1671–5, October 2005. ISSN 0959-4965. URL <http://www.ncbi.nlm.nih.gov/pubmed/16189475>.

L J Kirmayer. Cultural variations in the clinical presentation of depression and anxiety: implications for diagnosis and treatment. *J Clin Psychiatry*, 62 Suppl 1:22–30, 2001. URL http://www.ncbi.nlm.nih.gov/entrez/query.fcgi?cmd=Retrieve&db=PubMed&dopt=Citation&list_uids=11434415.

U M Klumpers, D J Veltman, R Boellaard, E F Comans, C Zucketo, M Yaqub, J E Mourik, M Lubberink, W J Hoogendijk, and A A Lammertsma. Compari-

son of plasma input and reference tissue models for analysing [(11)C]flumazenil studies. *J Cereb Blood Flow Metab*, 28(3):579–587, 2008. doi: 9600554[pii]10.1038/sj.jcbfm.9600554. URL http://www.ncbi.nlm.nih.gov/entrez/query.fcgi?cmd=Retrieve&db=PubMed&dopt=Citation&list_uids=17928801.

U M Klumpers, R Boellaard, D J Veltman, R W Kloet, W J Hoogendijk, and A A Lammertsma. Parametric [11C]flumazenil images. *Nucl Med Commun*, 33(4):422–430, 2012. doi: 10.1097/MNM.0b013e3283505f7b. URL http://www.ncbi.nlm.nih.gov/entrez/query.fcgi?cmd=Retrieve&db=PubMed&dopt=Citation&list_uids=22293497.

Victor D. Koechli and Borut Marincek. *Wie funktioniert MRI?* Springer-Verlag Berlin Heidelberg New Yor, 1998. ISBN 978-3540642954.

Yasunori Kotani, Yoshimi Ohgami, Yumiko Kuramoto, Tetsuji Tsukamoto, Yusuke Inoue, and Yasutsugu Aihara. The role of the right anterior insular cortex in the right hemisphere preponderance of stimulus-preceding negativity (SPN): an fMRI study. *Neuroscience letters*, 450(2):75–9, January 2009. ISSN 0304-3940. doi: 10.1016/j.neulet.2008.11.032. URL <http://www.ncbi.nlm.nih.gov/pubmed/19028549>.

N Kriegeskorte, W K Simmons, P S Bellgowan, and C I Baker. Circular analysis in systems neuroscience: the dangers of double dipping. *Nat Neurosci*, 12(5):535–540, 2009. doi: nn.2303[pii]10.1038/nn.2303. URL http://www.ncbi.nlm.nih.gov/entrez/query.fcgi?cmd=Retrieve&db=PubMed&dopt=Citation&list_uids=19396166.

Florian Kurth, Simon B Eickhoff, Axel Schleicher, Lars Hoemke, Karl Zilles, and Katrin Amunts. Cytoarchitecture and probabilistic maps of the human posterior insular cortex. *Cerebral cortex (New York, N.Y. : 1991)*, 20(6):1448–61, June 2010. ISSN 1460-2199. doi: 10.1093/cercor/bhp208. URL <http://www.pubmedcentral.nih.gov/articlerender.fcgi?artid=2871375&tool=pmcentrez&rendertype=abstract>.

C la Fougere, S Grant, A Kostikov, R Schirmacher, P Gravel, H M Schipper, A Reader, A Evans, and A Thiel. Where in-vivo imaging meets cytoarchitectonics: the relationship between cortical thickness and neuronal density measured with high-resolution [18F]flumazenil-PET. *Neuroimage*, 56(3): 951–960, 2011. doi: S1053-8119(10)01445-X[pii]10.1016/j.neuroimage.2010.11.015. URL http://www.ncbi.nlm.nih.gov/entrez/query.fcgi?cmd=Retrieve&db=PubMed&dopt=Citation&list_uids=21073964.

C Lamm and J Decety. Is the extrastriate body area (EBA) sensitive to the perception of pain in others? *Cereb Cortex*, 18(10):2369–2373, 2008. URL http://www.ncbi.nlm.nih.gov/entrez/query.fcgi?cmd=Retrieve&db=PubMed&dopt=Citation&list_uids=18270173.

C Lamm and T Singer. The role of anterior insular cortex in social emotions. *Brain Struct Funct*, 214(5-6):579–591, 2010. doi: 10.1007/s00429-010-0251-3. URL http://www.ncbi.nlm.nih.gov/entrez/query.fcgi?cmd=Retrieve&db=PubMed&dopt=Citation&list_uids=20428887.

A A Lammertsma and S P Hume. Simplified reference tissue model for PET receptor studies. *Neuroimage*, 4(3 Pt 1):153–158, 1996. doi: S1053-8119(96)90066-X[pii]10.1006/ning.1996.0066. URL http://www.ncbi.nlm.nih.gov/entrez/query.fcgi?cmd=Retrieve&db=PubMed&dopt=Citation&list_uids=9345505.

C G Last, M Hersen, A Kazdin, H Orvaschel, and S Perrin. Anxiety disorders in children and their families. *Archives of general psychiatry*, 48(10):928–34, October 1991. ISSN 0003-990X. URL <http://www.ncbi.nlm.nih.gov/pubmed/1929763>.

M Lauritzen, C Mathiesen, K Schaefer, and K J Thomsen. Neuronal inhibition and excitation, and the dichotomic control of brain hemodynamic and oxygen responses. *Neuroimage*, 2012. doi: S1053-8119(12)00057-2[pii]10.1016/j.neuroimage.2012.01.040. URL <http://www.ncbi.nlm.nih.gov/entrez/query.fcgi?cmd=Retrieve&db=>

PubMed&dopt=Citation&list_uids=22261372.

S Lehrl. MWT-B: Mehrfachwahl-Wortschatz-Intelligenztest. *Hogrefe, Goettingen*, 1995.

A J Levinson, P B Fitzgerald, G Favalli, D M Blumberger, M Daigle, and Z J Daskalakis. Evidence of cortical inhibitory deficits in major depressive disorder. *Biol Psychiatry*, 67(5):458–464, 2010. URL http://www.ncbi.nlm.nih.gov/entrez/query.fcgi?cmd=Retrieve&db=PubMed&dopt=Citation&list_uids=19922906.

David E J Linden, Isabelle Habes, Stephen J Johnston, Stefanie Linden, Ranjit Tatineni, Leena Subramanian, Bettina Sorger, David Healy, and Rainer Goebel. Real-time self-regulation of emotion networks in patients with depression. *PLoS one*, 7(6):e38115, January 2012. ISSN 1932-6203. doi: 10.1371/journal.pone.0038115. URL <http://www.pubmedcentral.nih.gov/articlerender.fcgi?artid=3366978&tool=pmcentrez&rendertype=abstract>.

M Liotti, H S Mayberg, S McGinnis, S L Brannan, and P Jerabek. Unmasking disease-specific cerebral blood flow abnormalities: mood challenge in patients with remitted unipolar depression. *Am J Psychiatry*, 159(11):1830–1840, 2002. URL http://www.ncbi.nlm.nih.gov/entrez/query.fcgi?cmd=Retrieve&db=PubMed&dopt=Citation&list_uids=12411216.

Zhifen Liu, Cheng Xu, Yong Xu, Yanfang Wang, Bing Zhao, Yating Lv, Xiaohua Cao, Kerang Zhang, and Chongxi Du. Decreased regional homogeneity in insula and cerebellum: a resting-state fMRI study in patients with major depression and subjects at high risk for major depression. *Psychiatry research*, 182(3):211–5, June 2010. ISSN 0165-1781. doi: 10.1016/j.psychresns.2010.03.004. URL <http://www.ncbi.nlm.nih.gov/pubmed/20493670>.

J Logan, J S Fowler, N D Volkow, G J Wang, Y S Ding, and D L Alexoff. Distribution volume ratios without blood sampling from graphical analysis of PET data. *J Cereb Blood Flow Metab*, 16(5):834–840, 1996. doi: 10.1097/

00004647-199609000-00008. URL http://www.ncbi.nlm.nih.gov/entrez/query.fcgi?cmd=Retrieve&db=PubMed&dopt=Citation&list_uids=8784228.

N K Logothetis. What we can do and what we cannot do with fMRI. *Nature*, 453(7197):869–878, 2008. doi: nature06976[pii]10.1038/nature06976. URL http://www.ncbi.nlm.nih.gov/entrez/query.fcgi?cmd=Retrieve&db=PubMed&dopt=Citation&list_uids=18548064.

N K Logothetis, J Pauls, M Augath, T Trinath, and A Oeltermann. Neurophysiological investigation of the basis of the fMRI signal. *Nature*, 412(6843):150–7, July 2001. ISSN 0028-0836. doi: 10.1038/35084005. URL <http://www.ncbi.nlm.nih.gov/pubmed/11449264>.

N K Logothetis, Y Murayama, M Augath, T Steffen, J Werner, and A Oeltermann. How not to study spontaneous activity. *Neuroimage*, 45(4):1080–1089, 2009. doi: S1053-8119(09)00023-8[pii]10.1016/j.neuroimage.2009.01.010. URL http://www.ncbi.nlm.nih.gov/entrez/query.fcgi?cmd=Retrieve&db=PubMed&dopt=Citation&list_uids=19344685.

a Lothe, a Didelot, a Hammers, N Costes, M Saoud, F Gilliam, and P Ryvlin. Comorbidity between temporal lobe epilepsy and depression: a [18F]MPPF PET study. *Brain : a journal of neurology*, 131(Pt 10):2765–82, October 2008. ISSN 1460-2156. doi: 10.1093/brain/awn194. URL <http://www.ncbi.nlm.nih.gov/pubmed/18765418>.

H C Lou, B Luber, M Crupain, J P Keenan, M Nowak, T W Kjaer, H A Sackeim, and S H Lisanby. Parietal cortex and representation of the mental Self. *Proc Natl Acad Sci U S A*, 101(17):6827–6832, 2004. doi: 10.1073/pnas.04000491010400049101[pii]. URL http://www.ncbi.nlm.nih.gov/entrez/query.fcgi?cmd=Retrieve&db=PubMed&dopt=Citation&list_uids=15096584.

B Luscher, Q Shen, and N Sahir. The GABAergic deficit hypothesis of major depressive disorder. *Mol Psychiatry*, 16(4):383–406, 2011. doi: mp2010120[pii]10.1038/mp.2010.

120. URL http://www.ncbi.nlm.nih.gov/entrez/query.fcgi?cmd=Retrieve&db=PubMed&dopt=Citation&list_uids=21079608.

Antoine Lutti, David L Thomas, Chloe Hutton, and Nikolaus Weiskopf. High-resolution functional MRI at 3 T: 3D/2D echo-planar imaging with optimized physiological noise correction. *Magnetic resonance in medicine : official journal of the Society of Magnetic Resonance in Medicine / Society of Magnetic Resonance in Medicine*, July 2012. ISSN 1522-2594. doi: 10.1002/mrm.24398. URL <http://www.ncbi.nlm.nih.gov/pubmed/22821858>.

J A Maldjian, P J Laurienti, R A Kraft, and J H Burdette. An automated method for neuroanatomic and cytoarchitectonic atlas-based interrogation of fMRI data sets. *Neuroimage*, 19(3):1233–1239, 2003. doi: S1053811903001691[pii]. URL http://www.ncbi.nlm.nih.gov/entrez/query.fcgi?cmd=Retrieve&db=PubMed&dopt=Citation&list_uids=12880848.

P Mansfield. Multi-planar image formation using NMR spin echoes. *Journal of Physics C: Solid State Physics*, 10:L55–L58, 1977.

M Marjanska, P G Henry, E J Auerbach, D Franc, B Mueller, K Ugurbil, and K O Lim. Reproducibility of In Vivo GABA Quantification in Anterior Cingulate at 3 Tesla. *Proc Intl Soc Mag Reson Med*, 15, 2007.

M F Mason, M I Norton, J D Van Horn, D M Wegner, S T Grafton, and C N Macrae. Wandering minds: The default network and stimulus independent thought. *Science*, 315:393–395, 2007.

G Massaweh, E Schirrmacher, C la Fougere, M Kovacevic, C Wangler, D Jolly, P Gravel, A J Reader, A Thiel, and R Schirrmacher. Improved work-up procedure for the production of [(18)F]flumazenil and first results of its use with a high-resolution research tomograph in human stroke. *Nucl Med Biol*, 36(7):721–727, 2009. doi: S0969-8051(09)00149-8[pii]10.1016/j.nucmedbio.2009.05.

008. URL http://www.ncbi.nlm.nih.gov/entrez/query.fcgi?cmd=Retrieve&db=PubMed&dopt=Citation&list_uids=19720284.

H S Mayberg. Modulating limbic-cortical circuits in depression: targets of antidepressant treatments. *Semin Clin Neuropsychiatry*, 7(4):255–268, 2002. URL http://www.ncbi.nlm.nih.gov/entrez/query.fcgi?cmd=Retrieve&db=PubMed&dopt=Citation&list_uids=12382208.

H S Mayberg. Modulating dysfunctional limbic-cortical circuits in depression: towards development of brain-based algorithms for diagnosis and optimised treatment. *Br Med Bull*, 65:193–207, 2003. URL http://www.ncbi.nlm.nih.gov/entrez/query.fcgi?cmd=Retrieve&db=PubMed&dopt=Citation&list_uids=12697626.

Erin B McClure, Abby Adler, Christopher S Monk, Jennifer Cameron, Samantha Smith, Eric E Nelson, Ellen Leibenluft, Monique Ernst, and Daniel S Pine. fMRI predictors of treatment outcome in pediatric anxiety disorders. *Psychopharmacology*, 191(1): 97–105, March 2007. ISSN 0033-3158. doi: 10.1007/s00213-006-0542-9. URL <http://www.ncbi.nlm.nih.gov/pubmed/16972100>.

M J McKeown, S Makeig, G G Brown, T P Jung, S S Kindermann, A J Bell, and T J Sejnowski. Analysis of fMRI data by blind separation into independent spatial components. *Hum Brain Mapp*, 6(3):160–188, 1998. doi: 10.1002/(SICI)1097-0193(1998)6:3<160::AID-HBM5>3.0.CO;2-1[pii]. URL http://www.ncbi.nlm.nih.gov/entrez/query.fcgi?cmd=Retrieve&db=PubMed&dopt=Citation&list_uids=9673671.

K A McKiernan, J N Kaufman, J Kucera-Thompson, and J R Binder. A parametric manipulation of factors affecting task-induced deactivation in functional neuroimaging. *J Cogn Neurosci*, 15(3):394–408, 2003. doi: 10.1162/089892903321593117. URL http://www.ncbi.nlm.nih.gov/entrez/query.fcgi?cmd=Retrieve&db=PubMed&dopt=Citation&list_uids=12729491.

Nick Medford and Hugo D Critchley. Conjoint activity of anterior insular

- and anterior cingulate cortex: awareness and response. *Brain structure & function*, 214(5-6):535–49, June 2010. ISSN 1863-2661. doi: 10.1007/s00429-010-0265-x. URL <http://www.pubmedcentral.nih.gov/articlerender.fcgi?artid=2886906&tool=pmcentrez&rendertype=abstract>.
- M. Mescher, H. Merkle, J. Kirsch, M. Garwood, and R. Gruetter. Simultaneous in vivo spectral editing and water suppression. *NMR in Biomedicine*, 11(6):266–272, 1998. URL http://phys.columbia.edu/~tosti/icidr/cm/spec/mega_garwood.pdf.
- M M Mesulam and E J Mufson. Insula of the old world monkey. I. Architectonics in the insulo-orbito-temporal component of the paralimbic brain. *The Journal of comparative neurology*, 212(1):1–22, November 1982. ISSN 0021-9967. doi: 10.1002/cne.902120102. URL <http://www.ncbi.nlm.nih.gov/pubmed/7174905>.
- H C Middleton and M Ashby. Clinical recovery from panic disorder is associated with evidence of changes in cardiovascular regulation. *Acta psychiatrica Scandinavica*, 91(2):108–13, March 1995. ISSN 0001-690X. URL <http://www.ncbi.nlm.nih.gov/pubmed/7778467>.
- Matthew S Milak, Ramin V Parsey, John Keilp, Maria A Oquendo, Kevin M Malone, and J John Mann. Neuroanatomic correlates of psychopathologic components of major depressive disorder. *Archives of general psychiatry*, 62(4):397–408, April 2005. ISSN 0003-990X. doi: 10.1001/archpsyc.62.4.397. URL <http://www.ncbi.nlm.nih.gov/pubmed/15809407>.
- P Millet, C Graf, A Buck, B Walder, and V Ibanez. Evaluation of the reference tissue models for PET and SPECT benzodiazepine binding parameters. *Neuroimage*, 17(2):928–942, 2002. doi: S1053811902912334[pii]. URL http://www.ncbi.nlm.nih.gov/entrez/query.fcgi?cmd=Retrieve&db=PubMed&dopt=Citation&list_uids=12377167.
- H Mohler. The GABA system in anxiety and depression and its potential for novel

therapeutics. *Neuropharmacology*, 2011. doi: S0028-3908(11)00373-X[pil]10.1016/j.neuropharm.2011.08.040. URL http://www.ncbi.nlm.nih.gov/entrez/query.fcgi?cmd=Retrieve&db=PubMed&dopt=Citation&list_uids=21889518.

Hanns Möhler. The GABA system in anxiety and depression and its therapeutic potential. *Neuropharmacology*, 62(1):42–53, January 2012. ISSN 1873-7064. doi: 10.1016/j.neuropharm.2011.08.040. URL <http://www.ncbi.nlm.nih.gov/pubmed/21889518>.

Christopher S Monk, Eva H Telzer, Karin Mogg, Brendan P Bradley, Xiaoqin Mai, Hugo M C Louro, Gang Chen, Erin B McClure-Tone, Monique Ernst, and Daniel S Pine. Amygdala and ventrolateral prefrontal cortex activation to masked angry faces in children and adolescents with generalized anxiety disorder. *Archives of general psychiatry*, 65(5):568–76, May 2008. ISSN 1538-3636. doi: 10.1001/archpsyc.65.5.568. URL <http://www.pubmedcentral.nih.gov/articlerender.fcgi?artid=2443697&tool=pmcentrez&rendertype=abstract>.

S A Montgomery and M Asberg. A new depression scale designed to be sensitive to change. *Br J Psychiatry*, 134:382–389, 1979. URL http://www.ncbi.nlm.nih.gov/entrez/query.fcgi?cmd=Retrieve&db=PubMed&dopt=Citation&list_uids=444788.

S D Muthukumaraswamy, R A Edden, D K Jones, J B Swettenham, and K D Singh. Resting GABA concentration predicts peak gamma frequency and fMRI amplitude in response to visual stimulation in humans. *Proc Natl Acad Sci U S A*, 106(20):8356–8361, 2009. doi: 0900728106[pil]10.1073/pnas.0900728106. URL http://www.ncbi.nlm.nih.gov/entrez/query.fcgi?cmd=Retrieve&db=PubMed&dopt=Citation&list_uids=19416820.

Suresh D Muthukumaraswamy, C John Evans, Richard A E Edden, Richard G Wise, and Krish D Singh. Individual variability in the shape and amplitude of the BOLD-HRF correlates with endogenous GABAergic inhibition. *Human Brain Mapping*, 33

(2):455–65, February 2012. doi: 10.1002/hbm.21223.

Luca Nanetti, Leonardo Cerliani, Valeria Gazzola, Remco Renken, and Christian Keysers. Group analyses of connectivity-based cortical parcellation using repeated k-means clustering. *NeuroImage*, 47(4):1666–77, October 2009. ISSN 1095-9572. doi: 10.1016/j.neuroimage.2009.06.014. URL <http://www.ncbi.nlm.nih.gov/pubmed/19524682>.

T Nichols and S Hayasaka. Controlling the familywise error rate in functional neuroimaging: a comparative review. *Stat Methods Med Res*, 12(5):419–446, 2003. URL http://www.ncbi.nlm.nih.gov/entrez/query.fcgi?cmd=Retrieve&db=PubMed&dopt=Citation&list_uids=14599004.

G Northoff. Psychopathology and pathophysiology of the self in depression - neuropsychiatric hypothesis. *J Affect Disord*, 104(1-3):1–14, 2007. URL http://www.ncbi.nlm.nih.gov/entrez/query.fcgi?cmd=Retrieve&db=PubMed&dopt=Citation&list_uids=17379318.

G Northoff, A Heinzel, M de Greck, F BERPpohl, H Dobrowolny, and J Panksepp. Self-referential processing in our brain—a meta-analysis of imaging studies on the self. *Neuroimage*, 31(1):440–457, 2006. URL http://www.ncbi.nlm.nih.gov/entrez/query.fcgi?cmd=Retrieve&db=PubMed&dopt=Citation&list_uids=16466680.

G Northoff, M Walter, R F Schulte, J Beck, U Dydak, A Henning, H Boeker, S Grimm, and P Boesiger. GABA concentrations in the human anterior cingulate cortex predict negative BOLD responses in fMRI. *Nat Neurosci*, 10(12):1515–1517, 2007. doi: nn2001[pil]10.1038/nn2001. URL http://www.ncbi.nlm.nih.gov/entrez/query.fcgi?cmd=Retrieve&db=PubMed&dopt=Citation&list_uids=17982452.

G Northoff, P Qin, and T Nakao. Rest-stimulus interaction in the brain: a review. *Trends Neurosci*, 2010a. URL http://www.ncbi.nlm.nih.gov/entrez/query.fcgi?cmd=Retrieve&db=PubMed&dopt=Citation&list_uids=20226543.

G Northoff, P Qin, and T E Feinberg. Brain imaging of the self—conceptual, anatomical and methodological issues. *Conscious Cogn*, 20(1):52–63, 2011a. doi: S1053-8100(10)00177-7[pii]10.1016/j.concog.2010.09.011. URL http://www.ncbi.nlm.nih.gov/entrez/query.fcgi?cmd=Retrieve&db=PubMed&dopt=Citation&list_uids=20932778.

G Northoff, C Wiebking, T Feinberg, and J Panksepp. The 'resting-state hypothesis' of major depressive disorder-A translational subcortical-cortical framework for a system disorder. *Neurosci Biobehav Rev*, 35(9):1929–1945, 2011b. doi: doi:10.1016/j.neubiorev.2010.12.007. URL http://www.ncbi.nlm.nih.gov/entrez/query.fcgi?cmd=Retrieve&db=PubMed&dopt=Citation&list_uids=21192971.

Georg Northoff, Christine Wiebking, Todd Feinberg, and Jaak Panksepp. The 'Resting-state Hypothesis' of Major Depressive Disorder-A Translational Subcortical-Cortical Framework for a System Disorder. *Neuroscience & Biobehavioral Reviews*, pages 1–17, 2010b. ISSN 18737528. doi: 10.1016/j.neubiorev.2010.12.007. URL <http://www.ncbi.nlm.nih.gov/pubmed/21192971>.

L Nyboe Jacobsen, I Smith Lassen, P Friis, P Videbech, and R Wentzer Licht. Bodily symptoms in moderate and severe depression. *Nord J Psychiatry*, 60(4):294–298, 2006. doi: R146371768552P81[pii]10.1080/08039480600790358. URL http://www.ncbi.nlm.nih.gov/entrez/query.fcgi?cmd=Retrieve&db=PubMed&dopt=Citation&list_uids=16923638.

Kevin N Ochsner, Rebecca D Ray, Jeffrey C Cooper, Elaine R Robertson, Sita Chopra, John D E Gabrieli, and James J Gross. For better or for worse: neural systems supporting the cognitive down- and up-regulation of negative emotion. *NeuroImage*, 23(2):483–99, October 2004. ISSN 1053-8119. doi: 10.1016/j.neuroimage.2004.06.030. URL <http://www.ncbi.nlm.nih.gov/pubmed/15488398>.

I Odano, C Halldin, P Karlsson, A Varrone, A J Airaksinen, R N Krasikova, and

- L Farde. [18F]flumazenil binding to central benzodiazepine receptor studies by PET–quantitative analysis and comparisons with [11C]flumazenil. *Neuroimage*, 45(3):891–902, 2009. doi: S1053-8119(08)01244-5[pii]10.1016/j.neuroimage.2008.12.005. URL http://www.ncbi.nlm.nih.gov/entrez/query.fcgi?cmd=Retrieve&db=PubMed&dopt=Citation&list_uids=19136064.
- S Ogawa, D W Tank, R Menon, J M Ellermann, S G Kim, H Merkle, and K Ugurbil. Intrinsic signal changes accompanying sensory stimulation: functional brain mapping with magnetic resonance imaging. *Proceedings of the National Academy of Sciences of the United States of America*, 89(13):5951–5, July 1992. ISSN 0027-8424. URL <http://www.pubmedcentral.nih.gov/articlerender.fcgi?artid=402116&tool=pmcentrez&rendertype=abstract>.
- Ruth L O’Gorman, Lars Michels, Richard A Edden, James B Murdoch, and Ernst Martin. In vivo detection of GABA and glutamate with MEGA-PRESS: reproducibility and gender effects. *Journal of Magnetic Resonance Imaging*, 33(5):1262–1267, 2011. URL <http://www.pubmedcentral.nih.gov/articlerender.fcgi?artid=3154619&tool=pmcentrez&rendertype=abstract>.
- Thomas H Ollendick and Dina R Hirshfeld-Becker. The developmental psychopathology of social anxiety disorder. *Biological psychiatry*, 51(1):44–58, January 2002. ISSN 0006-3223. URL <http://www.ncbi.nlm.nih.gov/pubmed/11801230>.
- R W Olsen. The GABA postsynaptic membrane receptor-ionophore complex. Site of action of convulsant and anticonvulsant drugs. *Molecular and cellular biochemistry*, 39:261–79, September 1981. ISSN 0300-8177. URL <http://www.ncbi.nlm.nih.gov/pubmed/6273709>.
- Jaak Panksepp. *Affective neuroscience : the foundations of human and animal emotions*. Oxford University Press, New York, 1998. ISBN 0195096738 (hardcover alk. paper). URL <http://www.loc.gov/catdir/enhancements/fy0635/98015955-d>.

html<http://www.loc.gov/catdir/enhancements/fy0635/98015955-t.html>.

Natalie A Paul, Steven J Stanton, Jeffrey M Greeson, Moria J Smoski, and Lihong Wang. Psychological and Neural Mechanisms of Trait Mindfulness in Reducing Depression Vulnerability. *Social cognitive and affective neuroscience*, June 2012. ISSN 1749-5024. URL <http://www.ncbi.nlm.nih.gov/pubmed/22717383>.

M P Paulus and M B Stein. An insular view of anxiety. *Biol Psychiatry*, 60(4):383–387, 2006. doi: S0006-3223(06)00476-8[pii]10.1016/j.biopsych.2006.03.042. URL http://www.ncbi.nlm.nih.gov/entrez/query.fcgi?cmd=Retrieve&db=PubMed&dopt=Citation&list_uids=16780813.

M P Paulus and M B Stein. Interoception in anxiety and depression. *Brain Struct Funct*, 214(5-6):451–463, 2010. doi: 10.1007/s00429-010-0258-9. URL <http://www.ncbi.nlm.nih.gov/pubmed/20490545>.

P L Pearl, K M Gibson, Z Quezado, I Dustin, J Taylor, S Trzcinski, J Schreiber, K Forester, P Reeves-Tyer, C Liew, S Shamim, P Herscovitch, R Carson, J Butman, C Jakobs, and W Theodore. Decreased GABA-A binding on FMZ-PET in succinic semialdehyde dehydrogenase deficiency. *Neurology*, 73(6):423–429, 2009. doi: 73/6/423[pii]10.1212/WNL.0b013e3181b163a5. URL http://www.ncbi.nlm.nih.gov/entrez/query.fcgi?cmd=Retrieve&db=PubMed&dopt=Citation&list_uids=19667317.

Cintia Azevedo-Marques Périco, Cesar R Skaf, Airton Yamada, Fábio Duran, Carlos A Buchpiguel, Cláudio C Castro, Jair C Soares, and Geraldo F Busatto. Relationship between regional cerebral blood flow and separate symptom clusters of major depression: a single photon emission computed tomography study using statistical parametric mapping. *Neuroscience letters*, 384(3):265–70, August 2005. ISSN 0304-3940. doi: 10.1016/j.neulet.2005.04.088. URL <http://www.ncbi.nlm.nih.gov/pubmed/15921853>.

- F Petty. GABA and mood disorders: a brief review and hypothesis. *J Affect Disord*, 34(4):275–281, 1995. doi: 016503279500025I[pii]. URL http://www.ncbi.nlm.nih.gov/entrez/query.fcgi?cmd=Retrieve&db=PubMed&dopt=Citation&list_uids=8550953.
- M E Phelps. Positron computed tomography studies of cerebral glucose metabolism in man: theory and application in nuclear medicine. *Seminars in nuclear medicine*, 11(1):32–49, January 1981. ISSN 0001-2998. URL <http://www.ncbi.nlm.nih.gov/pubmed/6972094>.
- M L Philips, W C Drevets, S L Rauch, and R Lane. Neurobiology of emotion perception II: implications for major psychiatric disorders. *Biological Psychiatry*, 54:515–528, 2003.
- A Pilc and G Nowak. GABAergic hypotheses of anxiety and depression: focus on GABA-B receptors. *Drugs Today (Barc)*, 41(11):755–766, 2005. doi: 904728[pii] 10.1358/dot.2005.41.11.904728. URL http://www.ncbi.nlm.nih.gov/entrez/query.fcgi?cmd=Retrieve&db=PubMed&dopt=Citation&list_uids=16395415.
- Daniel S Pine. Research review: a neuroscience framework for pediatric anxiety disorders. *Journal of child psychology and psychiatry, and allied disciplines*, 48(7): 631–48, July 2007. ISSN 0021-9630. doi: 10.1111/j.1469-7610.2007.01751.x. URL <http://www.ncbi.nlm.nih.gov/pubmed/17593144>.
- Daniel S Pine, Amanda E Guyer, and Ellen Leibenluft. Functional magnetic resonance imaging and pediatric anxiety. *Journal of the American Academy of Child and Adolescent Psychiatry*, 47(11):1217–21, November 2008. ISSN 1527-5418. doi: 10.1097/CHI.0b013e318185dad0. URL <http://www.pubmedcentral.nih.gov/articlerender.fcgi?artid=2635373&tool=pmcentrez&rendertype=abstract>.
- S Pitroda, M Angstadt, M S McCloskey, E F Coccaro, and K L Phan. Emotional experience modulates brain activity during fixation periods between tasks. *Neurosci*

- Lett*, 443(2):72–76, 2008. doi: S0304-3940(08)01004-5[pii]10.1016/j.neulet.2008.07.050. URL http://www.ncbi.nlm.nih.gov/entrez/query.fcgi?cmd=Retrieve&db=PubMed&dopt=Citation&list_uids=18674589.
- R A Poldrack and J A Mumford. Independence in ROI analysis: where is the voodoo? *Soc Cogn Affect Neurosci*, 4(2):208–213, 2009. doi: nsp011[pii]10.1093/scan/nsp011. URL http://www.ncbi.nlm.nih.gov/entrez/query.fcgi?cmd=Retrieve&db=PubMed&dopt=Citation&list_uids=19470529.
- O Pollatos, K Gramann, and R Schandry. Neural systems connecting interoceptive awareness and feelings. *Hum Brain Mapp*, 28(1):9–18, 2007a. doi: 10.1002/hbm.20258. URL http://www.ncbi.nlm.nih.gov/entrez/query.fcgi?cmd=Retrieve&db=PubMed&dopt=Citation&list_uids=16729289.
- O Pollatos, E Matthias, and R Schandry. Heartbeat perception and P300 amplitude in a visual oddball paradigm. *Clin Neurophysiol*, 118(10):2248–2253, 2007b. doi: S1388-2457(07)00327-6[pii]10.1016/j.clinph.2007.06.057. URL http://www.ncbi.nlm.nih.gov/entrez/query.fcgi?cmd=Retrieve&db=PubMed&dopt=Citation&list_uids=17709296.
- O Pollatos, R Schandry, D P Auer, and C Kaufmann. Brain structures mediating cardiovascular arousal and interoceptive awareness. *Brain Res*, 1141:178–187, 2007c. doi: S0006-8993(07)00070-4[pii]10.1016/j.brainres.2007.01.026. URL http://www.ncbi.nlm.nih.gov/entrez/query.fcgi?cmd=Retrieve&db=PubMed&dopt=Citation&list_uids=17296169.
- Robert A Pooley. AAPM/RSNA physics tutorial for residents: fundamental physics of MR imaging. *Radiographics : a review publication of the Radiological Society of North America, Inc*, 25(4):1087–99, January 2005. ISSN 1527-1323. doi: 10.1148/rg.254055027. URL <http://radiographics.rsna.org/content/25/4/1087.full>.

- S W Porges. Body Perception Questionnaire (German version). *Laboratory of Developmental Assessment, University of Maryland*, 1993.
- Joseph L Price and Wayne C Drevets. Neural circuits underlying the pathophysiology of mood disorders. *Trends in cognitive sciences*, 16(1):61–71, January 2012. ISSN 1879-307X. URL <http://www.ncbi.nlm.nih.gov/pubmed/22197477>.
- Pier J Prins and Thomas H Ollendick. Cognitive change and enhanced coping: missing mediational links in cognitive behavior therapy with anxiety-disordered children. *Clinical child and family psychology review*, 6(2):87–105, June 2003. ISSN 1096-4037. URL <http://www.ncbi.nlm.nih.gov/pubmed/12836579>.
- W. Proctor and F. Yu. The Dependence of a Nuclear Magnetic Resonance Frequency upon Chemical Compound. *Physical Review*, 77(5):717–717, March 1950. ISSN 0031-899X. doi: 10.1103/PhysRev.77.717. URL http://prola.aps.org/abstract/PR/v77/i5/p717_1.
- S W Provencher. Estimation of metabolite concentrations from localized in vivo proton NMR spectra. *Magn Reson Med*, 30(6):672–679, 1993. URL http://www.ncbi.nlm.nih.gov/entrez/query.fcgi?cmd=Retrieve&db=PubMed&dopt=Citation&list_uids=8139448.
- S W Provencher. Automatic quantitation of localized in vivo ¹H spectra with LCModel. *NMR in biomedicine*, 14(4):260–4, June 2001. ISSN 0952-3480. URL <http://www.ncbi.nlm.nih.gov/pubmed/11410943>.
- Pengmin Qin, Haibo Di, Yijun Liu, Senming Yu, Qiyong Gong, Niall Duncan, Xuchu Weng, Steven Laureys, and Georg Northoff. Anterior cingulate activity and the self in disorders of consciousness. *Human brain mapping*, 31(12):1993–2002, December 2010. ISSN 1097-0193. doi: 10.1002/hbm.20989. URL <http://www.ncbi.nlm.nih.gov/pubmed/20336686>.
- M E Raichle. A paradigm shift in functional brain imaging. *J Neurosci*, 29(41):12729–

- 12734, 2009. doi: 29/41/12729[pii]10.1523/JNEUROSCI.4366-09.2009. URL <http://www.ncbi.nlm.nih.gov/pubmed/19828783>.
- M E Raichle. Two views of brain function. *Trends Cogn Sci*, 14(4): 180–190, 2010. doi: S1364-6613(10)00029-X[pii]10.1016/j.tics.2010.01.008. URL http://www.ncbi.nlm.nih.gov/entrez/query.fcgi?cmd=Retrieve&db=PubMed&dopt=Citation&list_uids=20206576.
- M E Raichle and D A Gusnard. Intrinsic brain activity sets the stage for expression of motivated behavior. *J Comp Neurol*, 493(1):167–176, 2005. doi: 10.1002/cne.20752. URL http://www.ncbi.nlm.nih.gov/entrez/query.fcgi?cmd=Retrieve&db=PubMed&dopt=Citation&list_uids=16254998.
- M E Raichle and A Z Snyder. A default mode of brain function: A brief history of an evolving idea. *Neuroimage*, 37:1083–1090, 2007.
- M E Raichle, A M MacLeod, A Z Snyder, W J Powers, D A Gusnard, and G L Shulman. A default mode of brain function. *Proc Natl Acad Sci U S A*, 98(2):676–682, 2001. doi: 10.1073/pnas.98.2.67698/2/676[pii]. URL http://www.ncbi.nlm.nih.gov/entrez/query.fcgi?cmd=Retrieve&db=PubMed&dopt=Citation&list_uids=11209064.
- K A Rimes and E Watkins. The effects of self-focused rumination on global negative self-judgements in depression. *Behav Res Ther*, 43(12):1673–1681, 2005. doi: S0005-7967(05)00018-5[pii]10.1016/j.brat.2004.12.002. URL http://www.ncbi.nlm.nih.gov/entrez/query.fcgi?cmd=Retrieve&db=PubMed&dopt=Citation&list_uids=16239157.
- E Salmi, S Aalto, J Hirvonen, J W Langsjo, A T Maksimow, V Oikonen, L Metsahonkala, J Virkkala, K Nagren, and H Scheinin. Measurement of GABAA receptor binding in vivo with [¹¹C]flumazenil: a test-retest study in healthy subjects. *Neuroimage*, 41(2):260–269, 2008. doi: S1053-8119(08)00191-2[pii]10.1016/j.neuroimage.2008.02.

035. URL http://www.ncbi.nlm.nih.gov/entrez/query.fcgi?cmd=Retrieve&db=PubMed&dopt=Citation&list_uids=18411060.
- G Sanacora. Cortical inhibition, gamma-aminobutyric acid, and major depression: there is plenty of smoke but is there fire? *Biol Psychiatry*, 67(5):397–398, 2010. URL http://www.ncbi.nlm.nih.gov/entrez/query.fcgi?cmd=Retrieve&db=PubMed&dopt=Citation&list_uids=20159143.
- Gerard Sanacora, Giulia Treccani, and Maurizio Popoli. Towards a glutamate hypothesis of depression: an emerging frontier of neuropsychopharmacology for mood disorders. *Neuropharmacology*, 62(1):63–77, January 2012. doi: 10.1016/j.neuropharm.2011.07.036.
- R Saxe, M Brett, and N Kanwisher. Divide and conquer: a defense of functional localizers. *Neuroimage*, 30(4):1088–1089, 2006. URL http://www.ncbi.nlm.nih.gov/entrez/query.fcgi?cmd=Retrieve&db=PubMed&dopt=Citation&list_uids=16635578.
- Hillary S Schaefer, Katherine M Putnam, Ruth M Benca, and Richard J Davidson. Event-related functional magnetic resonance imaging measures of neural activity to positive social stimuli in pre- and post-treatment depression. *Biological psychiatry*, 60(9):974–86, November 2006. ISSN 0006-3223. doi: 10.1016/j.biopsych.2006.03.024. URL <http://www.ncbi.nlm.nih.gov/pubmed/16780808>.
- R Schandry. Heart beat perception and emotional experience. *Psychophysiology*, 18(4):483–488, 1981. URL http://www.ncbi.nlm.nih.gov/entrez/query.fcgi?cmd=Retrieve&db=PubMed&dopt=Citation&list_uids=7267933.
- L Schilbach, D Bzdok, B Timmermans, P T Fox, A R Laird, K Vogeley, and S B Eickhoff. Introspective minds: using ALE meta-analyses to study commonalities in the neural correlates of emotional processing, social & unconstrained cognition. *PLoS ONE*, 7(2):e30920, 2012. doi: 10.1371/journal.pone.

0030920PONE-D-11-20368[pii]. URL http://www.ncbi.nlm.nih.gov/entrez/query.fcgi?cmd=Retrieve&db=PubMed&dopt=Citation&list_uids=22319593.

C.S. Sherrington. *The Integrative Action of the Nervous System*. University Press, Cambridge, England, 1948.

A Shmuel, E Yacoub, J Pfeuffer, P F Van de Moortele, G Adriany, X Hu, and K Ugurbil. Sustained negative BOLD, blood flow and oxygen consumption response and its coupling to the positive response in the human brain. *Neuron*, 36(6):1195–1210, 2002. doi: S0896627302010619[pii]. URL http://www.ncbi.nlm.nih.gov/entrez/query.fcgi?cmd=Retrieve&db=PubMed&dopt=Citation&list_uids=12495632.

R G Shulman, F Hyder, and D L Rothman. Baseline brain energy supports the state of consciousness. *Proc Natl Acad Sci U S A*, 2009. doi: 0903941106[pii]10.1073/pnas.0903941106. URL http://www.ncbi.nlm.nih.gov/entrez/query.fcgi?cmd=Retrieve&db=PubMed&dopt=Citation&list_uids=19549837.

W. K Silverman. *Anxiety Disorders Interview Schedule for Children*. Graywind Publications, Boulder, CO, 1987.

W. K. Silverman and A. M. Albano. *The Anxiety Disorders Interview Schedule for DSM-IV Child and Parent Versions*. Graywind Publications, Boulder, CO, 1997.

Alan Simmons, Irina Strigo, Scott C Matthews, Martin P Paulus, and Murray B Stein. Anticipation of aversive visual stimuli is associated with increased insula activation in anxiety-prone subjects. *Biological psychiatry*, 60(4):402–9, August 2006. ISSN 0006-3223. doi: 10.1016/j.biopsych.2006.04.038. URL <http://www.ncbi.nlm.nih.gov/pubmed/16919527>.

W Kyle Simmons, Jason a Avery, Joel C Barcalow, Jerzy Bodurka, Wayne C Drevets, and Patrick Bellgowan. Keeping the body in mind: Insula functional organization and functional connectivity integrate interoceptive, exteroceptive, and emo-

- tional awareness. *Human brain mapping*, 000, June 2012. ISSN 1097-0193. doi: 10.1002/hbm.22113. URL <http://www.ncbi.nlm.nih.gov/pubmed/22696421>.
- J R Simpson Jr., W C Drevets, A Z Snyder, D A Gusnard, and M E Raichle. Emotion-induced changes in human medial prefrontal cortex: II. During anticipatory anxiety. *Proc Natl Acad Sci U S A*, 98(2):688–693, 2001. doi: 10.1073/pnas.98.2.68898/2/688[pii]. URL http://www.ncbi.nlm.nih.gov/entrez/query.fcgi?cmd=Retrieve&db=PubMed&dopt=Citation&list_uids=11209066.
- K S Smith and U Rudolph. Anxiety and depression: Mouse genetics and pharmacological approaches to the role of GABA(A) receptor subtypes. *Neuropharmacology*, 2011. doi: S0028-3908(11)00304-2[pii]10.1016/j.neuropharm.2011.07.026. URL http://www.ncbi.nlm.nih.gov/entrez/query.fcgi?cmd=Retrieve&db=PubMed&dopt=Citation&list_uids=21810433.
- S M Smith. Fast robust automated brain extraction. *Hum Brain Mapp*, 17(3):143–155, 2002. doi: 10.1002/hbm.10062. URL http://www.ncbi.nlm.nih.gov/entrez/query.fcgi?cmd=Retrieve&db=PubMed&dopt=Citation&list_uids=12391568.
- S M Smith, M Jenkinson, M W Woolrich, C F Beckmann, T E Behrens, H Johansen-Berg, P R Bannister, M De Luca, I Drobnjak, D E Flitney, R K Niazy, J Saunders, J Vickers, Y Zhang, N De Stefano, J M Brady, and P M Matthews. Advances in functional and structural MR image analysis and implementation as FSL. *Neuroimage*, 23 Suppl 1:S208–19, 2004. doi: S1053-8119(04)00393-3[pii]10.1016/j.neuroimage.2004.07.051. URL http://www.ncbi.nlm.nih.gov/entrez/query.fcgi?cmd=Retrieve&db=PubMed&dopt=Citation&list_uids=15501092.
- Reiner Sprengelmeyer, J Douglas Steele, Benson Mwangi, Poornima Kumar, David Christmas, Maarten Milders, and Keith Matthews. The insular cortex and the neuroanatomy of major depression. *Journal of affective disorders*, 133(1-2):120–7, September 2011. ISSN 1573-2517. URL <http://www.ncbi.nlm.nih.gov/pubmed/>

21531027.

Murray B Stein, Alan N Simmons, Justin S Feinstein, and Martin P Paulus. Increased amygdala and insula activation during emotion processing in anxiety-prone subjects. *The American journal of psychiatry*, 164(2):318–27, February 2007. ISSN 0002-953X. doi: 10.1176/appi.ajp.164.2.318. URL <http://www.ncbi.nlm.nih.gov/pubmed/17267796>.

Philipp Sterzer and Andreas Kleinschmidt. Anterior insula activations in perceptual paradigms: often observed but barely understood. *Brain structure & function*, 214(5-6):611–22, June 2010. ISSN 1863-2661. doi: 10.1007/s00429-010-0252-2. URL <http://www.ncbi.nlm.nih.gov/pubmed/20512379>.

S H Stewart, S E Buffett-Jerrott, and R Kokaram. Heartbeat awareness and heart rate reactivity in anxiety sensitivity: a further investigation. *J Anxiety Disord*, 15(6):535–553, 2001. URL http://www.ncbi.nlm.nih.gov/entrez/query.fcgi?cmd=Retrieve&db=PubMed&dopt=Citation&list_uids=11764311.

Irina A Strigo, Alan N Simmons, Scott C Matthews, Arthur D Bud Craig, and Martin P Paulus. Increased affective bias revealed using experimental graded heat stimuli in young depressed adults: evidence of "emotional allodynia". *Psychosomatic medicine*, 70(3):338–44, April 2008a. ISSN 1534-7796. doi: 10.1097/PSY.0b013e3181656a48. URL <http://www.pubmedcentral.nih.gov/articlerender.fcgi?artid=2742693&tool=pmcentrez&rendertype=abstract>.

Irina A Strigo, Alan N Simmons, Scott C Matthews, Arthur D Bud Craig, and Martin P Paulus. Association of major depressive disorder with altered functional brain response during anticipation and processing of heat pain. *Archives of general psychiatry*, 65(11):1275–84, November 2008b. ISSN 1538-3636. doi: 10.1001/archpsyc.65.11.1275. URL <http://www.pubmedcentral.nih.gov/articlerender.fcgi?artid=2702160&tool=pmcentrez&rendertype=abstract>.

J Sui, T Adali, G D Pearlson, and V D Calhoun. An ICA-based method for the identification of optimal fMRI features and components using combined group-discriminative techniques. *Neuroimage*, 46(1):73–86, 2009. doi: S1053-8119(09)00070-6[pii]10.1016/j.neuroimage.2009.01.026. URL http://www.ncbi.nlm.nih.gov/entrez/query.fcgi?cmd=Retrieve&db=PubMed&dopt=Citation&list_uids=19457398.

Petroc Sumner, Richard a E Edden, Aline Bompas, C John Evans, and Krish D Singh. More GABA, less distraction: a neurochemical predictor of motor decision speed. *Nature neuroscience*, 13(7):825–7, July 2010. ISSN 1546-1726. doi: 10.1038/nn.2559. URL <http://www.ncbi.nlm.nih.gov/pubmed/20512136>.

Umeda S. Terasawa Y, Shibata M, Moriguchi Y. Anterior insular cortex mediates bodily sensibility and social anxiety. *Soc Cogn Affect Neurosci*, 2012.

Janneke Terhaar, Filipa Campos Viola, Karl-Jürgen Bär, and Stefan Debener. Heart-beat evoked potentials mirror altered body perception in depressed patients. *Clinical neurophysiology : official journal of the International Federation of Clinical Neurophysiology*, April 2012. ISSN 1872-8952. doi: 10.1016/j.clinph.2012.02.086. URL <http://www.ncbi.nlm.nih.gov/pubmed/22541740>.

I Tkáč, Z Starcuk, I Y Choi, and R Gruetter. In vivo ¹H NMR spectroscopy of rat brain at 1 ms echo time. *Magnetic Resonance in Medicine*, 41(4):649–56, April 1999. ISSN 0740-3194. URL <http://www.ncbi.nlm.nih.gov/pubmed/10332839>.

W Treynor, R Gonzalez, and S Nolen-Hoeksema. Rumination Reconsidered: A Psychometric Analysis. *Cognitive Therapy and Research*, 27(3), 2003.

André Tylee and Paul Gandhi. The importance of somatic symptoms in depression in primary care. *Primary care companion to the Journal of clinical psychiatry*, 7(4): 167–76, January 2005. ISSN 1523-5998. URL <http://www.pubmedcentral.nih.gov/articlerender.fcgi?artid=1192435&tool=pmcentrez&rendertype=abstract>.

N Tzourio-Mazoyer, B Landeau, D Papathanassiou, F Crivello, O Etard, N Del-

croix, B Mazoyer, and M Joliot. Automated anatomical labeling of activations in SPM using a macroscopic anatomical parcellation of the MNI MRI single-subject brain. *Neuroimage*, 15(1):273–289, 2002. doi: 10.1006/nimg.2001.0978S1053811901909784[pii]. URL http://www.ncbi.nlm.nih.gov/entrez/query.fcgi?cmd=Retrieve&db=PubMed&dopt=Citation&list_uids=11771995.

Martijn P van den Heuvel, René C W Mandl, René S Kahn, and Hilleke E Hulshoff Pol. Functionally linked resting-state networks reflect the underlying structural connectivity architecture of the human brain. *Human brain mapping*, 30(10):3127–41, October 2009. ISSN 1097-0193. doi: 10.1002/hbm.20737. URL <http://www.ncbi.nlm.nih.gov/pubmed/19235882>.

A Vanhaudenhuyse, A Demertzi, M Schabus, Q Noirhomme, S Bredart, M Boly, C Phillips, A Soddu, A Luxen, G Moonen, and S Laureys. Two distinct neuronal networks mediate the awareness of environment and of self. *J Cogn Neurosci*, 23(3):570–578, 2011. doi: 10.1162/jocn.2010.21488. URL http://www.ncbi.nlm.nih.gov/entrez/query.fcgi?cmd=Retrieve&db=PubMed&dopt=Citation&list_uids=20515407.

F C Verhulst, J van der Ende, R F Ferdinand, and M C Kasius. The prevalence of DSM-III-R diagnoses in a national sample of Dutch adolescents. *Archives of general psychiatry*, 54(4):329–36, April 1997. ISSN 0003-990X. URL <http://www.ncbi.nlm.nih.gov/pubmed/9107149>.

J L Vincent, G H Patel, M D Fox, A Z Snyder, J T Baker, D C Van Essen, J M Zempel, L H Snyder, M Corbetta, and M E Raichle. Intrinsic functional architecture in the anaesthetized monkey brain. *Nature*, 447(7140):83–86, 2007. doi: nature05758[pii]10.1038/nature05758. URL http://www.ncbi.nlm.nih.gov/entrez/query.fcgi?cmd=Retrieve&db=PubMed&dopt=Citation&list_uids=17476267.

E Vul, C Harris, P Winkielman, and H Pashler. Puzzlingly High Correlations in fMRI

Studies of Emotion, Personality, and Social Cognition (a.k.a. Voodoo Correlations in Social Neuroscience). *Perspectives on Psychological Science*, 4(3):274–290, 2009.

M Walter, A Henning, S Grimm, R F Schulte, J Beck, U Dydak, B Schnepf, H Boeker, P Boesiger, and G Northoff. The relationship between aberrant neuronal activation in the pregenual anterior cingulate, altered glutamatergic metabolism, and anhedonia in major depression. *Arch Gen Psychiatry*, 66(5):478–486, 2009. doi: 66/5/478[pii] 10.1001/archgenpsychiatry.2009.39. URL http://www.ncbi.nlm.nih.gov/entrez/query.fcgi?cmd=Retrieve&db=PubMed&dopt=Citation&list_uids=19414707.

Carl F Weems, Chris Hayward, Joel Killen, and C Barr Taylor. A longitudinal investigation of anxiety sensitivity in adolescence. *Journal of abnormal psychology*, 111(3):471–7, August 2002. ISSN 0021-843X. URL <http://www.ncbi.nlm.nih.gov/pubmed/12150423>.

WHO. WHO The world health report 2002 - Reducing Risks, Promoting Healthy Life. Technical report, World Health Organisation, 2002. URL <http://www.who.int/whr/2002/en/>.

C Wiebking, A Bauer, M de Greck, N W Duncan, C Tempelmann, and G Northoff. Abnormal body perception and neural activity in the insula in depression: an fMRI study of the depressed "material me". *World J Biol Psychiatry*, 11(3):538–549, 2010. doi: 10.3109/15622970903563794. URL http://www.ncbi.nlm.nih.gov/entrez/query.fcgi?cmd=Retrieve&db=PubMed&dopt=Citation&list_uids=20146653.

C Wiebking, M de Greck, N W Duncan, A Heinzl, C Tempelmann, and G Northoff. Are emotions associated with activity during rest or interoception? An exploratory fMRI study in healthy subjects. *Neurosci Lett*, 491(1):87–92, 2011.

C Wiebking, N W Duncan, P Qin, D J Hayes, O Lyttelton, P Gravel, J Verhaege, A P Kostikov, R Schirrmacher, A J Reader, M Bajbouj, and G Northoff. External aware-

ness and GABA - A multimodal imaging study combining fMRI and [18F]flumazenil-PET. *Hum Brain Mapp*, in press, 2012a.

C. Wiebking, NW. Duncan, B. Tiret, DJ. Hayes, J. Doyon, M. Marjanska, M. Bajbouj, and G. Northoff. GABA in the insula - a predictor for the neural response to interoceptive awareness. *in submission*, 2012b.

Stefan Wiens. Interoception in emotional experience. *Current opinion in neurology*, 18(4):442–7, August 2005. ISSN 1350-7540. URL <http://www.ncbi.nlm.nih.gov/pubmed/16003122>.

J E Wiersma, P van Oppen, D J van Schaik, A J van der Does, A T Beekman, and B W Penninx. Psychological characteristics of chronic depression: a longitudinal cohort study. *J Clin Psychiatry*, 72(3):288–294, 2011. doi: 10.4088/JCP.09m05735blu. URL http://www.ncbi.nlm.nih.gov/entrez/query.fcgi?cmd=Retrieve&db=PubMed&dopt=Citation&list_uids=21450151.

M W Woolrich, S Jbabdi, B Patenaude, M Chappell, S Makni, T Behrens, C Beckmann, M Jenkinson, and S M Smith. Bayesian analysis of neuroimaging data in FSL. *Neuroimage*, 45(1 Suppl):S173–86, 2009. doi: S1053-8119(08)01204-4[pil]10.1016/j.neuroimage.2008.10.055. URL http://www.ncbi.nlm.nih.gov/entrez/query.fcgi?cmd=Retrieve&db=PubMed&dopt=Citation&list_uids=19059349.

Jamil Zaki, Joshua Ian Davis, and Kevin N Ochsner. Overlapping activity in anterior insula during interoception and emotional experience. *NeuroImage*, 62(1):493–9, August 2012. ISSN 1095-9572. URL <http://www.ncbi.nlm.nih.gov/pubmed/22587900>.

J Zhao, A-M Bao, X-R Qi, W Kamphuis, S Luchetti, J-S Lou, and D F Swaab. Gene expression of GABA and glutamate pathway markers in the prefrontal cortex of non-suicidal elderly depressed patients. *Journal of Affective Disorders*, 138(3):494–502, February 2012. doi: 10.1016/j.jad.2012.01.013.

K H Zou, D N Greve, M Wang, S D Pieper, S K Warfield, N S White, S Manandhar, G G Brown, M G Vangel, R Kikinis, and W M Wells 3rd. Reproducibility of functional MR imaging: preliminary results of prospective multi-institutional study performed by Biomedical Informatics Research Network. *Radiology*, 237(3):781–789, 2005. doi: 237/3/781[pii]10.1148/radiol.2373041630. URL http://www.ncbi.nlm.nih.gov/entrez/query.fcgi?cmd=Retrieve&db=PubMed&dopt=Citation&list_uids=16304101.

Q Zou, C W Wu, E A Stein, Y Zang, and Y Yang. Static and dynamic characteristics of cerebral blood flow during the resting state. *Neuroimage*, 48(3):515–524, 2009. doi: S1053-8119(09)00766-6[pii]10.1016/j.neuroimage.2009.07.006. URL http://www.ncbi.nlm.nih.gov/entrez/query.fcgi?cmd=Retrieve&db=PubMed&dopt=Citation&list_uids=19607928.

Chapter 10

Papers in peer-refereed journals

10.1 Year 2012

Christine Wiebking, Niall W. Duncan, Brice Tiret, David J. Hayes, Malgorzata Marjańska, Julien Doyon, Malek Bajbouj, Georg Northoff

GABA in the insula — a predictor of the neural response to interoceptive awareness

Submitted to Neuroimage and currently under review, 2012

Christine Wiebking, Moritz de Greck, Claus Tempelmann, Malek Bajbouj, Georg Northoff

Neural response to interoceptive awareness in the insula as state marker for depression - an fMRI study investigating healthy, depressed and remitted participants

Submitted, 2012

Christine Wiebking, Niall W. Duncan, Pengmin Qin, David J. Hayes, Oliver Lyttelton, Paul Gravel, J. Verhaeghe, A. P. Kostikov, Ralf Schirmacher, Anderw J. Reader, Malek Bajbouj, Georg Northoff

External awareness and GABA – A multimodal imaging study combining fMRI and [¹⁸F]flumazenil-PET

Human Brain Mapping 2012, doi: 10.1002/hbm.22166

Björn Enzi, Niall W. Duncan, Jörn Kaufmann, Claus Tempelmann, **Christine Wiebking**, Georg Northoff

Glutamate Modulates Resting State Activity in the Perigenual Anterior Cingulate Cortex
– A combined fMRI-MRS study

Neuroscience 2012, 227:102-109, doi: 10.1016/j.neuroscience.2012.09.039

Christine Wiebking und Georg Northoff

Selbst und Körper in der Depression

Zeitschrift für Psychiatrie, Psychologie und Psychotherapie 2012, 60(3), 2012, 177-183

D. Sliz, A. Smith, **C. Wiebking**, G. Northoff, S. Hayley

Neural correlates of a single-session massage treatment

Brain Imaging and Behavior 2012, 6(1):77-87 DOI 10.1007/s11682-011-9146-z

10.2 Year 2011

Christine Wiebking, Moritz de Greck, Niall W. Duncan, Alexander Heinzl, Claus Tempelmann, Georg Northoff

Are emotions associated with activity during rest or interoception? An exploratory fMRI study in healthy subjects

Neuroscience Letters 2011, 491, 87-92, doi:10.1016/j.neulet.2011.01.012

Georg Northoff, **Christine Wiebking**, Todd Feinberg, Jaak Panksepp

The 'resting-state hypothesis' of major depressive disorder—A translational subcortical–cortical framework for a system disorder

Neuroscience and Biobehavioral Reviews 2011, 35(9):1929-45

Niall W. Duncan, Björn Enzi, **Christine Wiebking**, Georg Northoff

Involvement of glutamate in rest-stimulus interaction between perigenual and supragenual anterior cingulate cortex: A combined fMRI-MRS study

Human Brain Mapping 2011, DOI: 10.1002/hbm.21179

10.3 Year 2010

Christine Wiebking, André Bauer, Moritz de Greck, Niall W. Duncan, Claus Tempelmann, Georg Northoff

Abnormal body perception and neural activity in the insula in depression – An fMRI study of the depressed „material me“

World Journal of Biological Psychiatry 2010, 11(3):538-49

10.4 Year 2009

Georg Northoff, Felix Schneider, Michael Rotte, Christian Matthiä, Claus Tempelmann, **Christine Wiebking**, Felix Bermpohl, Alexander Heinzl, Peter Danos, Hans-Jochen Heinze, Bernhard Bogerts, Martin Walter, Jaak Panksepp

Differential parametric modulation of self-relatedness and emotions in different brain regions

Human Brain Mapping 2009, 30: 369-382

Martin Walter, Christian Matthiä, **Christine Wiebking**, Michael Rotte, Claus Tempelmann, Bernhard Bogerts, Hans-Jochen Heinze, Georg Northoff

Preceding attention and the dorsomedial prefrontal cortex: Process specificity versus domain dependence

Human Brain Mapping 2009, 30(1):312-26

10.5 Year 2008

Felix Schneider, Felix Bermpohl, Alexander Heinzl, Michael Rotte, Martin Walter, Claus Tempelmann, **Christine Wiebking**, Henrik Dobrowolny, Hans Jochen Heinze, Georg Northoff

The resting brain and our Self: Self-relatedness modulates resting state neural activity in cortical midline structures

Neuroscience 2008, 157(1):120-31

10.6 Year 2007

Kolja Schiltz, Joachim Witzel, Georg Northoff, Kathrin Zierhut, Udo Gubka, Hermann Fellmann, Jörn Kaufmann, Claus Tempelmann, **Christine Wiebking**, Bernhard Bogerts
Brain Pathology in Pedophilic Offenders Evidence of Volume Reduction in the Right Amygdala and Related Diencephalic Structures

Arch Gen Psychiatry 2007, 64:737-746

Martin Walter, Joachim Witzel, **Christine Wiebking**, Udo Gubka, Michael Rotte, Kolja Schiltz, Felix Bermpohl, Claus Tempelmann, Bernhard Bogerts, Hans Jochen Heinze, and Georg Northoff

Pedophilia Is Linked to Reduced Activation in Hypothalamus and Lateral Prefrontal Cortex During Visual Erotic Stimulation

Biological Psychiatry 2007, 62(6):698-701

10.7 Year 2006

Christine Wiebking, Joachim Witzel, Martin Walter, Udo Gubka, Georg Northoff

Vergleich der emotionalen und sexuellen Prozessierung zwischen Gesunden und Patienten mit einer Pädophilie – eine kombinierte Studie aus Neuropsychologie und fMRT
Forensische Psychiatrie und Psychotherapie, Werkstattschriften (WsFPP), Pabst Science Publishers 13. Jahrgang 2006, Heft 2, 79-93

10.8 Book chapters

Neuroimaging in Forensic Psychiatry: from the clinic to the courtroom. Chapter 6: Pedophilia.

Authors: **Christine Wiebking**, Alexander Sartorius, Harald Dressing, Georg Northoff

Edited by Joseph R. Simpson, Wiley-Blackwell 2012. ISBN 978-0-470-97699-9

Neurobiologie forensisch-relevanter Störungen. Grundlagen, Störungsbilder, Perspektiven. Kapitel 32: Pädophilie.

Autoren: **Christine Wiebking** und Georg Northoff, S. 386-393. Jürgen Müller (Hrsg.),

Verlag W. Kohlhammer 2010. ISBN 978-3-17-020471-3

Chapter 11

List of contributions

A number of people have contributed to the research described in this work. Their exact contributions to each paper are outlined here.

11.1 Chapter 2: Are emotions associated with activity during rest or interoception? An exploratory fMRI study in healthy subjects [Wiebking et al., 2011]

Christine Wiebking - Designed study; recruited subjects; acquired data; conceived of and carried out analysis; wrote the manuscript.

Moritz de Greck² - Provided technical and conceptual input.

Niall W. Duncan³ - Reviewed the manuscript.

Alexander Heinzl⁵ - Reviewed the manuscript.

Claus Tempelmann⁴ - Provided technical input.

Georg Northoff³ - Designed study and provided conceptual input.

11.2 Chapter 3: Abnormal body perception and neural activity in the insula in depression – An fMRI study of the depressed “material me” [Wiebking et al., 2010]

Christine Wiebking- Designed study; recruited subjects; acquired data; conceived of and carried out analysis; wrote the manuscript.

André Bauer¹- Recruited subjects; acquired data.

Moritz de Greck²- Provided technical and conceptual input.

Niall W. Duncan³- Reviewed the manuscript.

Claus Tempelmann⁴- Provided technical input.

Georg Northoff³- Designed study and provided conceptual input.

11.3 Chapter 4: Neural response to interoceptive awareness in the insula as state marker for depression - an fMRI study investigating healthy, depressed and remitted participants

Christine Wiebking - Designed study; recruited subjects; acquired data; conceived of and carried out analysis; wrote the manuscript.

Moritz de Greck² - Provided technical and conceptual input.

Claus Tempelmann⁴ - Provided equipment.

Malek Bajbouj^{7,8} - Provided conceptual input.

Georg Northoff³- Designed study and provided conceptual input.

Affiliations

¹ State Hospital Uchtspringe, Saxony-Anhalt, Germany

² Department of Psychology, Peking University, 5 Yiheyuan Road, Beijing100871, China

³ Institute of Mental Health Research, University of Ottawa, Canada

⁴ Department of Neurology II, Otto-von-Guericke University, Magdeburg, Germany

⁵ Department of Nuclear Medicine, Heinrich-Heine University, Düsseldorf, Germany

⁶ McConnell Brain Imaging Centre, Montreal Neurological Institute, McGill University
Montreal, Canada

⁷ Department of Psychiatry, Charité-Universitätsmedizin Berlin, Campus Benjamin Franklin,
Berlin, Germany

⁸ Cluster of Excellence “Languages of Emotion” and Dahlem Institute for Neuroimaging
of Emotion (D.I.N.E.), Freie Universität Berlin, Germany

⁹ Functional Neuroimaging Unit and Department of Psychology, University of Montréal,
Canada

¹⁰Center for Magnetic Resonance Research and Department of Radiology, University
of Minnesota, Minneapolis, MN, USA

11.4 Chapter 5: External awareness and GABA – A multimodal imaging study combining fMRI and [¹⁸F]flumazenil-PET

[[Wiebking et al., 2012a](#)]

Christine Wiebking - Designed study; recruited subjects; acquired data; conceived of
and carried out analysis; wrote the manuscript.

Niall W. Duncan³ - Designed study; recruited subjects; acquired data; provided conceptual input; reviewed the manuscript.

Pengmin Qin³ - Provided conceptual input.

David J. Hayes³ - Designed study; recruited subjects; acquired data.

Oliver Lyttelton³ - Provided technical input.

Paul Gravel⁶ - PET reconstruction; provided technical input.

Jeroen Verhaeghe⁶ - Production radioligand.

Alexey P. Kostikov⁶ - Production radioligand.

Ralf Schirmacher⁶ - Provided equipment.

Andrew J. Reader⁶ - PET reconstruction; provided technical input.

Malek Bajbouj^{7,8} - Provided conceptual input.

Georg Northoff³ - Designed study and provided conceptual input.

11.5 Chapter 6: GABA in the insula — a predictor of the neural response to interoceptive awareness

Christine Wiebking - Designed study; recruited subjects; acquired data; conceived of and carried out analysis; wrote the manuscript.

Niall W. Duncan³ - Designed study; recruited subjects; acquired data; reviewed the manuscript.

Brice Tiret⁹ - Preprocessing of MRS data.

David J. Hayes³ - Designed study; recruited subjects; acquired data.

Malgorzata Marjańska¹⁰ - Provided equipment.

Julien Doyon⁹ - Provided equipment.

Malek Bajbouj^{7,8} - Provided conceptual input.

Georg Northoff³ - Designed study and provided conceptual input.

Appendix A

Supplementary material for Chapter 2

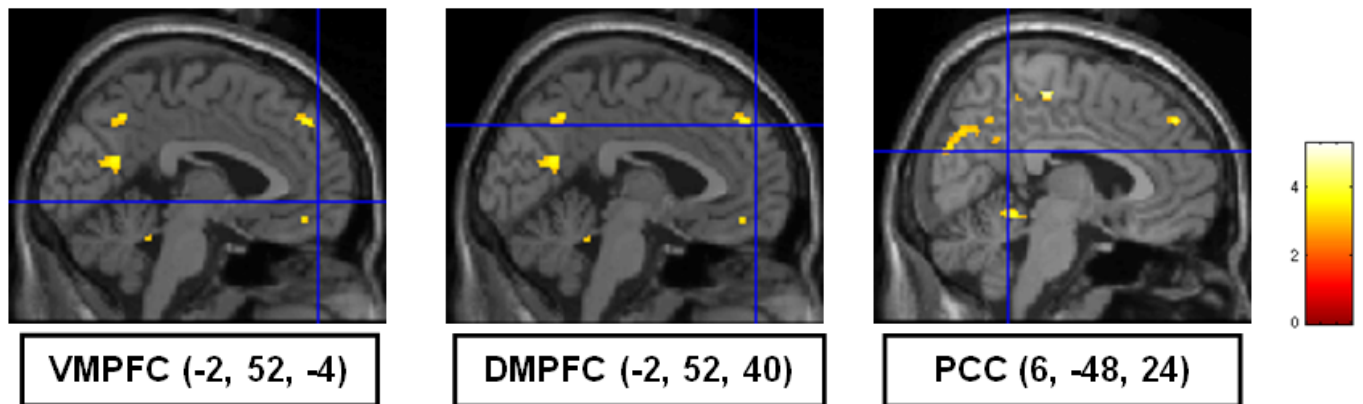


Figure A.1: The SPM images show the results of a whole brain regression analysis for the main contrast [Rest > Intero-/ Exteroception] with subject-specific scores of the FAB_8a ($P \leq 0.005$, non-corrected). Negative correlations occur near the regions of interest, which were defined independently from these results in the first step of our analysis. The position of the crosshair marks the center of each ROI. These SPM based results confirm the previous correlation results between extracted signal changes during rest and scores of FAB_8a (Table 2.2 B).

Regional Signal Changes Interoception					
		FAB 8a	BHS	BPQ_body	BPQ_total
Insula Cortex (-40, 8, -4)	<i>r</i>	-0.06	-0.16	0.27	0.22
	<i>P</i>	0.77	0.41	0.16	0.24
Insula Cortex (52, 6, 0)	<i>r</i>	0.001	-0.14	0.17	0.12
	<i>P</i>	1.0	0.45	0.38	0.52
Anterior Cingulate Cortex (4, 10, 46)	<i>r</i>	0.03	-0.29	0.18	0.24
	<i>P</i>	0.86	0.12	0.33	0.20
Lateral Somatomotor Cortex (56, -22, 24)	<i>r</i>	0.05	-0.12	0.08	0.55
	<i>P</i>	0.79	0.53	0.66	0.81
Lateral Somatomotor Cortex (62, -20, 30)	<i>r</i>	-0.44	0.06	0.07	-0.09
	<i>P</i>	0.02*	0.77	0.71	0.63
Lateral Somatomotor Cortex (-58, -22, 20)	<i>r</i>	0.15	-0.43	0.04	0.03
	<i>P</i>	0.42	0.02*	0.82	0.90

Table A.1: Main activated regions during interoception [Interoception > Exteroception] ($P \leq 0.05$, FWE corrected, $k \geq 10$) and their correlation with a behavioural test for emotional processing (FAB_8a), for depressed affect (BHS) and for body perception (BPQ) (* $P \leq 0.05$, P = significance (2-tailed), r = Pearson-correlation).

Appendix B

Supplementary material for Chapter 4

	H (<i>n</i> = 30)	D (<i>n</i> = 12)	R (<i>n</i> = 10)	Statistics	<i>P</i> -value
Age (mean ± SD)	33.7 ± 11.6	42.0 ± 14.2	37.9 ± 10.1	$F(2,49) = 2.1$	≥ 0.1
Gender (% female)	50	50	70	$X^2(2) = 1.3$	≥ 0.1
IQ	116.6 ± 12.0	109.4 ± 8.5	110.2 ± 10.7	$F(2,44) = 2.0$	≥ 0.1
BDI	n.a.	28.6 ± 10.3	17.4 ± 4.3	$t(8) = 2.7$	≤ 0.05*
BHS	4.6 ± 3.9	10.9 ± 4.6	n.a.	$t(35) = 3.7$	≤ 0.001**

Table B.1: Demographics and clinical variables for healthy (H), depressed (D), and remitted (R) participants.

Missing values: one in the healthy group for IQ, four in the depressed group for IQ. Beck Depression Inventory (BDI) and Beck Hopelessness Scale (BHS) contain seven subjects in the remitted and depressed group.

Region/ condition	F (df)	P	P-values ^a for pair-wise comparisons		
			H vs D	H vs R	D vs R
R_dAI/ IA	6.60 (2, 46)	0.007	0.003	1	0.037
R_vAI/ IA	6.02 (2, 46)	0.005	0.004	1	0.088
R_PI/ IA	5.23 (2, 46)	0.009	0.008	0.40	0.67
L_PI/ IA	3.84 (2, 46)	0.029	0.026	1	0.21
R_PI/ EA	3.86 (2, 46)	0.028	0.034	0.35	1
R_dAI/ EA	2.67 (2, 46)	0.08	0.123	0.41	1

Table B.2: Significant results as revealed by multivariate analysis of variance (MANOVA) occurred in the dorsal anterior insula (dAI), ventral anterior insula (vAI), and posterior insula (PI). Statistical group effects were mainly seen in IA conditions.

^a: P-values are given for significant contrasts based on Bonferroni post-hoc tests

	Healthy	Depressed	Remitted
R_dAI			
IA	0.05 ± 0.03	0.01 ± 0.03	0.05 ± 0.03
EA	0.03 ± 0.03	0.006 ± 0.03	0.01 ± 0.03
Fix	0.003 ± 0.03	-0.007 ± 0.03	0.01 ± 0.02
R_vAI			
IA	0.02 ± 0.03	-0.02 ± 0.04	0.01 ± 0.03
EA	0.01 ± 0.03	-0.02 ± 0.04	-0.002 ± 0.05
Fix	0.0004 ± 0.03	-0.01 ± 0.04	0.002 ± 0.02
R_PI			
IA	0.001 ± 0.03	-0.04 ± 0.02	-0.02 ± 0.04
EA	0.004 ± 0.03	-0.02 ± 0.03	-0.01 ± 0.03
Fix	0.002 ± 0.03	-0.01 ± 0.04	0.005 ± 0.03
L_PI			
IA	0.03 ± 0.03	-0.001 ± 0.03	0.02 ± 0.03
EA	0.02 ± 0.02	0.004 ± 0.03	0.01 ± 0.02
Fix	0.02 ± 0.03	0.01 ± 0.03	0.02 ± 0.02

IA: interoceptive awareness
EA: exteroceptive awareness
Fix: Fixation periods

R_dAI: right dorsal anterior insula
R_vAI: right ventral anterior insula
R_PI/ L_PI: right/ left posterior insula

Table B.3: Percent signal changes (mean ± SD) for healthy, depressed, and remitted participants in regions showing a significant group effect as revealed by MANOVA.

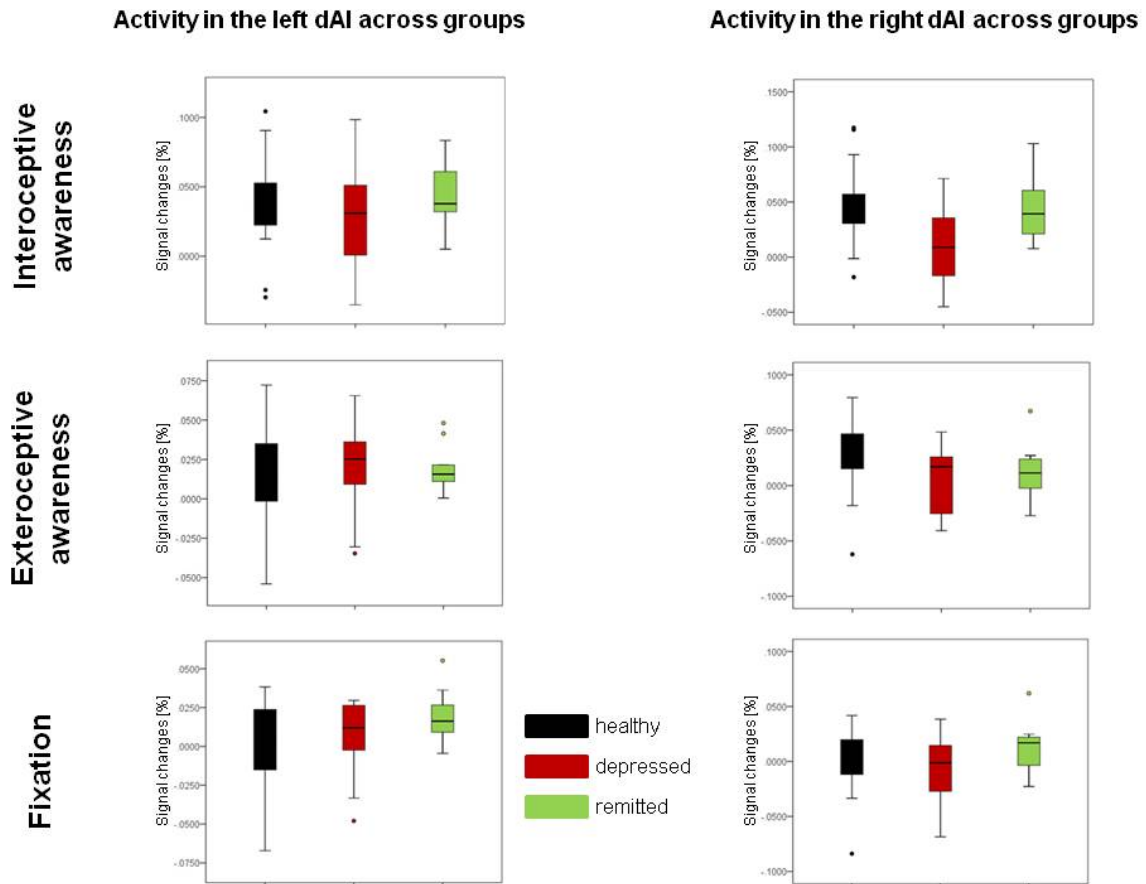


Figure B.1: Detailed overview of the distribution of neural activity in the left and right dAI across groups for different conditions (interoceptive awareness in the top, exteroceptive awareness in the middle, and Fixation in the bottom boxes).

	BHS Healthy	BHS Depr.	BDI Depr.	BDI Remitted
L_dAI				
IA	-0.39*	0.44	-0.19	-0.13
EA	-0.32 (*)	0.58	0.06	0.86*
Fix	-0.51***	0.35	0.09	0.22
R_dAI				
IA	-0.2	0.16	-0.38	0.33
EA	-0.19	0.36	-0.17	0.84*
Fix	-0.3(*)	0.31	0.22	0.50
L_PI				
IA	-0.13	0.24	-0.23	0.36
EA	-0.35(*)	0.44	0.12	0.89**
Fix	-0.36(*)	0.14	-0.03	0.42
R_PI				
IA	-0.23	0.07	0.01	0.41
EA	-0.55***	0.37	0.25	0.77*
Fix	-0.49**	0.21	0.13	0.43
***	P < 0.005			
**	P < 0.01			
*	P < 0.05			
(*)	P < 0.1			

Table B.4: Correlation (Pearson *r*-values, 2-tailed) between signal changes in the left and right dorsal anterior insula/ posterior insula and Beck Hopelessness Scale (BHS) or Beck Depression Inventory (BDI) in healthy, depressed, and remitted participants.

Appendix C

Supplementary material for Chapter 5

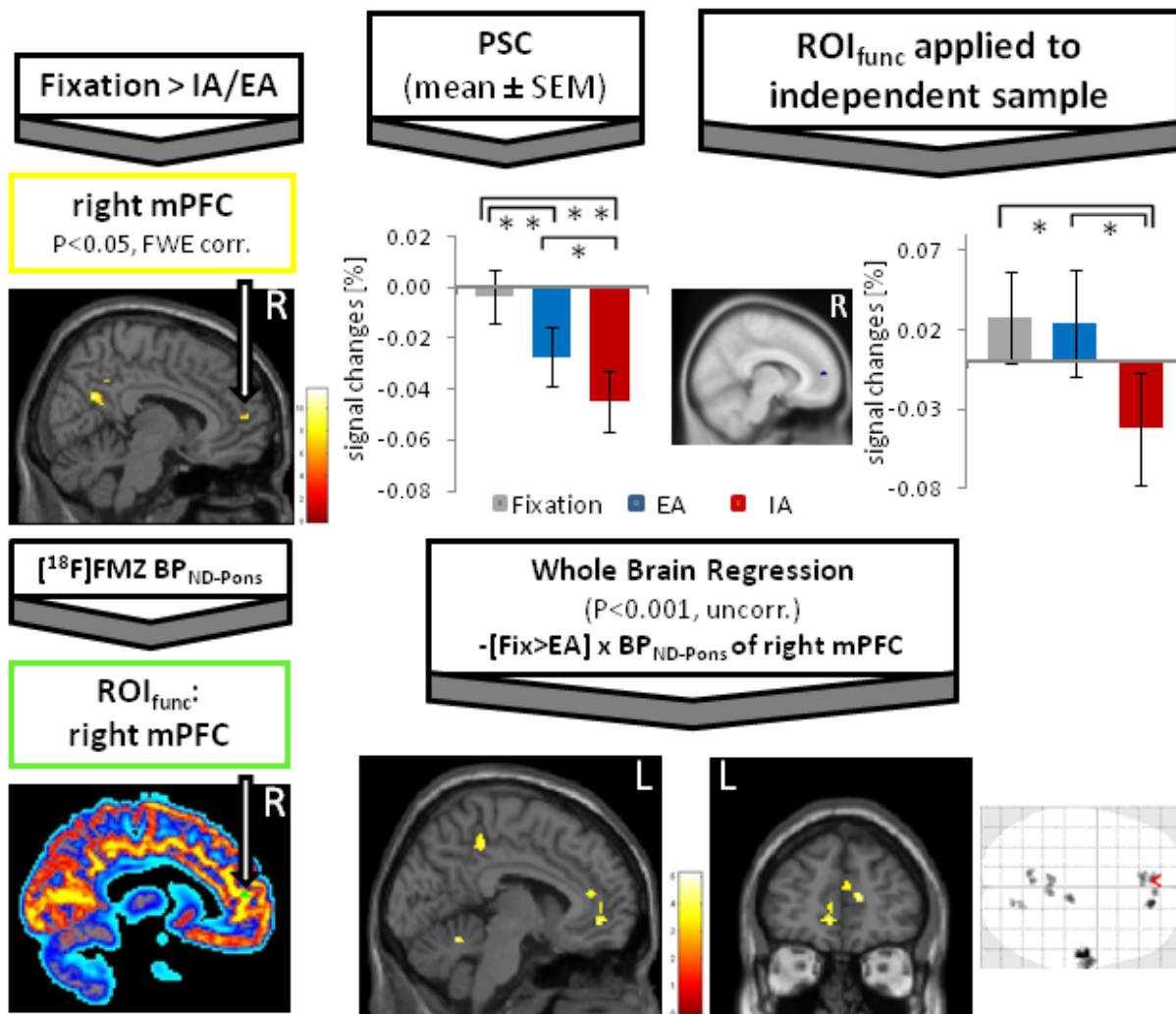


Figure C.1: The region of interest (ROI_{func}) in the right mPFC derived from the contrast [Fixation > Internal (IA)/ External Awareness (EA)] ($P \leq 0.05$, FWE corrected, $k \geq 5$, $n = 24$ subjects) (see SPM image in left upper corner). Bar diagrams show percent signal changes (PSC, mean \pm SEM) for $n = 20$ subjects as well as for an independent data sample ($n = 30$ subjects) during IA (red) and EA (blue) (** $P \leq 0.005$, * $P \leq 0.05$). This ROI was used to calculate binding potentials (BP_{ND-Pons}) for GABA_A receptors (see PET image in left lower corner). BP_{ND-Pons} values of the right mPFC were also entered into a whole brain regression analysis in SPM (right lower corner, negative correlation for the contrast [Fixation > External Awareness]) ($P \leq 0.001$, uncorrected, $k \geq 20$).

ROI _{func} (x,y,z)/ k/ T-value	BP _{ND-Pons}	BP _{ND-WM}	Partial correlation (controlled for grey matter)					
			PSC: Fixation		BP _{ND-Pons}		BP _{ND-WM}	
			PSC: IA	PSC: EA	PSC: Fix	PSC: IA	PSC: Fix	PSC: IA
			PSC: EA	PSC: Fix-IA	PSC: Fix-IA	PSC: EA	PSC: Fix-IA	PSC: Fix-IA
			PSC: Fix-EA	PSC: Fix-EA	PSC: Fix-EA	PSC: Fix-EA	PSC: Fix-EA	PSC: Fix-EA
				r-value	P-value		r-value	P-value
Hippocampus								
(-30,-26,-12)/ 50/ 8.51	3.6±0.8	5.3±1.1	0.01±0.04	r = -0.01	P = 1		r = -0.03	P = 0.9
			-0.03±0.04	r = 0.02	P = 0.9		r = -0.04	P = 0.9
			-0.02±0.04	r = 0.02	P = 0.9		r = 0.11	P = 0.7
			0.04±0.02	r = -0.04	P = 0.9		r = 0.02	P = 0.9
			0.03±0.02	r = -0.05	P = 0.8		r = -0.26	P = 0.3
(24,-10,-12)/ 12/ 7.35	1.8±0.8	3.8±1.1	0.01±0.05	r = 0.17	P = 0.5		r = 0.09	P = 0.7
			-0.03±0.05	r = 0.26	P = 0.3		r = 0.11	P = 0.6
			-0.01±0.05	r = 0.23	P = 0.3		r = 0.25	P = 0.3
			0.04±0.03	r = -0.22	P = 0.4		r = -0.07	P = 0.8
			0.03±0.02	r = -0.16	P = 0.5		r = -0.41	P = 0.1
(24,-24,-12)/ 17/ 8.55	2.1±1.2	3.6±1.5	0.02±0.06	r = -0.21	P = 0.4		r = -0.18	P = 0.5
			-0.02±0.07	r = -0.03	P = 0.9		r = -0.01	P = 1
			-0.02±0.05	r = -0.21	P = 0.4		r = -0.08	P = 0.8
			0.04±0.04	r = -0.23	P = 0.3		r = -0.23	P = 0.3
			0.04±0.03	r = 0.02	P = 0.9		r = -0.22	P = 0.4
Fusiform Gyrus								
(-34,-34,-16)/ 22/ 6.77	5.4±1.1	7.4±1.4	0.01±0.03	r = -0.32	P = 0.2		r = -0.34	P = 0.1
			-0.03±0.05	r = -0.21	P = 0.4		r = -0.29	P = 0.2
			-0.02±0.04	r = -0.27	P = 0.3		r = -0.33	P = 0.2
			0.03±0.02	r = -0.13	P = 0.6		r = 0.01	P = 1
			0.02±0.02	r = -0.13	P = 0.6		r = -0.07	P = 0.8
Amygdala								
(-18,-4,-18)/ 60/ 9.46	3.7±0.5	5.2±0.8	0.00±0.04	r = -0.22	P = 0.3		r = -0.19	P = 0.4
			-0.03±0.04	r = -0.28	P = 0.2		r = -0.33	P = 0.2
			-0.02±0.05	r = -0.27	P = 0.3		r = -0.16	P = 0.5
			0.04±0.02	r = 0.11	P = 0.6		r = 0.25	P = 0.3
			0.02±0.02	r = 0.25	P = 0.3		r = 0.02	P = 0.9
Middle Temporal Gyrus								
(60,2,-20)/ 68/ 8.96	5.3±1.0	7.2±1.7	0.00±0.03	r = 0.32	P = 0.2		r = -0.05	P = 0.8
			-0.05±0.04	r = 0.21	P = 0.4		r = -0.04	P = 0.9
			-0.03±0.04	r = 0.36	P = 0.1		r = -0.02	P = 0.9
			0.05±0.02	r = 0.07	P = 0.8		r = -0.01	P = 1
			0.03±0.02	r = -0.24	P = 0.3		r = -0.07	P = 0.8

Table C.1: Brain regions derived from the contrast [Fixation > IA/ EA] ($P \leq 0.05$, FWE-corrected, $k \geq 10$, $n = 24$ subjects, coordinates in MNI space) that were not located along the cortical midline. For each region, binding potential values ($BP_{ND-Pons}$ as well as BP_{ND-WM}) and percent signal changes (PSC) were calculated (mean \pm SD, $n = 20$ subjects). Results for the signal difference (Fix-EA) are grey shaded. Partial correlations (two-tailed, controlled for grey matter) showed no significant results across conditions and regions.

[Fixation>EA] x BP _{ND-Pons}	[Fixation>EA] x BP _{ND-WM}	[Fixation>IA] x BP _{ND-Pons}	[Fixation>IA] x BP _{ND-WM}
positive correlation	positive correlation	positive correlation	positive correlation
negative correlation	negative correlation	negative correlation	negative correlation
cluster-level \ k \ Z \ xyz	cluster-level \ k \ Z \ xyz	cluster-level \ k \ Z \ xyz	cluster-level \ k \ Z \ xyz
ROI_{func}			
Left mPFC			
no result for positive correlation	Puncorr 0.08 \ 55 \ 3.5 \ 50,-52,6	Puncorr 0.09 \ 46 \ 3.7 \ 50,-10,0	Puncorr 0.03 \ 88 \ 4.6 \ 58,-6,10
Puncorr 0.02 \ 102 \ 4.5 \ -12,46,6	Puncorr 0.02 \ 103 \ 3.8 \ 14,52,12	Puncorr 0.07 \ 56 \ 3.5 \ 14,44,-2	no result for negative correlation
P _{FWE} corr < 0.001 \ 587 \ 4.2 \ -8,-46,2	Puncorr 0.03 \ 94 \ 3.6 \ -4,38,12		
Puncorr 0.03 \ 76 \ 3.8 \ 8,26,-12	Puncorr 0.02 \ 115 \ 3.4 \ -18,-10,72		
Puncorr 0.002 \ 180 \ 3.6 \ 14,52,12	Puncorr 0.08 \ 56 \ 2.9 \ 28,54,18		
Puncorr 0.05 \ 61 \ 3.4 \ -6,18,-8			
Precuneus			
no result for positive correlation	Puncorr 0.07 \ 59 \ 3.9 \ 50,-54,4	no result for positive correlation	Puncorr 0.04 \ 72 \ 4.2 \ -56,-14,-4
Puncorr 0.04 \ 69 \ 4.0 \ -42,34,6	Puncorr 0.03 \ 86 \ 3.6 \ 30,-8,-16	no result for negative correlation	no result for negative correlation
Puncorr 0.008 \ 122 \ 3.9 \ -50,26,-8	Puncorr 0.006 \ 157 \ 3.4 \ -6,44,-12		
Puncorr 0.01 \ 111 \ 3.8 \ -18,-52,-24			
P _{FWE} corr 0.001 \ 435 \ 3.8 \ 12,48,10			
P _{FWE} corr 0.001 \ 412 \ 3.7 \ 4,-54,20			
Puncorr 0.06 \ 54 \ 3.6 \ -4,-6,30			
Puncorr 0.06 \ 56 \ 3.4 \ 62,-4,2			
Puncorr 0.02 \ 95 \ 3.1 \ 2,36,16			
Right mPFC			
no result for positive correlation	no result for positive correlation	Puncorr 0.07 \ 55 \ 4.1 \ 62,-32,20	no result for positive correlation
Puncorr 0.002 \ 183 \ 4.2 \ 54,-8,26	Puncorr 0.006 \ 150 \ 4.5 \ 30,26,42	Puncorr 0.01 \ 121 \ 4.0 \ 42,26,-6	Puncorr 0.07 \ 55 \ 3.8 \ 4,22,50
P _{FWE} corr < 0.001 \ 682 \ 4.0 \ 12,48,12	Puncorr 0.002 \ 201 \ 4.4 \ -52,-8,24	Puncorr 0.007 \ 137 \ 3.8 \ 6,34,36	
P _{FWE} corr 0.006 \ 335 \ 3.9 \ 62,-6,-6	Puncorr 0.03 \ 85 \ 4.1 \ 38,48,14		
Puncorr 0.03 \ 74 \ 3.8 \ 10,-22,38	P _{FWE} corr 0.001 \ 483 \ 4.0 \ -32,10,54		
Puncorr 0.007 \ 133 \ 3.8 \ -12,-58,-20	Puncorr 0.06 \ 59 \ 3.9 \ 52,12,-16		
Puncorr 0.06 \ 56 \ 3.8 \ -52,-10,28	Puncorr 0.02 \ 114 \ 3.8 \ 2,-58,-20		
Puncorr 0.02 \ 87 \ 3.8 \ 12,-68,4	Puncorr 0.06 \ 61 \ 3.7 \ 24,20,-16		
P _{FWE} corr 0.001 \ 469 \ 3.7 \ -2,-62,50	P _{FWE} corr 0.03 \ 273 \ 3.7 \ 36,-14,38		
Puncorr 0.06 \ 56 \ 3.7 \ 32,-44,-16	Puncorr 0.03 \ 91 \ 3.6 \ -4,-8,36		
Puncorr 0.008 \ 123 \ 3.7 \ 24,14,44	Puncorr 0.02 \ 105 \ 3.6 \ 18,34,58		
Puncorr 0.004 \ 149 \ 3.6 \ 14,-72,26	Puncorr 0.06 \ 62 \ 3.6 \ -18,6,60		
Puncorr 0.03 \ 78 \ 3.6 \ -50,24,-6	Puncorr 0.003 \ 178 \ 3.5 \ -10,60,-2		
Puncorr 0.08 \ 49 \ 3.5 \ -52,-16,-18	Puncorr 0.02 \ 104 \ 3.4 \ -24,52,16		
P _{FWE} corr 0.08 \ 207 \ 3.4 \ 16,-86,-26	Puncorr 0.04 \ 78 \ 3.3 \ -2,-62,50		
Puncorr 0.07 \ 51 \ 3.4 \ -32,18,42	Puncorr 0.02 \ 106 \ 3.3 \ 4,62,-2		
Puncorr 0.02 \ 99 \ 3.2 \ -2,-16,44	Puncorr 0.06 \ 63 \ 3.3 \ 24,-56,12		
Puncorr 0.06 \ 55 \ 3.1 \ -4,-70,8	Puncorr 0.08 \ 51 \ 3.2 \ 38,12,46		
Puncorr 0.08 \ 47 \ 3.1 \ 12,-54,26			

ROI _{ana} (colour code according to Figure 3)			
Front. Mid. Orb. Cortex, R			
no result for positive correlation	no result for positive correlation	no result for positive correlation	no result for positive correlation
P FWE corr 0.03 \ 170 \ 4.0 \ -2,-52,24	no result on cluster-level	P uncorr 0.07 \ 56 \ 3.2 \ 6,40,20	no result for negative correlation
P FWE corr 0.07 \ 136 \ 3.6 \ -8,46,6			
P uncorr 0.04 \ 80 \ 3.2 \ -8,54,26			
Front. Mid. Orb. Cortex, L			
no result for positive correlation	no result for positive correlation	no result for positive correlation	no result for positive correlation
P FWE corr 0.02 \ 209 \ 4.2 \ 16,62,0	P uncorr 0.07 \ 61 \ 3.1 \ 12,54,-6	no result on cluster-level	no result on cluster-level
P FWE corr 0.05 \ 149 \ 3.8 \ -12,46,6			
Front. Sup. Mid. Cortex, R			
no result for positive correlation	no result for positive correlation	no result for positive correlation	no result for positive correlation
P uncorr 0.02 \ 107 \ 4.0 \ -12,44,4	P FWE corr <0.001 \ 1294 \ 4.5 \ -12,62,2	no result for negative correlation	no result for negative correlation
P uncorr 0.06 \ 68 \ 3.6 \ 4,-60,16	P uncorr 0.02 \ 116 \ 3.2 \ -4,-62,50		
P uncorr 0.085 \ 54 \ 3.0 \ 2,-68,50			
Front. Sup. Mid. Cortex, L			
no result for positive correlation	no result for positive correlation	no result for positive correlation	no result for positive correlation
P uncorr 0.025 \ 96 \ 4.2 \ -12,44,4	P FWE corr 0.001 \ 409 \ 3.7 \ -4,40,12	no result for negative correlation	no result for negative correlation
P uncorr 0.03 \ 93 \ 3.3 \ 4,-60,14			
P uncorr 0.03 \ 88 \ 3.2 \ -8,-64,64			
Precuneus, R			
no result for positive correlation	no result for positive correlation	no result for positive correlation	no result for positive correlation
P uncorr 0.015 \ 118 \ 4.0 \ 14,-54,24	P uncorr 0.09 \ 52 \ 3.5 \ -8,50,0	no result for negative correlation	no result for negative correlation
P uncorr 0.04 \ 77 \ 3.6 \ -10,48,8			
Precuneus, L			
no result for positive correlation	no result for pos. correlation	no result for positive correlation	no result for positive correlation
P uncorr 0.03 \ 90 \ 4.3 \ 14,-54,24	no result on cluster-level	no result for negative correlation	no result for negative correlation
Anterior Cingulate, R			
no result for positive correlation	no result for positive correlation	no result for positive correlation	no result for positive correlation
no result for negative correlation	no result for negative correlation	no result for negative correlation	no result on cluster-level
Anterior Cingulate, L			
no result for positive correlation	no result for positive correlation	no result for positive correlation	no result for positive correlation
no result for negative correlation	no result for negative correlation	no result on cluster-level	no result for negative correlation
ROI_{ana} (non-medial regions)			
Amygdala, L			
no result for positive correlation	no result for positive correlation	no result for positive correlation	no result for positive correlation
P uncorr 0.06 \ 65 \ 4.2 \ -12,46,8	no result for negative correlation	no result for negative correlation	no result for negative correlation
P uncorr 0.03 \ 89 \ 3.8 \ 12,58,-2			
Amygdala, R			
no result for positive correlation	no result for positive correlation	no result for positive correlation	no result for positive correlation
P uncorr 0.08 \ 54 \ 3.9 \ 16,62,0	no result for negative correlation	no result for negative correlation	no result for negative correlation
Hippocampus, L			
no result for positive correlation	no result for positive correlation	no result for positive correlation	no result for positive correlation
P uncorr 0.04 \ 85 \ 3.9 \ 10,64,2	no result for negative correlation	no result for negative correlation	no result for negative correlation
Hippocampus, R			
no result on cluster-level	P uncorr 0.05 \ 66 \ 3.5 \ 4,-42,68	no result for positive correlation	no result for positive correlation
	P uncorr 0.02 \ 95 \ 3.5 \ -12,-46,66		
no result on cluster-level	no result for negative correlation	no result for negative correlation	no result on cluster-level

Table C.2: Detailed overview of the conducted whole brain regressions. The table contains results concerning the nature of contrast ([Fix-EA] is listed on the left side, [Fix-IA] is listed on the right side), the correlation value (BP_{ND-Pons} or BP_{ND-WM}) and the direction of the relationship (results for positive correlations have a white background, followed by grey shaded results for negative correlations) for each ROI_{ana}. Results concerning ROI_{func} (mPFC and precuneus, green coloured) are set to a threshold of $P \leq 0.005$ (uncorrected, $k \geq 40$). Results concerning ROI_{ana} are set to $P \leq 0.005$ (uncorrected, $k \geq 20$) and are inclusively masked and small volume corrected by the four bilateral ROI_{ana}. Note that reported results are restricted to $P \leq 0.09$ on the cluster-level and only provide the first relevant coordinate (x,y,z in MNI space) of a significant cluster (k). The BP_{ND} values of the left and right amygdala and hippocampus, regions which are also present in the initial fMRI contrast [Fix > IA/ EA] (see Suppl. table C.1), have also been used to perform whole brain regression analysis and are included at the end of this table.

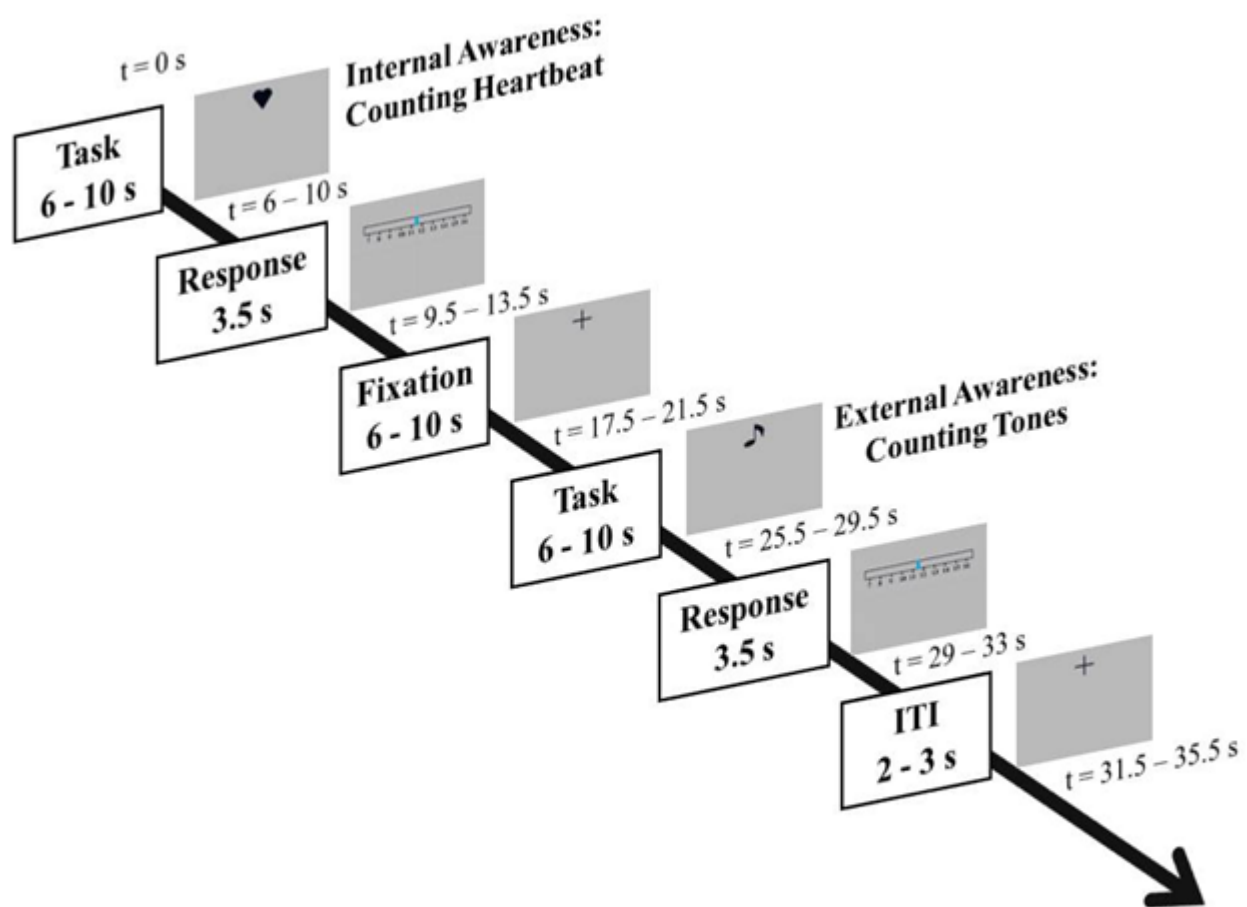


Figure C.2: The fMRI design was based on a paradigm introduced by Critchley and Pollatos [Pollatos et al., 2007b, Critchley et al., 2004]. Subjects were presented with three separate conditions: an internal task, an external task, and fixation periods, in a pseudo-randomised order (each jittered between 6-10 s).

Appendix D

Supplementary material for Chapter 6

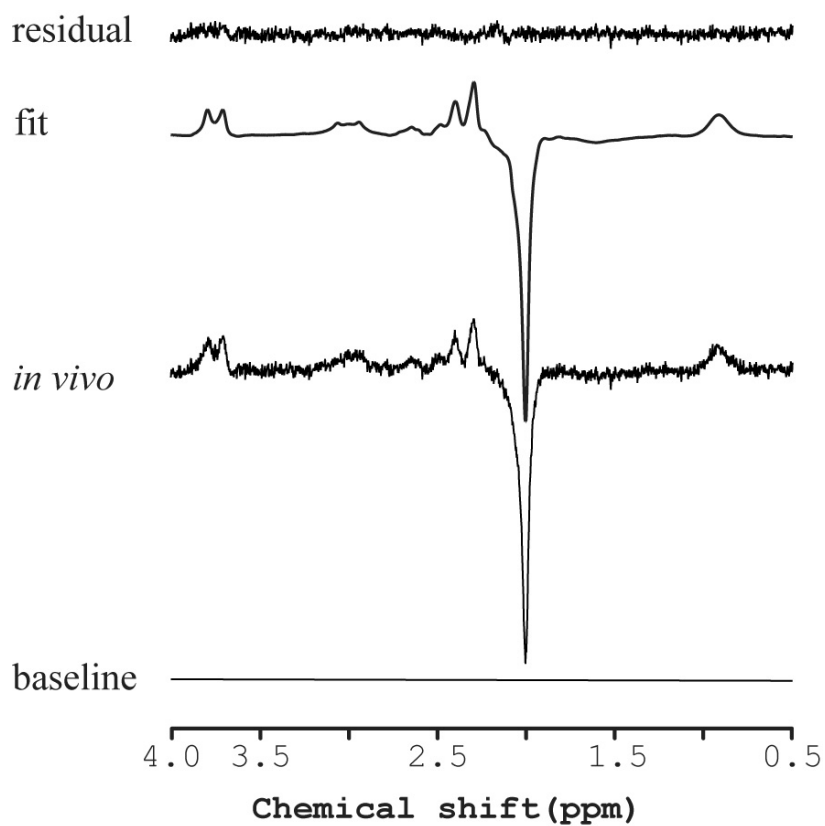


Figure D.1: LCModel quantification of the representative 1H NMR spectrum obtained using MEGA-PRESS [Mescher et al., 1998, Marjanska et al., 2007].

A)

		<u>Insula</u>			
concentration	(mean ± SD)	GABA ₁₅ /NAA	GlX ₁₄ /NAA	Glu ₁₄ /NAA	Gln ₁₄ /NAA
	min / max	0.07 ± 0.01 0.06 / 0.10	0.90 ± 0.10 0.73 / 1.12	0.69 ± 0.07 0.60 / 0.89	0.21 ± 0.04 0.13 / 0.29
CRLB	(mean ± SD)	GABA ₁₅	GlX ₁₄	Glu ₁₄	Gln ₁₄
	min / max	14.3 ± 2.1 11 / 19	2.4 ± 0.6 1 / 3	3.5 ± 0.8 2 / 5	13.8 ± 3.8 8 / 19
The correlation coefficient between Glu/Gln is -0.63 ± 0.09 (mean ± SD) with min / max values of -0.74 / -0.51.					
		<u>mPFC</u>			
concentration	(mean ± SD)	GABA ₉ /NAA	GlX ₁₈ /NAA	Glu ₁₈ /NAA	Gln ₁₈ /NAA
	min / max	0.06 ± 0.01 0.05 / 0.10	0.97 ± 0.07 0.87 / 1.12	0.71 ± 0.07 0.61 / 0.84	0.26 ± 0.05 0.18 / 0.37
CRLB	(mean ± SD)	GABA ₁₅	GlX ₁₄	Glu ₁₄	Gln ₁₄
	min / max	16.9 ± 2.0 14 / 20	2.3 ± 0.5 2 / 3	3.7 ± 0.7 3 / 5	11.9 ± 2.8 8 / 18
The correlation coefficient between Glu/Gln is -0.66 ± 0.08 (mean ± SD) with min / max values of -0.77 / -0.51.					

B)

		<u>Insula</u>			
Signal changes [%] (mean ± SD)		IA ₁₅	EA ₁₅	IA ₂₄	EA ₂₄
		0.00 ± 0.04 **	-0.01 ± 0.04	0.00 ± 0.04 **	-0.01 ± 0.04
Signal changes [%] (mean ± SD)		IA-Fix ₁₅	EA-Fix ₁₅	IA-Fix ₂₄	EA-Fix ₂₄
		0.01 ± 0.02 **	0.00 ± 0.02	0.00 ± 0.02 **	0.00 ± 0.02
		<u>mPFC</u>			
Signal changes [%] (mean ± SD)		IA ₉	EA ₉	IA ₁₈	EA ₁₈
		-0.01 ± 0.03 /	0.00 ± 0.02	-0.02 ± 0.03 (*)	-0.01 ± 0.03
Signal changes [%] (mean ± SD)		IA-Fix ₉	EA-Fix ₉	IA-Fix ₁₈	EA-Fix ₁₈
		-0.01 ± 0.01 /	-0.01 ± 0.01	-0.02 ± 0.02 (*)	-0.01 ± 0.02
				IA ₂₄	EA ₂₄
				-0.02 ± 0.03 (*)	-0.01 ± 0.03
				IA-Fix ₂₄	EA-Fix ₂₄
				-0.02 ± 0.02 (*)	-0.01 ± 0.02

Table D.1: A) Concentrations of brain metabolites (subscripted numbers indicate number of participants), Cramer-Rao lower bounds (CRLB) and correlation coefficients between Glu/Gln from the MRS voxel in left insula and mPFC (mean ± SD, min/max).

B) Signal changes from the MRS voxel in the left insula and mPFC (mean ± SD).

Values are compared by a paired t-test (** $P \leq 0.005$, *) $P \leq 0.1$).

Subscripted numbers indicate number of participants.

	[IA-Fix]	[EA-Fix]	[IA-EA]
	positive correlation	positive correlation	positive correlation
	negative correlation	negative correlation	negative correlation
	cluster-level\k\Z\xyz	cluster-level\k\Z\xyz	cluster-level\k\Z\xyz
GABA₁₅/NAA	** <i>P</i> FWE 0.003, <i>P</i> unc. 0.001\210\3.49\ -36 8 -8 3.37\ -36 4 2 3.30\ -42 -4 4 ...	no result for positive correlation	<i>P</i> FWE 0.12, <i>P</i> unc. 0.06\58\3.67\ -38 10 2
	no result for negative correlation	no result for negative correlation	no result for negative correlation
Glx₁₄/NAA	no result for positive correlation	no result for positive correlation	no result for positive correlation
	no result for negative correlation	no result for negative correlation	no result for negative correlation
Glu₁₄/NAA	no result for positive correlation	no result for positive correlation	no result for positive correlation
	no result for negative correlation	no result for negative correlation	no result for negative correlation
Gln₁₄/NAA	no result for positive correlation	no result for positive correlation	no result for positive correlation
	no result for negative correlation	no result for negative correlation	no result for negative correlation
BHS₁₅	no result for positive correlation	no result for positive correlation	no result for positive correlation
	** <i>P</i> FWE 0.002, <i>P</i> unc. 0.001\210\3.64\ -34 4 4 3.60\ -42 0 14 3.57\ -28 10 14 ...	no result for negative correlation	(* <i>P</i> FWE 0.055, <i>P</i> unc. 0.026\82\3.48\ -42 -2 6 3.37\ -34 4 2 2.82\ -30 -2 -2
BHS₂₄	no result for positive correlation	no result for positive correlation	no result for positive correlation
	** <i>P</i> FWE 0.007, <i>P</i> unc. 0.004\186\3.89\ -36 12 14 3.68\ -44 12 10 3.19\ -32 20 2 ...	no result for negative correlation	* <i>P</i> FWE 0.014, <i>P</i> unc. 0.008\149\3.87\ -34 6 2 3.53\ -30 -4 0 3.33\ -42 -2 2 ...

Table D.2: Neurochemical values (subscripted numbers indicate number of participants) and BHS scores were used as regressors in SPM analysis [$P \leq 0.005$, uncorrected, insula $k \geq 25$]. Positive correlations are marked in purple, negative correlations in blue. Results are shown for the left insula (small volume corrected for the MRS voxel in the left insula).

	[IA-Fix]	[EA-Fix]	[IA-EA]
	positive correlation	positive correlation	positive correlation
	negative correlation	negative correlation	negative correlation
	cluster-level\k\Z\xyz	cluster-level\k\Z\xyz	cluster-level\k\Z\xyz
GABA₉/NAA	no result for positive correlation	no result for positive correlation	no result for positive correlation
	no result for negative correlation	** <i>P</i> FWE 0.008, <i>P</i> unc. 0.003\87\3.90\ -2 36 -4	no result for negative correlation
		3.68\6 40 0	
		3.59\ -8 36 -2	
Glx₁₈/NAA	no result for positive correlation	no result for positive correlation	no result for positive correlation
	no result for negative correlation	no result for negative correlation	no result for negative correlation
Glu₁₈/NAA	no result for positive correlation	no result for positive correlation	no result for positive correlation
	no result for negative correlation	no result for negative correlation	no result for negative correlation
Gln₁₈/NAA	no result for positive correlation	no result for positive correlation	no result for positive correlation
	no result for negative correlation	no result for negative correlation	no result for negative correlation
BHS₁₈	no result for positive correlation	no result for positive correlation	no result for positive correlation
	no result for negative correlation	no result for negative correlation	no result for negative correlation
BHS₂₄	<i>P</i> FWE 0.11, <i>P</i> unc. 0.08\56\3.36\ -6 48 -8	no result for positive correlation	(*) <i>P</i> FWE 0.07, <i>P</i> unc. 0.05\75\3.8\ -18 38 -8
	3.31\ -18 46 -6		3.71\ -18 44 -6
	3.26\ -4 44 -8		3.67\ -8 48 -8
	no result for negative correlation	no result for negative correlation	no result for negative correlation

Table D.3: Neurochemical values (subscripted numbers indicate number of participants) and BHS scores were used as regressors in SPM analysis [$P \leq 0.005$, uncorrected, mPFC $k \geq 15$].

Positive correlations are marked in purple, negative correlations in blue.

Results are shown for the mPFC (small volume corrected for the MRS voxel in the mPFC).

GABA₁₅/NAA

Macroanatomical location	[IA-Fix]
	positive correlation
	negative correlation
	cluster-level $k \setminus Z \setminus xyz$
Right Supramarginal Gyrus	** P FWE 0.0, P unc. 0\567\4.41\58 -28 40 3.67\68 -16 24
Right Rolandic Operculum	3.57\54 -26 22
Right Superior Frontal Gyrus	** P FWE 0.0, P unc. 0\589\4.33\34 -6 60
Right Precentral Gyrus	4.3\40 -12 60 3.81\58 -10 50
Right Inferior Frontal Gyrus (p. Opercularis)	** P FWE 0.0, P unc. 0\768\4.21\48 12 16 4.0\40 16 6 3.92\56 12 14
Left Insula Lobe	(*) P FWE 0.08, P unc. 0.001\211\3.49\ -36 8 -8 3.37\ -36 4 2 3.3\ -42 -4 4
	no result for negative correlation
	[EA-Fix]
Right Angular Gyrus	** P FWE 0.0, P unc. 0\635\4.28\30 -54 42 4.11\36 -66 26
Right Superior Parietal Lobule	3.69\20 -60 50
Left Postcentral Gyrus	** P FWE 0.009, P unc. 0\295\4.22\ -40 -34 70 3.51\ -44 -30 58
Left SupraMarginal Gyrus	3.49\ -60 -22 40
Right Middle Frontal Gyrus	** P FWE 0.001, P unc. 0\390\3.89\36 -2 54 3.69\30 -12 48 3.62\40 -4 66
	no result for negative correlation
	[IA-EA]
	no result for positive correlation
	no result for negative correlation

Table D.4: Whole brain regressions using GABA values from the insula as regressor (masked by a grey matter mask). Reported results are restricted to P FWE ≤ 0.1 . All peaks were assigned to the most probable brain area by using the SPM Anatomy Toolbox [Eickhoff et al., 2007].

** P FWE ≤ 0.01 , * P FWE ≤ 0.05 , (*) P FWE ≤ 0.1

Appendix E

List of abbreviations

AAL: automated anatomical labeling

AC-PC: anterior commissure (AC) and posterior commissure (PC)

BDI: Beck Depression Inventory

BET: Brain Extraction Tool

BHS: Beck Hopelessness Scale

BOLD: blood oxygen level dependent

BP: binding potential

BP_{ND} : non-displaceable binding potential (ratio at equilibrium of specifically bound radioligand to non-displaceable radioligand)

$BP_{ND-Pons}$: ratio at equilibrium of specifically bound radioligand to non-displaceable radioligand using the pons as reference tissue

BP_{ND-WM} : ratio at equilibrium of specifically bound radioligand to non-displaceable radioligand using the white matter as reference tissue

BPQ: Body Perception Questionnaire

CMS: cortical midline structures

CRLB: Cramer-Rao lower bounds

CSF: cerebrospinal fluid

dAI: dorsal anterior insula

DMN: default-mode network

DMPFC: dorsomedial prefrontal cortex

DSM-IV: Diagnostic and Statistical Manual of Mental Disorders

EA: exteroceptive awareness

EPI: echo planar imaging

FAB: Florida Affect Battery (with subscales A: awareness, S: stress response, ANSR: autonomic nervous system reactivity, SS: stress style)

FDG: fluorodeoxyglucose

fMRI: functional magnetic resonance imaging

FMZ: flumazenil

FSL: FMRIB's Software Library

FWHM: full-width half-maximum

GABA: gamma-aminobutyric acid

Gln: glutamine

Glu: glutamate

HR: hemodynamic response

IA: interoceptive awareness

ICA: independent component analysis

LCModel: Linear Combination of Model *in vitro* spectra

LPS-3: Leistungsprüfsystem, Untertest 3

MADRS: Montgomery-Åsberg Depression Rating Scale

MANOVA: multivariate analysis of variance

MarsBaR: Marseille Region of Interest Toolbox software package

max: maximum

MDD: major depressive disorder

min: minimum

MNI: Montreal Neurological Institute

mPFC: medial prefrontal cortex

MRS: magnetic resonance spectroscopy

MWT-B: Mehrfachwahl-Wortschatz-Intelligenztest, Version B

NAA: N-acetylaspartate

NBR: negative BOLD response

NMR: nuclear magnetic resonance

OVS: outer volume suppression

PACC: perigenual anterior cingulate cortex

PBR: positive BOLD response

PCC: posterior cingulate cortex

PET: positron-emission-tomography

PI: posterior insula

PSC: percent signal change

ROI (ROI_{func} / ROI_{ana}): region of interest (defined by functional MRI contrast or anatomical structure)

rtfMRI: real-time fMRI

SD: standard deviation

SEM: standard error mean

SPM: statistical parametric mapping

SPSS: Statistical Package for the Social Sciences

T_1 / T_2 : longitudinal and transverse relaxation

T_E : echo time

TID: task-induced deactivation

T_R : time of repetition

vAI: ventral anterior insula

VMPFC: ventromedial prefrontal cortex

VOI: volume of interest

Appendix F

Copies of original publications

Not available in the electronic version of the dissertation.